

Design, modelling and simulation of a green building energy
efficient system

Thesis

Berhane Gebreslassie



Thesis submitted in fulfilment of the requirements for the degree of

Master of Engineering

March 2018

College of Engineering & Science

Abstract

Conventional commercial buildings are among the highest unwise consumers of enormous amounts of energy and hence produce significant amounts of carbon dioxide (CO₂). These have been built for years without considering their contribution to global warming. However, green buildings (GB) simulation for energy efficiency commenced in 1973 and many countries—in particular the United States—has responded positively to minimise energy consumption. Therefore, software companies have developed unique building energy efficiency simulation software, interoperable with Building Information Modelling. Hence, the past decade has witnessed a rapid increase in the number of studies on GB energy efficiency systems. However, similar studies also indicate that the results of current GB simulations are not yet satisfactory to meet GB objectives. In addition, most such studies did not run simulation to determine comprehensive building energy efficiency. This study aims to meet GB objectives through design, modelling and simulation of comprehensive ‘multilevel hexagonal-curve shape’ commercial office building, energy efficient system. In this study, every particular part of the building construction element was simulated for ensuring energy efficiency. Additionally, a control method is introduced that almost satisfies GB objectives by using appropriate modern cost-effective technologies, such as ‘Actuator Sensor Interface’. This method reduces the initial, running, and maintenance costs of electrical/electronic devices and limits wiring installations, leading to significant energy consumption reduction of about 50%. Further, renewable energy or green power, currently the key solution to tackle the energy crisis, plays a significant role in removing CO₂ (negative emissions). In this research, its use is significantly maximised, hence decreasing the impact of global greenhouse gas emissions. This study not only considers energy sufficient buildings, but also building occupant comfort and building stability through simulations. In conclusion, energy saving of **63.5%** is achieved overall, approaching **NetZero energy saving/building energy self-sufficiency**.

Master by Research Declaration

I, Berhane Gebreslassie, solemnly declare that the thesis I am submitting to Graduate Research Centre (GRC), Master by Research thesis entitled ‘Design, modelling and simulation of a Green Building energy efficient system’ is not more than 60,000 words in length including quotes and exclusive of tables, figures, references and footnotes. This thesis contains no material that has been submitted previously, in whole or in part, for the award of any other academic degree or diploma. Except where otherwise indicated, this thesis is my own work.

Signed



on: 12/06/2018

Acknowledgements

I am grateful to my supervisor, Professor Akhtar Kalam, and my associate supervisor, Adjunct Professor Aladin Zayegh, for the great support they provided me during this research. Without their support and directions, completing this thesis would have been difficult and might have taken a longer time than it should be. In addition, I am also grateful to Elite editing service for assist me to edit this thesis.

Table of Contents

Abstract	i
Master by Research Declaration	ii
Acknowledgements	iii
Table of Contents	iv
List of Tables	vii
List of Figures	x
List of Abbreviations	xiii
List of Publications	xv
Chapter 1: Thesis Overview	1
1.1 Introduction	1
1.2 Building Energy Rating Scheme	1
1.3 Building Element Energy Simulation.....	2
1.4 Building Integration with Modern Technology.....	2
1.5 History of Intelligent/Smart Building.....	3
1.6 Building Energy Simulation Progress	3
1.7 Intelligent Building Acceptance	4
1.8 Modelling and Designing of Sustainable Green Buildings	4
1.9 Greenhouse Gas Emissions	4
1.10 Renewable Energy Efficiency	5
1.11 Comprehensive Building Energy Simulation	6
1.12 Thesis Structure	6
1.13 Conclusion.....	8
Chapter 2: Literature Review	9
2.1 Introduction	9
2.2 Building Contribution to Greenhouse Gas Emissions.....	9
2.3 Building Energy Simulation History	10
2.4 Sustainable Building Design	10
2.5 Building Energy Usage Reduction	11
2.6 Building Energy Simulation and Analysis	12
2.7 Green Building Growth	13
2.8 Sustainable Building Structural Stability Simulation.....	13
2.9 Building Sustainable Design Covers	14
2.10 Renewable Energy Contribution	15
2.11 Sustainable Building Automation Control System.....	16
2.12 Intelligent Building.....	16
2.13 Sustainable Building Efficiency Achievements Demonstration	17
2.14 Occupant Health Issues in Sustainable Buildings	17
2.15 Conclusion.....	18
Chapter 3: Modelling and Designing of Green Building	19
3.1 Introduction	19
3.2 What Makes a Green Building	20
3.3 Green Building Versus Intelligent Building.....	21

3.4 Green Building Minimum Criteria Objectives	21
3.5 Sustainable Building Energy Efficient System	23
3.6 Conclusion	26
Chapter 4: Building Energy Simulation Heating and Cooling Requirement	27
4.1 Introduction	27
4.2 Building Space Utilisation.....	27
4.3 Space Heating and Cooling Load Calculation.....	29
4.4 Building Space Heating/Cooling Energy Reduction.....	74
4.5 Conclusion	75
Chapter 5: Base Run Building Solar Energy Simulation	76
5.1 Introduction	76
5.2 Building Solar Energy Simulation Process	77
5.3 Single Day Building Energy Solar Simulation.....	77
5.4 Base Run Simulation Parameter Data	78
5.5 Base Run Simulation Building Performance.....	79
5.5.1 Annual energy use intensity	80
5.5.2 Life-cycle energy use	80
5.5.3 Annual potential energy	81
5.5.4 Annual carbon emission	81
5.5.5 Annual energy usage cost.....	82
5.5.6 Annual fuel energy use.....	83
5.5.7 Annual electricity energy use	84
5.5.8 Annual, monthly heating load	85
5.5.9 Annual, monthly cooling load	86
5.5.10 Annual, monthly fuel consumption	88
5.5.11 Annual electricity consumption load.....	88
5.5.12 Annual, monthly peak load demand.....	89
5.6 Base Run Simulation, Weather Files Contribution	90
5.6.1 Regional wind speed distribution	91
5.6.2 Regional wind frequency distribution	92
5.6.3 Annual, monthly and hourly wind frequency distribution	93
5.6.4 Annual, monthly weather file collection data.....	94
5.6.5 Hourly temperature of bins.....	95
5.6.6 Annual, monthly weather file's average diurnal	96
5.6.7 Annual, monthly humidity variation	97
5.7 Base Run Building Energy Simulation Analysis.....	98
5.8 Base Run Water Efficiency	100
5.9 Renewable Energy Simulation	102
5.9.1 PV cell efficiency and performance	103
5.9.2 Extra-terrestrial radiation.....	105
5.9.3 Testing standard of PV cell	105
5.9.4 Generation of PV cell power	105
5.9.5 PV cell simulation	108
5.9.6 PV cell simulation analysis	111
5.9.7 Wind Turbine Description.....	115
5.9.8 Basic wind turbine simulation	116
5.9.9 Maximising wind turbine using power coefficient.....	117
5.9.10 Maximising wind turbine power using tip speed ratio	118
5.9.11 Maximising wind turbine power using optimal torque control	121

5.9.12 Calculation of renewable energy rated power	122
5.10 Conclusion	123
Chapter 6: Alternative Design Building Solar Energy Simulation.....	124
6.1 Introduction	124
6.2 Alternative Design Building Solar Energy Simulation Process	124
6.2.1 Alternative design method, number of run lists	126
6.3 Alternative Design Best Energy Simulation.....	156
6.4 Alternative Design Water Efficiency	161
6.5 Green Building Energy Efficient Achievements	164
6.6 Conclusion	165
Chapter 7: Sustainable Building Achievement	167
7.1 Introduction	167
7.2 Green Building Sustainability	168
7.3 Green Building Stability Simulation	169
7.4 Building Structural View.....	170
7.5 Building Structural Modelling.....	171
7.6 Building Structure Load Cases	172
7.7 Building Structure Load Reaction	174
7.8 Nodal Supporter Load Reactions.....	176
7.9 Structural Building Load Displacement	177
7.10 Force on Building Structure Elements.....	178
7.11 Load Forces in Slab Members	181
7.12 Building Occupant Comfort	187
7.12.1 Occupants' comfort satisfaction	187
7.12.2 Indoor air quality	188
7.12.3 Energy consumption and greenhouse gas emissions calculation	188
7.12.4 Outdoor air quality	189
7.12.5 Environmental comfort stability.....	189
7.13 Building Management Control System	190
7.13.1 AS-Interface network protocol method	190
7.13.2 Reasons to migrate to AS-Interface protocol for building automation	191
7.13.3 AS-Interface network protocol hierarchy	193
7.13.4 AS-Interface network protocol	195
7.13.5 Building internet of things.....	195
7.13.6 Benefit of AS-Interface protocol	196
7.14 Conclusion	198
Chapter 8: Conclusion and Further Research.....	200
8.1 Building Energy Simulation	200
8.2 Choosing Best Energy Simulation Results Package.....	200
8.3 Building Integrating with Renewable Energy	201
8.4 Building Structure Stability	201
8.5 Building Occupant Comfort	201
8.6 Building Management Control System	202
8.7 Further Research Recommendations	202
References.....	204

List of Tables

Table 4.1: Building project summary	30
Table 4.2: Building parameter summary	31
Table 4.3: Building zone summary—default	31
Table 4.4: Building default spaces	33
Table 4.5: Building space summary—1 space.....	34
Table 4.6: Building space summary—2 spaces	35
Table 4.7: Building space summary—4 spaces	36
Table 4.8: Building space summary—5 spaces	38
Table 4.9: Building space summary—6 spaces	39
Table 4.10: Building space summary—7 spaces	40
Table 4.11: Building space summary—8 spaces	41
Table 4.12: Building space summary—9 spaces	42
Table 4.13: Building space summary—13 spaces	44
Table 4.14: Building space summary—14 spaces	45
Table 4.15: Building space summary—15 spaces	46
Table 4.16: Building space summary—16 spaces	47
Table 4.17: Buildings space summary—17 spaces.....	48
Table 4.18: Building space summary—18 spaces	50
Table 4.19: Building space summary—19 spaces	51
Table 4.20: Building space summary—20 spaces	52
Table 4.21: Building space summary—23 spaces	53
Table 4.22: Building space summary—24 spaces	55
Table 4.23: Building space summary—25 spaces	56
Table 4.24: Building space summary—26 spaces	57
Table 4.25: Building space summary—27 spaces	58
Table 4.26: Building space summary—28 spaces	59
Table 4.27: Building space summary—29 spaces	61
Table 4.28: Building space summary—30 spaces	62
Table 4.29: Building space summary—31 spaces	63
Table 4.30: Building space summary—32 spaces	64
Table 4.31: Building space summary—33 spaces	65

Table 4.32: Building space summary—34 spaces	67
Table 4.33: Building space summary—35 spaces	68
Table 4.34: Building space summary—36 spaces	69
Table 4.35: Building space summary—37 spaces	70
Table 4.36: Building space summary—39 spaces	71
Table 4.37: Building space summary—40 spaces	73
Table 5.1: Base run building performance	80
Table 5.2: Annual energy use intensity	80
Table 5.3: Energy life-cycle use	81
Table 5.4: Annual estimated potential energy	81
Table 5.5: Base run solar building energy simulation result	100
Table 5.6: Base run solar building energy simulation water usage results	102
Table 5.7: PV cell parameters, performance during morning hours	112
Table 5.8: PV cell parameter, performance during midday hours.....	113
Table 5.9: PV cell input parameters, performance during afternoon hours	114
Table 5.10: Wind turbine maximum power extraction	118
Table 5.11: Wind turbine optimum TSR.....	120
Table 6.1: Alternative design, energy simulation package result list number 1.....	128
Table 6.2: Alternative design, energy simulation package result list number 2.....	130
Table 6.3: Alternative design, energy simulation package result list number 3.....	132
Table 6.4: Alternative design, energy simulation package result list number 4.....	134
Table 6.5: Alternative design, energy simulation package result list number 5.....	136
Table 6.6: Alternative design, energy simulation package result list number 6.....	138
Table 6.7: Alternative design, energy simulation package result list number 7.....	140
Table 6.8: Alternative design, energy simulation package result list number 8.....	142
Table 6.9: Alternative design, energy simulation package result list number 9.....	144
Table 6.10: Alternative design, energy simulation package result list number 10.....	146
Table 6.11: Alternative design, energy simulation package result list number 11.....	148
Table 6.12: Alternative design, energy simulation package result list number 12.....	150
Table 6.13: Alternative design, energy simulation package result list number 13.....	152
Table 6.14: Alternative design, energy simulation package result list number 14.....	154
Table 6.15: Alternative design, best energy simulation package result	159
Table 6.16: Alternative design, water usage improved efficiency	163
Table 6.17: Alternative design, water usage, approaching NetZero savings	164

Table 6.18: Base run simulation annual total energy result	165
Table 6.19: HVACTYPE_ASHRAE Package Terminal Heat Pump.....	165
Table 7.1: Building structure acting load	174
Table 7.2: Building structure acting load combinations.....	174
Table 7.3: Building structure load reaction	176
Table 7.4: Building structure load reaction cases.....	176
Table 7.5: Building structure load displacement	178
Table 7.6: Building structure force in column members	180
Table 7.7: Force in beam members	181

List of Figures

Figure 3.1: Architectural building structure of a five-storey commercial office building.....	20
Figure 3.2: Green building minimum objectives criteria	23
Figure 3.3: Green building design energy simulation process flow chart.....	25
Figure 4.1: Segregated space heating/cooling	28
Figure 4.2: Building space heating/cooling load calculation image.....	30
Figure 5.1: Base run building solar energy simulation.....	78
Figure 5.2: Annual carbon emission and net CO ₂ calculations	82
Figure 5.3: Annual energy usage cost	83
Figure 5.4: Annual fuel energy use	84
Figure 5.5: HVAC, lighting and other equipment annual energy usage	85
Figure 5.6: Annual energy usage, monthly heating load.....	86
Figure 5.7: Annual energy usage, monthly cooling load.....	87
Figure 5.8: Annual fuel consumption	88
Figure 5.9: Annual, monthly electricity consumption.....	89
Figure 5.10: Annual, monthly electricity energy peak demand	90
Figure 5.11: Weather files, regional wind speed distribution.....	92
Figure 5.12: Weather files, regional wind frequency distribution.....	93
Figure 5.13: Annual, monthly and hourly regional wind frequency distribution.....	94
Figure 5.14: Weather files, annual, monthly design data	95
Figure 5.15: Weather files, hourly temperature of bins.....	96
Figure 5.16: Annual, monthly diurnal average weather files	97
Figure 5.17: Annual, monthly humidity weather files, daily variations.....	98
Figure 5.18: PV cell characteristics	107
Figure 5.19: PV cell panel, sunlight effect influence	111
Figure 5.20: PV cell parameter respond performance during morning hours	112
Figure 5.21: PV cell parameter respond performance during midday hours.....	113
Figure 5.22: PV cell parameter respond performance during evening hours.....	114
Figure 5.23: PV cell panel, aligning with the Sun direction, configuring software tools	115
Figure 5.24: Wind turbine design for optimum performance.....	116

Figure 5.25: Wind turbine maximum power extraction	118
Figure 5.26: Wind turbine optimum TSR extraction.....	121
Figure 6.1: Whole building elements, solar building energy simulation.....	126
Figure 6.2: Best solar building energy simulation result chart 1	129
Figure 6.3: Best solar building energy simulation result chart 2.....	131
Figure 6.4: Best solar building energy simulation result chart 3.....	133
Figure 6.5: Best solar building energy simulation result chart 4.....	135
Figure 6.6: Best solar building energy simulation result chart 5.....	137
Figure 6.7: Best solar building energy simulation result chart 6.....	139
Figure 6.8: Best solar building energy simulation result chart 7.....	141
Figure 6.9: Best solar building energy simulation result chart 8.....	143
Figure 6.10: Best solar building energy simulation result chart 9.....	145
Figure 6.11: Best solar building energy simulation result chart 10.....	147
Figure 6.12: Best solar building energy simulation result chart 11	149
Figure 6.13: Best solar building energy simulation result chart 12.....	151
Figure 6.14: Best solar building energy simulation result chart 13.....	153
Figure 6.15: Best solar building energy simulation result chart 14.....	155
Figure 6.16: Base run energy simulation, energy end use result.....	160
Figure 6.17: Best simulation package, energy end use result.....	160
Figure 6.18 Building energy simulation, annual energy intensity result chart.....	161
Figure 7.1: Building structure internal & external force stability simulation	170
Figure 7.2: Building structure view	171
Figure 7.3: Model of building structural view.....	172
Figure 7.4: Building structure elements load supporter reaction view	175
Figure 7.5: Building structure load nodal supports	177
Figure 7.6: Building structure maximum load displacement	178
Figure 7.7: Maximum force in column members	180
Figure 7.8: Maximum force in beam members	181
Figure 7.9: View of Building structure slab load	182
Figure 7.10: Building structure slab with maximum load and directions	183
Figure 7.11: Building structure minimum force in slabs.....	183
Figure 7.12: Building structure minimum slab's loads and directions.....	184
Figure 7.13: Building structure with maximum of MYY slab loads.....	184
Figure 7.14: Building structure load case slab loads automatic direction.....	185

Figure 7.15: Building structure with minimum force in slabs.....	185
Figure 7.16: Building structure minimum slab loads with automatic direction	186
Figure 7.17: Building structure slab loads with maximum displacement	186
Figure 7.18: Slab load case with directions	187
Figure 7.19: AS-Interface network protocol wiring method	193
Figure 7.20: AS-Interface network protocol configuration method	194
Figure 7.21: AS-Interface network protocol influence factors & response.....	197
Figure 7.22: Benefit of AS-Interface protocol wiring configuration	198

List of Abbreviations

AS	Actuator Sensor
ASHRAE:	American Society for Heating, Refrigerating and Air-conditioning Engineers
BAS	Building Automation System
BAC:	Building Automation Control
BACS:	Building Automation Control System
BCA:	Building Code Australia
BEM:	Building Energy Modelling
BEMS:	Building Energy Management System
BIM:	Building Information and Modelling
BIOT:	Building Internet of Things
BMS	Building Management System
BREEAM:	Building Research Establishment Environmental Assessment Method
C/B:	Circuit Breaker
CAD:	Computer-aided Design
CO ₂ :	Carbon Dioxide
DCS:	Decentralised Control System
DHI:	Direct Horizontal Irradiation
DNI:	Direct Normal Irradiation
DOE:	US Department of Energy
EEB:	Energy Efficient Building
ETR:	Effective Tracking Range
EUI:	Energy Use Intensity
GB:	Green Building
GBAC:	Green Building Australian Council
GBIS:	Green Building Information System
GBS:	Green Building Studio
gbXML:	green building Extensible Text Mark-up Language
GHI:	Global Horizontal Irradiation
HMI:	Human Machine Interface

HVAC:	Heating, Ventilation and Air Conditioning
IAQ:	Indoor Air Quality
IB:	Intelligent Building
IGB:	Intelligent Green Building
IOT:	Internet of Things
IP:	Internet Protocol
LEED AP:	LEED Accredited Professional (AP)
LEED:	Leadership in Engineering and Environmental Design
MFP:	Model Free Predictive
MPPT:	Maximum Power Point Tracking
MXX:	Maximum Horizontal Force
MYV:	Maximum Vertical Force
NCC:	National Building Code
NNE:	North, North-East
NWN:	North-West, North
OLE:	Object Linking & Embedding
OPC:	Object Process Control
OTC:	Optimum Torque Control
PC:	Personal Computer
PV	Photovoltaic
PI:	PROFIBUS International
PMV:	Predictive Mean Value
RCC:	Reinforced Cement Concrete
RF:	Radio Frequency
R-value:	Insulation measurement value
SSW:	South, South-West
SW:	South-West
Tdb:	Dry-bulb Temperature
TSR:	Tip Speed Ratio
Twb:	Wet-bulb Temperature
WWR:	Wall-to-Window Ratio

List of Publications

- [1] B. Gebreslassie, A. Kalam, and A. Zayegh, "Energy saving, in commercial building by improving photovoltaic cell efficiency," in *2017 Australasian Universities Power Engineering Conference (AUPEC)*, 2017, pp. 1-6.
- [2] B. Gebreslassie, A. Zayegh, and A. Kalam, "Design, modeling of an intelligent green building using, actuator sensor interface network protocol," in *2017 Australasian Universities Power Engineering Conference (AUPEC)*, 2017, pp. 1-6.
- [3] B. Gebreslassie, "Design and Modeling of a Green Building Energy Efficient System T2 - World Academy of Science, Engineering and Technology, International Science Index, Energy and Power Engineering," vol. 12(2), pp. 1600-1600, 12/ 2018.
- [4] B. Gebreslassie "Design and modelling of an intelligent commercial building energy efficient system," Science Direct: Engineering, Science and Technology an International. Status: submitted.

Chapter 1: Thesis Overview

1.1 Introduction

Green building (GB) is also known as energy efficient construction. After the oil crisis that commenced in 1973–1974 [1], government institutions and private companies started searching for alternative methods for using their existing energy resources wisely and minimising unnecessary use. This opportunity led to the development of a wide range of energy research practices and simulations to reduce energy consumption in buildings. Current GB research shows that traditional/conventional buildings waste a huge amount of energy and produce the highest level of carbon dioxide (CO₂) emissions among the building industries. In addition, these studies have also identified the three highest contributors to greenhouse gas emissions: manufacturing industries, transportation and buildings [2]. In this regard, traditional/conventional buildings contribute up to 43% of the total global greenhouse gas emissions. The solutions to address this significant negative impact from the building sector is to implement GB globally as fast as possible as well as define GB and its objectives [3].

1.2 Building Energy Rating Scheme

Implementations of GB are classified according to the building energy rating values. GB is commissioned to comply with the energy rating credit point system designed by the accreditation authorities of countries. For example in Australia, Australia Green Building Council (AGBC), in the United States, Leadership in Energy and Environmental Design (LEED), in Hong Kong, Hong Kong Green Building Council, in China, GB Evolution Standard, in Finland, Green Building Council Finland, in Germany, German Sustainable Building Council, in India, Green Rating for Integrated Habitant Assessment and Indian Green Building Council, in the United Kingdom, Building Research Establishment Environmental Assessment Method (BREEAM); and in Qatar, Qatar Sustainability Assessment System. In addition, GB rating codes also differ from each country's credential authority codes; for example, AGBC uses Design as Built, star rating system and LEED uses LEED Accredited Professional (AP).

1.3 Building Element Energy Simulation

This research project focuses on investigating the extent of energy reduction possible on using comprehensive energy-saving methods on commercial office buildings. To this end, every particular building element and material used for construction of the building was simulated to identify energy wastage. For example, the orientation of windows and doors and types of building materials used have significant effect on energy consumption. In addition, massive concrete walls are used mainly for commercial buildings, because of their ability to provide significant building envelopes as a primary function. Moreover, such walls also play a major role in heating/cooling zones, owing to their natural thermal mass property, which enables building materials to absorb, store and later release heat [4]. These materials have a natural behaviour of absorbing energy slowly and retaining it for longer periods of time. This delayed response reduces heat transfer through thermal mass and shifts energy demand to off-peak time. Hence, energy is saved when reversal in heat flow occurs within walls. Since mass and heat flow play major roles to balance temperature fluctuations, significant energy is also saved during this period. Further, the window-to-wall ratio (WWR) also plays a major role in ensuring energy saving. Higher WWR in winter can let additional light into the building and also facilitate significant heat loss during summer [5]. In addition, windows and doors contribute a large part of the exterior building envelopes and have a major impact on human activities inside the building and also on energy use. Sustainable window design maximises the benefits of daylight while minimising energy use. Sustainable GB design and its objective goals are expected to provide 80% [6] of interior lighting through natural light as well as provide adequate natural ventilation by minimise/maximise windows size.

1.4 Building Integration with Modern Technology

Intelligent building (IB) is also known as sustainable intelligent green building (IGB) [7]. It usually involves constructing a new building or upgrading a conventional building. IGB implements sophisticated automated building control system programs using two or more of the following devices: personal computer (PC), programmable logic controller (PLC), distributed control system (DCS), object linked & embedding (OLE), object process control (OPC), human machine interface (HMI) or supervisor

control and data acquisition (SCADA) [8-10]. A highly sophisticated building automation program can save a significant amount of energy.

1.5 History of Intelligent/Smart Building

Historically, the term IB was adopted in the early 1980s from among the many competing names proposed and the term IBG is widely used instead. In Europe, the European IB Group coined a new definition stating it is an IB. In Asia, the definitions focused on the role of technology for building automation and control of building functions. In the late 1990s and early 2000s, with the introduction of the BREEAM codes and LEED programs, the IB spotlight tilted towards energy efficiency and sustainability. More recent definitions have commenced to consider elements such as the emerging Building Internet of Things (BIOT) technologies. An internet protocol (IP) network computer software application program connects all the building services to control, monitor and analyse any defects without human intervention. At present, major shifts are also occurring in the way that buildings are designed, operated and used. An energy efficient building leverages a state-of-the-art connectivity platform to address key corporate of building facilities and information technology. Its challenges are mainly to improve energy efficiency, space utilisation and occupant satisfaction.

1.6 Building Energy Simulation Progress

In addition to the above, the term IB commenced attracting increasing attention a few decades previously [11], when an energy crisis, in particular, the rising cost of fossil fuels, created economic instabilities globally and especially in the United States. Then, government institutions, industries, companies and nongovernment companies started to realise that in certain areas, energy was being wasted. This crisis was an opportunity for energy researchers, energy consultants, construction contractors and owners of companies to focus on three main energy consumers, Industries, Transportation and conventional buildings, as aforementioned. Since then, building energy-saving technology has grown rapidly from introducing simple automatic light control ON/OFF application to fully automated building control systems, such as the building automation system (BAS), building management system (BMS), building energy management system (BEMS) and building automation control system (BACS) [8]. These systems are just a few examples, and in reality, more advanced systems have been developed.

Further, building technology has gone beyond the scope of building automation with the help of BIOT and smart grid supply and currently focuses on an occupant density-centred approach to build smart cities [12], as well as a smart way of living.

1.7 Intelligent Building Acceptance

Following popular acceptance of IGB, the term IB emerged from conventional building in the early 1980s [13, 14] and the term GB dominates at present. In addition, GB appears in relation to saving energy and reducing greenhouse gas emissions [3, 7]. Moreover, GB is enhanced by green economy.

1.8 Modelling and Designing of Sustainable Green Buildings

Designing and modelling of sustainable GB, which satisfies the entire requirement or the scope and the objective of GB, is a very complex process that requires many collective bodies' efforts and economic achievements. However, an opportunity exists to design and model GB using cost-effective, modern, reliable, industry-proven technologies, such as the 'Actuator Sensor- (AS) Interface network protocol', which is now used by many industries to reduce the number of used parts, saving space as well as installation cost. Utilising this type of technology in building sector will improve the impact of energy consumption by the building and satisfies the scope and the objective of GB through reduced costs. In this research, the main aim is to model and design a smart commercial office building, using the most advanced technology, which would result in GB that is truly an energy efficient building (EEB).

1.9 Greenhouse Gas Emissions

Fossil oils produce CO₂, methane, nitrous oxide and fluorinated gases, and these chemicals have been found to be extremely dangerous, causing global climate change [15-17]. Although the benefit of fossil fuels is significant and crucial, it is necessary to cease using these gradually and replace these with renewable energy sources, which do not cause any adverse environmental effects.

1.10 Renewable Energy Efficiency

Energy efficiency in particular is the main issue related to the use of renewable energy since these have very low efficiency, except for hydropower [18-20]. Thus, even though significant effort has been made in the past and is still ongoing to improve the efficiency/performance of renewable energy sources, the results are not satisfactory especially as regards photovoltaic (PV) cell efficiency. For example, several studies have proposed different techniques to increase the efficiency of PV cells. The most used method is selecting highly efficient and suitable PV cell material, such as organic-metal halide perovskite, with improved sizing parameters that provide an efficiency up to 27.5% [21]. Another method is using PV cell material with a higher absorption coefficient to absorb more photons, because such materials absorb excess photons and excite more electrons to the conduction band. In this method, the absorption coefficient determines how far light of a particular wavelength can penetrate into a material before being absorbed [22]. In addition to these methods, the study of carrier multiplication absorbers based on semiconductor quantum dot increased PV cell efficiency up to 47.7% [23]. Another expensive method is using a concentrated incident light several times higher than the standard to increase the PV cell open voltage [24]. In addition, the maximum power point tracking (MPPT), model free predictive (MFP) and the model-based calibration approaching systems methods [25, 26] are three proven techniques that significantly improve PV cell efficiency. The MPPT method evolved and implements the concept of Perturb & Observe and is widely adapted by cutting-edge solar energy output efficiency researchers owing to its proven capability of optimising output power [25-28]. The MFP method uses the concept of a predefined solar system based on a Sun ephemeris orientation system using a stored algorithm. This type of technique predicts and implements astronomers' knowledge to track the Sun's position in the sky relative to the Earth's orbital position using pure software [26]. Conversely, the model-based calibrated approach is pure practical information collected from highly accurate intelligent fine sensors that calibrate to provide almost zero-tolerance measurements of the Sun's orientation position in the sky. The actual measured information is compared with the MFP-stored information obtained on basis of the concept of the Sun ephemeris system. In this method, the error or the feedback information is noticed as environmental affects [26]. Prediction of maximum output of the PV cell is also widely implemented using the I-V characteristic optimisation method

to obtain the desired result either by analytical invertible function or numerical technique approaches [29]. However, all these methods use complex mechanisms and techniques and implementing their actual process is time-consuming and very costly. This research thesis project develops an alternative method to ease the process of increasing the PV cell efficiency and also to reduce costs. In this method, the PV cells are designed and modelled using simulation software applications (Autodesk Revit and Dynamo) and the results are analysed to satisfy the target of PV efficiency.

1.11 Comprehensive Building Energy Simulation

This research is modelled and designed for minimum energy use in commercial building by applying comprehensive energy simulation possibilities, using computer software applications energy analysis, Autodesk Revit and Dynamo (script programming language) interfacing each other on the project design parameters. Hence, this research project uses the following steps to succeed its goals: (1) multilevel hexagonal-curve shape building design is drawn. (2) Energy analyses setting specifications, such as space/room, type of building and geographical location, are configured. (3) Weather files from the nearest weather station are loaded. (4) Base run (primary run) energy analysis is conducted. (5) Further, the Building Information Modelling (BIM), green building Extensible Mark-Up Language (gbXML) engineering information data are exported to Green Building Studio (GBS) for multiple alternative designs and for further energy simulation analysis. This approach was adopted to achieve the most comprehensive/optimum energy consumption reduction.

1.12 Thesis Structure

The contents of this thesis are presented in eight chapters and the thesis is structured according to the chapter's contribution to the research study.

Chapter 2

This chapter presents and emphasises a literature review of conventional/traditional buildings versus GB as the main topic. The history of GB, especially how the name GB was adopted, is briefly addressed. In addition, methods of building solar energy simulations with different simulation software applications are also briefly discussed. Further, BACS using different methods and configurations are also briefly discussed. Hence, the topics covered in this chapter are used to construct this thesis project.

Chapter 3

This chapter discusses the GB design process. The process is supported by procedures, and the procedures include flow charts, steps, tables and figures. These procedures are implemented in this chapter to explain how the design of GB is based on cost-effective economically achievable design methods.

Chapter 4

This chapter covers the pre-base run energy simulation, which focuses only on heating/cooling primary calculation results of building spaces. In this simulation, preliminary heating/cooling simulation results per segregated space of the building are obtained. Hence, this chapter considers a prerequisite simulation to the base run simulation.

Chapter 5

This chapter covers the first/primary (base run) building solar energy simulation, which is the basic simulation part in this research and introductory simulation to the alternative design energy simulation. Hence, the simulation results obtained from this chapter do not reflect significant energy reduction. These results help to compare with the alternative design simulation result, and also act as a reference point. In addition, it also covers the use and contribution of renewable energy in GB design, in relation to the building being energy efficient. In this chapter, PV cell and wind turbine efficiency and performance are maximised using cost-effective techniques and methods.

Chapter 6

This chapter covers the main part of this research project. It is the alternative design part of the building solar energy simulation and concludes this research simulation process by achieving significant results. In this chapter, the construction elements of the whole building are simulated for their energy efficient capabilities by automatically changing the construction elements for different options of design called 'alternative design methods'. Hence, the results presented in this chapter are compared with these of the previous simulations to choose the best energy reduction simulation results. Among 254 alternative design runs, energy package lists conducted, one energy package list was found the best, with substantial reduced energy results.

Chapter 7

This chapter covers three main topics

GB structural stability simulation: This section covers building structural stability in terms of the building being physically stable during internal and external environmental incidents. Hence, the aim of this simulation is to detect defects in any structural elements prior to commencing practical work.

Building occupant comfortableness: This section explains briefly the GB capability of responding to occupants according to their desired interests by providing not only thermal comfort but also intelligently acting and responding to their activities. In this section, indoor/outdoor air quality is briefly discussed.

Building automation control system: This section covers the BACS and explains the introduction of a modern cost-effective control method, ‘AS-Interface network protocol’, aiming to replace the current BACS, which is categorised in this research thesis project as non-cost-effective methods. In this section, the benefit of the ‘AS-Interface network protocol’ is discussed in depth.

Chapter 8

This chapter presents the main conclusion of this research thesis project and discusses the contribution and the achievements of this thesis in terms of buildings’ energy efficiency briefly. It also provides directions and recommendations for further studies.

1.13 Conclusion

This chapter covers the main introductory information in relation to this research thesis project topic. It describes the formation or evolution of GB in brief as well as the main contents of this thesis, such as the type of methods used, building solar energy simulation process, implementation of renewable energy sources and the method to optimise their efficiency/ performance.

In addition, building stability simulation, occupant comfort and the building automation control method used are also discussed.

Chapter 2: Literature Review

2.1 Introduction

Green building (GB) is also known as green construction or sustainable building, which refers to building structures in which intelligent electrical, electronic and electromechanical devices are in use. These smart devices sense and control the occupants' activities and excess energy use as well as monitor the building in terms of security [30]. Moreover, GB practice expands and complements the classical building design by addressing issues related to economy, utility, durability and comfort. New technologies are constantly being developed to complement current practices in creating greener structures. The common objective is to ensure that the GB is designed to reduce the overall impact of the building environment on human health and the natural environment by efficiently using all types of available energy resources, thus protecting occupant health, increasing occupant comfort, improving productivity, reducing waste or pollution as well as preventing environmental degradation.

2.2 Building Contribution to Greenhouse Gas Emissions

Buildings have been designed and modelled traditionally for years, without consideration or notice of their negative impact with respect to global CO₂ emissions as well as their lack of energy efficiency contribution. Conventional buildings, regardless of their attractive structural or masonry designs, waste significant amounts of energy. Hence, conventional buildings are among the highest energy consumers and also among the highest contributors to greenhouse gas emissions, accounting for approximately 40% and 33% of CO₂ emissions produced by developed countries and the rest of the world respectively. This situation persists despite the US Government spending approximately US\$1 trillion per year on construction, renovation and operation of buildings [31]. In addition, US buildings are the largest energy consumers of energy worldwide and consume 71% of the electricity and 54% of the natural gas the country produces annually. Hence, the US Army spends more than US\$1 billion dollars on building energy bills to reduce energy consumption in buildings. As a consequence, the US Army aims to achieve buildings energy efficiency of between 25 to 30% by 2023

and net zero building energy efficiency by 2058 [32]. This is the best initiative taken by the US Army in this regard.

2.3 Building Energy Simulation History

Building energy simulation with a specific focus on GB simulation was started by US Department of Energy (DOE) in consultation with industries and universities after the oil crisis commenced during 1973–1974. The oil crisis led to energy shortfall in the country and resulted in significant negative effects on the US economy; however, the simulation conducted at that time was merely to control nothing more than a room temperature. After 1990, PC-based simulation software applications rapidly developed to the point that a graphical user interface could significantly help in simulations and was quicker than other methods [31]. Energy sustainability can also be defined as meeting the needs of the present generation without comprising the ability of future generations to meet their needs. Some green construction building programs do not address the issue of retrofitting of existing buildings, unlike others. Green construction principles can easily be applied to retrofit work as well as new construction. Thus, the advantage of GB over conventional building is also significant; an experimental report released by the US general services administration in 2009 found 12 sustainably designed buildings cost less to operate and had excellent energy performance. In addition, occupants were more satisfied with the overall building than those in conventional commercial buildings. Thus, conventional buildings waste a huge quantity of energy and generate significant quantity of CO₂, which in turn accounts for a large volume of carbon emissions [33] and decrease occupants' quality of life, and increase costs.

2.4 Sustainable Building Design

For GB, a close integration of building systems, with special focus on energy saving, is one of the required criteria. Thus, using design process modelling, visualisation of tools, material analysis and effective team work make a significant contribution to the design of sustainable GB. Hence, high-performance green buildings can be achieved, which will reduce energy consumption and improve peoples' health, their lifestyles and their comfort [34] in general. To achieve this, the most useful tool currently used by many companies is BIM [35]. Hence, as BIM has become popular, there is an urgent need in

the market for green construction simulation and modelling using BIM. However, the current GB construction software simulation application has limited services and requires an updated or new construction software simulation program that will solve the time management difficulties in interoperability with BIM [36]. Facility engineers, managers and building designers are increasingly concerned that modelling and simulation analysis of the EEB process is time and labour-consuming. Hence, efforts on how to improve the energy efficiency modelling process are also increasing to develop cost-effective useful software program tools [34, 37]. Although building simulation and modelling prior to making a decision to build are necessary to achieve the desired high energy efficiency, the current simulation software available is not sufficiently intelligent [38] to make significant changes.

2.5 Building Energy Usage Reduction

Building accounts for 27–40% of electrical usage. On designing GB exterior walls using steel studs by applying energy efficient methods per the global building standard as well as by applying similar methods when installing electrical devices and appliances, 27% energy efficiency can be achieved. Similarly, energy reduction can be obtained when a thermal wall insulation system calculates the R-values, in which the larger the value is, the less is the heat flow. Conversely, a smaller R-value implies better thermal continuous insulation [39]. Thus, the use of steel exterior studs has produced highly significant improvements in temperature and also improves energy consumption in buildings by minimising thermal bridging through the steel studs. This improves the performance of insulation, moderating wall cavity temperature, lessening condensation within the wall cavity and decreasing heating/cooling use [39]. Moreover, GB will be more efficient if the predesign model formation satisfies the eco-charrette goal [40]. An eco-charrette, also known as the kick-off meeting, is an interactive brainstorming and team-building exercise that generates and targets sustainability goals for a GB. It brings together members of the design team, the owner, architect, civil engineer, mechanical engineer and landscape designer with the general contractor, maintenance staff, tenants, neighbours and concerned officials. The aim is to collaboratively contribute ideas to the building's design and functions [40]. Eco-charrettes are becoming a common element in the design of high-performance buildings and have been used successfully on some of

the most progressive US buildings [40]. Hence, GB predesign is the smart way of achieving the goal of an EEB. Thus, one of the predesign works is simulation.

2.6 Building Energy Simulation and Analysis

GB energy analysis simulation software uses BIM as the source of engineering data information, to achieve high performance of GB predesign objectives [41]. Since 1990, many software companies have developed their own unique software simulation packages; however, each package has its advantages and disadvantages. Some packages have good functionality but poor interfaces, while others have brilliant interfaces and limited functionality. Effective use depends on the aim of using the software and whether users have the skills and the knowledge to implement the software. eQUEST is a part of the energy design resources supported and funded by California utility customers and administrated by three utility companies; it is the quickest and most comprehensive building graphical analysis energy simulation tool and consists of enhanced DOE-2 + Wizard + Graphics. Modelling and simulation of GB using eQUEST is simple, easy and straightforward and does not require drawing the model manually—the model is automatically drawn as the user enters the required parameter inputs. This is the reason eQUEST is widely used in the United States; however, to use it outside the United States and Canada, the user has to provide weather data manually from the building location [36, 40]. Bentley AECOSim Building Designer, Bentley Building Mechanical/Electrical System and Bentley Speedikon Architectural are building modelling and energy analysis simulation application software. Thus, these three similar simulation software packages are fast, powerful modern advanced technology, integrated BIM applications for micro station and computer-aided design (CAD) applications. Similar software is the Nemetschek-Vectorworks Architecture, which is used for various types of world-class building modelling design and energy efficiency analyses. This software has the robust and flexible capability of BIM with ease of design, intelligence tools, greater documentation and direct support for exporting gbXML format BIM data to a wide variety of energy efficient analysis simulation application software. Similarly, GBS is known worldwide as a single web-based energy efficient analysis service software application. It can be integrated with existing 3D CAD/BIM software tools [36]. Design Builder is known as the state-of-the-art software application mostly used for checking building energy, CO₂, lighting and

comfort performance. This software has been designed to ease the process of building modelling and simulation; in addition, Design Builder allows users fast comparability function tools to deliver results on time and on budget [36, 42]. Solar computer, also known as green building information system (GBIS), is a CAD application with the functionality of bidirectional gbXML and is mostly used for energy analysis of heating, ventilation and air conditioning (HVAC) load. GBIS enhances the gbXML file CAD data; this enables GBIS to be a very detailed building model, which sets it apart from similar software [36]. Autodesk Ecotect Analysis is the most sustainable modelling design energy analysis application compared with similar software. Ecotect analysis offer a wide range functionality of simulation tools that enables the user to improve performance of existing building and new building designs [36]. However, Ecotect software has not been updated for many years and is being overtaken by other similar powerful modern software.

2.7 Green Building Growth

During the past decade, commercial GB has rapidly increased. However, this rapid growth is not supported by all types of buildings; there has been non-uniform growth in all or most of types of buildings. Although the debate on what GB should include and exclude is inconclusive [43], an important measure of energy efficiency GB is the overall thermal transfer value, which plays significant role in reducing energy usage. This has been widely adapted by many countries for enhancing energy efficient GB designs. Hence, it is showing remarkably increased use since the past decade; however, because building evaluation is performed based on the bare of tradition building, GB designers are currently facing difficulties [44]. Hence, GB designers and researchers in this field are currently seeking ways to minimise these difficulties.

2.8 Sustainable Building Structural Stability Simulation

Building stability simulation is out of the scope of this research. However, the aim of this thesis is to achieve ultimate energy saving (to reach almost NetZero energy reductions in commercial building), and hence, when a commercial building theoretically becomes stable as regards energy consumption, it must also be physically and structurally stable. Such stability is required to ensure occupants of the building not only feel safe and secure in terms of energy consumption as well security, but also in

terms of the building's physical firmness and safety, leading to building occupants' comfort satisfaction achievement. Owing to these reasons, building structural stability simulation was carried out prior to energy simulation. The generated report indicates the defects of the building elements and where these defective elements should be subject to adjustments prior to commencing practical work.

2.9 Building Sustainable Design Covers

Energy efficiency and sustainable GB designs are features for new/existing buildings and have become the top priorities for GB developers and researchers since the 1970s [1]. Analysis of correlation of BIM data using data mining technology management system is necessary to simplify the GB designer's process, and hence to develop optimum energy efficiency and sustainable buildings [45]. Sustainable building design concepts are likely to create capabilities to enhance building performance, increase energy efficiency, reduce operating costs and hence also encourage green economy investors [46]. Any type of building sustainability is a worldwide challenging issue, especially, for example, for GB designers of smart/intelligent buildings and city/urban planners, including policymakers [35]. Sustainable building is not only sustainable in term of its building erection and being strong against environmental forces. In addition, it is also sustainable in terms of minimised energy use within the buildings. This is considered an effort to reduce and/or to eliminate unnecessary energy usages in buildings globally.

In the United States alone, conventional buildings use one-third of the total amount of energy generated and are responsible for 50% of greenhouse gas emissions [1, 47]. Thus, the consequences of unnecessary energy usage are an energy impact, a crisis and a shortage of energy supply in some sectors. Hence, a global trend to save energy exists and it has become the main priority for public and private sectors since the oil crisis. At present, intelligent GB is progressing towards NetZero energy [48], especially those buildings integrated with the improved efficiency of renewable energy sources. In intelligent GB, PV cells and wind turbines are mainly used owing to their energy efficiency and PV cells are, in particular the most commonly used in GB. This is because of their tendency to increase their efficiencies using different types of techniques. For example, one proven type of technique is which the PV cell is mainly fitted with an automatic 180 degrees (azimuth angle) sunlight incident irradiation ray

tracking mechanism to help to increase its efficiency from a basic 5 to 15%, to an average of 39% to 42%. This is practically proven technology, in countries that mostly have a cold climate, and 8% increase has been reported in the hottest climate regions [49-51] of the world.

2.10 Renewable Energy Contribution

Renewable energies are sustainable sources of energy efficiency in buildings. However, the most important concern globally is the increase in CO₂ by 25–30% over the past century. Climate experts are extremely worried about the amount and the rate of change of CO₂ in the atmospheric levels and hence the amount of carbon in biomass [52]. The literature on green energy that considers post occupancy on energy consumption is yet to arrive at a conclusion on green energy efficiency; debates concerning the research results on dry and cool simulations are ongoing. There is also ongoing disagreement on accepting a geographic atmospheric concentration for hot and dry climates. The results of LEED-based GB simulation conducted in Arizona are not satisfactory [53]. Hence, in designing for the ultimate EEB, strong computer-aided simulation is required. This is to simulate the whole building for energy efficiency. This can be performed by considering the solar thermal mass for cost-effective daylight savings, using all types of renewable energy sources and applying natural ventilation methods. In addition, commercial GB should be implemented with maximum types of renewable energy regardless of their minor negative effects, such as the commercial wind turbine that could be located on the roof or in the building compound. The wind turbine technology developed since the late 1970s by pioneers in Denmark was widely used from the 1980s to 1990s and was the base of wind energy expansion in countries such as Spain, Denmark and Germany during the 1990s [54]. The first fixed speed wind turbines were designed and constructed under the concept of reusing many electrical and mechanical components. The main concepts related to this technology are as follows: The fixed speed is related to the fact that an asynchronous machine coupled to a fixed frequency electrical network rotates at a qualified mechanical speed independent of the wind speed. Wind turbine is not considered low or high efficiency; its maximum efficiency is governed by the Betz Limit, an equation that proves solid efficiency of 59.26% [55] and its performance in maximising the output power is categorised by three main methods, namely, using the (1) power coefficient [55], (2) tip speed ratio (TSR) [56] and (3)

optimum torque control (OTC) technique [57]. There are many other emerging renewable energies but their discussion is excluded in this thesis because the simulation software used to simulate the energy analysis for this thesis project did not include these in the simulation result report.

2.11 Sustainable Building Automation Control System

As regards GB designs, the early stages of GB were implemented with basic BACS or BMS to control the activities of the electrical/electronic components and pneumatic and hydraulic machinery equipment to energise/de-energise at the demand time only. A control system such as this proven to ensure significant energy reduction and substantial energy saving in kilowatt-hours (kWh), and when off-peak usages are implemented in the computer program saving can be increased up to 30-35%. Currently, many building energy reduction application tools are in use. For example, in an automatic control system for building, using predicted mean vote reduced the energy usage by around 30% [58].

2.12 Intelligent Building

Further, in the history of GB, the term IB appeared a few decades ago [11], when an energy crisis, namely the high cost of fossil fuels, created economic instabilities globally and in the United States in particular. Then, government institutions, industries, companies and nongovernment companies started to realise that energy was being wasted in certain areas. Thus, opportunities were created for energy researchers, energy consultants, construction contractors and owners of companies to focus on mainly the three highest energy consumers. They found that the highest energy consumers are Industries, Transportation and traditional buildings. This led to the emergence of building energy-saving technologies, starting from simple automatic lighting control ON/OFF application. After a transition period in the early design stage of GB, these technologies rapidly developed from smart homes and buildings to fully automated building control systems, such as the intelligent BAS, BMS, BEMS and BACS [8]. At present, building using modern technology has gone beyond the scope of BAS, with the help of the internet of things (IOT) and ancillary services offered by the power supply of grid currently focusing on an occupant density-centred approach to develop smart cities [12]. Thus, owing to the popular acceptance of IB and rapid growth, although not

as anticipated, the term smart or intelligent building emerged from the conventional building in the early 1980s [13, 14]. Further, GB appears in relation to saving energy and reducing greenhouse gas emissions, which is also known as sustainable GB [3, 7]. Designing and modelling of sustainable GB that satisfies the entire requirement or the scope and the objective of GB is a complex process that requires the efforts of many collective bodies and economic achievements. However, an opportunity exists to design and model GB using economically cost-effective, modern, reliable, industry-proven technologies, such as the ‘AS-Interface network protocol’, which is now used by many industries to reduce their electrical device costs as well as installation costs. Migrating this type of technology to the building sector will improve the impact of energy consumption by the building and satisfy the scope and the objective of GB by reducing costs.

2.13 Sustainable Building Efficiency Achievements Demonstration

This research project demonstrates that comprehensive saving of GB is obtained from mainly four different sources:

1. fuel and electricity energy usage reductions, mainly from the building fuel energy simulation, related to HVAC annual consumption
2. optimised implementation of renewable energies, especially PV cell
3. building water usages: the highest savings occurred when GB is associated with efficient facilities that reduce the amount of water required for cooling and heating and minimise the energy needed to perform these tasks, which in turn reduces costs; several studies show that up to 15% of a commercial building’s energy consumption is owing to heating water [59]
4. control method used for building facilities, electrical/electronic devices and plugin appliances. This type of energy saving is achieved by controlling and monitoring the activities of these devices to function in the demand periods only.

2.14 Occupant Health Issues in Sustainable Buildings

In addition to the above, this thesis research project uses an ultimate energy-saving method in commercial building to approach almost NetZero energy saving in a five-storey commercial office building. Results obtained from this energy simulation

demonstrate significant achievements, which contribute to the energy reduction in building and minimised CO₂ contribution to the global greenhouse gas emissions. In addition to the CO₂ emission reduction obtained by GB, a significant issue is that the GB should be comfortable and free of worries for occupants. GB designed and implemented with extreme wireless communication decreases occupants' comfort, since the use of short-wave/higher energy radio frequency (RF) can cause health issues [60-62]. Thus, a significant contribution of this research thesis is avoiding the use of an extended/excessive wireless control system in the building, and instead, using a single-cable two-wire 'AS-Interface network protocol' control system that is free from any RF radiation influence in the field. In this method, occupants being affected by power density influence of excessive RF wireless devices is minimised, and hence, occupants would be derive with maximum comfort and satisfaction.

The results of the simulations conducted in this study would be useful for reference or for predesigning when using GB designing and modelling methods.

2.15 Conclusion

This chapter presents a literature review on conventional/traditional buildings in the first few sections in which the brief history of conventional building, GB and solar energy simulation in relation to energy usage reduction is discussed. In addition, other sections describe the derivation of GB from conventional building. Further, the capability of commercial building to be energy efficient and structurally stable, in terms of physical stability and occupants' comfort, including health safety, is briefly discussed.

Chapter 3: Modelling and Designing of Green Building

3.1 Introduction

Green building (GB) is defined, a building structure, which incorporates design, construction and operational practices that substantially reduces/eliminates its negative impact on the environment space and is modernised suitable for occupants. Hence, GB offers an opportunity to use resources efficiently while creating healthier environments. In addition to the energy and CO₂ reductions, the building provides comfortable indoor weather for its occupants uniformly throughout the year, regardless of seasonal weather variations. Owing to the thermal comfort of GB, common perceptions are that GB only involves providing air-conditioned services and that significant costs must be incurred to construct it. This was partially correct in the early development of GB a few decades ago when GB was an emerging technology. However, GB users have proven these perceptions to be incorrect. Hence, the recent literature review shows that there are many options to build GB at a cost similar or lower than that incurred on a conventional building. This is true when the right BACS is implemented in the GB, such as the ‘AS-Interface network protocol’ that reduces the building wiring cost by at least by 50%, as aforementioned.

Moreover, GB provides thermal comfort, and now, the benefit of GB is unlimited, ranging from energy saving to the extent of providing an objected-oriented automatic activity control system to the point that the term has changed to smart/intelligent building, offering new benefits. This smart building reacts/responds to occupants’ activities, space occupation and entry and exit from the building without their activating any switches physically. Thus, this implies that the building becomes a multifunctional service provider. Hence, the purpose of this research is to ensure ultimate energy reduction and increase energy efficiency, for which all construction materials are simulated or considered in relation to maximum energy reduction. The whole building elements, as shown in in Figure 3.1, are simulated to maximise energy reductions. In parallel, PV cell and wind turbines are also simulated to extract maximum power generation and their performance is also maximised. Base run energy simulation is conducted, after the space-zone heating/cooling is calculated. Based on these estimated simulation results, the alternative automatic design simulation is conducted.



Figure 3.1: Architectural building structure of a five-storey commercial office building

3.2 What Makes a Green Building

The term GB originates from the fact that the construction of the building is environmentally friendly throughout its life-cycle, which reduces energy usage of fossil oils and increases implementation of renewable energy. Thus, it implies fossil oil energy use in the buildings is restricted or, in other words, green energy is used, which minimises CO₂ emissions and does not pollute the atmosphere or unbalance the global weather. The control method and energy rating scheme used to achieve these energy reductions have resulted in these buildings being called GB. For example, some of these control systems currently used in the building sector are the BAS, BEMS and BACS. Furthermore, the energy rating scheme accredited organisation such as Green Building Council (AGBC) and others similar organisation emphasises the name of GB publicly.

3.3 Green Building Versus Intelligent Building

GB highly emphasises energy saving, while intelligent GB places more emphasis on building smartness/being sufficiently intelligent in terms of sense and response of building control systems.

3.4 Green Building Minimum Criteria Objectives

For GB, the minimum criteria are that the building has been complying with and is built according to the GBCA, LEED and other similar accreditations [63] of different countries:

1. Buildings should be developed that use the natural resources to the minimum at the time of construction as well as during continuous operations. Hence, the resource usage efficiency of the three Rs, reduce, reuse and recycle [3, 64], known as 'RRR', should be emphasised.
2. GB should maximise the use of efficient construction materials and practices; boost the use of natural sources and sinks in the building's surroundings; minimise the energy usage to run itself; use highly proficient equipment for the indoor area; and use highly proficient methods for water and waste management. Hence, minimum negative impact on the environment by the construction and operation of a building should be ensured. The external environment at the building location, the internal area for the occupants of the building and the areas not close to the building [65] should also be preserved.
3. Ensure energy saving through the GB concept through two methods. First is reducing the amount of energy that is consumed by building. Second is increasing the usage of energy sources that do not produce any greenhouse gases and are renewable in nature. Thus, GB emphasises more on natural lighting, concepts of temperature control and efficient design to further reduce the carbon footprint as well as reduce the cost of operation [66] of the building.
4. GB uses various methods to reduce water usage, treat and reuse waste water and filter water sourced from precipitation. The target is to achieve zero impact on water table and contribute to increasing it. Hence, waste is to be reduced. The GB concept emphasises improving the design of the product, reusing and

recycling materials. It results in significant waste reduction and also helps to reduce the environmental impact of the building [67].

5. Improving health and productivity by ensuring hygiene in the building helps in boosting human productivity. Thus, the GB concept provides cleanliness and neat living conditions for the building occupants [68] and others as well.

To satisfy the objectives of GB, it is necessary to use minimum resources of building materials and use EEB materials and implement an IB control system, as shown in Figures 3.2 and 3.3. The disadvantage of constructing GB is that the current conventional building construction and control system costs are much lesser than that of the GB. This means the GB construction costs are higher than the conventional building cost [10]. This is because any GB constructed with the current building control system consumes a huge amount of wiring cables and several large cabinets. If the GB is constructed with the 'AS-Interface protocol', the number of electrical or electronic devices used in the building will be reduced. Consequently, the installation and tradesman (skilled labour) cost will also be significantly reduced.

In the AS-Interface protocol, there are three main wiring requirements only, the main grid supply, the AC power supply and the 30VDC power supply. The AS-Interface power supply uses the same wire for transmitting/receiving signals as well as to power the gateway/scanner master and slave nodes and it also has a capability of handling up to maximum of 8 amps per network with minimum 3 V voltage drop allowed. There is no change in the grid main supply wiring. The changes are only in the AC power supply wiring system and in the control wiring system. The AS-Interface protocol wiring method is distinguished from the other wiring methods because the AS-Interface uses one continuous AC power supply cable running to every device from the main circuit breaker (C/B) without entering ON/OFF switches or having control of switches. A separate 'AS-Interface bus cable' runs to each device's slave nodes, as shown in Chapter 7, Figures, 7.19 and 7.20. This type of wiring method saves a number of C/B, switches, cables, relays, contactors and uses a minimum-size control cabinet. In addition, the flow chart components shown in Figure 3.2 demonstrate the minimum criteria to satisfy the requirements to design a GB with minimum sources. Utilising these materials and concept leads the building to energy sustainability. Hence, the acceptance criteria to apply for building energy efficient credit rating points can be met.

Further, Figure 3.2 shows six items and each of them play an important role in terms of reducing energy consumption and cost. However, it is too difficult to achieve the first three items ('apply sustainable materials', 'use minimum materials' and 'use energy efficient materials') in practice, since sustainable and energy efficient materials have never been cheap. This is the reason this research is important. This research thesis reduces the cost gap between the GB and conventional building. Using this method, the GB costs can match those of the latter.

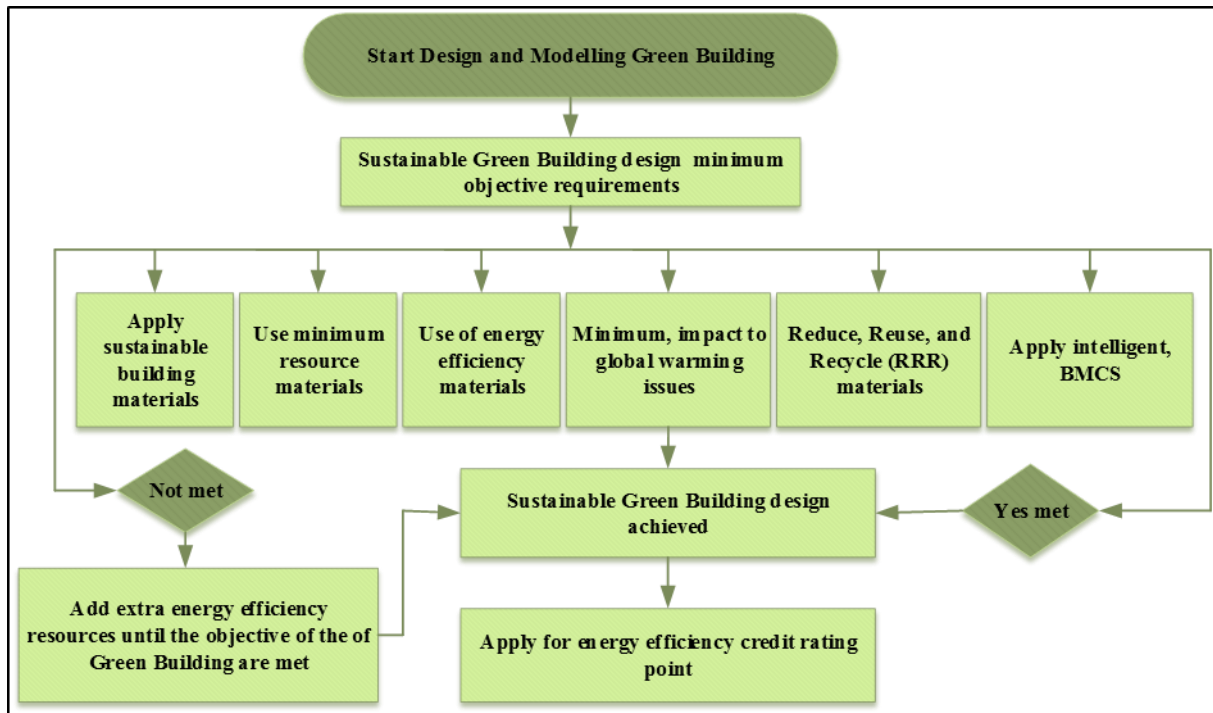


Figure 3.2: Green building minimum objectives criteria

3.5 Sustainable Building Energy Efficient System

Designing and modelling of GB is not an easy task; actually, it is a complex process in which a collection of engineering expertise, green energy researchers, construction contractors and an echo chart organisation contribute. Construction of sustainable GB is less significantly non-economical than the construction of conventional buildings [69], and this is one of the reasons that GB is not growing as fast as anticipated. In addition, in the design and the modelling of GB, appropriate modern technology must be carefully selected to satisfy the objectives of GB without adding extra construction costs over the conventional buildings. An overall design of this research project is outlined as shown in the flow chart in Figure 3.3. The design is mainly focused on the BIM energy simulation to obtain maximised reductions. Design and modelling of the GB is chosen

to be central hexagonal shape, five-storey commercial office building. The central hexagonal shape is chosen for the following reasons:

1. to have significant side shading effect by the top curved side edge shape of the roof when reflected light from the opposite curtain wall approaches the area below the curved roof
2. to ensure the office rooms inside remain cold/warm for longer periods during all seasons. This is owing to the fact that the curved outer body of the building will be heated/cooled first before the cold/heat approaches the inner-side rooms.

The building is designed using the Autodesk Revit architectural drawing template. Modelling of the building was first constructed using randomly selected construction materials. Since every location/region in the world has specific atmospheric weather, the location of the project has to be selected to load the correct weather files into the buildings software. For this thesis research project, Sydney, Australia, was chosen as the location. Then, from the weather station nearest to Sydney, weather files were loaded into the buildings software. A base run energy simulation was carried out using Autodesk Revit energy simulation analysis. For further analysis and multiple alternative designs runs, the BIM engineering data green building Extensible Mark-up Language (gbXML) files were exported automatically to cloud-based GBS. In this method, the base run acts as the reference point and construction materials and building elements, such as energy efficiency walls (massive super-high insulation), double glazing windows, low-e glazing, wall-to-window ratio (WWR), window shading ratio and roofs, are automatically replaced by the system for better energy rating. In addition, the building orientation was also rotated to different angles, such as to $+45^\circ$, -45° , $+90^\circ$ and -90° , for the solar energy to be absorbed into the building envelope at optimum level. GBS runs a number of alternative design options by automatically selecting different energy packages. In those energy packages, American Society of Heating, Refrigerating and Air-Conditioning Engineers (ASHRAE) packages were found to be the best energy-saving methods. Choosing the final best energy simulation result was not easy because most of the alternative designs have similar best reduction of annual total electrical energy. Since the aim of this research project study is to save energy and increase energy efficiency in commercial office buildings, 'The HVAC_TYPES_ ASHRAE_ Package Terminal Heat Pump' was chosen because of the

fuel energy reduction result is significantly higher amount, almost by 50% than the base run result.

The overall design also includes a simulation process for renewable energy potential, which is proposed for this building by the base run simulation. The proposed renewable energy sources are three types of roof-mounted PV cells, with low, medium and high efficiency, and one type of 15-inch wind turbine. Energy potentials from these renewables are estimated at 24,147 kWh, 48,295 kWh, 72,442 kWh and 2,208 kWh respectively.

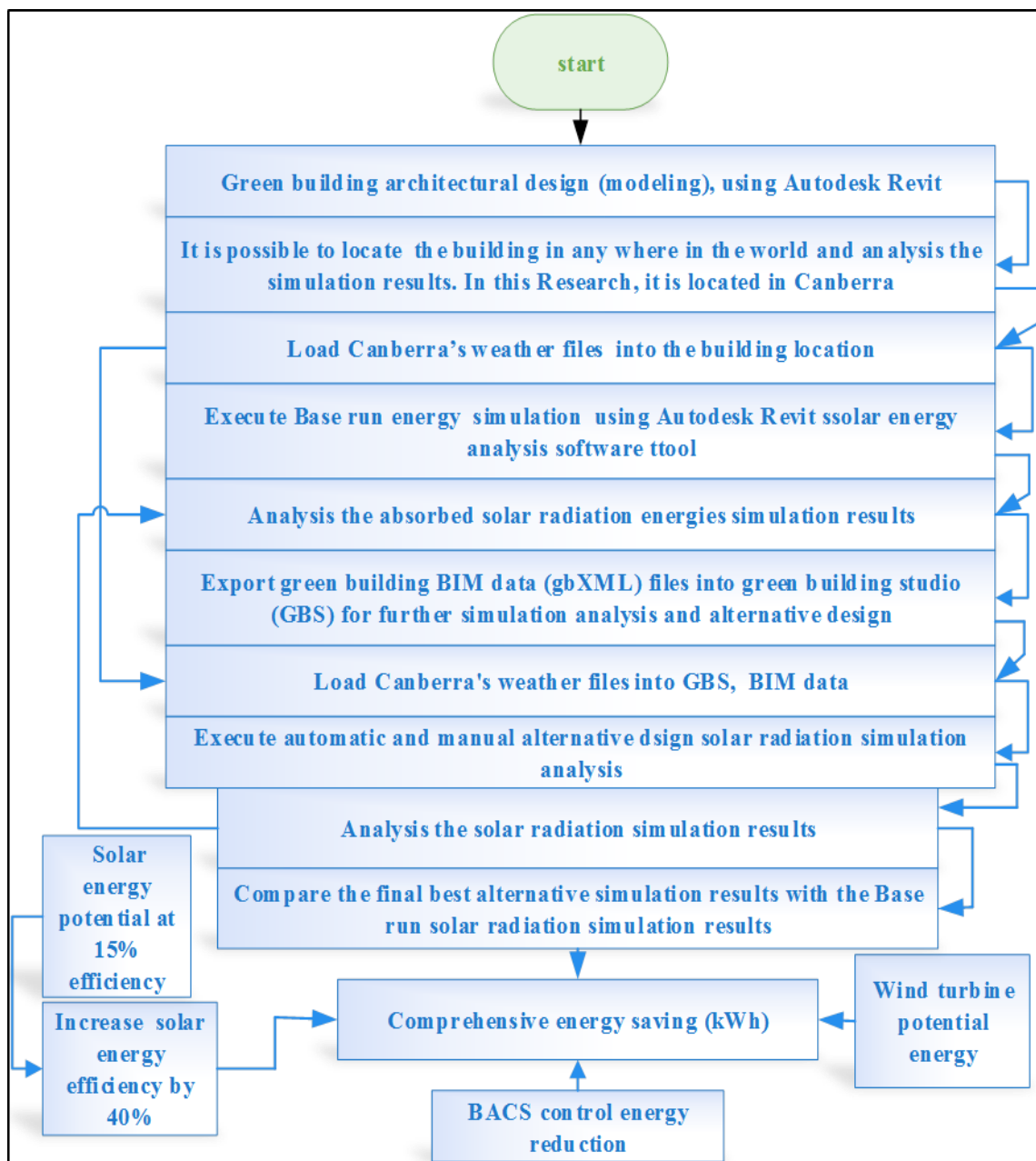


Figure 3.3: Green building design energy simulation process flow chart

3.6 Conclusion

This chapter attempts to resolve the complex issues of GB by developing a method to simplify these issues. However, the developed method is purely theoretical method, which uses only pure software simulation application. Using this research method, simulation results are shown to achieve significant minimised energy annual usages. However, further practical research work is required to prove the achieved simulation results obtained from chapters 4, 5, 6 and 7.

Chapter 4: Building Energy Simulation Heating and Cooling Requirement

4.1 Introduction

Autodesk Revit energy analysis for heating/cooling uses ‘building area space segregation’, ‘volume computations’ and ‘placing space’. Space segregation is created under certain criteria during the project space heating/cooling analysis process; meanwhile the created spaces are required to calculate the volumes of the areas that demand heating/cooling. This computation volume is for the specific created space based on its room-bounding components and is calculated as the area of its base multiplied by the height of the space. Hence, an accurate heating/cooling load analysis can only be accomplished when spaces are placed in all areas to account for the entire volume of the building model. However, accounting for the volume of cavities, shafts and chases is critical as well as to the heating and cooling load analysis; this is to account for the entire building volume. To minimise the critical volumes of cavities, shafts and chases, the interior and exterior room-bounding components must be correctly identified for an accurate analysis of heating and cooling loads.

In this research project, the heating/cooling energy simulation was conducted prior to the Base run energy simulation and it is simply a path of preparation for the base run and alternative design simulations. This early simulation mainly involves space/room division to segregate each space zone of the building area in a different boundary to calculate the basic monthly heating/ cooling consumption in a summarised method. This method uses space specification rather than rooms and segregates the building into 38 spaces; each of the spaces draws its own heating/cooling loads depend upon its area, volume and air flow routes.

4.2 Building Space Utilisation

Building space utilisation in a commercial office has a significant effect on reducing energy use when the work area is designed to obtain maximum natural energy from daylight. By arranging office furniture around the curtain walls and windows, applying efficient lighting design, fitting lights with motion-based sensors and applying daylight

responsive light dimming, lighting bill costs can be reduced by 35–40% [70]. Figures 4.1 and 4.1 show space utilisation for the commercial office building, with the outer envelope of the building fitted with curtain wall, which will allow adequate light into the inner spaces during winter and reflect greater portion of the light during summer. This is so that the inner side of the building has relatively constant temperature, so that the HVAC loads can be kept at minimum in the inner space.

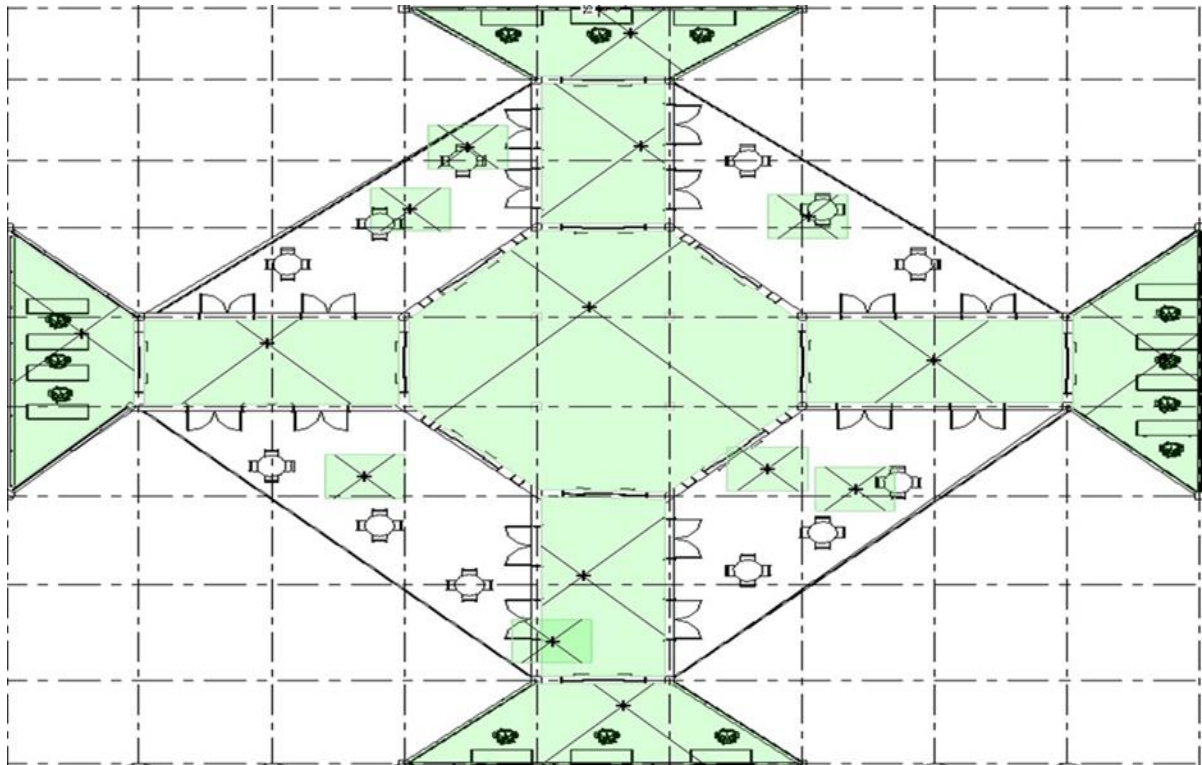


Figure 4.1: Segregated space heating/cooling

Legend:



Office Table



Office Chair



Office Table

4.3 Space Heating and Cooling Load Calculation

Knowing the fundamental rules of heat and cold transfer and how these opposite energies translate into energy flows in a building is critical, especially when designing high-performance buildings. Studying the different forms of heat transfer, material properties such as U-factor and R-value, heating, cooling loads, energy use intensity (EUI) and the difference between site and building source of energy is useful in predesign.

Constructing and operating buildings requires energy but high-performance buildings use the right blend of passive and active design strategies to minimise the energy use while ensuring occupant comfort [71]. Autodesk Revit energy simulation uses building space/room classification and conducts pre-simulation heating/cooling calculations as shown in Figure 4.2, space model analytical segregation; in Tables 4.1 to 4.36, the analytical model space, heating/cooling calculations of specific components brief summary results are presented.

In these basic heating/cooling calculations, the summarised simulation results include the entire analytical model's segregated spaces and basic elements used in constructing the real building. Thus, the space under the building, the area and the volume of the building are properly addressed. These results are summarised and displayed in these tables. Thus, the first four Tables, Tables 4.1 to 4.4, present the project summary, building's element summary, project zone/space summary and project default summary respectively. Tables 4.5 to 4.36 present information on the total default spaces and building heating/cooling details of the summaries.

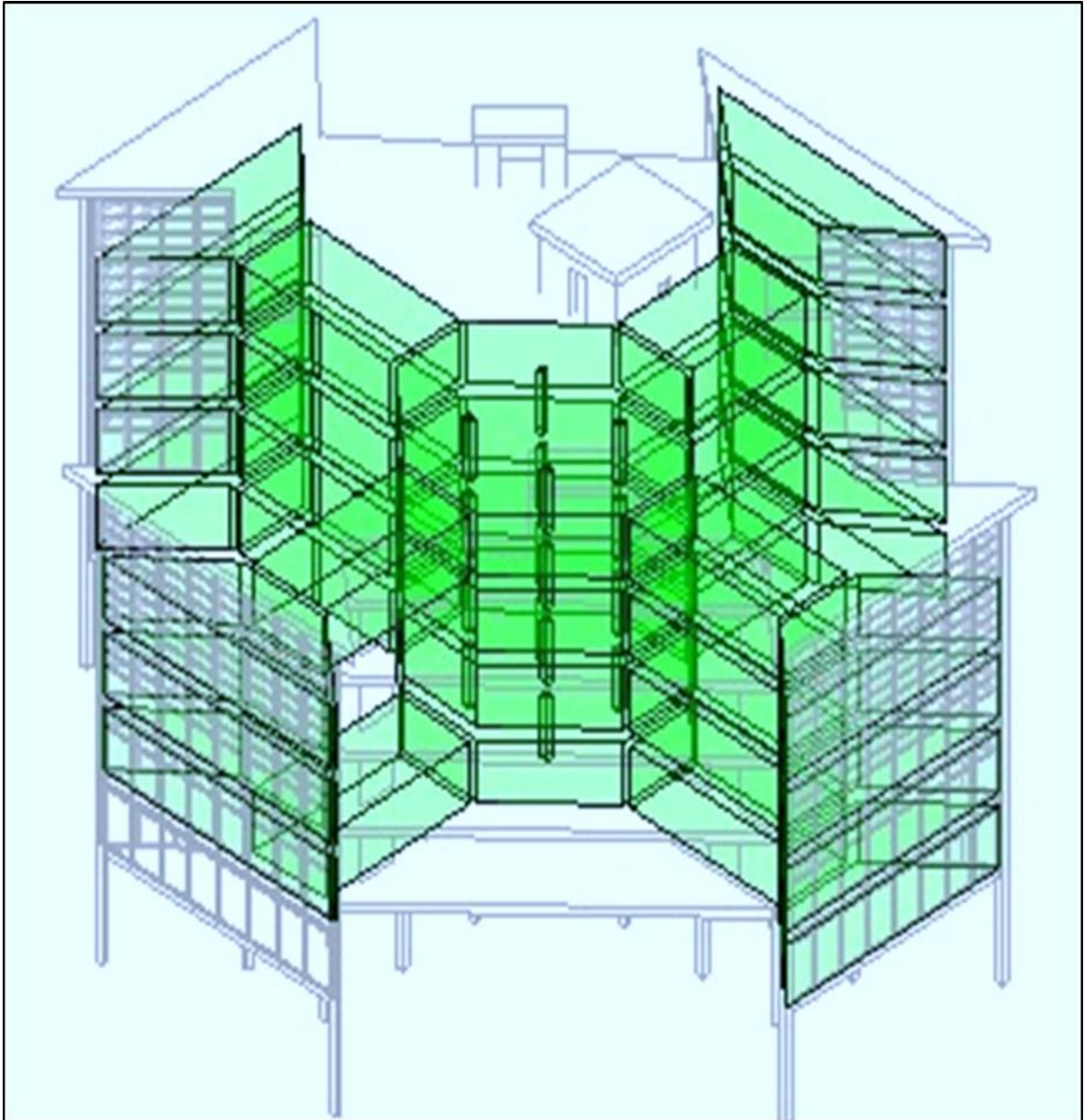


Figure 4.2: Building space heating/cooling load calculation image

Table 4.1: Building project summary

Project	Location and Weather
	Project Name
Address	Sydney, Australia
Calculation Time	Saturday, 6 January 2018, 2:02 PM
Report Type	Standard
Latitude	-33.87°
Longitude	151.21°
Summer Dry Bulb	34 °C

Summer Wet Bulb	23 °C
Winter Dry Bulb	9 °C
Mean Daily Range	7 °C

Table 4.2: Building parameter summary

Inputs	
Building Type	Office
Area (m ²)	1,158
Volume (m ³)	2,824.30
Calculated Results	
Peak Cooling Total Load (W)	101,971
Peak Cooling Month and Hour	January; 4:00 PM
Peak Cooling Sensible Load (W)	99,713
Peak Cooling Latent Load (W)	2,257
Maximum Cooling Capacity (W)	101,971
Peak Cooling Airflow (L/s)	7,537.5
Peak Heating Load (W)	46,246
Peak Heating Airflow (L/s)	3,231.0
Checksums	
Cooling Load Density (W/m ²)	88.04
Cooling Flow Density (L/(s·m ²))	6.51
Cooling Flow/Load (L/(kW))	73.92
Cooling Area/Load (m ² /kW)	11.36
Heating Load Density (W/m ²)	39.93
Heating Flow Density (L/(s·m ²))	2.79

Table 4.3: Building zone summary—default

Inputs	
Area (m ²)	1,158
Volume (m ³)	2,824.30
Cooling Set point	23 °C
Heating Set point	21 °C
Supply Air Temperature	12 °C
Number of People	41
Infiltration (L/s)	0.0

Air Volume Calculation Type	VAV–Dual Duct
Relative Humidity	46.00% (Calculated)
Psychometrics	
Psychrometric Message	None
Cooling Coil Entering Dry-Bulb Temperature	23 °C
Cooling Coil Entering Wet-Bulb Temperature	16 °C
Cooling Coil Leaving Dry-Bulb Temperature	11 °C
Cooling Coil Leaving Wet-Bulb Temperature	11 °C
Mixed Air Dry-Bulb Temperature	23 °C
Calculated Results	
Peak Cooling Load (W)	101,971
Peak Cooling Month and Hour	January; 4:00 PM
Peak Cooling Sensible Load (W)	99,713
Peak Cooling Latent Load (W)	2,257
Peak Cooling Airflow (L/s)	7,537.5
Peak Heating Load (W)	46,246
Peak Heating Airflow (L/s)	3,231.0
Peak Ventilation Airflow (L/s)	0.0
Checksums	
Cooling Load Density (W/m ²)	88.04
Cooling Flow Density (L/(s·m ²))	6.51
Cooling Flow/Load (L/(kW))	73.92
Cooling Area/Load (m ² /kW)	11.36
Heating Load Density (W/m ²)	39.93
Heating Flow Density (L/(s·m ²))	2.79
Ventilation Density (L/(s·m ²))	0.00
Ventilation/Person (L/s)	0.0

Components	Cooling		Heating	
	Loads (W)	Percentage of Total	Loads (W)	Percentage of Total
Wall	7,135	7.00	6,099	13.19

Window	47,554	46.63	26,229	56.72
Door	15,781	15.48	13,918	30.10
Roof	0	0.00	0	0.00
Skylight	0	0.00	0	0.00
Partition	0	0.00	0	0.00
Infiltration	0	0.00	0	0.00
Ventilation	0	0.00	0	0.00
Lighting	10,381	10.18		
Power	13,495	13.23		
People	4,697	4.61		
Plenum	0	0.00		
Fan Heat	2,928	2.87		
Reheat	0	0.00		
Total	101,971	100	46,246	100

Table 4.4: Building default spaces

Space Name	Area (m²)	Volume(m³)	Peak Cooling Load (W)	Cooling Airflow (L/s)	Peak Heating Load (W)	Heating Airflow (L/s)
1 Space	22	53.77	1,291	97.1	557	38.9
2 Spaces	23	56.60	3,375	256.9	1,881	131.4
4 Spaces	100	243.43	3,988	303.5	1,261	88.1
5 Spaces	27	65.59	1,497	113.9	902	63.0
6 Spaces	29	71.86	4,289	326.4	1,891	132.1
7 Spaces	28	68.55	2,231	169.8	1,190	83.1
8 Spaces	27	66.70	1,523	115.9	912	63.7
9 Spaces	26	63.00	4,269	324.9	1,516	105.9
13 Spaces	23	56.60	3,375	256.9	1,881	131.4
14 Spaces	22	53.77	1,682	128.0	810	56.6
15 Spaces	100	243.43	4,556	346.8	1,764	123.2
16 Spaces	27	66.70	1,532	116.6	920	64.2
17 Spaces	27	65.59	1,497	113.9	902	63.0
18 Spaces	29	71.86	4,289	326.4	1,891	132.1
19 Spaces	28	67.75	3,862	293.9	2,262	158.0

20 Spaces	26	63.05	4,278	325.5	1,520	106.2
23 Spaces	23	56.60	3,375	256.9	1,881	131.4
24 Spaces	22	53.77	1,682	128.0	810	56.6
25 Spaces	100	243.43	4,556	346.8	1,764	123.2
26 Spaces	27	65.59	1,497	113.9	902	63.0
27 Spaces	29	71.86	4,289	326.4	1,891	132.1
28 Spaces	27	66.70	1,532	116.6	920	64.2
29 Spaces	28	67.75	3,862	293.9	2,262	158.0
30 Spaces	26	63.05	4,278	325.5	1,520	106.2
31 Spaces	23	56.60	3,375	256.9	1,881	131.4
32 Spaces	22	53.77	1,682	128.0	810	56.6
33 Spaces	100	243.43	4,266	324.6	1,463	102.2
34 Spaces	27	65.59	1,497	113.9	902	63.0
35 Spaces	27	66.70	1,532	116.6	920	64.2
36 Spaces	29	71.86	4,289	326.4	1,891	132.1
37 Spaces	28	67.75	3,594	273.5	1,961	137.0
39 Spaces	28	68.55	1,942	147.8	889	62.1
40 Spaces	26	63.05	4,278	325.5	1,520	106.2

Table 4.5: Building space summary—1 space

Inputs	
Area (m ²)	22
Volume (m ³)	53.77
Wall Area (m ²)	30
Roof Area (m ²)	0
Door Area (m ²)	18
Partition Area (m ²)	0
Window Area (m ²)	0
Skylight Area (m ²)	0
Lighting Load (W)	237
Power Load (W)	309
Number of People	1
Sensible Heat Gain/Person (W)	73
Latent Heat Gain/Person (W)	59
Infiltration Airflow (L/s)	0.0

Space Type	Office (inherited from building type)
Calculated Results	
Peak Cooling Load (W)	1,291
Peak Cooling Month and Hour	January; 9:00 AM
Peak Cooling Sensible Load (W)	1,248
Peak Cooling Latent Load (W)	43
Peak Cooling Airflow (L/s)	97.1
Peak Heating Load (W)	557
Peak Heating Airflow (L/s)	38.9

Components	Cooling		Heating	
	Loads (W)	Percentage of Total	Loads (W)	Percentage of Total
Wall	302	23.43	233	41.79
Window	0	0.00	0	0.00
Door	471	36.50	324	58.21
Roof	0	0.00	0	0.00
Skylight	0	0.00	0	0.00
Partition	0	0.00	0	0.00
Infiltration	0	0.00	0	0.00
Lighting	188	14.55		
Power	244	18.92		
People	85	6.60		
Plenum	0	0.00		
Total	1,291	100	557	100

Table 4.6: Building space summary—2 spaces

Inputs	
Area (m ²)	23
Volume (m ³)	56.60
Wall Area (m ²)	53
Roof Area (m ²)	0
Door Area (m ²)	6
Partition Area (m ²)	0
Window Area (m ²)	52

Skylight Area (m ²)	0
Lighting Load (W)	250
Power Load (W)	325
Number of People	1
Sensible Heat Gain/Person (W)	73
Latent Heat Gain/Person (W)	59
Infiltration Airflow (L/s)	0.0
Space Type	Office (inherited from building type)
Calculated Results	
Peak Cooling Load (W)	3,375
Peak Cooling Month and Hour	January; 4:00 PM
Peak Cooling Sensible Load (W)	3,330
Peak Cooling Latent Load (W)	45
Peak Cooling Airflow (L/s)	256.9
Peak Heating Load (W)	1,881
Peak Heating Airflow (L/s)	131.4

Components	Cooling		Heating	
	Loads (W)	Percentage of Total	Loads (W)	Percentage of Total
Wall	14	0.42	14	0.73
Window	2,783	82.44	1,868	99.27
Door	0	0.00	0	0.00
Roof	0	0.00	0	0.00
Skylight	0	0.00	0	0.00
Partition	0	0.00	0	0.00
Infiltration	0	0.00	0	0.00
Lighting	210	6.23		
Power	273	8.09		
People	95	2.82		
Plenum	0	0.00		
Total	3,375	100	1,881	100

Table 4.7: Building space summary—4 spaces

Inputs

Area (m ²)	100
Volume (m ³)	243.43
Wall Area (m ²)	65
Roof Area (m ²)	0
Door Area (m ²)	34
Partition Area (m ²)	0
Window Area (m ²)	0
Skylight Area (m ²)	0
Lighting Load (W)	1,075
Power Load (W)	1,397
Number of People	4
Sensible Heat Gain/Person (W)	73
Latent Heat Gain/Person (W)	59
Infiltration Airflow (L/s)	0.0
Space Type	Office (inherited from building type)
Calculated Results	
Peak Cooling Load (W)	3,988
Peak Cooling Month and Hour	January; 4:00 PM
Peak Cooling Sensible Load (W)	3,793
Peak Cooling Latent Load (W)	195
Peak Cooling Airflow (L/s)	303.5
Peak Heating Load (W)	1,261
Peak Heating Airflow (L/s)	88.1

Components	Cooling		Heating	
	Loads (W)	Percentage of Total	Loads (W)	Percentage of Total
Wall	605	15.17	486	38.56
Window	0	0.00	0	0.00
Door	933	23.39	775	61.44
Roof	0	0.00	0	0.00
Skylight	0	0.00	0	0.00
Partition	0	0.00	0	0.00
Infiltration	0	0.00	0	0.00
Lighting	890	22.32		

Power	1,157	29.01		
People	403	10.10		
Plenum	0	0.00		
Total	3,988	100	1,261	100

Table 4.8: Building space summary—5 spaces

Inputs				
Area (m ²)	27			
Volume (m ³)	65.59			
Wall Area (m ²)	39			
Roof Area (m ²)	0			
Door Area (m ²)	25			
Partition Area (m ²)	0			
Window Area (m ²)	0			
Skylight Area (m ²)	0			
Lighting Load (W)	290			
Power Load (W)	376			
Number of People	1			
Sensible Heat Gain/Person (W)	73			
Latent Heat Gain/Person (W)	59			
Infiltration Airflow (L/s)	0.0			
Space Type	Office (inherited from building type)			
Calculated Results				
Peak Cooling Load (W)	1,497			
Peak Cooling Month and Hour	January; 4:00 PM			
Peak Cooling Sensible Load (W)	1,445			
Peak Cooling Latent Load (W)	52			
Peak Cooling Airflow (L/s)	113.9			
Peak Heating Load (W)	902			
Peak Heating Airflow (L/s)	63.0			
Components	Cooling		Heating	
	Loads (W)	Percentage of Total	Loads (W)	Percentage of Total
Wall	235	15.72	254	28.12

Window	0	0.00	0	0.00
Door	602	40.19	648	71.88
Roof	0	0.00	0	0.00
Skylight	0	0.00	0	0.00
Partition	0	0.00	0	0.00
Infiltration	0	0.00	0	0.00
Lighting	240	16.02		
Power	312	20.82		
People	109	7.25		
Plenum	0	0.00		
Total	1,497	100	902	100

Table 4.9: Building space summary—6 spaces

Inputs	
Area (m ²)	29
Volume (m ³)	71.86
Wall Area (m ²)	54
Roof Area (m ²)	0
Door Area (m ²)	6
Partition Area (m ²)	0
Window Area (m ²)	52
Skylight Area (m ²)	0
Lighting Load (W)	317
Power Load (W)	412
Number of People	2
Sensible Heat Gain/Person (W)	73
Latent Heat Gain/Person (W)	59
Infiltration Airflow (L/s)	0.0
Space Type	Office (inherited from building type)
Calculated Results	
Peak Cooling Load (W)	4,289
Peak Cooling Month and Hour	January; 4:00 PM
Peak Cooling Sensible Load (W)	4,231
Peak Cooling Latent Load (W)	57
Peak Cooling Airflow (L/s)	326.4

Peak Heating Load (W)	1,891
Peak Heating Airflow (L/s)	132.1

Components	Cooling		Heating	
	Loads (W)	Percentage of Total	Loads (W)	Percentage of Total
Wall	29	0.69	21	1.13
Window	3,525	82.19	1,870	98.87
Door	0	0.00	0	0.00
Roof	0	0.00	0	0.00
Skylight	0	0.00	0	0.00
Partition	0	0.00	0	0.00
Infiltration	0	0.00	0	0.00
Lighting	267	6.22		
Power	347	8.09		
People	121	2.82		
Plenum	0	0.00		
Total	4,289	100	1,891	100

Table 4.10: Building space summary—7 spaces

Inputs	
Area (m ²)	28
Volume (m ³)	68.55
Wall Area (m ²)	48
Roof Area (m ²)	0
Door Area (m ²)	20
Partition Area (m ²)	0
Window Area (m ²)	0
Skylight Area (m ²)	0
Lighting Load (W)	303
Power Load (W)	393
Number of People	1
Sensible Heat Gain/Person (W)	73
Latent Heat Gain/Person (W)	59
Infiltration Airflow (L/s)	0.0

Space Type	Office (inherited from building type)
Calculated Results	
Peak Cooling Load (W)	2,231
Peak Cooling Month and Hour	January; 4:00 PM
Peak Cooling Sensible Load (W)	2,176
Peak Cooling Latent Load (W)	55
Peak Cooling Airflow (L/s)	169.8
Peak Heating Load (W)	1,190
Peak Heating Airflow (L/s)	83.1

Components	Cooling		Heating	
	Loads (W)	Percentage of Total	Loads (W)	Percentage of Total
Wall	380	17.02	283	23.82
Window	0	0.00	0	0.00
Door	1,162	52.06	907	76.18
Roof	0	0.00	0	0.00
Skylight	0	0.00	0	0.00
Partition	0	0.00	0	0.00
Infiltration	0	0.00	0	0.00
Lighting	251	11.23		
Power	326	14.60		
People	113	5.08		
Plenum	0	0.00		
Total	2,231	100	1,190	100

Table 4.11: Building space summary—8 spaces

Inputs	
Area (m ²)	27
Volume (m ³)	66.70
Wall Area (m ²)	40
Roof Area (m ²)	0
Door Area (m ²)	20
Partition Area (m ²)	0
Window Area (m ²)	0
Skylight Area (m ²)	0

Lighting Load (W)	294
Power Load (W)	383
Number of People	1
Sensible Heat Gain/Person (W)	73
Latent Heat Gain/Person (W)	59
Infiltration Airflow (L/s)	0.0
Space Type	Office (inherited from building type)
Calculated Results	
Peak Cooling Load (W)	1,523
Peak Cooling Month and Hour	January; 4:00 PM
Peak Cooling Sensible Load (W)	1,470
Peak Cooling Latent Load (W)	53
Peak Cooling Airflow (L/s)	115.9
Peak Heating Load (W)	912
Peak Heating Airflow (L/s)	63.7

Components	Cooling		Heating	
	Loads (W)	Percentage of Total	Loads (W)	Percentage of Total
Wall	250	16.41	264	28.93
Window	0	0.00	0	0.00
Door	602	39.52	648	71.07
Roof	0	0.00	0	0.00
Skylight	0	0.00	0	0.00
Partition	0	0.00	0	0.00
Infiltration	0	0.00	0	0.00
Lighting	244	16.01		
Power	317	20.81		
People	110	7.25		
Plenum	0	0.00		
Total	1,523	100	912	100

Table 4.12: Building space summary—9 spaces

Inputs	
Area (m ²)	26

Volume (m ³)	63.00
Wall Area (m ²)	53
Roof Area (m ²)	0
Door Area (m ²)	0
Partition Area (m ²)	0
Window Area (m ²)	38
Skylight Area (m ²)	0
Lighting Load (W)	278
Power Load (W)	362
Number of People	1
Sensible Heat Gain/Person (W)	73
Latent Heat Gain/Person (W)	59
Infiltration Airflow (L/s)	0.0
Space Type	Office (inherited from building type)
Calculated Results	
Peak Cooling Load (W)	4,269
Peak Cooling Month and Hour	January; 4:00 PM
Peak Cooling Sensible Load (W)	4,218
Peak Cooling Latent Load (W)	50
Peak Cooling Airflow (L/s)	324.9
Peak Heating Load (W)	1,516
Peak Heating Airflow (L/s)	105.9

Components	Cooling		Heating	
	Loads (W)	Percentage of Total	Loads (W)	Percentage of Total
Wall	201	4.72	150	9.89
Window	3,424	80.20	1,366	90.11
Door	0	0.00	0	0.00
Roof	0	0.00	0	0.00
Skylight	0	0.00	0	0.00
Partition	0	0.00	0	0.00
Infiltration	0	0.00	0	0.00
Lighting	234	5.48		
Power	304	7.12		

People	106	2.48		
Plenum	0	0.00		
Total	4,269	100	1,516	100

Table 4.13: Building space summary—13 spaces

Inputs	
Area (m ²)	23
Volume (m ³)	56.60
Wall Area (m ²)	53
Roof Area (m ²)	0
Door Area (m ²)	6
Partition Area (m ²)	0
Window Area (m ²)	52
Skylight Area (m ²)	0
Lighting Load (W)	250
Power Load (W)	325
Number of People	1
Sensible Heat Gain/Person (W)	73
Latent Heat Gain/Person (W)	59
Infiltration Airflow (L/s)	0.0
Space Type	Office (inherited from building type)
Calculated Results	
Peak Cooling Load (W)	3,375
Peak Cooling Month and Hour	January; 4:00 PM
Peak Cooling Sensible Load (W)	3,330
Peak Cooling Latent Load (W)	45
Peak Cooling Airflow (L/s)	256.9
Peak Heating Load (W)	1,881
Peak Heating Airflow (L/s)	131.4

Components	Cooling		Heating	
	Loads (W)	Percentage of Total	Loads (W)	Percentage of Total
Wall	14	0.42	14	0.73
Window	2,783	82.44	1,868	99.27

Door	0	0.00	0	0.00
Roof	0	0.00	0	0.00
Skylight	0	0.00	0	0.00
Partition	0	0.00	0	0.00
Infiltration	0	0.00	0	0.00
Lighting	210	6.23		
Power	273	8.09		
People	95	2.82		
Plenum	0	0.00		
Total	3,375	100	1,881	100

Table 4.14: Building space summary—14 spaces

Inputs	
Area (m ²)	22
Volume (m ³)	53.77
Wall Area (m ²)	30
Roof Area (m ²)	0
Door Area (m ²)	25
Partition Area (m ²)	0
Window Area (m ²)	0
Skylight Area (m ²)	0
Lighting Load (W)	237
Power Load (W)	309
Number of People	1
Sensible Heat Gain/Person (W)	73
Latent Heat Gain/Person (W)	59
Infiltration Airflow (L/s)	0.0
Space Type	Office (inherited from building type)
Calculated Results	
Peak Cooling Load (W)	1,682
Peak Cooling Month and Hour	January; 4:00 PM
Peak Cooling Sensible Load (W)	1,639
Peak Cooling Latent Load (W)	43
Peak Cooling Airflow (L/s)	128.0

Peak Heating Load (W)	810
Peak Heating Airflow (L/s)	56.6

Components	Cooling		Heating	
	Loads (W)	Percentage of Total	Loads (W)	Percentage of Total
Wall	228	13.54	162	19.97
Window	0	0.00	0	0.00
Door	913	54.29	648	80.03
Roof	0	0.00	0	0.00
Skylight	0	0.00	0	0.00
Partition	0	0.00	0	0.00
Infiltration	0	0.00	0	0.00
Lighting	197	11.69		
Power	256	15.19		
People	89	5.29		
Plenum	0	0.00		
Total	1,682	100	810	100

Table 4.15: Building space summary—15 spaces

Inputs	
Area (m ²)	100
Volume (m ³)	243.43
Wall Area (m ²)	75
Roof Area (m ²)	0
Door Area (m ²)	45
Partition Area (m ²)	0
Window Area (m ²)	0
Skylight Area (m ²)	0
Lighting Load (W)	1,075
Power Load (W)	1,397
Number of People	4
Sensible Heat Gain/Person (W)	73
Latent Heat Gain/Person (W)	59
Infiltration Airflow (L/s)	0.0

Space Type	Office (inherited from building type)
Calculated Results	
Peak Cooling Load (W)	4,556
Peak Cooling Month and Hour	January; 4:00 PM
Peak Cooling Sensible Load (W)	4,362
Peak Cooling Latent Load (W)	195
Peak Cooling Airflow (L/s)	346.8
Peak Heating Load (W)	1,764
Peak Heating Airflow (L/s)	123.2

Components	Cooling		Heating	
	Loads (W)	Percentage of Total	Loads (W)	Percentage of Total
Wall	568	12.47	472	26.77
Window	0	0.00	0	0.00
Door	1,539	33.77	1,292	73.23
Roof	0	0.00	0	0.00
Skylight	0	0.00	0	0.00
Partition	0	0.00	0	0.00
Infiltration	0	0.00	0	0.00
Lighting	890	19.53		
Power	1,157	25.39		
People	403	8.84		
Plenum	0	0.00		
Total	4,556	100	1,764	100

Table 4.16: Building space summary—16 spaces

Inputs	
Area (m ²)	27
Volume (m ³)	66.70
Wall Area (m ²)	41
Roof Area (m ²)	0
Door Area (m ²)	25
Partition Area (m ²)	0
Window Area (m ²)	0

Skylight Area (m ²)	0
Lighting Load (W)	294
Power Load (W)	383
Number of People	1
Sensible Heat Gain/Person (W)	73
Latent Heat Gain/Person (W)	59
Infiltration Airflow (L/s)	0.0
Space Type	Office (inherited from building type)
Calculated Results	
Peak Cooling Load (W)	1,532
Peak Cooling Month and Hour	January; 4:00 PM
Peak Cooling Sensible Load (W)	1,479
Peak Cooling Latent Load (W)	53
Peak Cooling Airflow (L/s)	116.6
Peak Heating Load (W)	920
Peak Heating Airflow (L/s)	64.2

Components	Cooling		Heating	
	Loads (W)	Percentage of Total	Loads (W)	Percentage of Total
Wall	259	16.90	271	29.50
Window	0	0.00	0	0.00
Door	602	39.29	648	70.50
Roof	0	0.00	0	0.00
Skylight	0	0.00	0	0.00
Partition	0	0.00	0	0.00
Infiltration	0	0.00	0	0.00
Lighting	244	15.92		
Power	317	20.69		
People	110	7.20		
Plenum	0	0.00		
Total	1,532	100	920	100

Table 4.17: Buildings space summary—17 spaces

Inputs

Area (m ²)	27
Volume (m ³)	65.59
Wall Area (m ²)	39
Roof Area (m ²)	0
Door Area (m ²)	25
Partition Area (m ²)	0
Window Area (m ²)	0
Skylight Area (m ²)	0
Lighting Load (W)	290
Power Load (W)	376
Number of People	1
Sensible Heat Gain/Person (W)	73
Latent Heat Gain/Person (W)	59
Infiltration Airflow (L/s)	0.0
Space Type	Office (inherited from building type)
Calculated Results	
Peak Cooling Load (W)	1,497
Peak Cooling Month and Hour	January; 4:00 PM
Peak Cooling Sensible Load (W)	1,445
Peak Cooling Latent Load (W)	52
Peak Cooling Airflow (L/s)	113.9
Peak Heating Load (W)	902
Peak Heating Airflow (L/s)	63.0

Components	Cooling		Heating	
	Loads (W)	Percentage of Total	Loads (W)	Percentage of Total
Wall	235	15.72	254	28.12
Window	0	0.00	0	0.00
Door	602	40.19	648	71.88
Roof	0	0.00	0	0.00
Skylight	0	0.00	0	0.00
Partition	0	0.00	0	0.00
Infiltration	0	0.00	0	0.00
Lighting	240	16.02		

Power	312	20.82		
People	109	7.25		
Plenum	0	0.00		
Total	1,497	100	902	100

Table 4.18: Building space summary—18 spaces

Inputs	
Area (m ²)	29
Volume (m ³)	71.86
Wall Area (m ²)	54
Roof Area (m ²)	0
Door Area (m ²)	6
Partition Area (m ²)	0
Window Area (m ²)	52
Skylight Area (m ²)	0
Lighting Load (W)	317
Power Load (W)	412
Number of People	2
Sensible Heat Gain/Person (W)	73
Latent Heat Gain/Person (W)	59
Infiltration Airflow (L/s)	0.0
Space Type	Office (inherited from building type)
Calculated Results	
Peak Cooling Load (W)	4,289
Peak Cooling Month and Hour	January; 4:00 PM
Peak Cooling Sensible Load (W)	4,231
Peak Cooling Latent Load (W)	57
Peak Cooling Airflow (L/s)	326.4
Peak Heating Load (W)	1,891
Peak Heating Airflow (L/s)	132.1

Components	Cooling		Heating	
	Loads (W)	Percentage of Total	Loads (W)	Percentage of Total

Wall	29	0.69	21	1.13
Window	3,525	82.19	1,870	98.87
Door	0	0.00	0	0.00
Roof	0	0.00	0	0.00
Skylight	0	0.00	0	0.00
Partition	0	0.00	0	0.00
Infiltration	0	0.00	0	0.00
Lighting	267	6.22		
Power	347	8.09		
People	121	2.82		
Plenum	0	0.00		
Total	4,289	100	1,891	100

Table 4.19: Building space summary—19 spaces

Inputs	
Area (m ²)	28
Volume (m ³)	67.75
Wall Area (m ²)	66
Roof Area (m ²)	0
Door Area (m ²)	6
Partition Area (m ²)	0
Window Area (m ²)	54
Skylight Area (m ²)	0
Lighting Load (W)	299
Power Load (W)	389
Number of People	1
Sensible Heat Gain/Person (W)	73
Latent Heat Gain/Person (W)	59
Infiltration Airflow (L/s)	0.0
Space Type	Office (inherited from building type)
Calculated Results	
Peak Cooling Load (W)	3,862
Peak Cooling Month and Hour	January; 4:00 PM
Peak Cooling Sensible Load (W)	3,808
Peak Cooling Latent Load (W)	54

Peak Cooling Airflow (L/s)	293.9			
Peak Heating Load (W)	2,262			
Peak Heating Airflow (L/s)	158.0			
Components	Cooling		Heating	
	Loads (W)	Percentage of Total	Loads (W)	Percentage of Total
Wall	64	1.65	66	2.92
Window	2,876	74.46	1,937	85.66
Door	230	5.96	258	11.42
Roof	0	0.00	0	0.00
Skylight	0	0.00	0	0.00
Partition	0	0.00	0	0.00
Infiltration	0	0.00	0	0.00
Lighting	252	6.51		
Power	327	8.47		
People	114	2.95		
Plenum	0	0.00		
Total	3,862	100	2,262	100

Table 4.20: Building space summary—20 spaces

Inputs	
Area (m ²)	26
Volume (m ³)	63.05
Wall Area (m ²)	53
Roof Area (m ²)	0
Door Area (m ²)	6
Partition Area (m ²)	0
Window Area (m ²)	38
Skylight Area (m ²)	0
Lighting Load (W)	278
Power Load (W)	362
Number of People	1
Sensible Heat Gain/Person (W)	73
Latent Heat Gain/Person (W)	59

Infiltration Airflow (L/s)	0.0
Space Type	Office (inherited from building type)
Calculated Results	
Peak Cooling Load (W)	4,278
Peak Cooling Month and Hour	January; 4:00 PM
Peak Cooling Sensible Load (W)	4,227
Peak Cooling Latent Load (W)	50
Peak Cooling Airflow (L/s)	325.5
Peak Heating Load (W)	1,520
Peak Heating Airflow (L/s)	106.2

Components	Cooling		Heating	
	Loads (W)	Percentage of Total	Loads (W)	Percentage of Total
Wall	208	4.87	153	10.05
Window	3,425	80.06	1,367	89.95
Door	0	0.00	0	0.00
Roof	0	0.00	0	0.00
Skylight	0	0.00	0	0.00
Partition	0	0.00	0	0.00
Infiltration	0	0.00	0	0.00
Lighting	234	5.47		
Power	304	7.11		
People	106	2.48		
Plenum	0	0.00		
Total	4,278	100	1,520	100

Table 4.21: Building space summary—23 spaces

Inputs	
Area (m ²)	23
Volume (m ³)	56.60
Wall Area (m ²)	53
Roof Area (m ²)	0
Door Area (m ²)	6
Partition Area (m ²)	0

Window Area (m ²)	52
Skylight Area (m ²)	0
Lighting Load (W)	250
Power Load (W)	325
Number of People	1
Sensible Heat Gain/Person (W)	73
Latent Heat Gain/Person (W)	59
Infiltration Airflow (L/s)	0.0
Space Type	Office (inherited from building type)
Calculated Results	
Peak Cooling Load (W)	3,375
Peak Cooling Month and Hour	January; 4:00 PM
Peak Cooling Sensible Load (W)	3,330
Peak Cooling Latent Load (W)	45
Peak Cooling Airflow (L/s)	256.9
Peak Heating Load (W)	1,881
Peak Heating Airflow (L/s)	131.4

Components	Cooling		Heating	
	Loads (W)	Percentage of Total	Loads (W)	Percentage of Total
Wall	14	0.42	14	0.73
Window	2,783	82.44	1,868	99.27
Door	0	0.00	0	0.00
Roof	0	0.00	0	0.00
Skylight	0	0.00	0	0.00
Partition	0	0.00	0	0.00
Infiltration	0	0.00	0	0.00
Lighting	210	6.23		
Power	273	8.09		
People	95	2.82		
Plenum	0	0.00		
Total	3,375	100	1,881	100

Table 4.22: Building space summary—24 spaces

Inputs				
Area (m ²)	22			
Volume (m ³)	53.77			
Wall Area (m ²)	30			
Roof Area (m ²)	0			
Door Area (m ²)	25			
Partition Area (m ²)	0			
Window Area (m ²)	0			
Skylight Area (m ²)	0			
Lighting Load (W)	237			
Power Load (W)	309			
Number of People	1			
Sensible Heat Gain/Person (W)	73			
Latent Heat Gain/Person (W)	59			
Infiltration Airflow (L/s)	0.0			
Space Type	Office (inherited from building type)			
Calculated Results				
Peak Cooling Load (W)	1,682			
Peak Cooling Month and Hour	January; 4:00 PM			
Peak Cooling Sensible Load (W)	1,639			
Peak Cooling Latent Load (W)	43			
Peak Cooling Airflow (L/s)	128.0			
Peak Heating Load (W)	810			
Peak Heating Airflow (L/s)	56.6			
Components	Cooling		Heating	
	Loads (W)	Percentage of Total	Loads (W)	Percentage of Total
Wall	228	13.54	162	19.97
Window	0	0.00	0	0.00
Door	913	54.29	648	80.03
Roof	0	0.00	0	0.00
Skylight	0	0.00	0	0.00
Partition	0	0.00	0	0.00

Infiltration	0	0.00	0	0.00
Lighting	197	11.69		
Power	256	15.19		
People	89	5.29		
Plenum	0	0.00		
Total	1,682	100	810	100

Table 4.23: Building space summary—25 spaces

Inputs				
Area (m ²)	100			
Volume (m ³)	243.43			
Wall Area (m ²)	75			
Roof Area (m ²)	0			
Door Area (m ²)	45			
Partition Area (m ²)	0			
Window Area (m ²)	0			
Skylight Area (m ²)	0			
Lighting Load (W)	1,075			
Power Load (W)	1,397			
Number of People	4			
Sensible Heat Gain/Person (W)	73			
Latent Heat Gain/Person (W)	59			
Infiltration Airflow (L/s)	0.0			
Space Type	Office (inherited from building type)			
Calculated Results				
Peak Cooling Load (W)	4,556			
Peak Cooling Month and Hour	January; 4:00 PM			
Peak Cooling Sensible Load (W)	4,362			
Peak Cooling Latent Load (W)	195			
Peak Cooling Airflow (L/s)	346.8			
Peak Heating Load (W)	1,764			
Peak Heating Airflow (L/s)	123.2			
Components	Cooling		Heating	
	Loads (W)	Percentage of	Loads (W)	Percentage of

		Total		Total
Wall	568	12.47	472	26.77
Window	0	0.00	0	0.00
Door	1,539	33.77	1,292	73.23
Roof	0	0.00	0	0.00
Skylight	0	0.00	0	0.00
Partition	0	0.00	0	0.00
Infiltration	0	0.00	0	0.00
Lighting	890	19.53		
Power	1,157	25.39		
People	403	8.84		
Plenum	0	0.00		
Total	4,556	100	1,764	100

Table 4.24: Building space summary—26 spaces

Inputs	
Area (m ²)	27
Volume (m ³)	65.59
Wall Area (m ²)	39
Roof Area (m ²)	0
Door Area (m ²)	25
Partition Area (m ²)	0
Window Area (m ²)	0
Skylight Area (m ²)	0
Lighting Load (W)	290
Power Load (W)	376
Number of People	1
Sensible Heat Gain/Person (W)	73
Latent Heat Gain/Person (W)	59
Infiltration Airflow (L/s)	0.0
Space Type	Office (inherited from building type)
Calculated Results	
Peak Cooling Load (W)	1,497
Peak Cooling Month and Hour	January; 4:00 PM
Peak Cooling Sensible Load (W)	1,445

Peak Cooling Latent Load (W)	52
Peak Cooling Airflow (L/s)	113.9
Peak Heating Load (W)	902
Peak Heating Airflow (L/s)	63.0

Components	Cooling		Heating	
	Loads (W)	Percentage of Total	Loads (W)	Percentage of Total
Wall	235	15.72	254	28.12
Window	0	0.00	0	0.00
Door	602	40.19	648	71.88
Roof	0	0.00	0	0.00
Skylight	0	0.00	0	0.00
Partition	0	0.00	0	0.00
Infiltration	0	0.00	0	0.00
Lighting	240	16.02		
Power	312	20.82		
People	109	7.25		
Plenum	0	0.00		
Total	1,497	100	902	100

Table 4.25: Building space summary—27 spaces

Inputs	
Area (m ²)	29
Volume (m ³)	71.86
Wall Area (m ²)	54
Roof Area (m ²)	0
Door Area (m ²)	6
Partition Area (m ²)	0
Window Area (m ²)	52
Skylight Area (m ²)	0
Lighting Load (W)	317
Power Load (W)	412
Number of People	2
Sensible Heat Gain/Person (W)	73

Latent Heat Gain/Person (W)	59
Infiltration Airflow (L/s)	0.0
Space Type	Office (inherited from building type)
Calculated Results	
Peak Cooling Load (W)	4,289
Peak Cooling Month and Hour	January; 4:00 PM
Peak Cooling Sensible Load (W)	4,231
Peak Cooling Latent Load (W)	57
Peak Cooling Airflow (L/s)	326.4
Peak Heating Load (W)	1,891
Peak Heating Airflow (L/s)	132.1

Components	Cooling		Heating	
	Loads (W)	Percentage of Total	Loads (W)	Percentage of Total
Wall	29	0.69	21	1.13
Window	3,525	82.19	1,870	98.87
Door	0	0.00	0	0.00
Roof	0	0.00	0	0.00
Skylight	0	0.00	0	0.00
Partition	0	0.00	0	0.00
Infiltration	0	0.00	0	0.00
Lighting	267	6.22		
Power	347	8.09		
People	121	2.82		
Plenum	0	0.00		
Total	4,289	100	1,891	100

Table 4.26: Building space summary—28 spaces

Inputs	
Area (m ²)	27
Volume (m ³)	66.70
Wall Area (m ²)	41
Roof Area (m ²)	0
Door Area (m ²)	25

Partition Area (m ²)	0
Window Area (m ²)	0
Skylight Area (m ²)	0
Lighting Load (W)	294
Power Load (W)	383
Number of People	1
Sensible Heat Gain/Person (W)	73
Latent Heat Gain/Person (W)	59
Infiltration Airflow (L/s)	0.0
Space Type	Office (inherited from building type)
Calculated Results	
Peak Cooling Load (W)	1,532
Peak Cooling Month and Hour	January; 4:00 PM
Peak Cooling Sensible Load (W)	1,479
Peak Cooling Latent Load (W)	53
Peak Cooling Airflow (L/s)	116.6
Peak Heating Load (W)	920
Peak Heating Airflow (L/s)	64.2

Components	Cooling		Heating	
	Loads (W)	Percentage of Total	Loads (W)	Percentage of Total
Wall	259	16.90	271	29.50
Window	0	0.00	0	0.00
Door	602	39.29	648	70.50
Roof	0	0.00	0	0.00
Skylight	0	0.00		0.00
Partition	0	0.00	0	0.00
Infiltration	0	0.00	0	0.00
Lighting	244	15.92		
Power	317	20.69		
People	110	7.20		
Plenum	0	0.00		
Total	1,532	100	920	100

Table 4.27: Building space summary—29 spaces

Inputs				
Area (m ²)	28			
Volume (m ³)	67.75			
Wall Area (m ²)	66			
Roof Area (m ²)	0			
Door Area (m ²)	6			
Partition Area (m ²)	0			
Window Area (m ²)	54			
Skylight Area (m ²)	0			
Lighting Load (W)	299			
Power Load (W)	389			
Number of People	1			
Sensible Heat Gain/Person (W)	73			
Latent Heat Gain/Person (W)	59			
Infiltration Airflow (L/s)	0.0			
Space Type	Office (inherited from building type)			
Calculated Results				
Peak Cooling Load (W)	3,862			
Peak Cooling Month and Hour	January; 4:00 PM			
Peak Cooling Sensible Load (W)	3,808			
Peak Cooling Latent Load (W)	54			
Peak Cooling Airflow (L/s)	293.9			
Peak Heating Load (W)	2,262			
Peak Heating Airflow (L/s)	158.0			
Components	Cooling		Heating	
	Loads (W)	Percentage of Total	Loads (W)	Percentage of Total
Wall	64	1.65	66	2.92
Window	2,876	74.46	1,937	85.66
Door	230	5.96	258	11.42
Roof	0	0.00	0	0.00
Skylight	0	0.00	0	0.00
Partition	0	0.00	0	0.00

Infiltration	0	0.00	0	0.00
Lighting	252	6.51		
Power	327	8.47		
People	114	2.95		
Plenum	0	0.00		
Total	3,862	100	2,262	100

Table 4.28: Building space summary—30 spaces

Inputs				
Area (m ²)	26			
Volume (m ³)	63.05			
Wall Area (m ²)	53			
Roof Area (m ²)	0			
Door Area (m ²)	6			
Partition Area (m ²)	0			
Window Area (m ²)	38			
Skylight Area (m ²)	0			
Lighting Load (W)	278			
Power Load (W)	362			
Number of People	1			
Sensible Heat Gain/Person (W)	73			
Latent Heat Gain/Person (W)	59			
Infiltration Airflow (L/s)	0.0			
Space Type	Office (inherited from building type)			
Calculated Results				
Peak Cooling Load (W)	4,278			
Peak Cooling Month and Hour	January; 4:00 PM			
Peak Cooling Sensible Load (W)	4,227			
Peak Cooling Latent Load (W)	50			
Peak Cooling Airflow (L/s)	325.5			
Peak Heating Load (W)	1,520			
Peak Heating Airflow (L/s)	106.2			
Components	Cooling		Heating	
	Loads (W)	Percentage of	Loads (W)	Percentage of

		Total		Total
Wall	208	4.87	153	10.05
Window	3,425	80.06	1,367	89.95
Door	0	0.00	0	0.00
Roof	0	0.00	0	0.00
Skylight	0	0.00	0	0.00
Partition	0	0.00	0	0.00
Infiltration	0	0.00	0	0.00
Lighting	234	5.47		
Power	304	7.11		
People	106	2.48		
Plenum	0	0.00		
Total	4,278	100	1,520	100

Table 4.29: Building space summary—31 spaces

Inputs	
Area (m ²)	23
Volume (m ³)	56.60
Wall Area (m ²)	53
Roof Area (m ²)	0
Door Area (m ²)	6
Partition Area (m ²)	0
Window Area (m ²)	52
Skylight Area (m ²)	0
Lighting Load (W)	250
Power Load (W)	325
Number of People	1
Sensible Heat Gain/Person (W)	73
Latent Heat Gain/Person (W)	59
Infiltration Airflow (L/s)	0.0
Space Type	Office (inherited from building type)
Calculated Results	
Peak Cooling Load (W)	3,375
Peak Cooling Month and Hour	January; 4:00 PM
Peak Cooling Sensible Load (W)	3,330

Peak Cooling Latent Load (W)	45			
Peak Cooling Airflow (L/s)	256.9			
Peak Heating Load (W)	1,881			
Peak Heating Airflow (L/s)	131.4			
Components	Cooling		Heating	
	Loads (W)	Percentage of Total	Loads (W)	Percentage of Total
Wall	14	0.42	14	0.73
Window	2,783	82.44	1,868	99.27
Door	0	0.00	0	0.00
Roof	0	0.00	0	0.00
Skylight	0	0.00	0	0.00
Partition	0	0.00	0	0.00
Infiltration	0	0.00	0	0.00
Lighting	210	6.23		
Power	273	8.09		
People	95	2.82		
Plenum	0	0.00		
Total	3,375	100	1,881	100

Table 4.30: Building space summary—32 spaces

Inputs	
Area (m ²)	22
Volume (m ³)	53.77
Wall Area (m ²)	30
Roof Area (m ²)	0
Door Area (m ²)	25
Partition Area (m ²)	0
Window Area (m ²)	0
Skylight Area (m ²)	0
Lighting Load (W)	237
Power Load (W)	309
Number of People	1
Sensible Heat Gain/Person (W)	73

Latent Heat Gain/Person (W)	59
Infiltration Airflow (L/s)	0.0
Space Type	Office (inherited from building type)
Calculated Results	
Peak Cooling Load (W)	1,682
Peak Cooling Month and Hour	January; 4:00 PM
Peak Cooling Sensible Load (W)	1,639
Peak Cooling Latent Load (W)	43
Peak Cooling Airflow (L/s)	128.0
Peak Heating Load (W)	810
Peak Heating Airflow (L/s)	56.6

Components	Cooling		Heating	
	Loads (W)	Percentage of Total	Loads (W)	Percentage of Total
Wall	228	13.54	162	19.97
Window	0	0.00	0	0.00
Door	913	54.29	648	80.03
Roof	0	0.00	0	0.00
Skylight	0	0.00	0	0.00
Partition	0	0.00	0	0.00
Infiltration	0	0.00	0	0.00
Lighting	197	11.69		
Power	256	15.19		
People	89	5.29		
Plenum	0	0.00		
Total	1,682	100	810	100

Table 4.31: Building space summary—33 spaces

Inputs	
Area (m ²)	100
Volume (m ³)	243.43
Wall Area (m ²)	65
Roof Area (m ²)	0
Door Area (m ²)	45

Partition Area (m ²)	0
Window Area (m ²)	0
Skylight Area (m ²)	0
Lighting Load (W)	1,075
Power Load (W)	1,397
Number of People	4
Sensible Heat Gain/Person (W)	73
Latent Heat Gain/Person (W)	59
Infiltration Airflow (L/s)	0.0
Space Type	Office (inherited from building type)
Calculated Results	
Peak Cooling Load (W)	4,266
Peak Cooling Month and Hour	January; 4:00 PM
Peak Cooling Sensible Load (W)	4,071
Peak Cooling Latent Load (W)	195
Peak Cooling Airflow (L/s)	324.6
Peak Heating Load (W)	1,463
Peak Heating Airflow (L/s)	102.2

Components	Cooling		Heating	
	Loads (W)	Percentage of Total	Loads (W)	Percentage of Total
Wall	527	12.35	430	29.37
Window	0	0.00	0	0.00
Door	1,289	30.22	1,033	70.63
Roof	0	0.00	0	0.00
Skylight	0	0.00	0	0.00
Partition	0	0.00	0	0.00
Infiltration	0	0.00	0	0.00
Lighting	890	20.86		
Power	1,157	27.12		
People	403	9.44		
Plenum	0	0.00		
Total	4,266	100	1,463	100

Table 4.32: Building space summary—34 spaces

Inputs				
Area (m ²)	27			
Volume (m ³)	65.59			
Wall Area (m ²)	39			
Roof Area (m ²)	0			
Door Area (m ²)	25			
Partition Area (m ²)	0			
Window Area (m ²)	0			
Skylight Area (m ²)	0			
Lighting Load (W)	290			
Power Load (W)	376			
Number of People	1			
Sensible Heat Gain/Person (W)	73			
Latent Heat Gain/Person (W)	59			
Infiltration Airflow (L/s)	0.0			
Space Type	Office (inherited from building type)			
Calculated Results				
Peak Cooling Load (W)	1,497			
Peak Cooling Month and Hour	January; 4:00 PM			
Peak Cooling Sensible Load (W)	1,445			
Peak Cooling Latent Load (W)	52			
Peak Cooling Airflow (L/s)	113.9			
Peak Heating Load (W)	902			
Peak Heating Airflow (L/s)	63.0			
Components	Cooling		Heating	
	Loads (W)	Percentage of Total	Loads (W)	Percentage of Total
Wall	235	15.72	254	28.12
Window	0	0.00	0	0.00
Door	602	40.19	648	71.88
Roof	0	0.00	0	0.00
Skylight	0	0.00	0	0.00
Partition	0	0.00	0	0.00

Infiltration	0	0.00	0	0.00
Lighting	240	16.02		
Power	312	20.82		
People	109	7.25		
Plenum	0	0.00		
Total	1,497	100	902	100

Table 4.33: Building space summary—35 spaces

Inputs				
Area (m ²)	27			
Volume (m ³)	66.70			
Wall Area (m ²)	41			
Roof Area (m ²)	0			
Door Area (m ²)	25			
Partition Area (m ²)	0			
Window Area (m ²)	0			
Skylight Area (m ²)	0			
Lighting Load (W)	294			
Power Load (W)	383			
Number of People	1			
Sensible Heat Gain/Person (W)	73			
Latent Heat Gain/Person (W)	59			
Infiltration Airflow (L/s)	0.0			
Space Type	Office (inherited from building type)			
Calculated Results				
Peak Cooling Load (W)	1,532			
Peak Cooling Month and Hour	January; 4:00 PM			
Peak Cooling Sensible Load (W)	1,479			
Peak Cooling Latent Load (W)	53			
Peak Cooling Airflow (L/s)	116.6			
Peak Heating Load (W)	920			
Peak Heating Airflow (L/s)	64.2			
Components	Cooling		Heating	
	Loads (W)	Percentage of	Loads (W)	Percentage of

		Total		Total
Wall	259	16.90	271	29.50
Window	0	0.00	0	0.00
Door	602	39.29	648	70.50
Roof	0	0.00	0	0.00
Skylight	0	0.00	0	0.00
Partition	0	0.00	0	0.00
Infiltration	0	0.00	0	0.00
Lighting	244	15.92		
Power	317	20.69		
People	110	7.20		
Plenum	0	0.00		
Total	1,532	100	920	100

Table 4.34: Building space summary—36 spaces

Inputs	
Area (m ²)	29
Volume (m ³)	71.86
Wall Area (m ²)	54
Roof Area (m ²)	0
Door Area (m ²)	6
Partition Area (m ²)	0
Window Area (m ²)	52
Skylight Area (m ²)	0
Lighting Load (W)	317
Power Load (W)	412
Number of People	2
Sensible Heat Gain/Person (W)	73
Latent Heat Gain/Person (W)	59
Infiltration Airflow (L/s)	0.0
Space Type	Office (inherited from building type)
Calculated Results	
Peak Cooling Load (W)	4,289
Peak Cooling Month and Hour	January; 4:00 PM
Peak Cooling Sensible Load (W)	4,231

Peak Cooling Latent Load (W)	57
Peak Cooling Airflow (L/s)	326.4
Peak Heating Load (W)	1,891
Peak Heating Airflow (L/s)	132.1

Components	Cooling		Heating	
	Loads (W)	Percentage of Total	Loads (W)	Percentage of Total
Wall	29	0.69	21	1.13
Window	3,525	82.19	1,870	98.87
Door	0	0.00	0	0.00
Roof	0	0.00	0	0.00
Skylight	0	0.00	0	0.00
Partition	0	0.00	0	0.00
Infiltration	0	0.00	0	0.00
Lighting	267	6.22		
Power	347	8.09		
People	121	2.82		
Plenum	0	0.00		
Total	4,289	100	1,891	100

Table 4.35: Building space summary—37 spaces

Inputs	
Area (m ²)	28
Volume (m ³)	67.75
Wall Area (m ²)	56
Roof Area (m ²)	0
Door Area (m ²)	6
Partition Area (m ²)	0
Window Area (m ²)	54
Skylight Area (m ²)	0
Lighting Load (W)	299
Power Load (W)	389
Number of People	1
Sensible Heat Gain/Person (W)	73

Latent Heat Gain/Person (W)	59
Infiltration Airflow (L/s)	0.0
Space Type	Office (inherited from building type)
Calculated Results	
Peak Cooling Load (W)	3,594
Peak Cooling Month and Hour	January; 4:00 PM
Peak Cooling Sensible Load (W)	3,540
Peak Cooling Latent Load (W)	54
Peak Cooling Airflow (L/s)	273.5
Peak Heating Load (W)	1,961
Peak Heating Airflow (L/s)	137.0

Components	Cooling		Heating	
	Loads (W)	Percentage of Total	Loads (W)	Percentage of Total
Wall	26	0.73	24	1.21
Window	2,876	80.01	1,937	98.79
Door	0	0.00	0	0.00
Roof	0	0.00	0	0.00
Skylight	0	0.00	0	0.00
Partition	0	0.00	0	0.00
Infiltration	0	0.00	0	0.00
Lighting	252	7.00		
Power	327	9.10		
People	114	3.17		
Plenum	0	0.00		
Total	3,594	100	1,961	100

Table 4.36: Building space summary—39 spaces

Inputs	
Area (m ²)	28
Volume (m ³)	68.55
Wall Area (m ²)	38
Roof Area (m ²)	0
Door Area (m ²)	25

Partition Area (m ²)	0
Window Area (m ²)	0
Skylight Area (m ²)	0
Lighting Load (W)	303
Power Load (W)	393
Number of People	1
Sensible Heat Gain/Person (W)	73
Latent Heat Gain/Person (W)	59
Infiltration Airflow (L/s)	0.0
Space Type	Office (inherited from building type)
Calculated Results	
Peak Cooling Load (W)	1,942
Peak Cooling Month and Hour	January; 4:00 PM
Peak Cooling Sensible Load (W)	1,887
Peak Cooling Latent Load (W)	55
Peak Cooling Airflow (L/s)	147.8
Peak Heating Load (W)	889
Peak Heating Airflow (L/s)	62.1

Components	Cooling		Heating	
	Loads (W)	Percentage of Total	Loads (W)	Percentage of Total
Wall	339	17.46	241	27.11
Window	0	0.00	0	0.00
Door	913	47.02	648	72.89
Roof	0	0.00	0	0.00
Skylight	0	0.00	0	0.00
Partition	0	0.00	0	0.00
Infiltration	0	0.00	0	0.00
Lighting	251	12.91		
Power	326	16.78		
People	113	5.84		
Plenum	0	0.00		
Total	1,942	100	889	100

Table 4.37: Building space summary—40 spaces

Inputs				
Area (m ²)	26			
Volume (m ³)	63.05			
Wall Area (m ²)	53			
Roof Area (m ²)	0			
Door Area (m ²)	6			
Partition Area (m ²)	0			
Window Area (m ²)	38			
Skylight Area (m ²)	0			
Lighting Load (W)	278			
Power Load (W)	362			
Number of People	1			
Sensible Heat Gain/Person (W)	73			
Latent Heat Gain/Person (W)	59			
Infiltration Airflow (L/s)	0.0			
Space Type	Office (inherited from building type)			
Calculated Results				
Peak Cooling Load (W)	4,278			
Peak Cooling Month and Hour	January; 4:00 PM			
Peak Cooling Sensible Load (W)	4,227			
Peak Cooling Latent Load (W)	50			
Peak Cooling Airflow (L/s)	325.5			
Peak Heating Load (W)	1,520			
Peak Heating Airflow (L/s)	106.2			
Components	Cooling		Heating	
	Loads (W)	Percentage of Total	Loads (W)	Percentage of Total
Wall	208	4.87	153	10.05
Window	3,425	80.06	1,367	89.95
Door	0	0.00	0	0.00
Roof	0	0.00	0	0.00
Skylight	0	0.00	0	0.00
Partition	0	0.00	0	0.00

Infiltration	0	0.00	0	0.00
Lighting	234	5.47		
Power	304	7.11		
People	106	2.48		
Plenum	0	0.00		
Total	4,278	100	1,520	100

4.4 Building Space Heating/Cooling Energy Reduction

Annual energy reductions are obtained from the different components of the building as illustrated in the above table. Those contribution of these components are as follows:

1. Concrete wall: The thermal mass property of concrete walls enables building materials to absorb, store and later release significant amounts of heat. Buildings constructed with concrete and masonry have a unique energy-saving advantage because of their inherent thermal mass. These building material elements absorb energy slowly and hold it for much longer periods of time than do less massive concrete wall materials. This type of delay reduces heat transfer through a thermal mass building component, leading to many important advantages.
2. Energy efficient window: Such windows are an important consideration for both new and existing buildings. Heat gain and loss through windows are currently responsible for 25–30% of commercial heating and cooling energy use.
3. Light: Light-reflective floors and walls improve illumination inside buildings by reflecting light from both natural and artificial sources. These surfaces provide a background that reduces shadows from large stationary objects. Instead of adding more costly lighting units or increasing their intensity, creating a light surface is a passive means of improving illumination. For example, ordinary concrete and other reflective surfaces can reduce energy costs associated with indoor and outdoor lighting. Reflective surfaces will reduce the number of fixtures and lighting required. Concrete wall exposed to the interior could help reduce interior lighting requirements. In addition, coloured exterior walls can reduce outdoor lighting requirements. Energy costs for lighting concrete parking lots can be 35% less than those for asphalt parking lots.

4.5 Conclusion

This chapter covers the first simulation part in the building solar energy simulation. Autodesk Revit building energy analysis requires space/room segregation to estimate energy required against space utilisation. The contents of the spaces are fed as input parameters and the component values are displayed as output. This chapter is mainly focused on space heating/cooling load calculations. Hence, these heating/cooling data on spaces prepare the pathway to the base run (chapter 5) building solar energy simulation.

Chapter 5: Base Run Building Solar Energy Simulation

5.1 Introduction

This chapter covers two main topics, ‘Base run solar building energy simulation’ and ‘Renewable energy sources simulations’ as subchapter sections, and hence their introductory descriptions are outlined:

1. Base run solar building energy simulation

Sun’s solar irradiation energy simulation for building focused on the concept of the amount of solar irradiation energy that can be absorbed by the building elements during a non-cloudy day (clear sunny day). This type of simulation method can be performed using many different techniques and step procedures; it depends upon the researcher’s skills and selection of the appropriate tools. One of the techniques is building orientation.

Orientation is defined as the positioning of a building considering seasonal variations in the Sun’s path since the solar irradiation intensity varies correspondingly. The best building orientation could increase the energy efficiency of buildings, making it more comfortable for occupants to live or to work in the building and also making the operations of the building less expensive.

For the purpose of this research, a procedure in three steps or chapters was chosen to complete the research aim and achieve significant maximised outcomes, which this chapter details in the second part.

2. Renewable energy source simulation

Renewable energies are clean and inexhaustible. Renewable energy differs from fossil fuel energy principally in terms of diversity. Renewable energy is abundant and has the potential for use anywhere on the planet, owing to its not producing greenhouse gases or polluting emissions. In addition, the costs of renewable energies are also falling and at a sustainable rate, whereas the general cost trend for fossil fuels is in the opposite direction in spite of their present volatility. Growth in clean energies is currently unstoppable, as reflected in the 2015 statistics of the International Energy Agency:

Renewable energy represented nearly half of all new electricity generation capacity installed in 2014. According to the study, world electricity demand will have increased by 70% by 2040. Clean energy development is vital for combating climate change and limiting its most devastating effects.

5.2 Building Solar Energy Simulation Process

Base run building energy simulation is a continuation of simulation part of building heating/cooling requirement (chapter 4), but it is more in depth and covers all parts in the building. Building solar energy simulation can be carried out either using ‘conceptual mass’ or the ‘whole building elements’: ‘Conceptual mass’ simulates the building as a block of mass and conversely, the ‘whole building element’ covers every building part used in this thesis project. Thus, creating building elements, such as walls, roofs, floors and windows, as room/space elements are optional. Defining energy settings, especially location and building type, and submitting the whole building energy simulation to web-based energy simulation is also possible.

Further, the energy analytical model (building engineering data) created from the building elements can also be exported to third-party applications for further analysis, in a variety of common formatted files: for example, gbXML can be exported to US Department of Energy (DOE-2) and Energy Plus [72] building energy simulation software applications.

5.3 Single Day Building Energy Solar Simulation

For the purpose of this thesis research project, building solar irradiation simulation was conducted using Autodesk Revit energy analysis for a single day for a period of six hours from 10 am to 4 pm during summer solstice seasons, as shown in Figure 5.1. During the six hours, in the building solar irradiation simulation the sunlight intensity continues to increase until it approaches the maximum intensity at midday. Thus, at this time the building absorbs maximum solar energy. After midday, the sunlight intensity steadily reduces and its maximum intensity also reduces until it reduces to zero after 6 pm.

The six-hour simulation period was an adequate length of time, which helps to calculate the building’s average estimated annual energy consumption, particularly the HVAC

load consumption, because during this period the HVAC load demand increases. During this solar building simulation process, every building element exhibits/experiences solar irradiation intensity. Thus, this ensures no part of the building is excluded from being tested for the solar energy absorption.

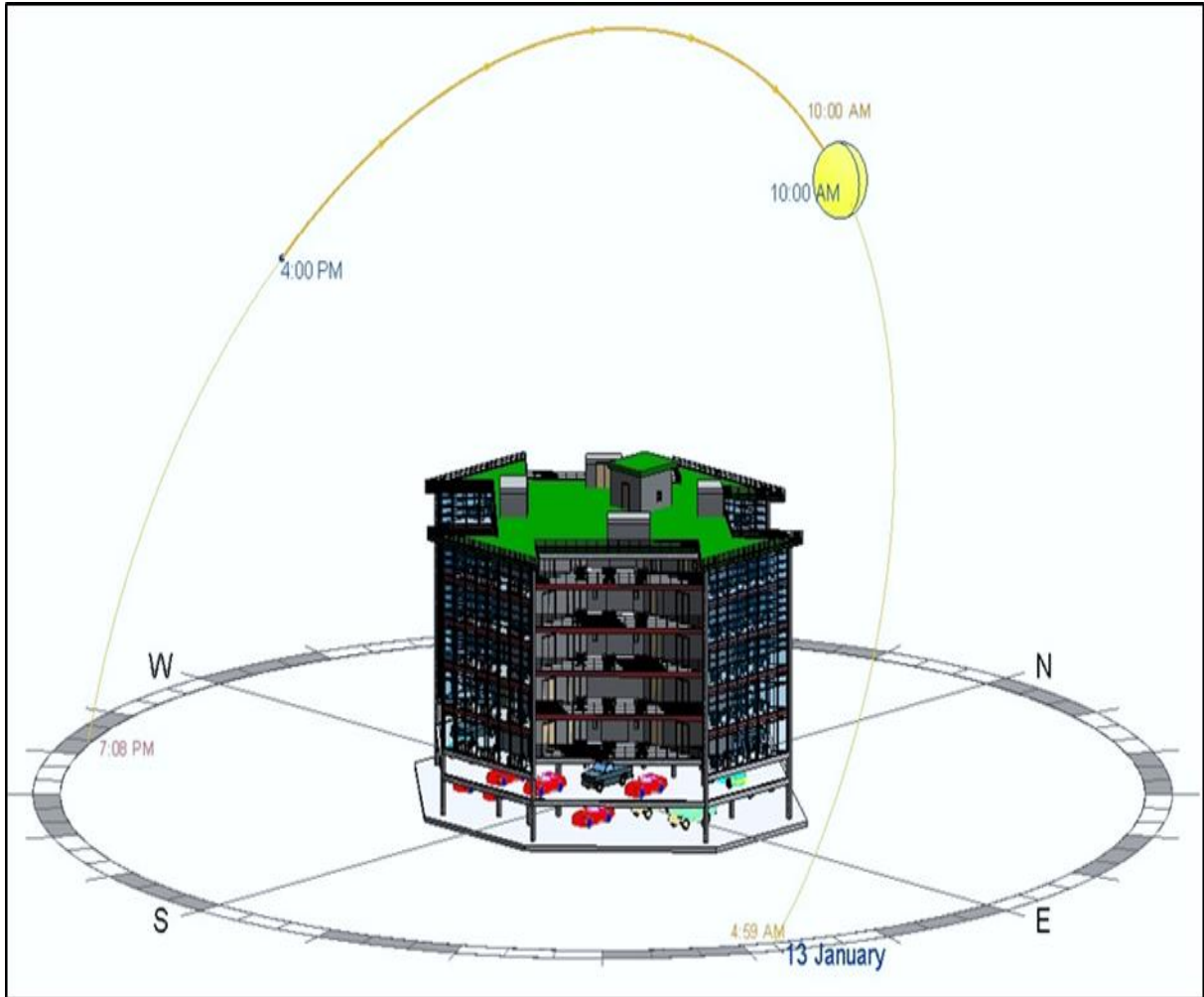


Figure 5.1: Base run building solar energy simulation

5.4 Base Run Simulation Parameter Data

Energy simulation requires data, such as BIM, as parameters with specific details and units to enable the algorithm to compute the given task correctly and efficiently in minimal time. Thus, these input parameters, whose values are shown in Tables 5.1 and 5.2, have significant effect on the energy simulation process and produced significant energy reductions. Similar to the input parameters, output parameters are proposed by the simulation system with significant cost-effective economic values, which also lead to GB approaching system/NetZero-energy. Thus, this base run energy simulation,

which also acts as a reference point for the alternative design simulation, demonstrates the building performance, annual estimated energy usage, life-cycle energy use and cost and renewable potential energies with their specific data, signifying the controllable use of energy. In addition, it also demonstrates net CO₂ emissions, annual energy use/cost, annual fuel energy use, annual electric energy use, annual monthly heating/cooling loads, annual monthly fuel/electricity consumption and annual monthly peak demand. Further, in this section, weather file parameters, such as annual monthly wind speed/frequency distribution, annual monthly weather file design data, average diurnal temperature and average humidity, are briefly analysed as the major contributors to the building solar energy simulation. Thus, the actual processing of the simulations was performed briefly based on the effects of environmental weather files [73, 74]. Hence, the action of weather files affects the actual building size and area to produce output results. Further, the action of weather files is forced also to the alternative design energy simulation to demonstrate/produce output in detail with much reduced results. Hence, forecasting/estimating using simulations of specific regional weather files annual monthly speed/frequency distribution behaviour in general is used to determine a plan for energy usage estimations. For example, the weather station used for this research thesis project is Sydney's weather station, as specified in the Location Weather and Site dialog of Sydney. Files of forecasted weather for these regions can be accessed from this station or from any other nearby weather station.

5.5 Base Run Simulation Building Performance

During this simulation, maximum/minimum temperatures at the project location are used and gross floor area of the analysed model space was formed by subtracting the net wall area. In this office commercial building spaces/rooms, heating and cooling loads are driven by internal gains from heat emitted by people, lighting and equipment and by the building envelope. Thus, HVAC loads are directly dependent on weather files, and the lights depend on the building conditioned indoor space. Hence, the building performance shown in Table 5.1 is an example of the regional weather file definition.

Table 5.1: Base run building performance

Location:	Sydney NSW, Australia
Weather Station:	600300
Outdoor Temperature:	Max: 37°C/Min: 6°C
Floor Area:	1,306 m ²
Exterior Wall Area:	633 m ²
Average Lighting Power:	10.23 W / m ²
People:	52 people
Exterior Window Ratio:	1.48
Electrical Cost:	\$0.06 / kWh
Fuel Cost:	\$0.78 / Therm

5.5.1 Annual energy use intensity

Table 5.2 shows annual average electricity, EUI per kilo-watt hour, per square meter, per year (kWh/m²/year) in the first row, annual average fuel, EUI per Mega joule, per square meter, per year (MJ/m²/year) in the second row and total of both annual average EUI in the third row. EUI is a measurement of per-area metric, and it is a convenient method of comparing energy consumption when the analysed building model uses different energy sources. 710MJ/m²/year signifies good energy performance.

Table 5.2: Annual energy use intensity

Electricity EUI:	125 kWh / sm / yr
Fuel EUI:	262 MJ / sm / yr
Total EUI:	710 MJ / sm / yr

5.5.2 Life-cycle energy use

The average energy simulation results for the building life-cycle period are shown in Table 5.3, with average annual life-cycle electricity use in the first row, average annual life-cycle fuel use in the second row, average annual life-cycle total cost in the third row and average annual life-cycle discount rate in the fourth row. Thus, the Autodesk Revit energy analysis simulation system algorithm is intelligent enough to include the estimated discount rate (6.1%) of the average annual cycle-life for 30 years. These results signify best energy performance.

Table 5.3: Energy life-cycle use

Life Cycle Electricity Use:	5,073,816 kWh
Life Cycle Fuel Use:	10,676,574 MJ
Life Cycle Energy Cost	\$176,519
*30-year life and 6.1% discount rate for costs	

5.5.3 Annual potential energy

The Autodesk Revit energy analysis tool analyses the weather at the building's roof surfaces for the estimated potential to generate electricity when PV cell panels and wind turbine are planted. Table 5.4 presents three different types of PV cell efficiency, reflecting the PV cells' ability to convert sunlight into electricity and wind power that can be generated from one 15-inch-diameter horizontal axis. These renewable potential energy simulation results provided by the system are from, as mentioned previously, three significant options of solar PV cells, low, medium and high efficiency, ranging from 5 to 15%. From the highest efficiency, an average amount of power can be extracted, approximately over 72,442kWh/yr. This is high potential energy compared with the annual building energy consumption. Conversely, the proposed wind turbine potential energy simulation result is low compared with the annual building energy consumption. The wind potential energy of this region lacks the capacity to generate adequate energy. Conversely, the PV cell renewable potential energy indicates it is worthwhile using it, even when the initial cost and the maintenance cost are added.

Table 5.4: Annual estimated potential energy

Roof Mounted PV System (Low efficiency):	24,147 kWh / yr
Roof Mounted PV System (Medium efficiency):	48,295 kWh / yr
Roof Mounted PV System (High efficiency):	72,442 kWh / yr
Single 15' Wind Turbine Potential:	2,208 kWh / yr
*PV efficiencies are assumed to be 5%, 10% and 15% for low, medium and high efficiency systems	

5.5.4 Annual carbon emission

The annual carbon emissions, as shown in Figure 5.2, consist of the annual energy use, energy generation potential and the net CO₂, with the net CO₂ emissions shown in light blue colour obtained by adding the total known amount of carbon released (70 + 17 = 87) and subtracting the negative carbon emission [87 - (30 + 0) = 57]

generated by the renewable energy sources mainly from the PV cells. The net CO₂ was found to be equivalent to 57 metric tons per year. This is a significant reduction in energy usage versus achieving carbon neutralities, which means that when energy consumption increases, especially that of fuel energy, the CO₂ emission, also, increases proportionally. Further, the PV cell not only yields high potential energy kilowatt-hour, but also acts in the CO₂ negativity process (removing carbon CO₂ from the compound area) where the wind turbine is of use only ensuring CO₂ neutrality only.

To calculate CO₂ emissions for the project located in Sydney Australia, Autodesk Revit used utility emissions data from Carbon Monitoring for Action data. Emissions data for the project are based on the on-site fuel usage and fuel sources' generated of electricity usage in the region. For example, a project located in a region with electrical power plants powered by coal has higher CO₂ emissions per kWh of electricity consumption than a similar project located in a region where electrical power plants are powered by hydroelectricity.

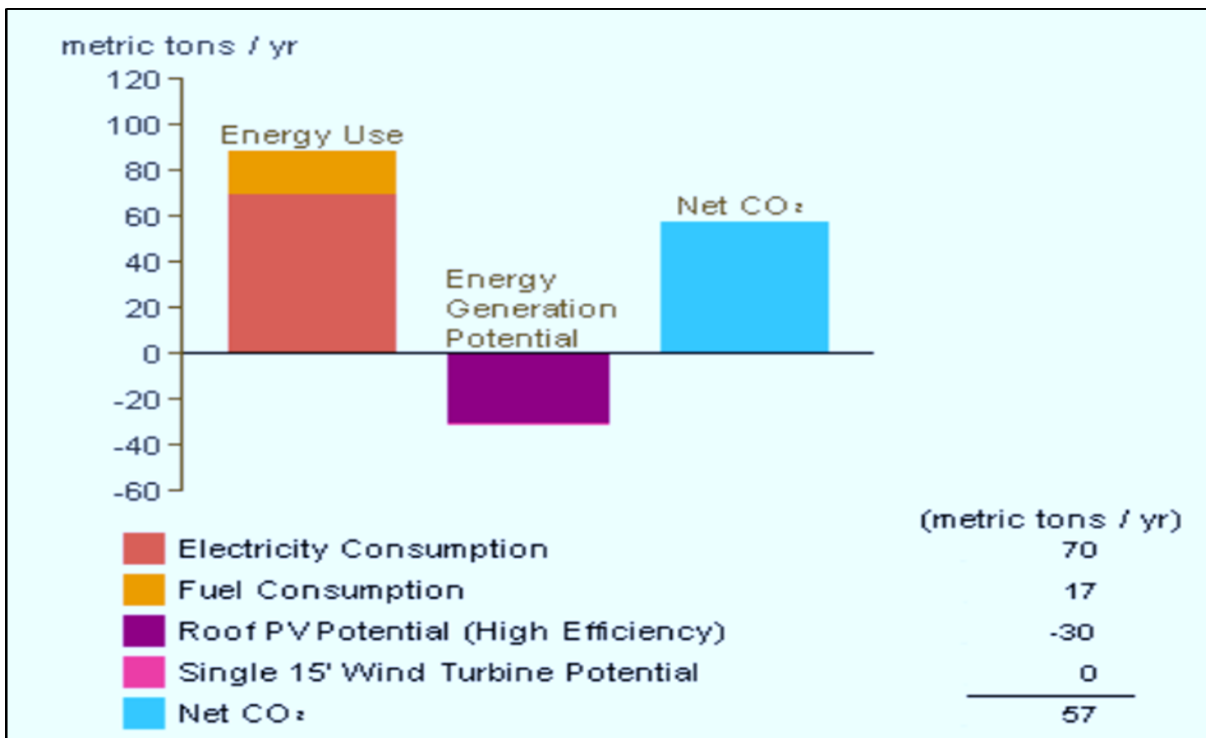


Figure 5.2: Annual carbon emission and net CO₂ calculations

5.5.5 Annual energy usage cost

The base run simulation report in Figure 5.3 shows total annual energy usage cost of electricity and fuel. The fuel and electricity usages are dissimilar. However, the cost of

electricity per kWh is higher than the fuel cost for the same kWh. This is a good option to use alternative cost-effective energy. The Autodesk Revit base run energy simulation list shown in Table 5.5 states the cost of electricity per unit of kWh as \$0.06 and the cost fuel energy per unit of MJ as \$0.007. MJ is converted to kWh using the universal energy conversion formula of $1\text{kWh} = 3.6\text{MJ}$; then, the calculation shows $\$0.007 \times 3.6 = \0.0252 . Thus, the usage cost of fuel energy is very economical compared with electricity energy usage cost. Annualised energy cost and consumption information can inform building energy cost comparisons and early design decisions. Costs are estimated using state-wide, territory-wide or nation-wide average utility rates.

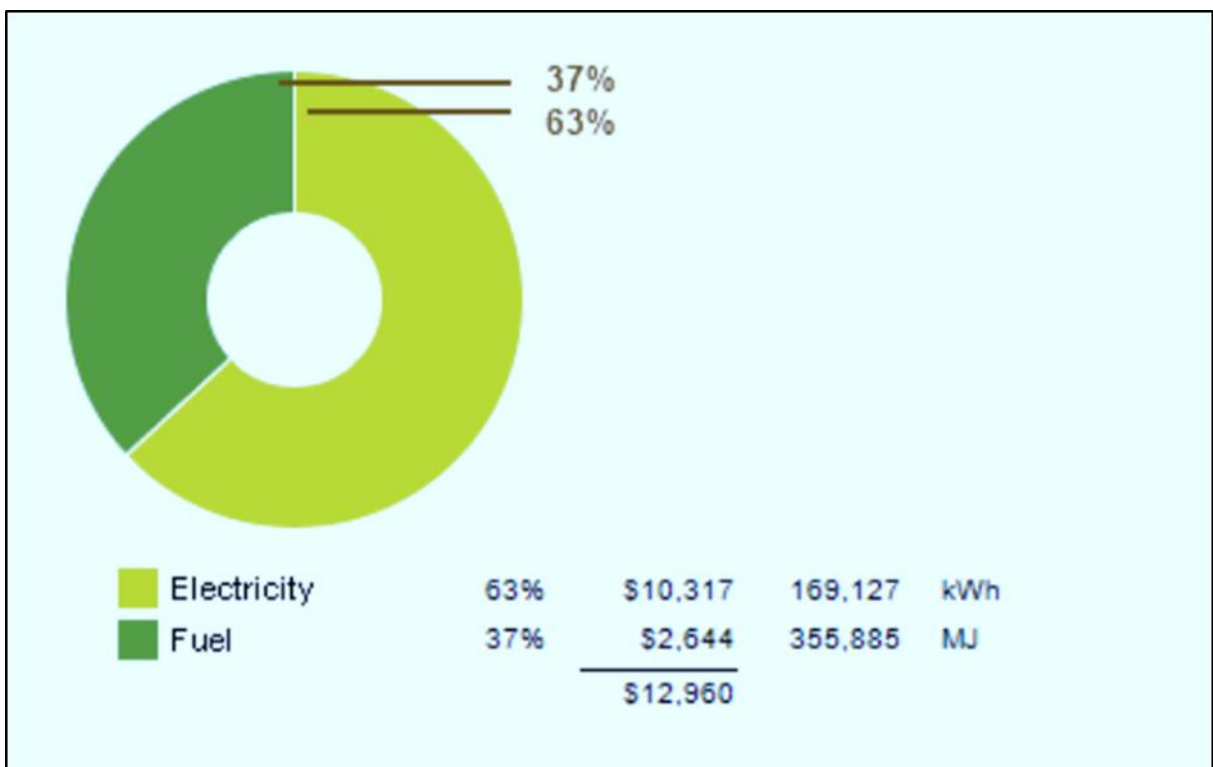


Figure 5.3: Annual energy usage cost

5.5.6 Annual fuel energy use

Building energy is mainly consumed by the HVAC system and both draw significant amounts of energy (electricity and fuel). The HVAC and hot water load analyses report chart shown in Figure 5.4 presents the amount of energy used by each. From this chart report analysis, it can be noticed that the HVAC loads dominate (92%) the usage of energy, while hot water energy usage is significantly limited, at the minimum of 8%. This implies that the simulation system used to analysis this energy simulation is a very effective method that uses/programmed the hot water to function by avoiding on peak-

demand periods, while it is too difficult to avoid functioning of the HVAC loads during on peak-demand hours. This is one of the causes that the HVAC loads draw significant amount of power. However, it is not easy to significantly minimise usage of HVAC loads during both opposite (hot/cold) seasons, especially on peak- demand periods. This chart shows the percentage of total fuel use, costs and individual unit for each end use, which is helpful in identifying most estimated end usage. Hence, a strategic plan to reduce energy consumption can be established for the project.

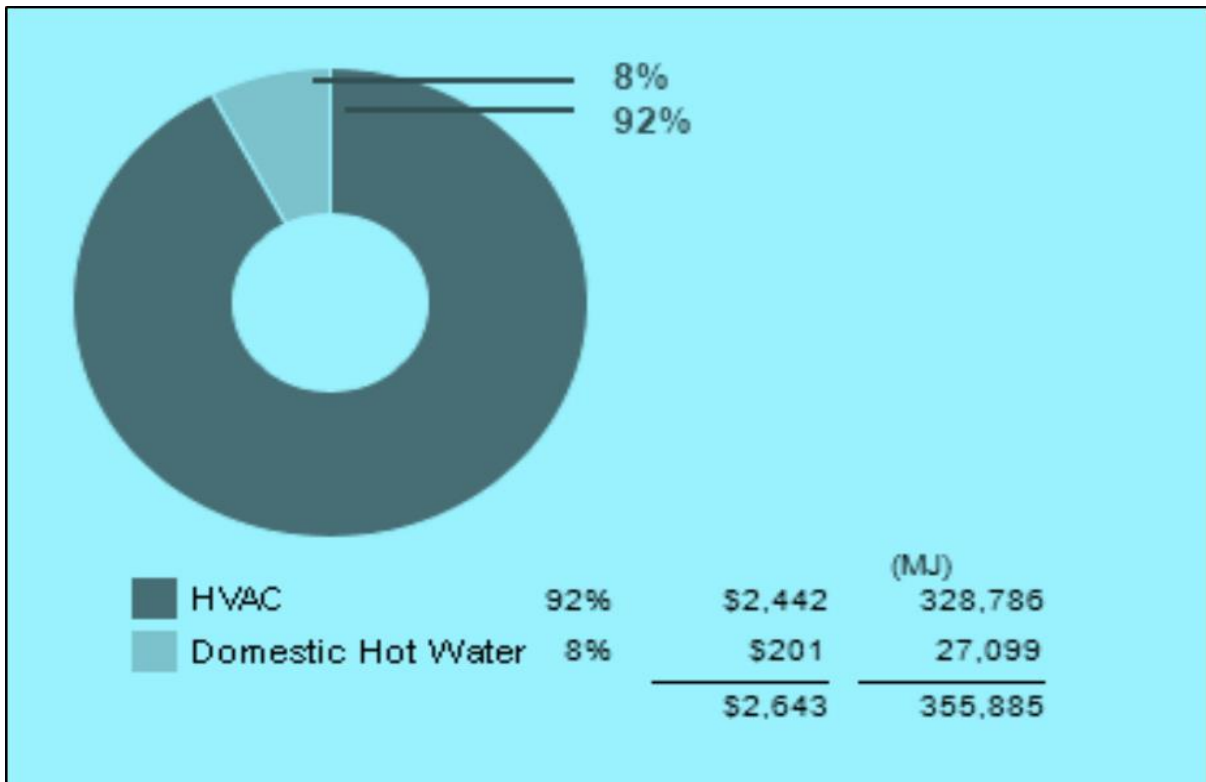


Figure 5.4: Annual fuel energy use

5.5.7 Annual electricity energy use

The base run energy simulation summarised usages for each energy source to provide the user a hint about where to save energy and to avoid using energy unnecessarily. Figure 5.5 shows how the end use energy loads are supplied among the building’s main energy usages. In this configuration, it can be noticed that the supply energy and costs are equivalently balanced between the HVAC, lighting and miscellaneous equipment loads. Miscellaneous equipment includes computers, elevators and miscellaneous appliances. For each end use, the chart shows the percentage of total electricity usage, costs and kWh. By understanding the end use that requires the most electricity, this can

be focused on in the strategic plan to reduce overall energy consumption for the project. For example, the strategic plan will be very helpful in determining ways to program/schedule equipment function time, to ensure cost-effective use to according to the utility energy Supply Company's rate for the peak-demand and nonpeak-demand periods.

Peak-demand period rates information data can be found from the utility energy supply energy company website or by directly calling the company call centre.

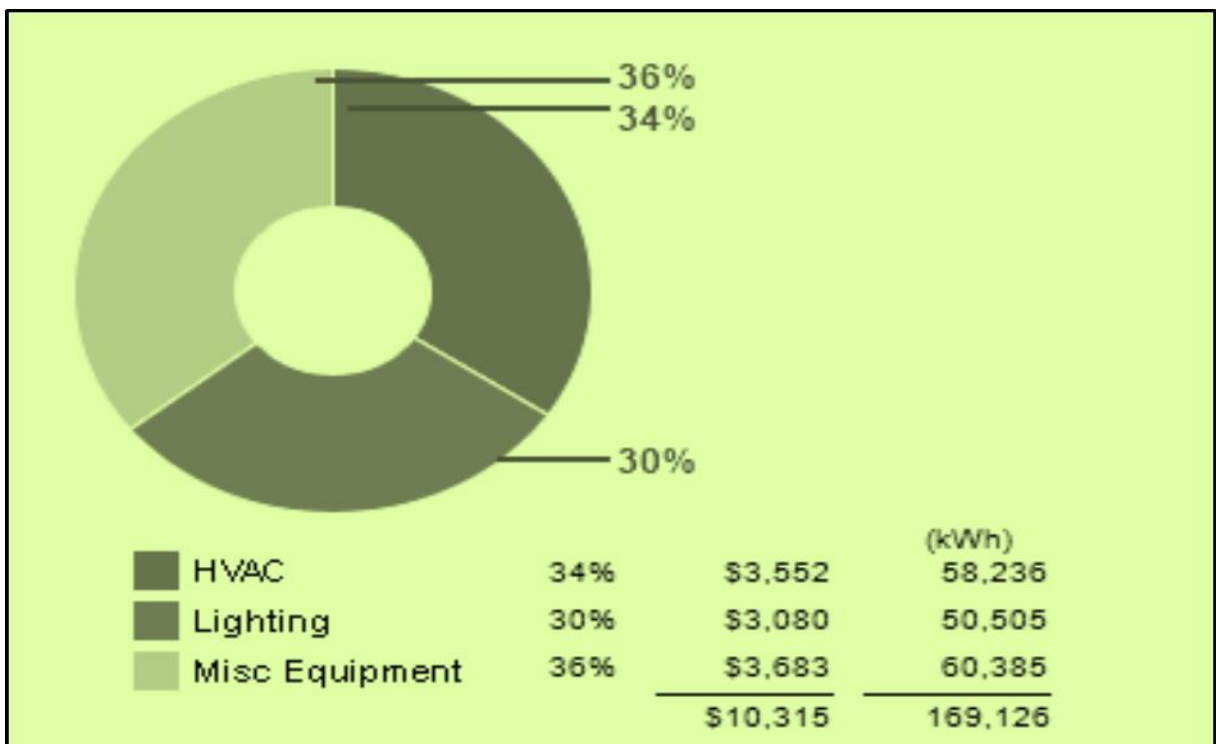


Figure 5.5: HVAC, lighting and other equipment annual energy usage

5.5.8 Annual, monthly heating load

The base run energy simulation calculates the building's annual energy in annually summarised reports, but in addition, it also calculates monthly details of cooling, heating, fuel, electric and peak-demand loads, as shown in Figure 5.6, where each particular building element/part is simulated against its capabilities of being energy efficient and ability to absorb solar energies, such as concrete walls, curtain walls, roofs and conductive windows, which are substantial examples. At present, the concept of green roof is emerging for its ability to reduce heat flow into and out of the surface covered. There is also evidence that the benefit is much greater in summer time because the reflectivity of the leaves of the plants and the evaporation rates are maximised in the

summer. Green roofs reduce the heat flux through the roof, and reduction in energy for cooling or heating can lead to significant cost savings. Shading the outer surface of the building envelope has been shown to be more effective than internal insulation. In summer, green roofs protect buildings from direct solar heat.

The largest negative value for June is window conduction; heat loss from conduction through windows represents the largest single monthly demand for heat in June. However, miscellaneous equipment, which includes plug loads, computers and office equipment, reduces the demand for heat. To reduce the heating load on the project, this graph is used to identify the critical component. In this example, windows cause the greatest amount of heat loss. Roofs and walls result in a significantly smaller amount of heat loss. Thus, the focuses holding on the windows and their U-value should be decreased to reduce the heating load.

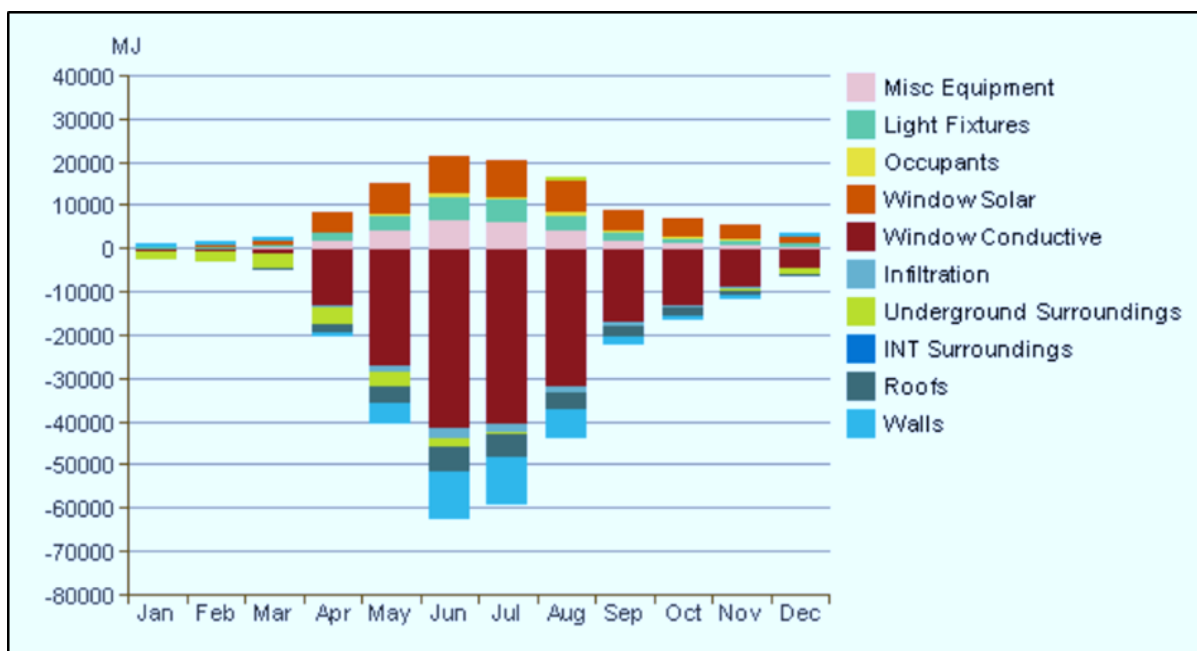


Figure 5.6: Annual energy usage, monthly heating load

5.5.9 Annual, monthly cooling load

Monthly cooling load, as shown in Figure 5.7, is contributed by each of the building element materials. The highest cooling contributor is the wall followed by the roof and conductive windows. Massive concrete walls are used mainly for commercial buildings, because of their ability to provide significant building envelope functions. In addition to their primary function as building envelope, play a major role in heating/cooling zone

climate situations, owing to their natural thermal mass property that enables building materials to absorb, store and later release significant amounts of heat. Buildings constructed using concrete and masonry have a unique, significant energy-saving advantage because of their inherent thermal mass. These materials have natural behaviour that they absorb energy slowly and hold it for much longer periods of time than do less massive materials. Mass and reversal of heat flow play a major role to gain a benefit in climates with large daily temperature fluctuations above and below the point of balance. For these conditions, the concrete mass building envelope can be easily cooled by natural ventilation during the night and then be allowed to absorb heat or to float during the warmer day. When outdoor temperatures are at their peak, the inner part of the building remains cool because the heat has not yet penetrated the mass. Positive values represent cooling demands that must be satisfied by a cooling system or other means, and negative values offset the need for cooling. For example, conduction through a closed window may provide some cooling to a building at night if the ambient temperature is low enough. The largest cumulative cooling loads occur in June, with the greatest contribution from window solar, or radiant solar heat gain through windows. However, heat gains through walls are small by comparison. Thus, it should be improving the glass to reduce the windows' solar heat gain coefficient before investing in improvements to the wall insulation values.

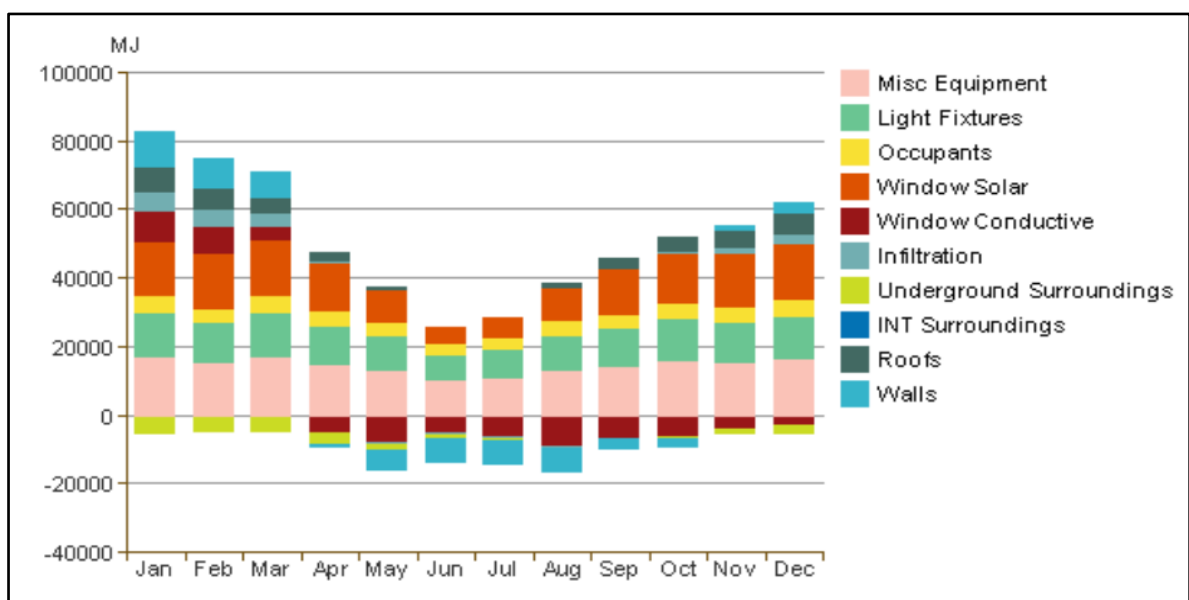


Figure 5.7: Annual energy usage, monthly cooling load

5.5.10 Annual, monthly fuel consumption

The monthly fuel energy consumption shown in Figure 5.8 indicates where or in which month consumption is high, and it can be observed from the graph that the fuel energy consumption starts with smooth linear increase for the period of two months, January and February, and starts increasing in March by semi-linear inclination for the period of three months. This semi-linear inclination reaches the maximum in the middle of June and drops down nonlinearly for a period of three months again. The project uses fuel energy sources for heating as opposed to electric heating sources, and fuel energy usage increases during the colder months of the year.

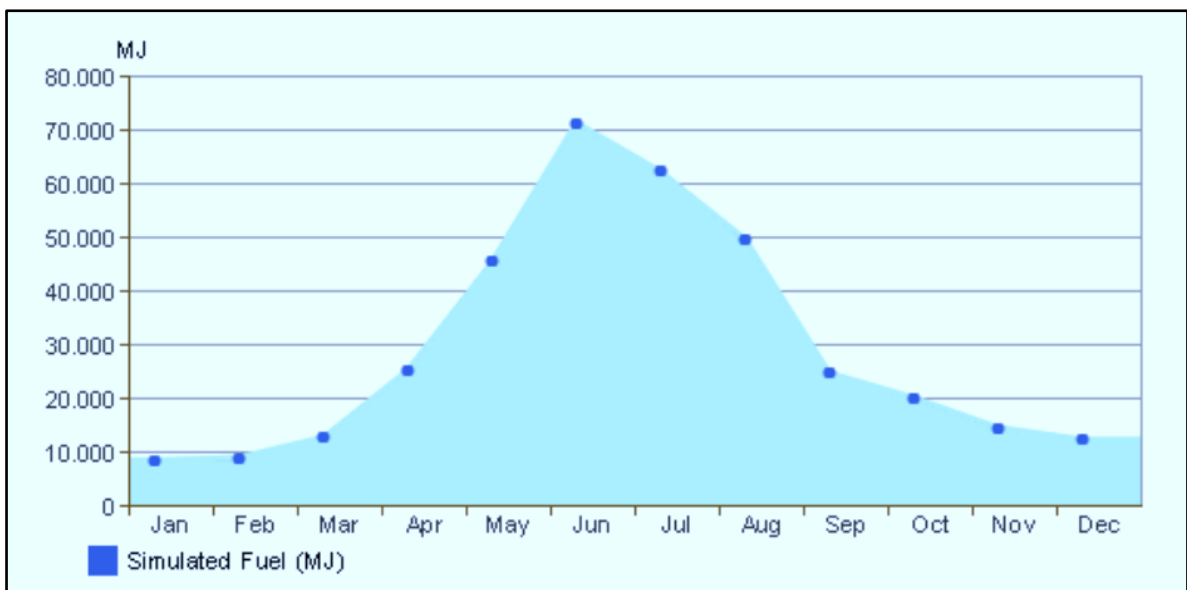


Figure 5.8: Annual fuel consumption

5.5.11 Annual electricity consumption load

Electrical load is an electrical component or portion of a circuit that consumes (active) electric power. This is opposed to a power source, such as a battery or generator, which produces power. In electric power circuits, examples of loads are appliances and lights. Electric consumption load shown in Figure 5.9 affects the performance of circuits with respect to output voltages or currents, such as in sensors, voltage sources and amplifiers. Mains power outlets provide full rated supply power at constant voltage, with electrical hardwired components/appliances connected to the power circuit collectively making up the load. Thus, when high-power appliances are plugged in or switched on, it dramatically reduces the load impedance. In case the load impedance is not very much

higher than the power supply impedance, voltage drop will occur immediately. In commercial/domestic building environments, switching on a heating appliance may cause incandescent lights to dim noticeably. On using air-conditioning as the main cooling supply to the building rather than using duct gas cooling supply, electricity usage increases during the hotter months of the year, as shown in Figure 5.9 which is during the months of January and March, when the electrically supplied usage loads approach the maximum point. The simulation picks the months of January and March by skipping February, which is the hottest month as well. This needs further investigation.

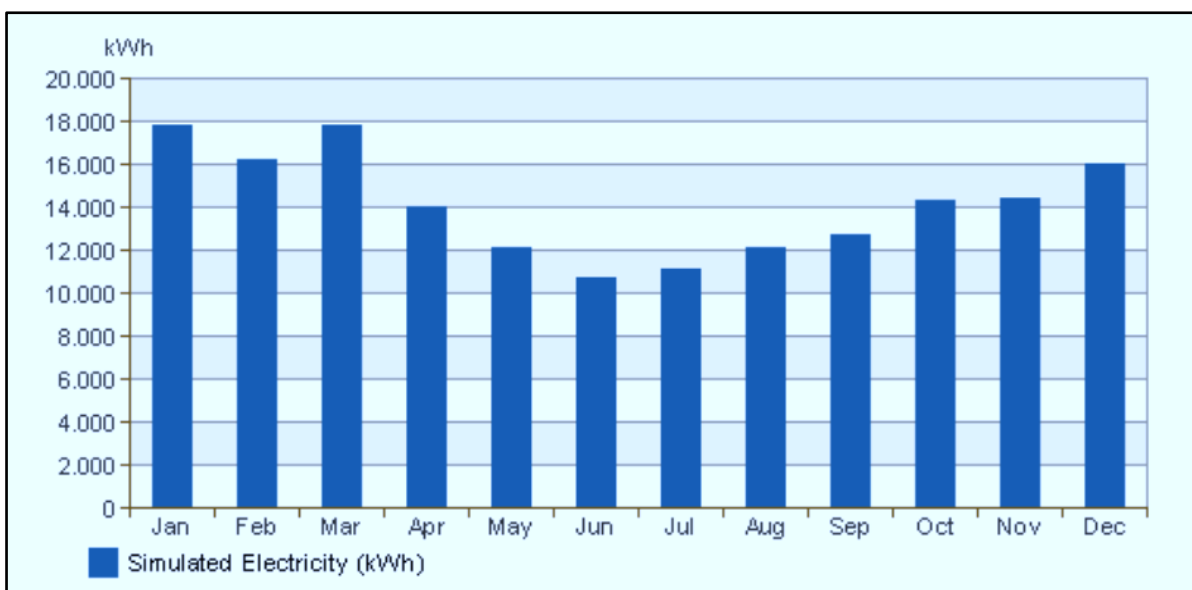


Figure 5.9: Annual, monthly electricity consumption

5.5.12 Annual, monthly peak load demand

Electricity consumption peak load shown in Figure 5.10 occurred during peak- demand periods, which are when electricity usages on the grid network are at highest demand times. It can strain the electricity grid network and lead to power outages. A rapidly growing population also adds to peak demand. Peak-demand time at work varies depending on the types of businesses in the area. For example, a shopping centre may have a peak demand in the middle of the day when the air-conditioning is working at full load and lights and other appliances are on. Peak-demand time for industrial sites, such as factories and mines, varies depending on how they operate. ‘Peak demand’ refers to the total amount of electricity used at any given time. This is different to energy usages, which is the total amount of electricity consumed over a period, which is

measured in kWh. Watched demand on the grid network and undertaking necessary regular forecasting to predict grid network demand is possible. The aim is to reduce the chance of outages owing to demand from all customers exceeding the capacity of the local grid network. When the total customer demand exceeds capacity, in some cases, financial incentives may be provided to customers to reduce their demand, where it is subjected to a cost-effective alternative method. However, these costs are also one of the contributors to electricity price rises. When reviewing an energy analysis, this chart displays the building's estimated annual peak electricity load demand in a monthly dispatch configuration. The peak demand is the maximum instantaneous electrical load in a given limited period.

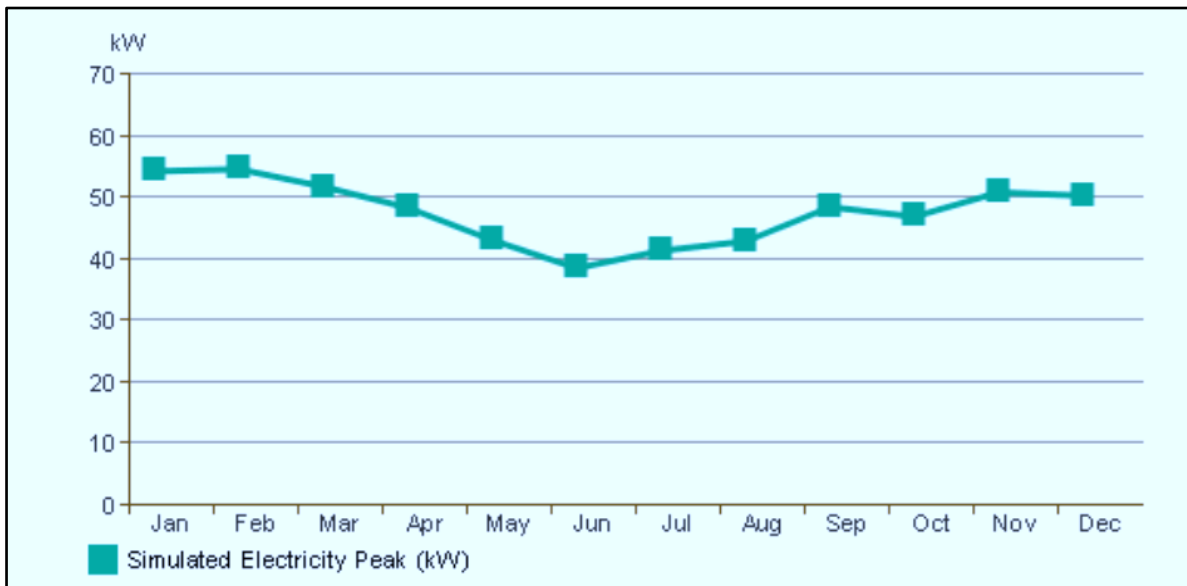


Figure 5.10: Annual, monthly electricity energy peak demand

5.6 Base Run Simulation, Weather Files Contribution

Building solar energy simulations use weather files as measurement factors/parameters to achieve accurate energy usages and cost. Hence, energy costs are highly affected by weather files, such as annual Wind Rose (wind speed). This wind speed distribution is used in building solar irradiation energy simulations as factors or parameters to enable the simulation process system, in which the estimated annual total energy, the total life-cycle energy and the annual renewable potential energy simulations are calculated based on the exact current distribution of the annual wind speed. Knowing the annual current wind speed is not only useful to obtain accurate estimated building energy simulation, but it also contributes significantly to building sustainable GB in terms of stability. In

addition, the hourly Wind Rose contributes in a similar role as the wind speed. Wind hourly frequency is measured in frequency (Hz), which means how much quantity of air repeatedly occurs or is present in that area in one hour. In this region, the highest wind frequency was found around the centre towards the north-west north (NWN) sides and towards the east side of Sydney. Conversely, the lowest wind frequency is found around north north-East (NNE) sides and towards the south-west (SW) sides.

5.6.1 Regional wind speed distribution

The wind speed is shown in Figure 5.11 in 16 cardinal directions with a variety of speed distributions. Thus, this type of wind speed configuration data can be useful to building designers to make necessary design changes according to the location of the building. The annual wind speed and directions are not only useful for building designers and to obtain accurate estimated building solar irradiation energy simulation analysis results, but it also makes significant contributions to building sustainable GB in terms of stability, as mentioned previously.

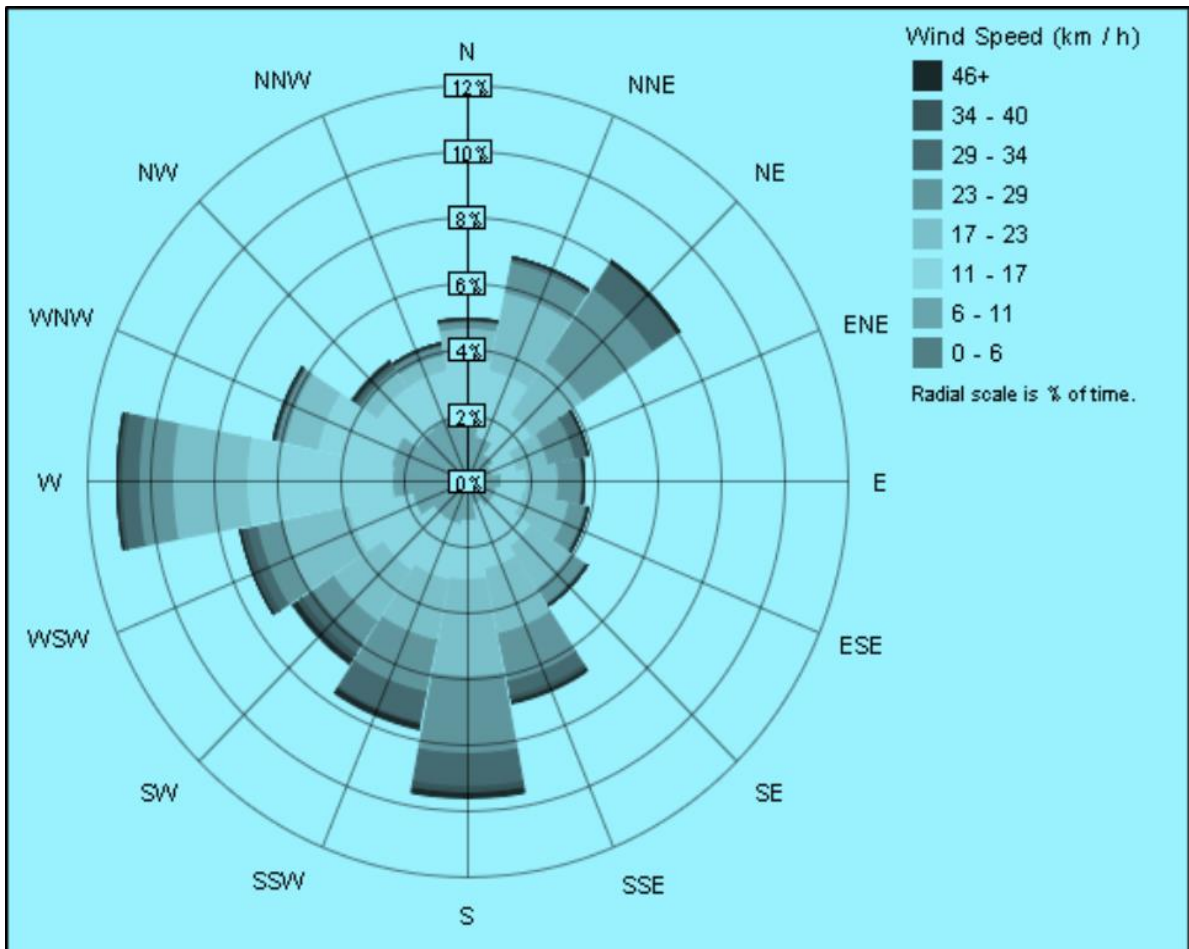


Figure 5.11: Weather files, regional wind speed distribution

5.6.2 Regional wind frequency distribution

In Figure 5.12, moving outward on the radial scale, the frequency associated with wind from that direction increases. Each spoke is divided by colour into wind speed ranges. The radial length of each spoke around the circle is the percentage of time that the wind blows from those directions. In this simulation of the sample wind speed frequency distribution, Sydney’s annual wind speed frequency from the NW and SSW directions is the most common and for more than 10% of the total annual hours. When analysing this region’s wind frequency distribution, the highest wind frequency is found around the centre towards the NWN side and east side of Sydney. Conversely, the lowest wind frequency is found around NNE side and SW side. The wind frequency distribution is a very useful tool when evaluating accurately the estimated building solar irradiation energy simulation analysis and also to achieve a sustainable GB design. As the chart in Figure 5.12 illustrates, there are six varieties of wind speed frequency, starting from the lowest frequency, 0 km/h, to the highest frequency, 45 km/h.

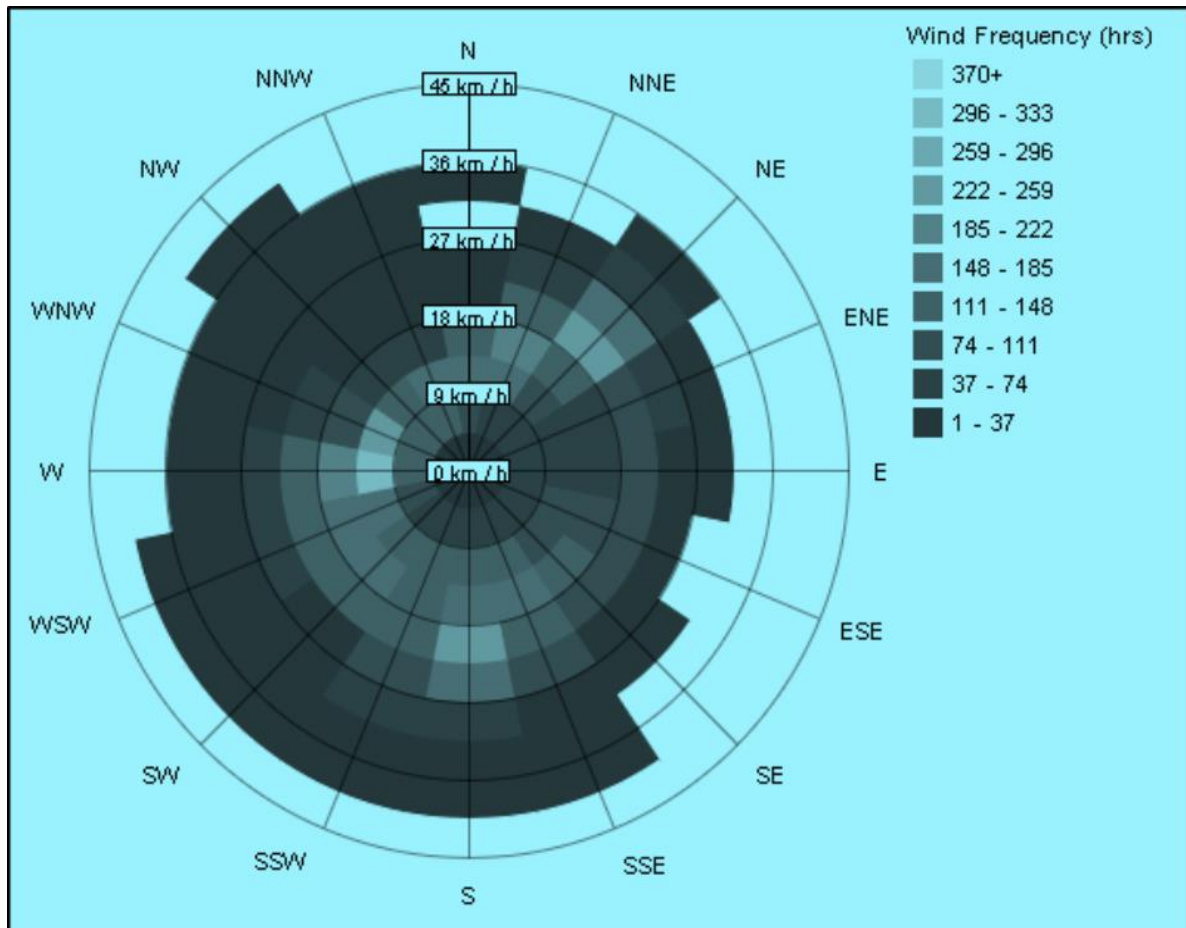


Figure 5.12: Weather files, regional wind frequency distribution

5.6.3 Annual, monthly and hourly wind frequency distribution

The base run Autodesk Revit energy simulation analysis formats hourly weather files to define external conditions during the simulation process. Each location has a separate file describing the external temperature, solar radiation and atmospheric conditions for every hour of the year at that location. These hourly weather data sets are often typical data derived from hourly observations at a specific location by the country's national weather service authorities or meteorological office. Occasionally, since hourly weather data are not always available for every location in a specific period, it is often necessary to use weather data for a nearby location that represents the weather at the actual site.

Figure 5.13 shows the annual, monthly and hourly wind speed/frequency distribution of Sydney specified for each month from minimum to maximum speed/frequency distribution, as shown in the chart. This is very significant information for building designers and area developers to design the building to resist the hourly repeated wind speed/frequency according to the wind force that will be exerted on the building.

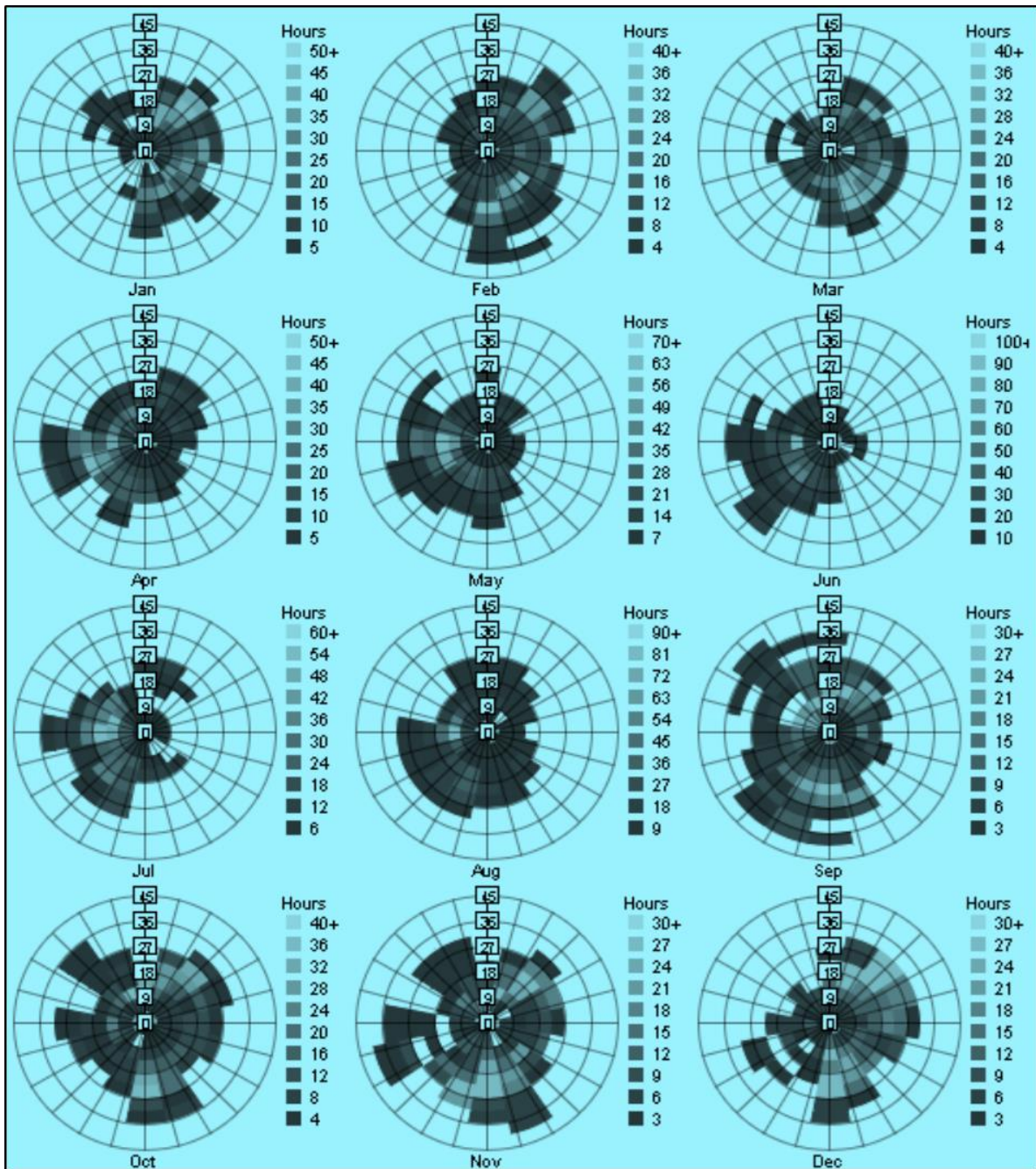


Figure 5.13: Annual, monthly and hourly regional wind frequency distribution

5.6.4 Annual, monthly weather file collection data

Dry and wet bulb are points of temperatures, particularly to relative humidity, vapour pressure and saturated vapour pressure, which significantly describe sea level pressure and station level pressure data for all stations across Australia. The graph in Figure 5.14 shows not only monthly temperatures averaged from historical climate data, but also two levels of uncommon extremes. The green boxes show the historical averages of monthly highest and lowest dry-bulb temperatures. Thus, this site is virtually guaranteed

to experience such temperatures in these months. The extensions of the boxes show extreme temperatures, which were recorded only 1% of the time in historical data. The site is not likely to experience these often, but for a robust design the data should be included. Conversely, the box with blue colour extension shows the dry-bulb heating temperature.

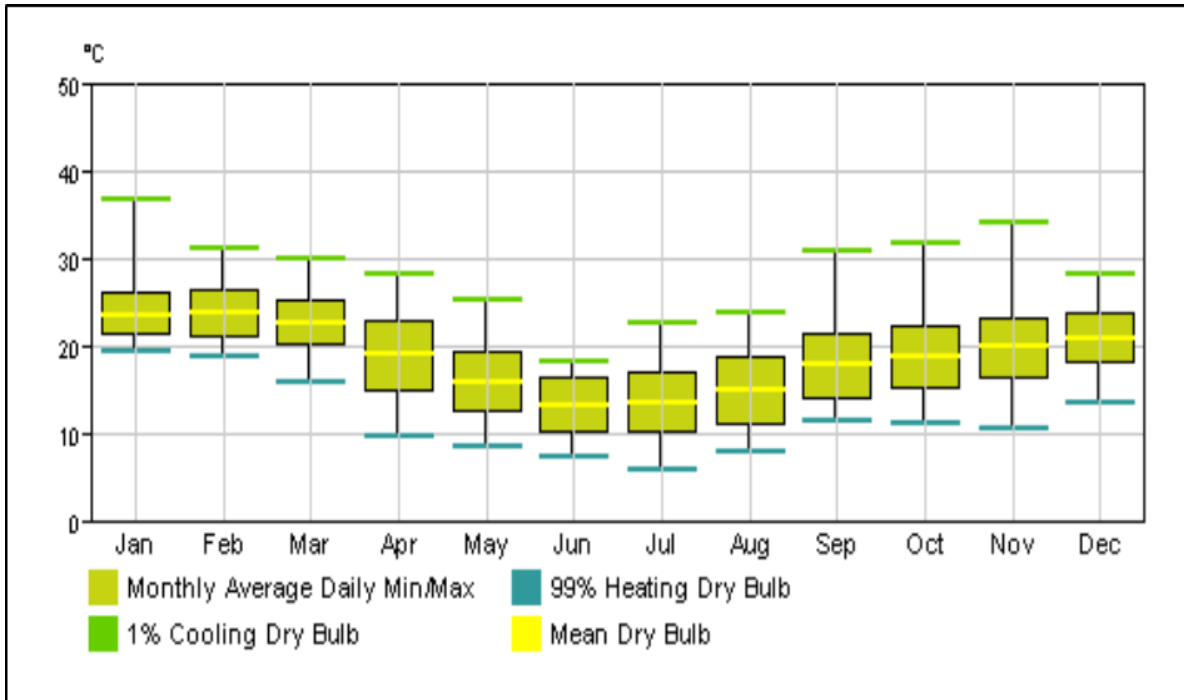


Figure 5.14: Weather files, annual, monthly design data

5.6.5 Hourly temperature of bins

In the Autodesk Revit energy analysis, the base run simulation process also analysed the hourly temperature at different sites. According to the location's weather file configuration, different sites are affected by different weather characteristics, such as in some sites, heating dominates the design requirements for most of the year. Similarly, for other sites cooling dominates. This is referred to as annual temperature bins. Colder sites mostly require heating for their comfort and vice versa for hotter sites. Figure 5.6.5.1 chart displays the frequency of wet- and dry-bulb temperatures, suggesting the climate does not have humid summers. Thus, using outdoor dry-bulb temperatures (Tdb) and wet-bulb temperatures (Twb) measurements, to analyse building energy consumption reductions is another helpful method. Dry climates that experience large diurnal temperature swings, the building is ventilated at night and closed in the morning to retain the cool air. Figure 5.15 further indicates that the highest Twb occurred under

10°C and lasted for more than 20 hours. This indicates that during these hours, the air contained a mixture of water vapour that is the weather was humid. Conversely, the Tdb reaches its maximum at 20°C and lasts for maximum 14 hours. Hence, this type of configuration is used for the building control to program/schedule the cooling/heating unit to operate according to the Twb and Tdb hourly variations. This is for the HVAC system to operate cost effectively and hence achieve maximum building energy usage reductions.

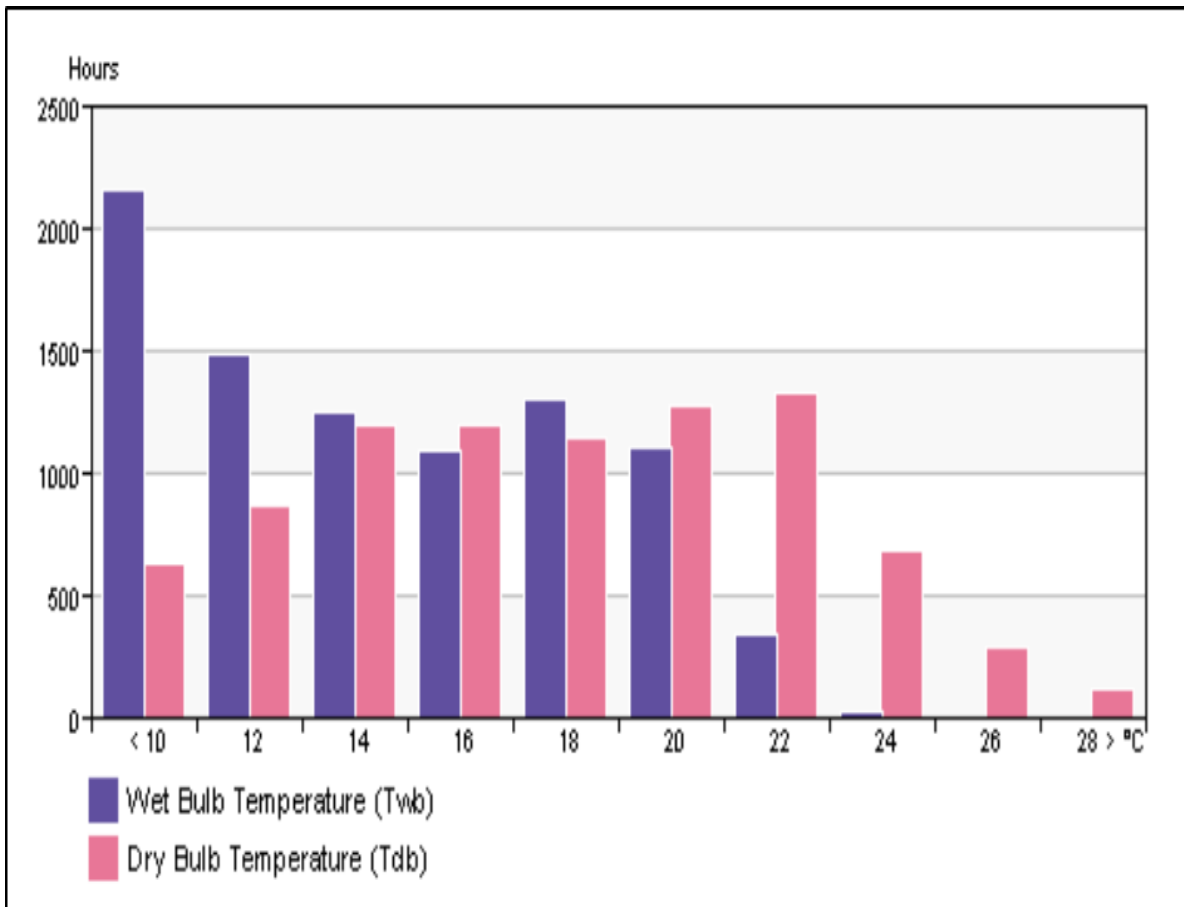


Figure 5.15: Weather files, hourly temperature of bins

5.6.6 Annual, monthly weather file's average diurnal

Weather data shown in Figure 5.16 are annual average files of weather throughout the year in Sydney. As can be noticed from the graph, the weather files consist of four major contributors: the temperature of dry bulb; the temperature of wet bulb; the direct solar watt per meter square and the diffuse solar watt per meter square. GB solar energy irradiation simulation process was conducted by considering these weather file data as

main factors and their contribution to the simulation process was significantly high because without the correct weather files it is difficult to build a sustainable GB.

Diurnal temperature data show daily cycles of temperature and radiation on the site. The data typically include dry-bulb temperature, wet-bulb temperature, direct solar radiation and diffuse solar radiation as a daily average for each month. From this data, the difference between dry- and wet-bulb temperatures can be studied. The difference between night-time temperatures and daytime temperatures is known as the diurnal swing. GB energy simulation is significantly affected by the peak hour's variation times and diurnal swings.

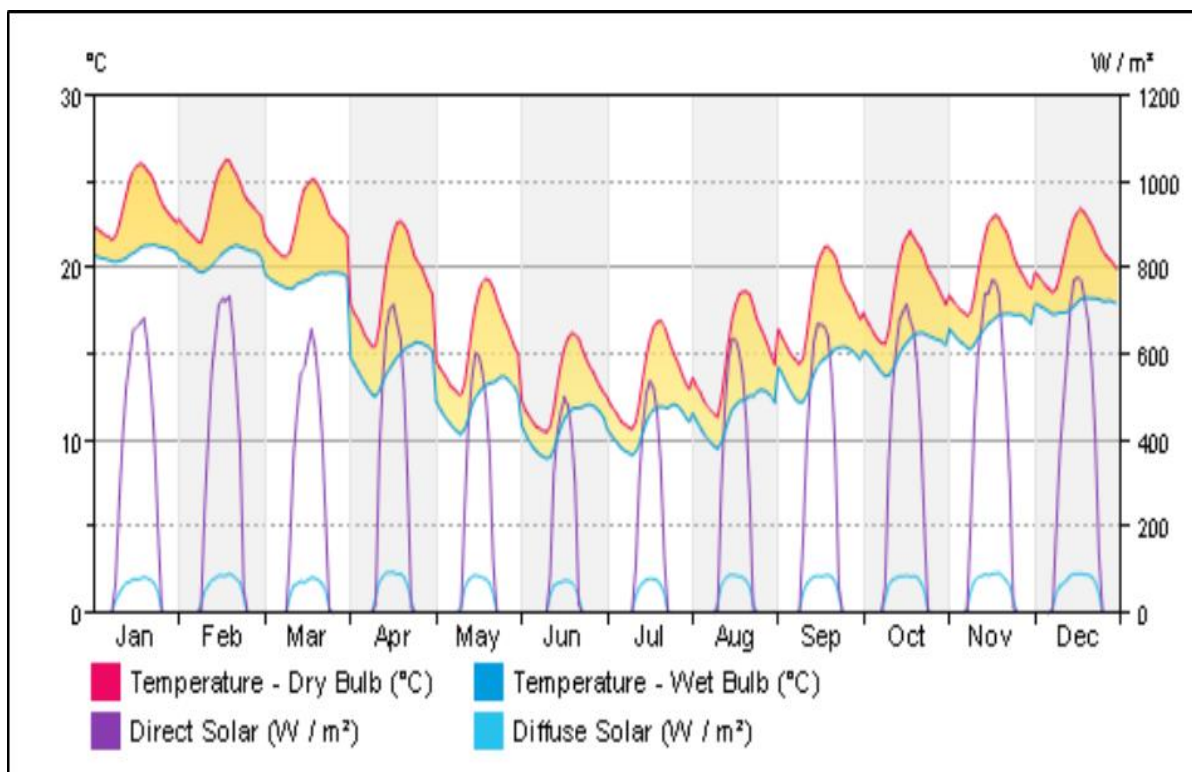


Figure 5.16: Annual, monthly diurnal average weather files

5.6.7 Annual, monthly humidity variation

In the Autodesk Revit energy analysis, the base run building solar energy simulation uses ‘humidity distribution’ as the main input data. Figure 5.17 shows the average annual monthly humidity timely variation range in Sydney. As can be noticed from the chart, the average annual humidity differs from morning to afternoon. In the morning, the average annual humidity increases to 70% and as the day approaches midday and afternoon, the average humidity decreases to 50%. GB energy simulation estimated results were

calculated in consideration of the average daily humidity data, including the peak periodic humidity data. Thus, the humidity can vary greatly throughout the course of one day and is typically higher in the mornings. The mean daily range is the difference between the averages of the daily maximum and minimum of relative humidity for the month and the full range is a record of the absolute maximum and minimum of relative humidity for the month. This is an important part of the monthly recorded humidity variation range, especially for the HVAC system building designers and engineers, because it helps to identify the times at which the humidity varies and the minimum and maximum points; accordingly, the building HVAC system can be designed for optimised operation. Hence, building energy reduction is obtained by using clever operating algorithms. Using these types of humidity variation helps to operate the HVAC system of the building to utilise the maximum benefit in regard to saving energy.

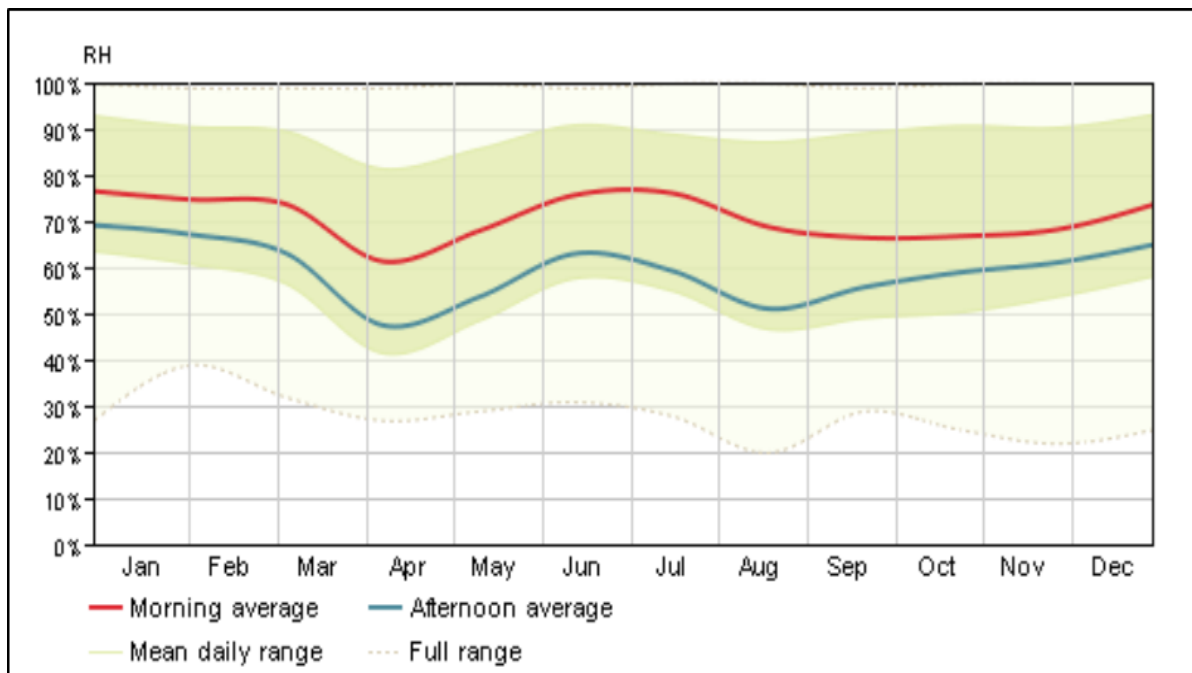


Figure 5.17: Annual, monthly humidity weather files, daily variations

5.7 Base Run Building Energy Simulation Analysis

To achieve maximum energy in GB, whole building energy modelling (BEM) is necessary and it is a versatile multipurpose tool that can be used in a new building and for example, for retrofit design, code compliance, green certification, qualification for tax credits, utility incentives and real-time building control. In addition, BEM is also used on a large scale in analyses to develop building energy efficiency classification

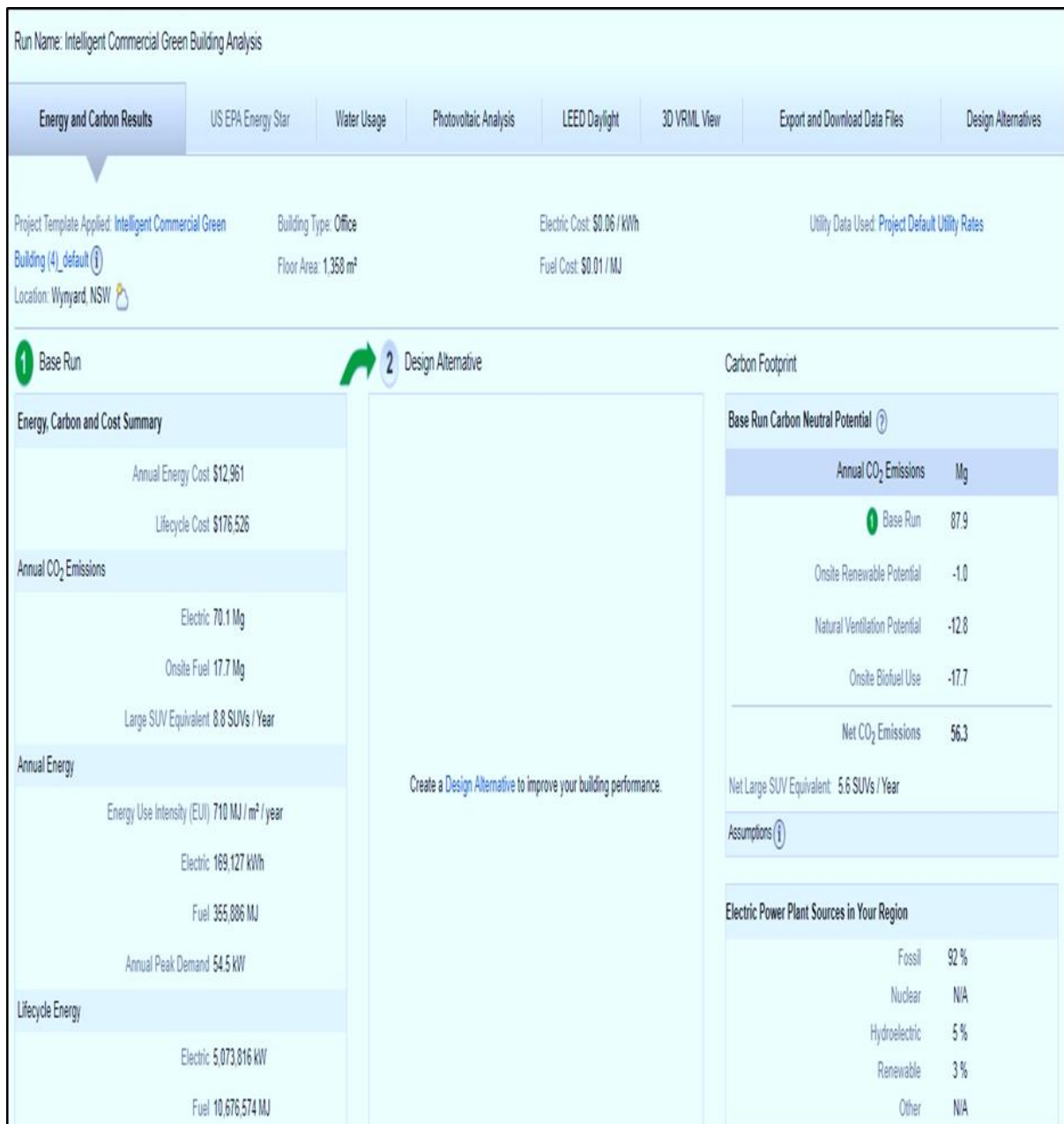
codes. These codes are used to help responsible authorities and policy decision makers [75].

The Autodesk Revit energy analysis, base run building energy simulation is fed information data in the first step (simulation part one). The data are fed as parameters' inputs with specific details and units to enable the simulation software application to compute the given task correctly and efficiently in minimal time. Examples of the information data used are data on building space/rooms, location, weather files from the nearest weather station and energy current unities energy cost as shown in detail in Tables 5.1 and 5.2.

In the second step (part two simulation) of the simulation process, the computer simulation uses these randomly selected building element materials and building information data as input parameters to produce base run energy simulation analytical model as basic outputs, as also shown in Table 5.5. Thus, the content of Table 5.5 focuses mainly on four building energy simulation result summaries: energy cost summary, annual CO₂ emission, annual energy usages and building life-cycle energy usage in the first column. The second column of the Table is left blank because this column is designed for the advanced/alternative design simulation results. The third column is related to carbon footprint and other energy potentials available in the region. From this column content, the base run annual net CO₂ emission is 56.3 Mg. This is not a significant reduction but is to be improved in the advanced (alternative design simulation).

These base run energy simulation results are to be improved in the advanced alternative design energy simulation process because a number of alternative energy simulation packages are sequentially simulated. Thus, this type of method facilitates selection of the best building energy simulation packages by comparing each simulation package against the other and also against the base run simulation results. This is the way to find the best energy reduction packages from 254 numbers of alternative runs. Hence, the base run simulation method acts as a reference point for the alternative design methods.

Table 5.5: Base run solar building energy simulation result



5.8 Base Run Water Efficiency

Most significant savings for a GB associated with water efficiency reduce energy costs. Reducing the amount of water for cooling and heating minimises the amount of energy needed to perform these tasks, which in turn reduces costs. Several studies show that up to 15% [76] of a commercial building's energy consumption is owing to water heating. Efficient hot water usage and generation through alternative methods, such as 'geothermal heating', can lead to significant energy savings and also reduce the pollution related to the production of energy. In addition, the studies also show that

water efficiency directly affects to natural scenery and human well-being and both of them are directly affected if groundwater and reservoirs are depleted. Lower water levels concentrate natural contaminants, such as radon and arsenic, and human pollution from chemical wastes are also added to water bodies.

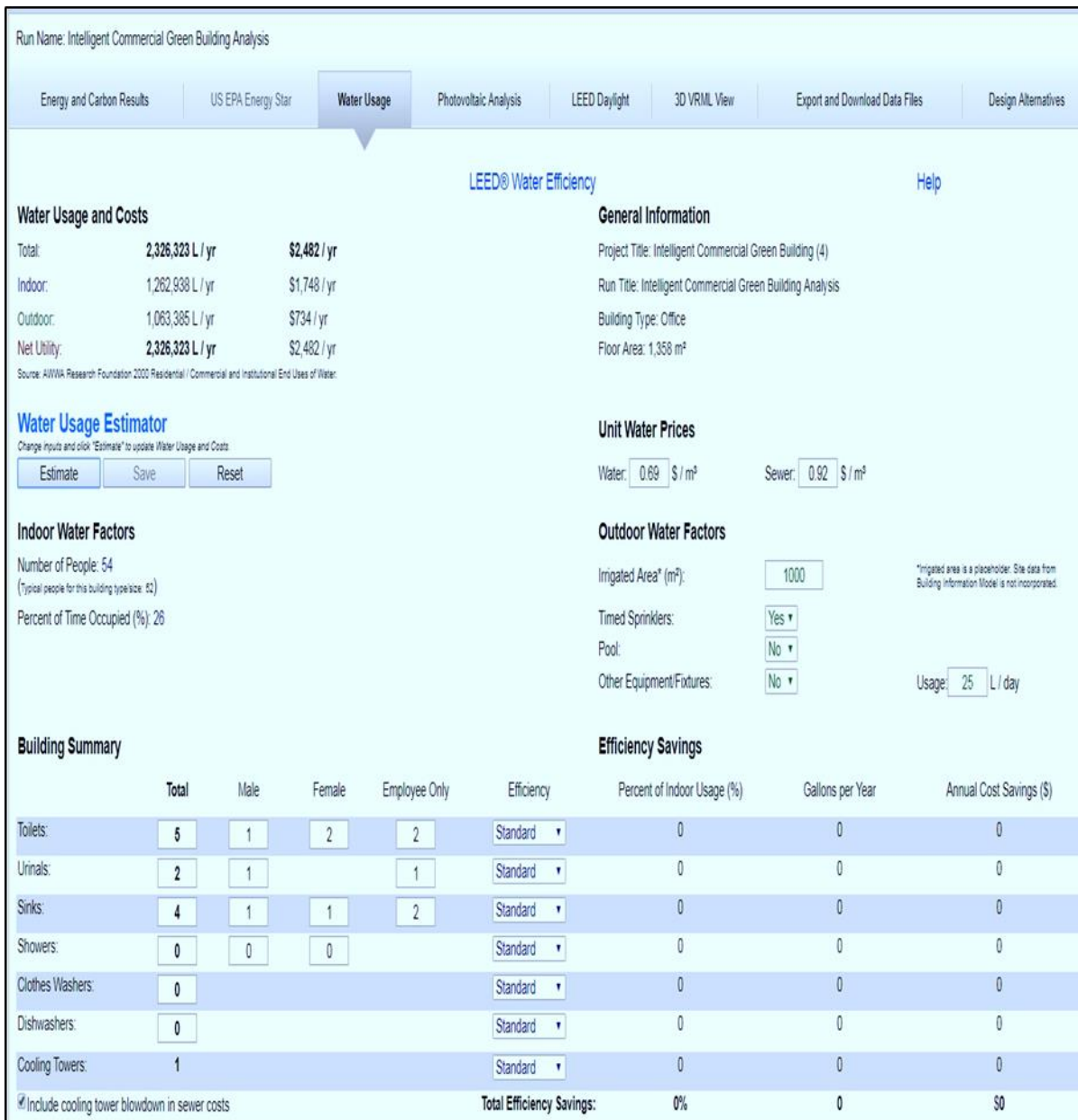
One of the objective criteria of GB is to increase development of worldwide GB projects, especially those related to the Leadership in Engineering and Environmental Design and Green Building Council Australia (LEED/GBCA) standard, provide the contextual basis for the implementation of water conservation strategies. Water efficiency strategies in GB practices are becoming paramount to new and existing building construction efforts. Thus, a wide range of terms is associated with water efficiency in GB to satisfy the objectives of GB from the water efficient side.

Numerous terms are used to describe key elements in the design and implementation of water conservation strategies in GB. Thus, one of the most important elements of understanding water efficiency is the diversification of water terms in green GB practices. In particular, the LEED/GBCA standard water efficient steps of procedure identify four key types' potable water, greywater, black water and process water all of which provide different utilities in GB water efficiency processes.

Beside these four key types of water diversification, several other definitions related to each type of water in the LEED/GBCA standard is necessary to implement the GB water efficiency diversification process. Thus, to provide greater understanding of utility in the GB engineering process and to achieve significant water usage reduction in GB [77].

Table 5.6 shows the base run energy simulation at standard water usage efficiency. In this table, all the water facilities are set to standard rate of water usage without any improvement attempted to reduce the usage of the water in the building. At this standard water usage, the average annual total usage is 23,263,262 L/year, and the net water usage is the same, which clearly indicates no attempt is made to reduce the water usage at this stage. As previously mentioned, the part two simulation is a basic standard simulation to the part three simulation, and significant water usage is expected in the part three simulation.

Table 5.6: Base run solar building energy simulation water usage results



5.9 Renewable Energy Simulation

Simulation of renewable energy covers many emerging alternative energy sources. However, the most valuable ones, especially in commercial buildings, are PV cell and wind turbine. Thus, this thesis research project uses the guideline proposed by base run simulation in regard to renewable energy implementation and excludes the other renewable energy sources. The proposed renewable energy sources are 15% efficiency PV cell and 15-inch wind turbine. Knowing these sources are at initial efficiency and performance, boosting/optimising of their efficiency and performance are one of the

tasks in designing energy sustainability of GB. Hence, this research section focuses on how to optimise the current commercially available renewable energy, in particular from the PV cell and the wind turbine.

5.9.1 PV cell efficiency and performance

To understand the PV cell electricity generation, the first aspects to be understood are the basic theory of the solar irradiation, orientation of the Sun above the horizon, sunlight incidence angles and sunlight intensities and their calculations, such as the angle of declination (δ), the angle of latitude (ϕ), the angle of azimuth or bearing angle (A_z), the angle of zenith (Θ_z), the angle of solar altitude (α) and the hourly angle (W).

The following symbols are recognised globally:

N = number of solar days

ω = the hour angle

α = the altitude angle

A_z = the solar azimuth angle

δ = the declination angle = 23.45° tilt angle

ϕ = observer's latitude = 0° at equator, 23.45° at summer and winter solstices and 66.55° at the Arctic Circle and Antarctic Circle. The declination angle in radians at any given day and time is: $\delta = [(23.45\pi) \div (180)] \sin[2\pi\{(284 + n) \div 36.25\}]$.

The azimuth angle at any location is given by $A_z = \sin^{-1}(\sin \omega \times \cos \alpha) / \cos \delta$.

The hourly angle is given by $\sin \omega = \sin \alpha - \sin \delta \sin \phi / \cos \delta \cos \phi$.

The altitude angle is given by $\sin \alpha = \sin \delta \sin \phi + \cos \delta \cos \omega \cos \phi$.

The zenith angle is also the angle of incidence and it is given by $\sin \theta_i = \cos \theta_z = \cos \delta \cos \phi \cos \omega + \sin \delta \sin \phi$.

As mentioned previously, this research project chose Sydney, Australia, as the GB location, and adequate information regarding the solar path of one complete cycle or full turn in one year was required for this region to conduct successful energy simulation. This means numerical calculation of all angles related to our research project is derived from these collected data. Sydney is located on the latitude and longitude geometric coordination of the global geographic region, about 35° south and about 149° East

in the southern hemisphere. Thus, to use the best orientation for our PV cells position, it is very important to know the geographic solar orientation of the locations, so that the PV cell panel can be positioned to the best orientation to maximise the PV cell output power. Since Sydney is located in the southern hemisphere, as a general rule, the PV cell panel is to be installed facing north because it would be the most efficient position and vice versa for a location in the northern hemisphere.

Before PV cell installation, it is important to have adequate knowledge about the general solar irradiation and its fundamental phenomena of occurring, starting from the Sun to the Earth, as mentioned previously. Thus, the Sun is spherical shape consisting of hydrogen and hydrogen energy fusion creator [78], known as the prime energy source, located about 1.5×10^{11} meters away from the Earth. The Sun produces or radiates uniformly equal average energy of 3.8×10^{26} watt to all directions from its surface. The Earth receives only a portion of it, about 1.7×10^{11} watt, which is enough to keep the Earth warm and also to maintain life on Earth [79]. The Earth's entire energy portion does not reach its surface; solar energy radiation faces a lot of obstacles before it approaches the Earth's atmosphere. The Sun radiates a composite of different energy levels, which is called the solar radiation spectrum. It is composed of 40% infrared wavelengths or longer, 50% visible light wavelengths and 10% ultraviolet wavelengths or shorter. A part of these radiations approaches the Earth's surface at different incident angles and intensities. The total solar radiation reaching the Earth's surface is approximately 950 watt/m^2 and approaches in three directions, which are known as global horizontal irradiation (GHI), diffuse horizontal irradiation (DHI) and direct normal irradiation (DNI) [80]. The atmospheric medium significantly distorts the solar irradiation, dividing it into portions, and some portion of it is reflected straight away from the medium, some portion is refracted horizontally and most of it passes through the medium and reaches the surface. The incident ray that reaches the ground is composed of mainly two radiations, the DHI and the DNI, which is equal to GHI. It is important to know how the solar radiation approaches the Earth's surface. Except at 12 noon, irradiance never approaches the surface at maximum intensities. This is because the position and orientation of the Earth relative to the sun is not constant, and hence, the irradiation or the light from the sun mostly reaches the surface at angle, which reduces the intensity of the irradiation as well as the PV cell efficiency. To compensate for these reductions, many researchers have developed solar irradiance intensity

tracking mechanism systems, using sophisticated technologies. For example, intelligent sensors, servo motor, algorithm to take control of the motions, MPPT trackers and GPS controlling system of mechanism.

5.9.2 Extra-terrestrial radiation

Extra-terrestrial radiation (watt/meter square) is the amount of solar radiation incident tangential to surface of Earth's atmosphere on a function of time and it is expressed either for an hour (I_0) or a day (H_0)

$$I_0 = \frac{12.3600}{\pi} G_{sc} \left(1 + 0.033 \cdot \cos \frac{360 \cdot n}{365} \right) \left[\cos \varphi \cdot \cos \delta \cdot (\sin \omega_2 - \sin \omega_1) + \left\{ \frac{\pi \cdot (\omega_2 - \omega_1)}{180} \right\} \sin \varphi \cdot \sin \delta \right]$$

$$H_0 = \frac{24.3600}{\pi} G_{sc} \left\{ 1 + 0.033 \cdot \cos \frac{360 \cdot n}{365} \right\} (\cos \varphi \cdot \cos \delta \cdot \sin \omega_s + \frac{\pi \cdot \omega_s}{180} \sin \varphi \cdot \sin \delta)$$

Where Solar Constant, $G_{sc} = \text{watt/m}^2$

Hourly Radiation = J/m^2

Daily Radiation = $\text{J/day} \cdot \text{m}^2$

5.9.3 Testing standard of PV cell

The PV cell average testing standard irradiation is 1,000 watt/m^2 (known also as 1 sun flat plate) at air mass 1.5 and at standard temperature 25°C or kelvin, k ($25 + 273 = 298$ k). The ideal PV cell characteristics are: $V_{oc} = 0.623$, Ideal $I_{sc} = 35 \text{ mA/cm}^2$, $\text{FF}_{\text{ideal}} = 0.83$, and the real cell: $V_{oc} = 612$, $I_{sc} = 34.6 \text{ mA/cm}^2$ and $\text{FF}_{\text{real}} = 0.67$.

5.9.4 Generation of PV cell power

Light contains particles called photons and when these photons incident on the surface of a semiconductor, these are either reflected from the top surface or absorbed in the material or, missing these two chances, transmitted through the material. For PV cell devices, reflection and transmission are typically considered a loss since photons that are not absorbed do not generate power. If the photon is absorbed, it has the possibility of exciting an electron from the valence band to the conduction band. A significant factor in the determining of photon energy is whether it is absorbed or transmitted.

Therefore, only if the photon has enough energy will the electron be excited into the conduction band from the valence band. When the energy of a photon is equal to or greater than the band gap of the material, the photon is absorbed by the material and excites an electron into the conduction band. Further, materials with higher absorption coefficient $\left(a = \frac{4\pi K}{\lambda}\right)$ more readily absorb photons [81], which also excites electrons into the conduction band. The absorption coefficient determines how far into a material can light of a particular wavelength penetrate before it is absorbed. The absorption coefficient depends on the material and also on the wavelength of light being absorbed. To generate adequate PV cell power, the sunlight intensity, which is a composite of many types of different wavelengths as well energies, should be able to absorb sufficient photons of short wavelengths and the PV cell material must have higher absorption coefficients. Thus, when the photon's energy $\left(E = \frac{hc}{\lambda}\right)$, where E is energy in joules, h is Plank's constant (6.626×10^{-34} joules), c is light speed (2.998×10^8 m/s), and λ is wavelengths in meters, an inverse relationship equation is derived from the above equation $\left(\lambda = \frac{hc}{E} = \frac{6.626 \times 10^{-34} \cdot 2.998 \times 10^8}{E} = \frac{1.99 \times 10^{-25} \text{ joules-m}}{E}\right)$. The inverse relationship means that light consisting of high energy photons (such as blue lights) has a short wavelength and light consisting of low energy photons (such as red lights) has a long wavelength. Mostly, when we deal with particles such as photons or electrons a commonly used unit of energy is the electron volt (eV) rather than the joule (J) and an electron volt is the energy required to raise an electron through 1 volt. Thus, for a photon with energy of $1 \text{ eV} = 1.602 \times 10^{-19} \text{ J}$, its wavelength is calculated as

$$\left(\lambda = \frac{hc}{E} = \frac{6.626 \times 10^{-34} \cdot 2.998 \times 10^8}{1.602 \times 10^{-19} \text{ J}} = \frac{1.99 \times 10^{-25} \text{ joules-m}}{1.602 \times 10^{-19} \text{ J}} = 1.24 \times 10^{-6} \text{ meter}\right); \text{ hence,}$$

this micro wavelength is sufficient to knock an electron of PV cell.

Figure 5.18 (a), (b) and (c) show the PV cell's ideal and non-ideal diode characteristics in regard to light intensity penetration and maximum output voltage generation, which are called IV characteristics. In this section, the diode characteristics are briefly described in regard to its dark, shunt and series currents; current density, light intensity density and open voltage as well in respect to their corresponding values. The shunt short circuit current and open circuit voltage values are simulated to increase the PV cell efficiency.

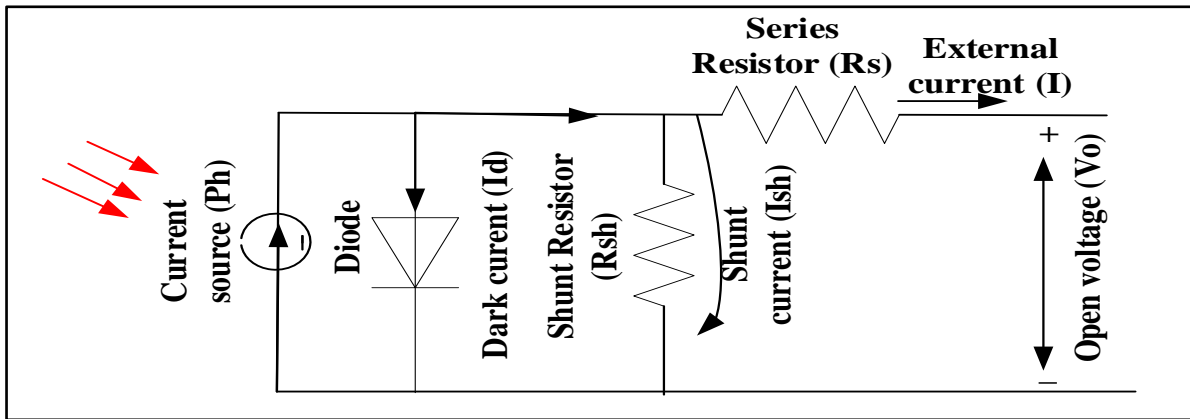
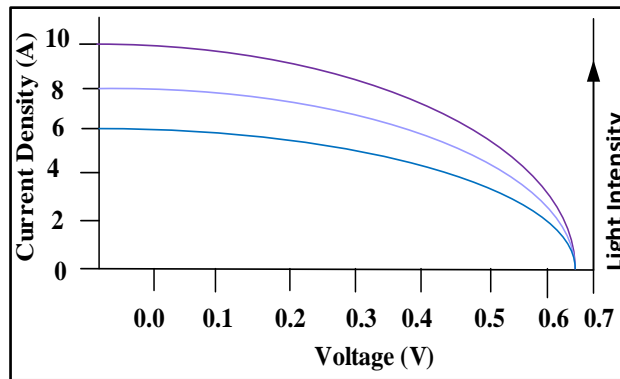
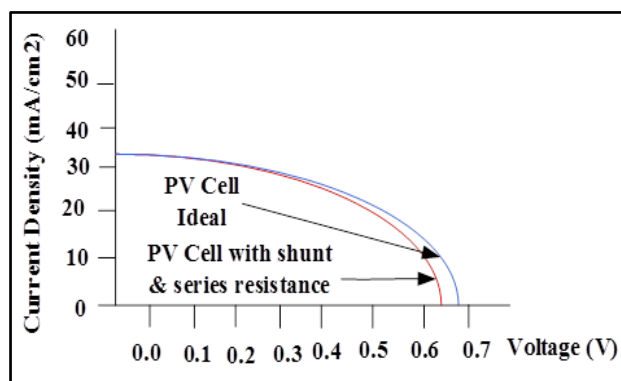


Figure 5.18: PV cell characteristics

- a) PV cell diode characteristics, dark current, shunt resistance and series resistor



(b) PV cell diode current density



(c) PV cell diode light intensity

Where: $I_{sc} = qG(L_p + L_n)$, $V_{oc} = \frac{nKT}{q} \ln \left(\frac{I_{sc}}{I_0} + 1 \right)$, and Fill factor (FF) = $\left(\frac{V_m I_m}{V_0 I_{sc}} \right)$

$$\text{External current (I)} = I_{ph} - I_o \left(e^{q(V + IR_s)/aKT} - 1 \right) - \left\{ V + \frac{R_s}{R_{sh}} \right\}, \text{ maximum power (P}_m) \\ = (I_m V_m), \text{ and the efficiency (}\eta) = \left(\frac{V_o I_{sc} FF}{P_{in}} \right)$$

Where: I_{ph} = current source, I_o = Open current, a = Ideal defector, K = Plank's constant, T = standard temperature, q = electronic charge, G = generation rate, L_p = hole diffusion lengths and L_n = electronic diffusion lengths. The equations and the figures show the basic introduction of PV cell power generation and how to reach the maximum IV curve characterises. Thus, this leads to understanding PV cell maximum power tracking simulation. The base run proposed PV cell highest efficiency is 72,442kWh/year = $\frac{72442kWh}{1824h} = 39.72 \text{ kw}$; this is the rated power of the PV cell and for the calculation of the hours, refer to section 5.10.5.

5.9.5 PV cell simulation

As mentioned previously on the overall research project design, the main aim of this research project is to simulate the PV cell Sun incident light tracking system, which is previously proven by several researchers using a mechatronic system of controlling practices. This research project developed an alternative method that works on the similar concept but using a simple method and at less cost.

The way developed in this research project is that the PV cell generates current depending on the sunlight intensity, by which the closer the sunlight is shining on PV cell perpendicular to its position; the PV cell generates current proportional to the sunlight sensitivity. Thus, around midday hours, the PV cell receives maximum sunlight intensity and during these hours the PV cell generates the maximum power. However, the PV cell generating capacity is affected by many factors. For example, the position of the Sun in the sky during morning and evening in relation to the azimuth angle, the Earth's seasonal tilting angle (declination angle) and how far is the position of the Sun above the horizon in relation the zenith angle are all factors affecting the sunlight intensity. Considering all these factors, this alternative method system is developed to compensate the power loss by these affecting factors to achieve the maximum output power approximately from morning to evening. This alternative method also works on a very simple concept that when the PV cell semiconductor is covered with curtain wall adaptive component or material, this adaptive component has the ability to sense the

sunlight intensity and to rotate with the sun's orientation position. This means by tilting the PV cell panel to a flexible tilting angle position and programming it to follow the Sun's orientation position in the sky, the PV cell will receive approximately constant normal incident light to its plane. However, the intensity of the light will vary during the morning and the evening hours owing to the Sun being at a greater distance from the PV cell, but the incidence light will always be focused on the PV cell in the straight and normal position angles.

The concept has been proved using software simulation application as shown in Figs 5.19 to 5.21 and Tables 5.7 to 5.9. Thus, the simulation process algorithm programs vectors point towards the Sun and towards PV cell to align/misalign each other, as shown in Figure 5.18. Then depending on the Sun's position, three main positions are identified as position 1, 2 and 3. Position 1 is during morning hours (7.12 am), position 2 is during after midday (1.46 pm) and position 3 is during starting of evening hours (at 2.12 pm).

1) Position 1

At position 1, the Sun is not in effect because it is still rising above the horizon and the vector angle is opened, as shown in Figure 5.20 and Table 5.7

2) Position 2

At position 2, as the Sun keeps rising, the vector angles between it and the PV cell approach to zero and the azimuth angle approaches close to 90° as shown in Figure 5.21 and Table 5.8 and at about after midday, the PV cell panel is fully closed. At this position, the Sun has the greatest effect over the PV cell panel and maximum power generation is achieved.

3) Position 3

At position 3, the Sun is approaching the other side of the world. The actual time is during early evening hours. The Sun's effectiveness on the PV cell panel is very similar to that at position one except that the azimuth angle has negative sign and the PV cell panel is partially closed. The efficiency of PV cell increases as the output power increases and the output power increase is owing to the current increase. As aforementioned, the current of the PV cell varies propositionally with variation of

sunlight irradiation. In Tables 5.7 to 5.9, all the required parameters are shown and except the area of the PV cell panel, the initial real current, the real potential difference, the initial efficiency and the thickness of the PV cell panels, the rest of the parameters are supposed to vary according to the sun's light irradiation intensity. When the Sun moves from one position to the other, the software script program shown in Figure 5.23 takes control over the Autodesk Revit parameters and adjusts the values of the parameters according to the Sun's position in the sky. As the intensity of the light increases, the PV cell reaches its maximum generation ideally above 8 Amps, say 10 Amps and there are 36 PV cell panels ($10 \times 36 = 360$ Amp). During morning hours, the incident angle is zero and the current is also zero, but when the Sun continues its ascent above the horizon, the incident angle approaches towards 90° . The current and the efficiency are also approaching the maximum point, as shown in Table 5.9.

The highest efficiency of PV cells currently in the market without using sunlight tracking system is in the range of 5% to 27%, and this efficiency is not very satisfactory or not feasible when all the costs incurred and the maintenance cost are added. Several studies currently show that many types of different methods have been proposed to improve the low efficiency of PV cells; one of these is the sunlight intensity tracking system and it has been proven that especially in a mostly cold climate region, the efficiency of the PV cell sunlight tracking system could increase from the basic low efficiency to more than 40% efficiency. This is a significant, good approach that involves adding minor, expensive high-technology devices to increase the basic efficiency by more than double. However, this type of method is still not cost-effective. The main aim of this research article is to develop a method that works on similar concepts of the sunlight tracking system, but it has to be very cost-effective and produce the same, or close to the same, amount of power. In this method, the PV cell approaches its maximum current at 1.45 pm and at angle of 80.754° . Theoretically, the maximum power should approach at 12 pm and at the angle of 90° , but the mismatch could result from the performance of the software in relation to the Sun's orientation.

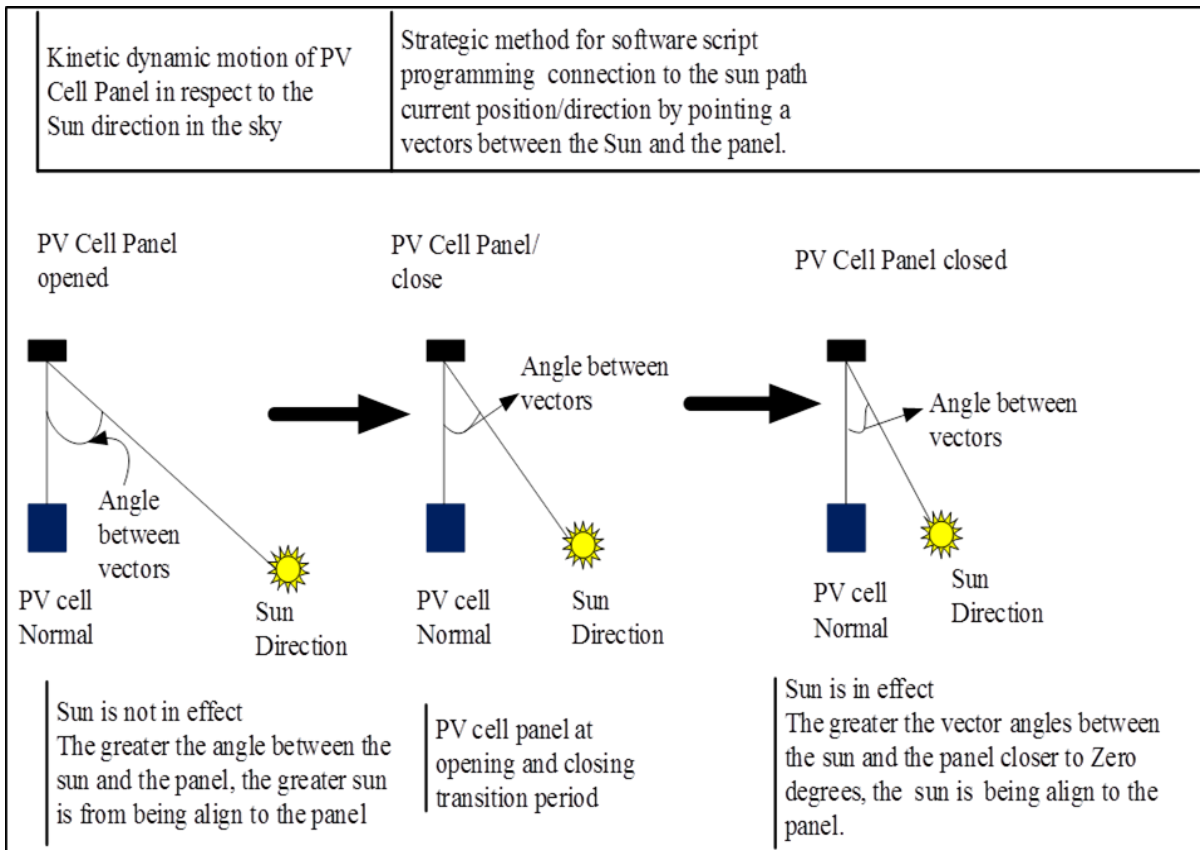


Figure 5.19: PV cell panel, sunlight effect influence

5.9.6 PV cell simulation analysis

As mentioned previously, the highest efficiency of PV cell currently in the market without using boosting mechanism to increase its efficiency is in the range of 15 to 27%, and this efficiency is not very satisfactory. A current literature review of PV cell efficiency articles shows that a number of different methods have been attempted to improve the efficiency of PV cells, one of which is sunlight intensity tracking system and this method has significantly proved the PV cell efficiency. Nevertheless, this is a significant clever method. However, this type of method is not cost-effective. Thus, this research thesis chapter deals and develops a method that works on similar concepts of the sunlight tracking system, but using a cost-effective method, and produces the same or close to the same amount of efficiency. In this method, the PV cell panels are simulated by the Autodesk Revit and Dynamo software application algorithm to follow the sunlight irradiation intensity direction once the Sun is above the horizon using natural phenomenon, as shown in Tables 5.7 to 5.9 and Figures 5.20 to 5.23. The method costs the minimum, and the cost could be negligible if compared with the other similar methods that produce similar results.

Table 5.7: PV cell parameters, performance during morning hours

Electrical Engineering		
PV Cell Maximum Current	360.00 A	= 10 A * 36
PV Cell Improved current (default)	0.00 A	= sin(Rotate_Middle) * PV Cell Maximum Current
PV Cell Inial Current	124.56 A	= 3.46 A * 36
PV Cell Potential Difference	21.96 V	= 0.61 V * 36
Electrical - Loads		
PV Cell Improved Output Power (default)	0.00 W	= (PV Cell Potential Difference) * PV Cell Improved current
PV Cell Initial Output Power	2735.34 W	= (PV Cell Inial Current) * PV Cell Potential Difference
Dimensions		
Area of Solar Panel	18.581 m ²	= (3.048 m * 6.096)
L (report)	3048.0	=
Rotate_Middle (default)	0.000°	=
Rotation_Botom (default)	0.000°	=
Rotion_Top (default)	0.000°	=
Thicknes	76.2	=
Energy Analysis		
PV Cell Improved Efficiency (default)	0.000000	= (PV Cell Improved Output Power) / PV Cell Input Energy Capacity
PV Cell Initial Efficiency	0.147219	= (PV Cell Initial Output Power) / PV Cell Input Energy Capacity
PV Cell Input Energy Capacity	18580.00 W	= (18.58 W) * 1000
Analytical Properties		

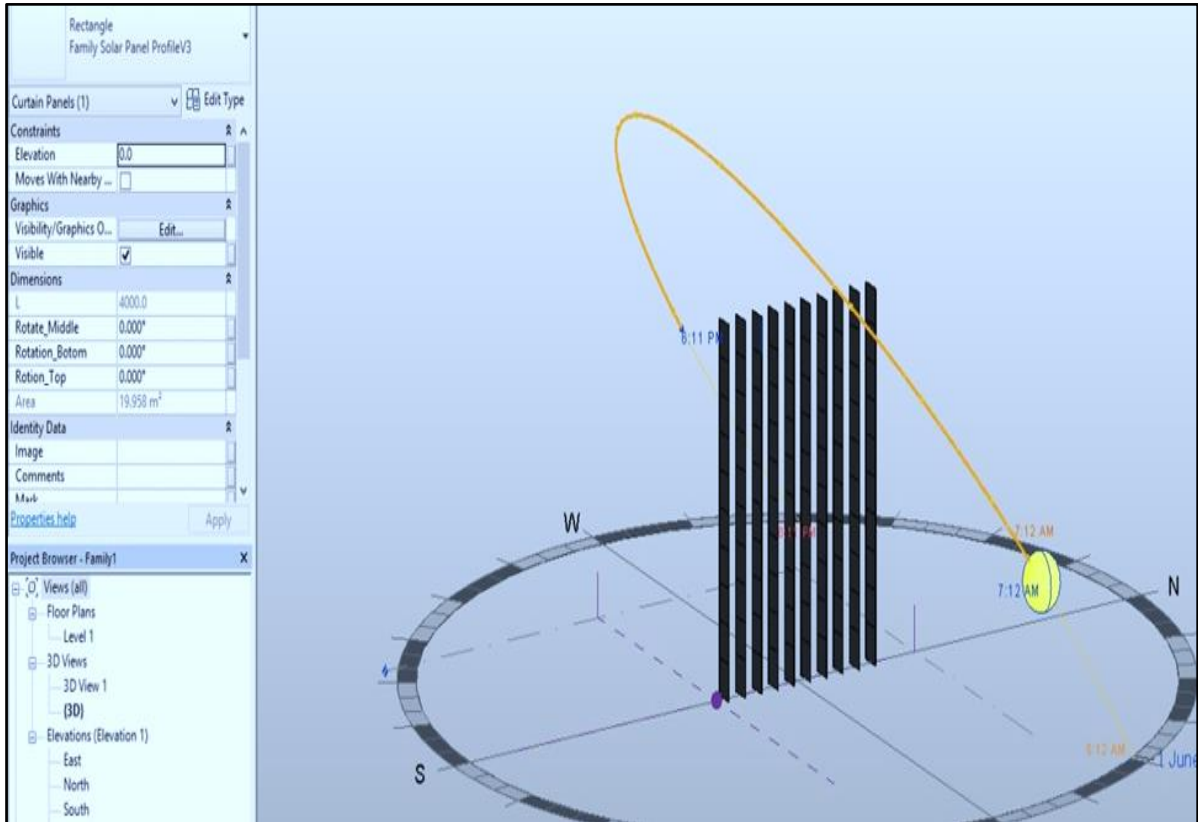


Figure 5.20: PV cell parameter respond performance during morning hours

Table 5.8: PV cell parameter, performance during midday hours

Electrical Engineering		
PV Cell Maximum Current	360.00 A	= 10 A * 36
PV Cell Improved current (default)	320.01 A	= sin(Rotate_Middle) * PV Cell Maximum Current
PV Cell Inial Current	124.56 A	= 3.46 A * 36
PV Cell Potential Difference	21.96 V	= 0.61 V * 36
Electrical - Loads		
PV Cell Improved Output Power (default)	7027.46 W	= (PV Cell Potential Difference) * PV Cell Improved current
PV Cell Initial Output Power	2735.34 W	= (PV Cell Inial Current) * PV Cell Potential Difference
Dimensions		
Area of Solar Panel	18.581 m ²	= (3.048 m ² * 6.096)
L (report)	3048.0	=
Rotate_Middle (default)	62.738°	=
Rotation_Botom (default)	62.738°	=
Rotion_Top (default)	62.738°	=
Thicknes	76.2	=
Energy Analysis		
PV Cell Improved Efficiency (default)	0.378227	= (PV Cell Improved Output Power) / PV Cell Input Energy Capacity
PV Cell Initial Efficiency	0.147219	= (PV Cell Initial Output Power) / PV Cell Input Energy Capacity
PV Cell Input Energy Capacity	18580.00 W	= (18.58 W) * 1000
Analytical Properties		

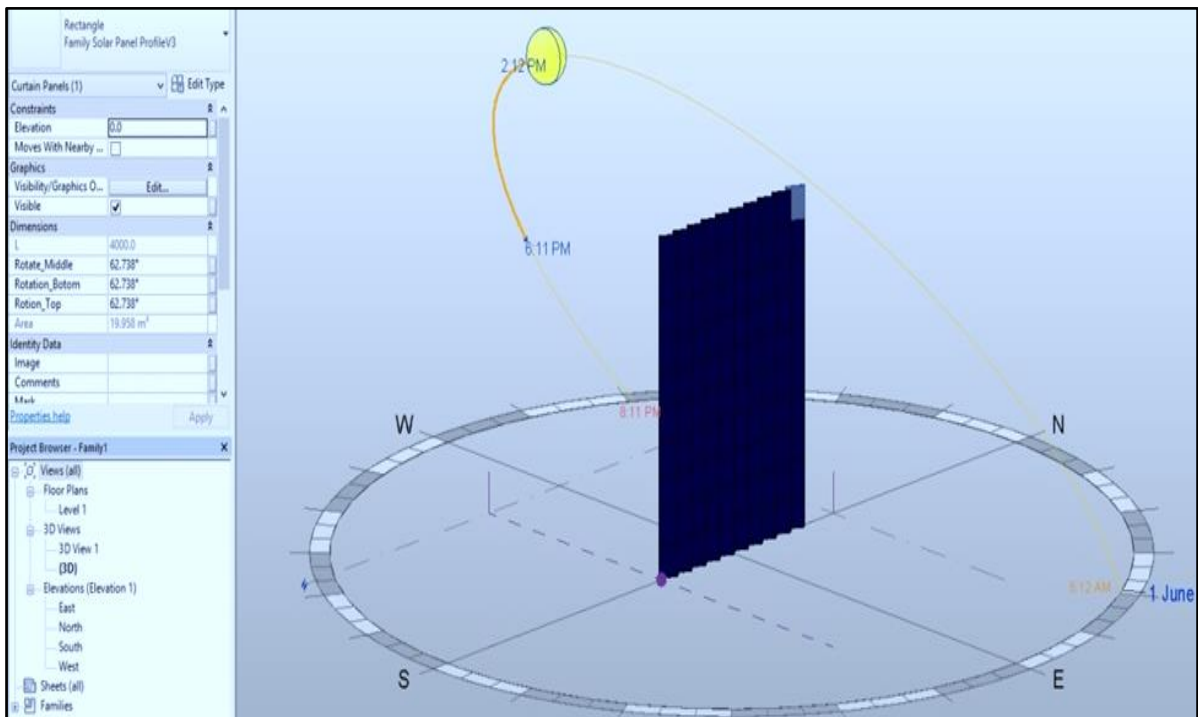


Figure 5.21: PV cell parameter respond performance during midday hours

Table 5.9: PV cell input parameters, performance during afternoon hours

Electrical Engineering		
PV Cell Maximum Current	360.00 A	= 10 A * 36
PV Cell Improved current (default)	355.32 A	= sin(Rotate_Middle) * PV Cell Maximum Current
PV Cell Inial Current	124.56 A	= 3.46 A * 36
PV Cell Potential Difference	21.96 V	= 0.61 V * 36
Electrical - Loads		
PV Cell Improved Output Power (default)	7802.89 W	= (PV Cell Potential Difference) * PV Cell Improved current
PV Cell Initial Output Power	2735.34 W	= (PV Cell Inial Current) * PV Cell Potential Difference
Dimensions		
Area of Solar Panel	18.581 m ²	= (3.048 m ² * 6.096)
L (report)	3048.0	=
Rotate_Middle (default)	80.754°	=
Rotation_Botom (default)	80.754°	=
Rotion_Top (default)	80.754°	=
Thicknes	76.2	=
Energy Analysis		
PV Cell Improved Efficiency (default)	0.419962	= (PV Cell Improved Output Power) / PV Cell Input Energy Capacity
PV Cell Initial Efficiency	0.147219	= (PV Cell Initial Output Power) / PV Cell Input Energy Capacity
PV Cell Input Energy Capacity	18580.00 W	= (18.58 W) * 1000
Analytical Properties		

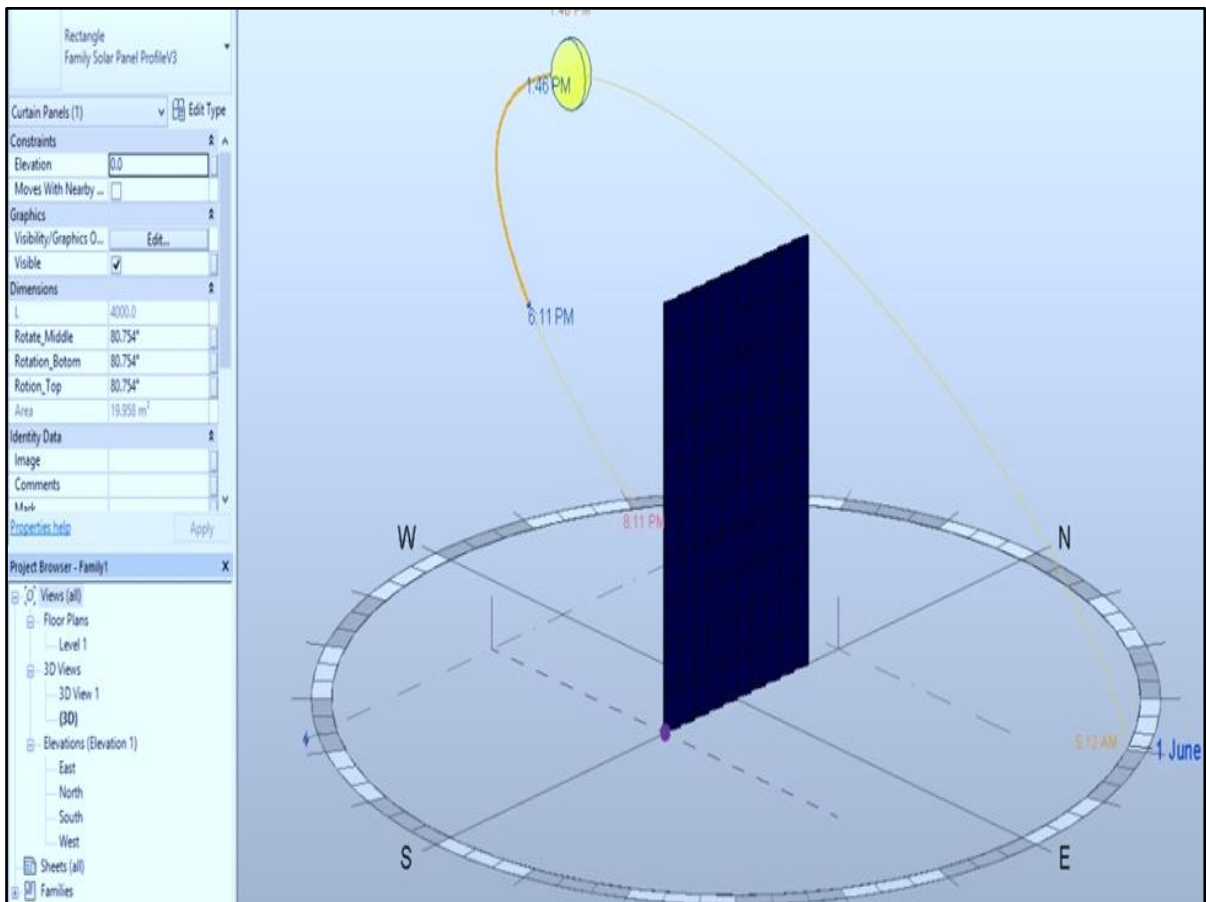


Figure 5.22: PV cell parameter respond performance during evening hours

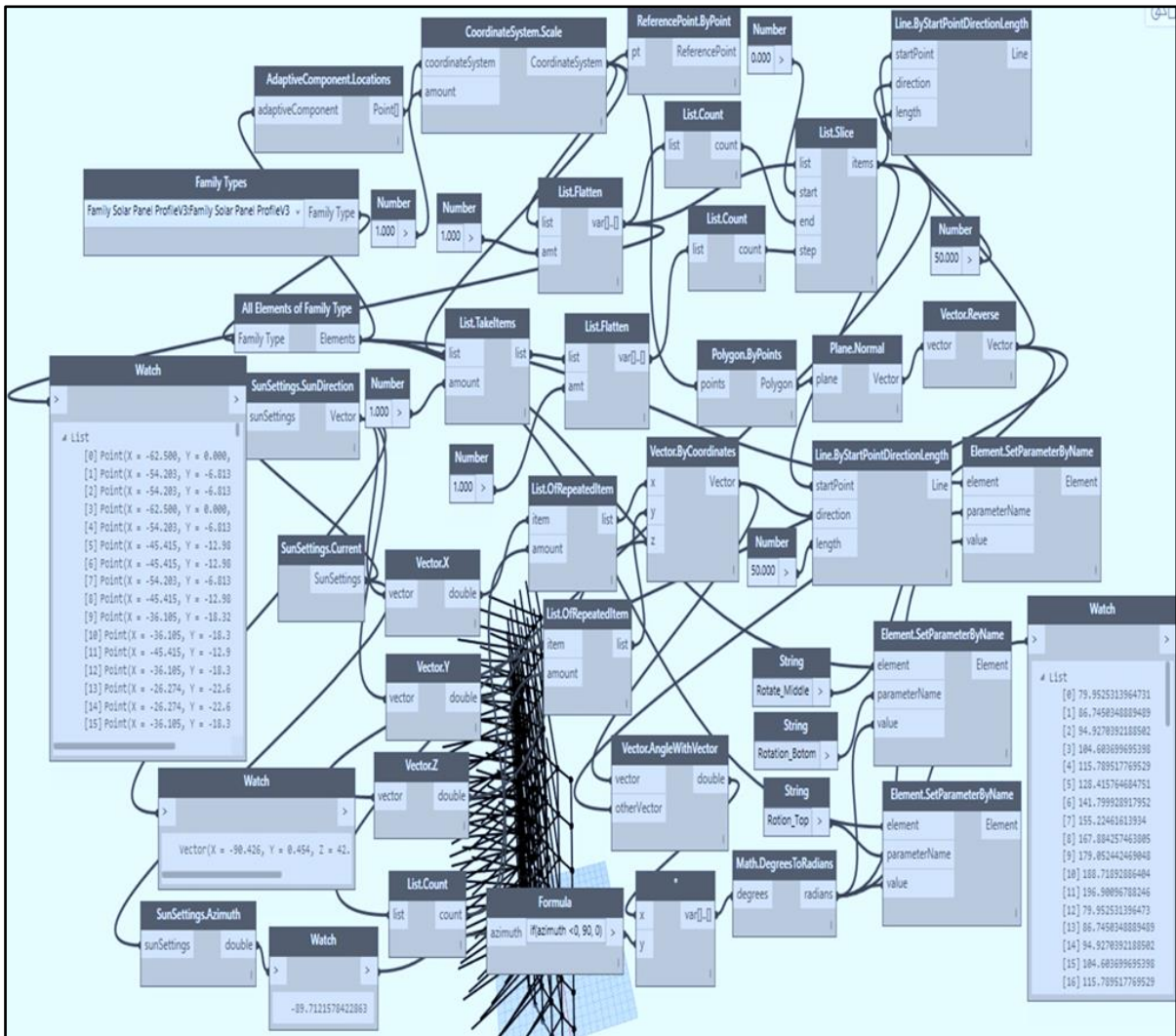


Figure 5.23: PV cell panel and simulated vectors aligning/misaligning with the sun position, and direction on the sky

5.9.7 Wind Turbine Description

The term wind turbine or wind power is described by the process used to generate electric power from kinetic mechanical power. Aerodynamics is an important concept to consider when designing an effective wind turbine, but size also matters: the longer the turbine blades are, the greater the diameter of the rotor, and more the energy a turbine can capture from the wind and thus the greater the electricity generating capacity. Generally, doubling the rotor diameter produces a fourfold increase in energy output [82, 83]. In some cases, the reverse results in better performance, such as in a lower-wind-speed area, a smaller diameter rotor can produce more wind power than a larger diameter rotor. This is because with smaller rotor diameter and shorter blades, it takes less wind power to spin the smaller generator. Thus, the turbine can run at full capacity

continuously. In addition, tower height is also a major factor in production capacity. The higher the turbine, the more energy it can capture because wind speeds increase proportionally with elevation height, that is, about 12% increase in wind speed with each doubling of elevation height [82]. Currently, most efficiently used wind turbines sizes and configuration are horizontal/vertical axis. However, the horizontal axis turbine with three blades configurations as shown in Figure 5.24 is widely used globally owing to its speed and aerodynamic turbulence stability.

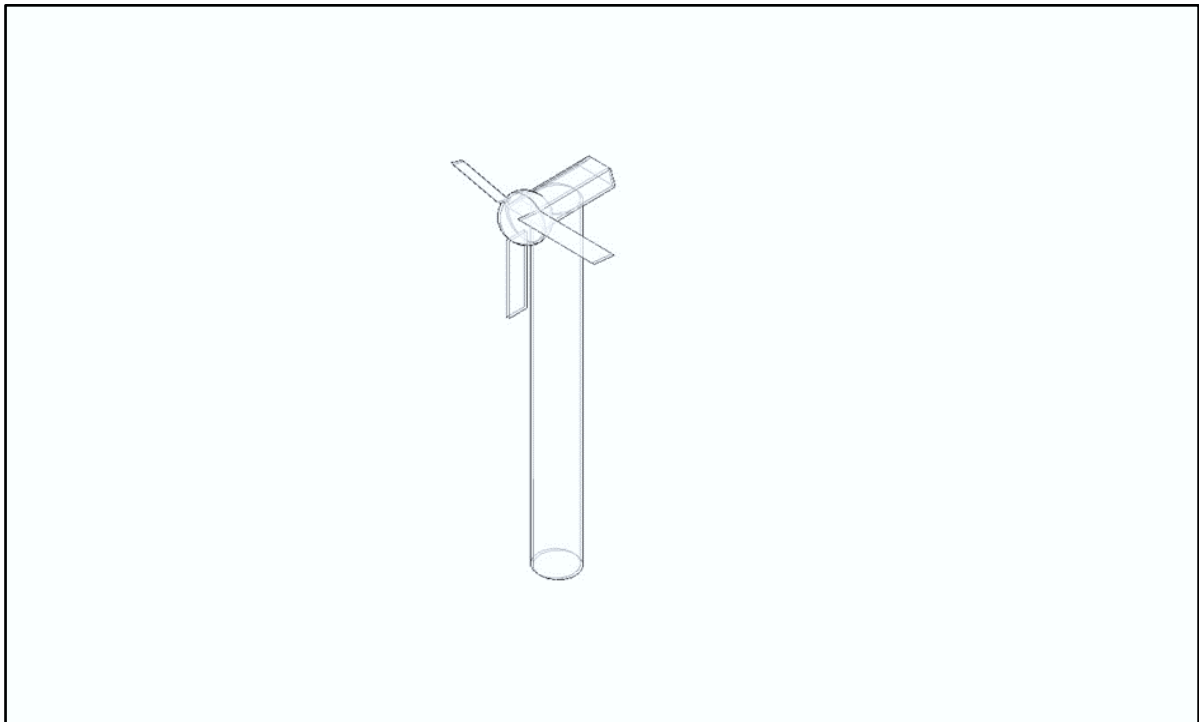


Figure 5.24: Wind turbine design for optimum performance

5.9.8 Basic wind turbine simulation

From the base run (part two) building energy simulation, annual wind power potential is recommended by the system as shown in Table 5.24, and based on this assumption, it was necessary to maximise the output power to keep tracking its performance. Wind turbine blades and rotor diameter were theoretically designed to meet the maximum optimisation of wind turbine. Thus, starting from the aerodynamic blade design, wind turbine blades and the rotor diameter are designed correctly maximised to suit wind turbine turbulence and its performance is also theoretically maximised. However, the study of wind turbine at maximum extraction shows that it is a complex issue. In addition, the study also shows three main types of proven methods that demonstrate that the MPPT system can improve the performance of the wind turbine. The methods are

(1) the wind turbine power coefficient, (C_p), (2) TSR and (3) OTC. As the aim of this thesis is designing the ultimate energy efficiency building, it is necessary to use the wind turbine also at maximum power extraction.

5.9.9 Maximising wind turbine using power coefficient

Power coefficient is a measurement of wind turbine efficiency. C_p is the ratio of actual electric power produced by a wind turbine divided by the total wind power moving into the turbine blades at a specific wind speed. The power coefficient represents the combined efficiency of the various wind power system components, which include the turbine blades, the shaft bearings and gear train, the generator and power electronics. The C_p for a particular turbine is measured or calculated by the manufacturer and usually provided at various wind speeds. Information about the C_p at any given wind speeds for a specific type of turbine can be used to estimate the electrical power output. Thus, the C_p of a particular wind turbine varies with operating conditions, such as wind speed, turbine blade angle, turbine rotation speed and other parameters. Overall, it is a measurement of a particular wind turbine's overall system efficiency.

$C_p = \frac{P_{out}}{P_{in}} = \frac{\text{Actual Power Produced}}{\text{Wind power in to the turbine}}$; this equation demonstrates that as the wind power approaching into the turbine increases, electrical power extracted increases [55].

In an effective wind turbine design, there are two types of wind speed velocities, V_1 , upper stream velocity and V_2 , downstream velocity. Theoretically, when $V_1 < V_2$, it implies breaking action upon the wind and when $V_1 = V_2 = 0$, no effective action occurs. Thus, the effective action occurs when the power of change in kinetic energy from upstream to downstream transform process occurs and this introduces interference factor, b , as the ratio of the two velocities, $b = \frac{V_1}{V_2}$ [84].

The rate of changing (kinetic energy) power, P , $= \frac{\Delta E}{\Delta t} = \frac{\frac{1}{2}(m(V_1^2) - m(V_2^2))}{\Delta t} = \frac{1}{2}m(V_1^2 - V_2^2)$, when $\Delta t \rightarrow 0$. Substituting for 'm' by the swept area, $P = \frac{1}{2}\rho SV(V_1^2 - V_2^2)$.

Where, S is the cross-sectional area of the rotor, ρ is the air density and m is the swept area of the wind turbine turbulence, which appears as cubic volume, $m = \rho S_1 V_1 = \rho S V = \rho S_2 V_2$

Thus, power density (P_d) = $\frac{p}{s} = \frac{\frac{1}{2}\rho s V^3}{s}$, $w = \frac{1}{2}\rho s V_1^3$, $C_p = \frac{p}{w} = \frac{\frac{1}{4}\rho s V_1^3(1-b^2)(1+b)}{\frac{1}{2}\rho s V_1^3} = \frac{1}{2}(1 - b^2)(1 + b)$. Table 5.10 and Figure 5.25 show that when $b = 0$, $C_p = 0.5$ and so on. Then, maximum power occurs when $b = 0.33$, according the calculation, $C_{p\text{maximum}} = 0.59$.

Table 5.10: Wind turbine maximum power extraction

b	0.0	0.1	0.3	0.4	0.5	0.6	0.7	0.8	0.9	1	1.1	1.2	1.3
C_p	0.5	0.54	0.59	0.58	0.26	0.51	0.34	0.32	0.18	0.00	-	-	-
											0.22	0.26	0.44

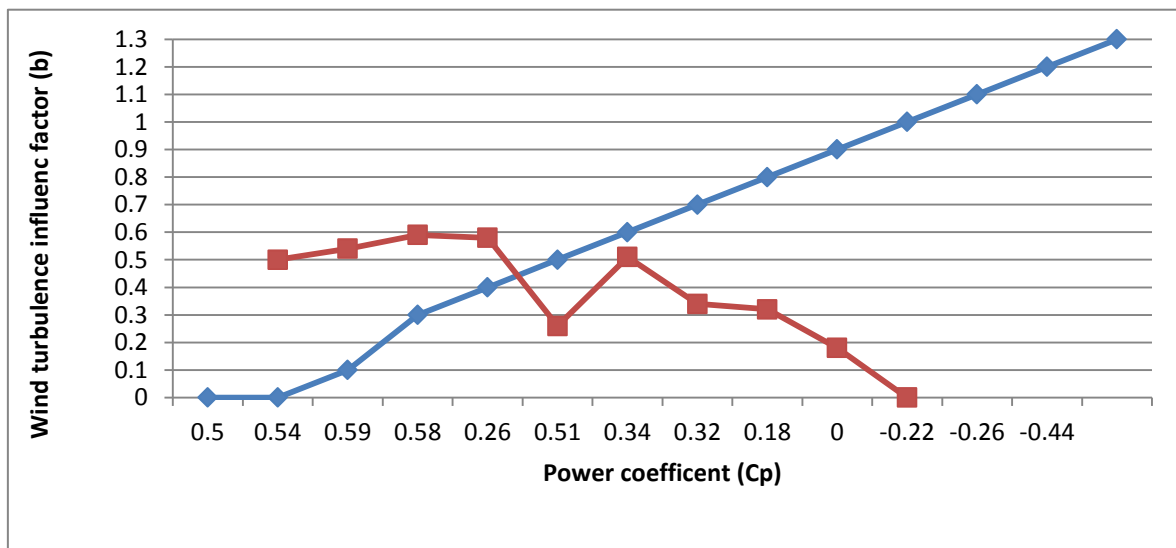


Figure 5.25: Wind turbine maximum power extraction

As derived earlier in this chapter, the maximum achievable power coefficient is 59%, which is the Betz Limit. In practice, however, obtainable values are involved and reduce the power coefficient to around 45%. These values are inefficiency and losses attributed by different configurations, rotor blades profiles, finite wings, friction and turbine designs. As mentioned earlier, the maximum power extraction occurs at the optimal TSR [84].

5.9.10 Maximising wind turbine power using tip speed ratio

TSR is the speed of the blade at its tips, divided by the speed of the wind. The tip of a blade travels at a meter per hour (mph) rate as does the wind. However, these two different speeds are never equal in practice, and the tip of the blade speed is always

higher the wind speed. Thus, the tip ratio becomes important for maximising wind turbine power calculation. This practical fundamental demonstrates facts of wind speed and tip relationships; when the blade set spins too slowly, most of the wind will pass by the rotor without being captured by the blades. Conversely, if the blades spin too fast, the blades will always be traveling through used/turbulent wind. It is important that to extract maximum power, enough time should be allowed to lapse between two blades traveling through the same location so that new/unused wind can enter this location. Thus, the next blade that passes through this location will be able to harness fresh/unused wind.

$TSR = \frac{\text{Actual tipping speed of the blade}}{\text{Current speed of the wind, where the generator is located}}$; this formula is used for each particular generator location [55, 56, 84].

Effective TSR depends on the blade of the aerofoil, number of blades and type of the wind turbine, and generally, a wind turbine with three blades that operates between 6 and 8 TSR is the most valuable.

Thus, for power extraction, the effective $TSR = \lambda = \frac{\omega r}{V}$, where V = the wind turbine speed, ω = rotor tip speed of the angular velocity (radians) and r = the wind turbine rotor blade radius.

The optimal TSR for maximum power extraction is governed by relating the time taken for the disturbed wind to re-establish itself to the time required for the next blade to move into the location of the preceding blade. These times are arranged by the following equations.

$T_s = \frac{2\pi}{n\omega} sec$, $T_w = \frac{S}{V} sec$, where n = number of blades, S = the length of the Windstream and ω = the rotor angular speed. The characteristics of these times for their being significant effective to produce optimised power is governed by the following comparisons:

If $T_s > T_w$, some wind is unaffected, and if $T_w > T_s$, some wind is not allowed to pass through the rotor blades. Hence, the maximum power extraction occurs when these two times are approximately equal, that is, when $T_s \cong T_w$, which yields this equation,

$\frac{2\pi}{n\omega} \cong \frac{S}{V} \Rightarrow \frac{n\omega}{V} \cong \frac{2\pi}{S}$, expressing this equation in terms of the optimum angular velocity,

$\omega_{Optimum} = \frac{2\pi V}{nS}$. Thus, to obtain optimal power extraction, the rotor blade rotates at angular speed, which is related to the speed of the oncoming wind. Because the rotor angular velocity decreases as the radius of the rotor increases, the characteristics of the rotor angular speed are governed by the optimal TSR, $\lambda_{Optimum} = \frac{\omega_{Optimum}}{V} r = \frac{2\pi}{n} \left(\frac{r}{S}\right)$

As mentioned previously, the optimal TSR depends on the number of rotor blades of the wind turbine. The lesser the number of rotor blades, the faster, the wind turbine rotates to extract the maximum power from the wind. For any n, the number of wind turbine blades, the empirical experience of the length of the Windstream time (S) is approximately equal to 50% of the rotor radius [84]. That is, $\frac{S}{r} \cong \frac{1}{2}$, $\lambda_{Optimal} \cong \frac{2\pi}{n} \left(\frac{r}{S}\right) \cong \frac{4\pi}{n}$ and TSR with 3 blades = 4.14 is the most effective and valuable.

Table 5.11 and Figure 5.26 show TSR for n = 2, 3 and 4 is 6.28, 4.19 and 3.14 respectively. With proper aerofoil design, the optimal TSR values may be approximately 25–30% above these values. These highly efficient rotor blade aerofoils increase the rotational speed of the blade and thus generate more power. Using this assumption, the optimal TSR for a three-bladed rotor would be in the range of 5.24–5.45. Poorly designed rotor blades that yield too low TSR would cause the wind turbine to exhibit a tendency to slow and stall. Conversely, if the TSR is too high, the wind turbine will rotate very rapidly and may experience larger stresses and become uncontrollable, which may lead to catastrophic failure in highly turbulent wind conditions [84].

Table 5.11: Wind turbine optimum TSR

n	2	3	4	5	6	7	8	9	10	11	12
λ	6.28	4.14	3.14	2.51	2.09	1.79	1.57	1.39	1.25	1.14	1.04

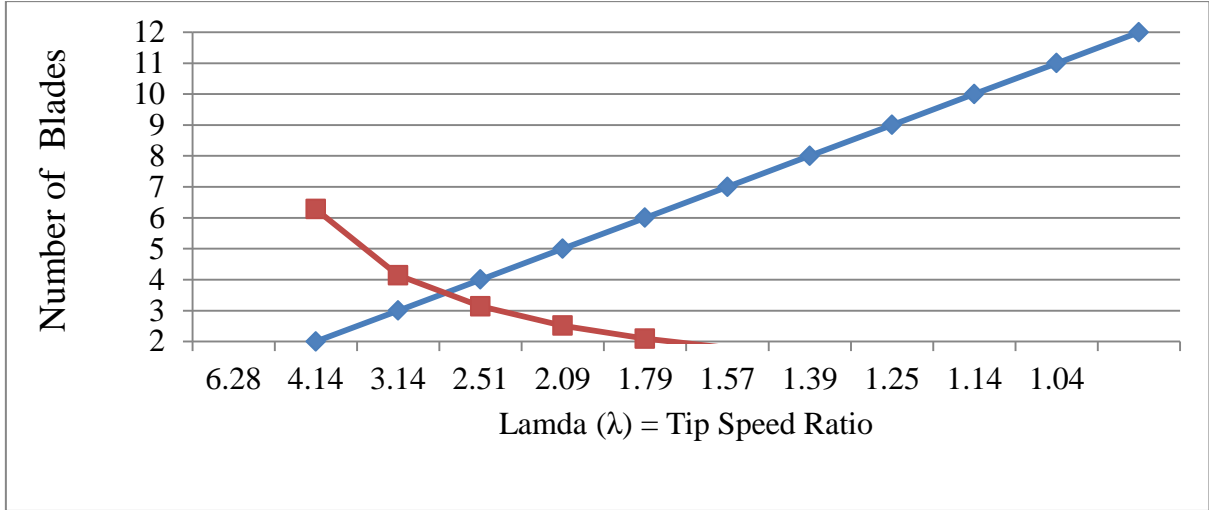


Figure 5.26: Wind turbine optimum TSR extraction

5.9.11 Maximising wind turbine power using optimal torque control

OTC is a method used for MPPT extraction. Owing to the sluggish response of wind turbines with high inertia, conventional OTC method was improved to increase the wind turbine efficiency by dynamically modifying the generator torque versus rotor speed. An effective tracking range (ETR) that corresponds to the local interval of wind speed with concentrated wind energy distribution is proposed and an improved OTC based on ETR was developed. In this method, based on a direct relationship between ETR and wind conditions, the torque curve can be quickly optimised so that higher and more stable MPPT efficiency can be achieved under varying wind conditions [57, 85].

Hence, OTC depends on $C_{p\text{maximum}}$ and $\text{TSR}_{\text{optimum}} = \lambda_{\text{optimum}}$, that is, when, $\lambda = \frac{\omega r}{v}$,

$$P_m = T_m \omega, P_m = \frac{1}{2} \rho \pi r^5 \frac{C_{p\text{maximum}}}{\lambda_{\text{optimum}}^3} \omega^3,$$

where $C_{p\text{maximum}}$ = maximum power extraction, and T_m = the generated control torque [86]. Thus, when the measurements of the parameters are almost perfectly taken and the wind turbine correctly modelled, the standard torque control system leads to the optimum power operation during the steady state and that is where the maximum OTC becomes effective. Thus, the maximum power is

$$P_m = \frac{1}{2} \rho \pi r^5 \frac{C_{p\text{maximum}}}{\lambda_{\text{optimum}}^3} \omega_m^3; \text{ rearranging the torque equation above, } T_m = \frac{P_m}{\omega_m} =$$

$$\frac{\frac{1}{2} \rho \pi r^5 \frac{C_{p\text{maximum}}}{\lambda_{\text{optimum}}^3} \omega_m^3}{\omega_m} = \frac{1}{2} \rho \pi r^5 \frac{C_{p\text{maximum}}}{\lambda_{\text{optimum}}^3} \omega_m^2. \text{ To calculate the maximum torque control,}$$

let us calculate the unknown parameters first, the rotor blade radius (r) and ω_m . Let us also use the maximum wind speed, approximately 15 m/sec, and the average turbine rotor to generator gear ratio unit as 1:100. Then, the generator should be running at least 1,500 rpm to generate effective electricity. From the gear ratio unit, the calculation of rotor blade rotation is 15 rpm. Then, conversion, the rpm to radian/sec, is $\omega = \omega_m = \frac{2\pi}{60} \times 15 = 1.57 \text{ rev/sec}$. For this case, assume $\omega = \omega_m$. Then, the air density of Sydney, Australia, using the international air density standard calculation formula is $\rho = \frac{\text{Air Pressure } (P)}{\text{Dry air } (R) \text{ Temperature } (T) \text{ in } (^{\circ}k)} = \frac{101325}{288.15 \times 287.05} = 1.23$. Next, from the TSR formula, $r = \frac{\lambda \times V}{\omega} = \frac{4.14 \times 15}{1.57} = 39.3 \cong 40 \text{ m}$. Then, the maximum torque is $T_m = \frac{1}{2} \times 1.23 \times 3.14 \times 40^5 \frac{0.59}{4.14^3} 1.57^2 = 4053962.86 \text{ w} = 4.05396286 \text{ Mw}$. This maximum torque shall be used for the MPPT. The computer algorithm software technique with sensing feedback of this torque will keep operating at maximum power extraction for the wind turbine mechanical power. This calculated torque is applied only for this rotor radius blade.

5.9.12 Calculation of renewable energy rated power

The base run energy building energy simulation proposed renewable energy potential in the New South Wales region where the building is located. For the wind turbine, the proposed annual rated power is 2,208 kWh from single 15-inch wind turbine. This 15-inch wind turbine can be planted on the compound ground or in the roof. For this thesis, it is planted on the top of the roof. As mentioned previously, the building is a commercial office building. According to the Australian work trading hours, the building will be in operation for at least eight hours a day for five days a week, except on public holidays. If the wind turbine is established to be in operation during working hours, that is 5 days a week $\times 4 = 20$ days in a month $\times 12 = 240$ days in a year. According to the NSW industrial relations website, there are 12 days public holidays per year, and hence, $240 - 12 = 228$ days working days a year. As mentioned previously the building is in operation for at least 8 hours: thus, $228 \text{ days} \times 8 = 1,824$ hours in a year. To find the rated power of the Wind turbine, the 2,208 kWh is divided by the operating hours, that is: $\frac{2208 \text{ kWh}}{1824 \text{ h}} = 1.22 \text{ kw}$. Hence, using the above concept and calculations, the wind turbine must be operated at its rated power or above.

5.10 Conclusion

Base run building energy simulation analysis covers the second main simulation part. The simulation processes simulate all the building elements for their capability of being energy efficient. However, the simulation results of this chapter revealed that base run simulation did not reduce energy usage. Hence, these are compared with the simulation part three results from the next chapter. In other words, this chapter acts as reference point to the part three simulation. In addition, this chapter focuses on optimum usage of renewable energy with minimum resource usage in predesigning energy efficient GB.

As is known, renewable energy is a key solution to tackle the energy cost, shortage of sustainable power supply and the global climate pollution produced by fossil oils and other similar substances. Increasing the productivity of renewable energy with optimised usage will eliminate fossil oil use in long term. Thus, this chapter proposed for this commercial office building three types of PV cell efficiency, classified as low, medium and high (5%, 10% and 15%) respectively and one type of 15-inch wind turbine. The PV cell efficiency of 15% is increased to 40% using the Sun intensity tracking method. Conversely, the performance of wind turbine potential energy is theoretically optimised using three main, proven different techniques (C_p , TSR and OTC). Thus, energy reduction obtained from this chapter is added to the previous chapter's annual energy reductions to summarise overall annual building energy usage reduction.

Chapter 6: Alternative Design Building Solar Energy Simulation

6.1 Introduction

Autodesk Revit energy simulation uses the Revit model as the basis for energy analysis, and then this energy analytical model (BIM) is packaged in gbXML files and exported to Autodesk GBS for further analysis. GBS uses the concept of a project as a means of storing simulation runs for the model and defines the building type, location, project operation schedule and other information that is used for the simulation. Hence, by performing energy analysis at regular intervals during the design process it can be ensured that the building model uses cost-effective strategies to achieve the desired sustainable energy efficient ratings.

6.2 Alternative Design Building Solar Energy Simulation Process

Alternative design solar building energy simulation is just a continuation part of base run (Chapter 5) solar building energy simulations. In this simulation, many significant alternative designs have been conducted, using several alternative energy packages.

Solar energy provides the largest untapped potential for global energy generation, while on-site production allows the possibilities of buildings to entirely erase their carbon footprint. In addition, in considering increased energy production, optimal methods of energy usage reduction are considered. Understanding solar energy allows us to reduce the heating in the winter, the cooling in the summer and the lighting energy usages throughout the year [87].

Alternative design energy simulation uses data from formatted gbXML files or BIM as parameters with specific details and units to enable the algorithm to compute the given task correctly and efficiently in minimal time. Tables 6.1 to 6.14 show the input parameters and the values of those parameters that have significant effect on the energy simulation process. Similar to the input parameters, output parameters are also proposed by the system. For example, similar to the base run simulation but more advanced, the alternative design simulation demonstrates building solar energy simulation in numerous alternative runs by automatically changing the Energy Efficient Building

(EEB) elements as a set of packages and by loading the actual regional currently updated weather files from the nearest weather station. Thus, the calculation of the simulations was performed briefly based on the fact of environmental weather files effect [73, 74].

The weather files action is to affect the actual building size and area to produce the output of solar building simulation results. Further, the action of weather files forced the alternative design run to demonstrate in detail with much reduced results, as shown in the second column in Table 6.15, parameters such as annual electricity use intensity per kWh/m²/year; annual fuel use intensity per MJ/m²/year, and total annual EUI per MJ/m²/year, average estimated life-cycle electricity use in kWh; average estimated life-cycle fuel use in MJ and the average estimated life-cycle cost in Australian dollars.

Figure 6.1 shows the complete design of GB fitted with a number of PV cell panels and one single 15-inch wind turbine. The PV cell panels and wind turbine are designed based on the base run building solar energy simulation (part two) output proposal for the regional area of Sydney's weather suffice.

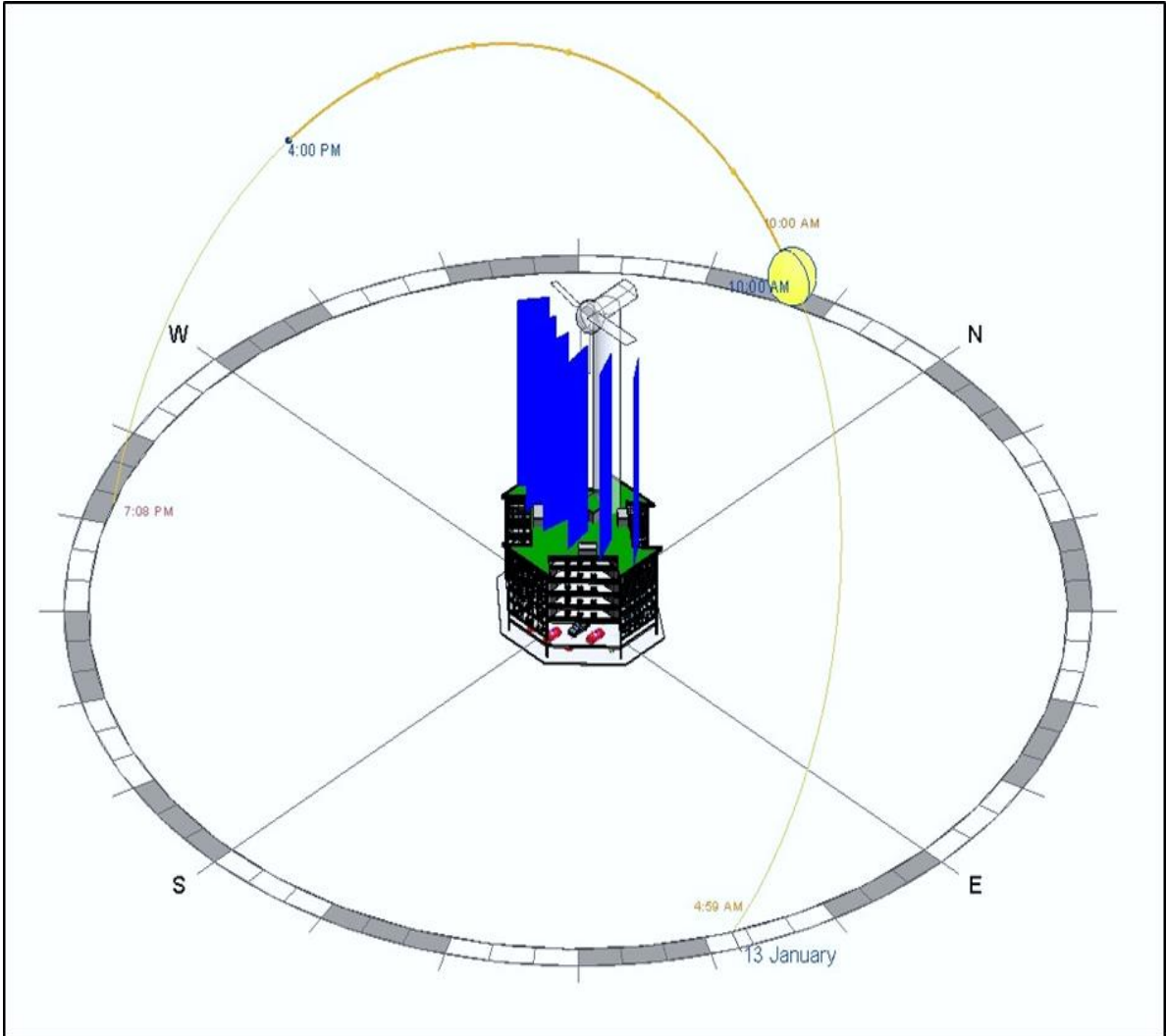


Figure 6.1: Whole building elements, solar building energy simulation

6.2.1 Alternative design method, number of run lists

Autodesk Revit, base run energy simulation run one cycle, which is one list of energy simulation processes and obtains one lists of results, is used as the reference point for the advanced alternative designs. Conversely, the alternative design runs several different configuration methods as ‘energy reduction alternative packages’ to archive the best and significantly reduced annual energy consumption results.

Alternative design building energy simulation was conducted using the cloud-based GBS tool designed by the Autodesk Revit for advanced alternative optional design to obtain the best reduced annual energy of fuel and electricity usages and hence to achieve much reduced cost of both energies. In this section, the GBS energy simulation processed 254 different simulations’ alternative run lists packages. Thus, these

alternative run list packages have been conducted sequentially by changing/replacing for their being best EEB elements. As shown in the Tables 6.1 to 6.14 list of energy package runs, the main interchangeable building elements are wall-to-window ratio (WWR) of all sides of the building, windows' shading, windows' shading height, windows' glass type, building orientation, wall insulation type, roof insulation type, infiltration, lighting efficiency, daylight control, occupancy energy control, plug load efficiency, ASHRAE energy packages, operating schedule and minimum/maximum internal loads.

As can be noticed from the above paragraph, every particular building element used to construct the building is being simulated and each possible method to reduce energy usages has been conducted, as shown in Tables 6.1 to 6.14, which present 254 alternative energy reduction simulation option lists.

Among the entire run lists, 'ASHRAE' energy packages were the best energy-saving methods out of all the alternative design run lists. To find the best energy simulation package from the entire run list, an analytical graph is used for each table list of content as shown from Figure 6.2 to 6.15. The last table in section, which is Table 6.14, presents details of the best simulation result (the HVACTYPES_ ASHRAE_ Package Terminal Heat Pump), as shown also in the analytical graph in the last figure in this section, which is Figure 6.15.

Table 6.1: Alternative design, energy simulation package result list number 1

Name	Date	User Name	Floor Area (m ²)	Energy Use Intensity (MJ/m ² year) (?)	Electric Cost (kWh)	Fuel Cost (MJ)	Total Annual Cost ¹			Total Annual Energy ¹			Carbon Emissions (Mg)	Compare	Potential Energy Savings									
							Electric	Fuel	Energy	Electric (kWh)	Fuel (MJ)	Energy												
Project Default Utility Rates													Weather Data: GBS_06M12_09_130095											
Project Default Utility Rates													--	--	--	--	--	--	--	--	--	--	--	--
Base Run																								
<input type="checkbox"/>	Intelligent Commercial Green Building Analysis	1/8/2018 12:27 AM	Berhanegw	1,358	710.4	\$0.06	\$0.007	\$10,317	\$2,643	\$12,960	169,127	355,886	87.9											
Alternate Run(s) of Intelligent Commercial Green Building Analysis																								
<input type="checkbox"/>	Intelligent Commercial Green Building Analysis_ASHRAE 90.1-2010	1/8/2018 12:30 AM	Berhanegw	1,358	582.2	\$0.06	\$0.007	\$10,513	\$1,264	\$11,776	172,340	170,137	80.0											
<input type="checkbox"/>	WWR - Northern Walls_95% -- Window Shades - North_No change -- Window Glass Types - North_No change	1/8/2018 12:30 AM	Berhanegw	1,358	723.1	\$0.06	\$0.007	\$10,315	\$2,772	\$13,087	169,093	373,204	88.7											
<input type="checkbox"/>	WWR - Northern Walls_95% -- Window Shades - North_No change -- Window Glass Types - North_Sgl Clr	1/8/2018 12:30 AM	Berhanegw	1,358	890.0	\$0.06	\$0.007	\$13,761	\$2,944	\$16,706	225,592	396,406	115.2											
<input type="checkbox"/>	WWR - Northern Walls_95% -- Window Shades - North_No change -- Window Glass Types - North_Dbl Clr	1/8/2018 12:30 AM	Berhanegw	1,358	853.8	\$0.06	\$0.007	\$13,546	\$2,674	\$16,220	222,062	360,019	111.8											
<input type="checkbox"/>	WWR - Northern Walls_95% -- Window Shades - North_No change -- Window Glass Types - North_Dbl LoE	1/8/2018 12:30 AM	Berhanegw	1,358	857.5	\$0.06	\$0.007	\$13,938	\$2,539	\$16,477	228,495	341,825	113.8											
<input type="checkbox"/>	WWR - Northern Walls_95% -- Window Shades - North_No change -- Window Glass Types - North_Tip LoE	1/8/2018 12:30 AM	Berhanegw	1,358	742.1	\$0.06	\$0.007	\$11,942	\$2,250	\$14,192	195,776	302,927	97.2											
<input type="checkbox"/>	WWR - Northern Walls_95% -- Window Shades - North_1/3 Win Height -- Window Glass Types - North_No ch	1/8/2018 12:30 AM	Berhanegw	1,358	723.8	\$0.06	\$0.007	\$10,211	\$2,824	\$13,036	167,399	380,232	88.3											
<input type="checkbox"/>	WWR - Northern Walls_95% -- Window Shades - North_1/3 Win Height -- Window Glass Types - North_Sgl C	1/8/2018 12:30 AM	Berhanegw	1,358	846.0	\$0.06	\$0.007	\$12,652	\$2,987	\$15,639	207,409	402,136	107.4											
<input type="checkbox"/>	WWR - Northern Walls_95% -- Window Shades - North_1/3 Win Height -- Window Glass Types - North_Dbl C	1/8/2018 12:30 AM	Berhanegw	1,358	811.7	\$0.06	\$0.007	\$12,510	\$2,703	\$15,214	205,088	363,960	104.4											
<input type="checkbox"/>	WWR - Northern Walls_95% -- Window Shades - North_1/3 Win Height -- Window Glass Types - North_Dbl L	1/8/2018 12:30 AM	Berhanegw	1,358	810.9	\$0.06	\$0.007	\$12,804	\$2,567	\$15,371	209,907	345,555	105.6											
<input type="checkbox"/>	WWR - Northern Walls_95% -- Window Shades - North_1/3 Win Height -- Window Glass Types - North_Tip L	1/8/2018 12:30 AM	Berhanegw	1,358	714.1	\$0.06	\$0.007	\$11,332	\$2,235	\$13,568	185,774	300,932	92.6											
<input type="checkbox"/>	WWR - Northern Walls_95% -- Window Shades - North_2/3 Win Height -- Window Glass Types - North_No ch	1/8/2018 12:30 AM	Berhanegw	1,358	725.8	\$0.06	\$0.007	\$10,147	\$2,873	\$13,020	166,348	386,805	88.2											

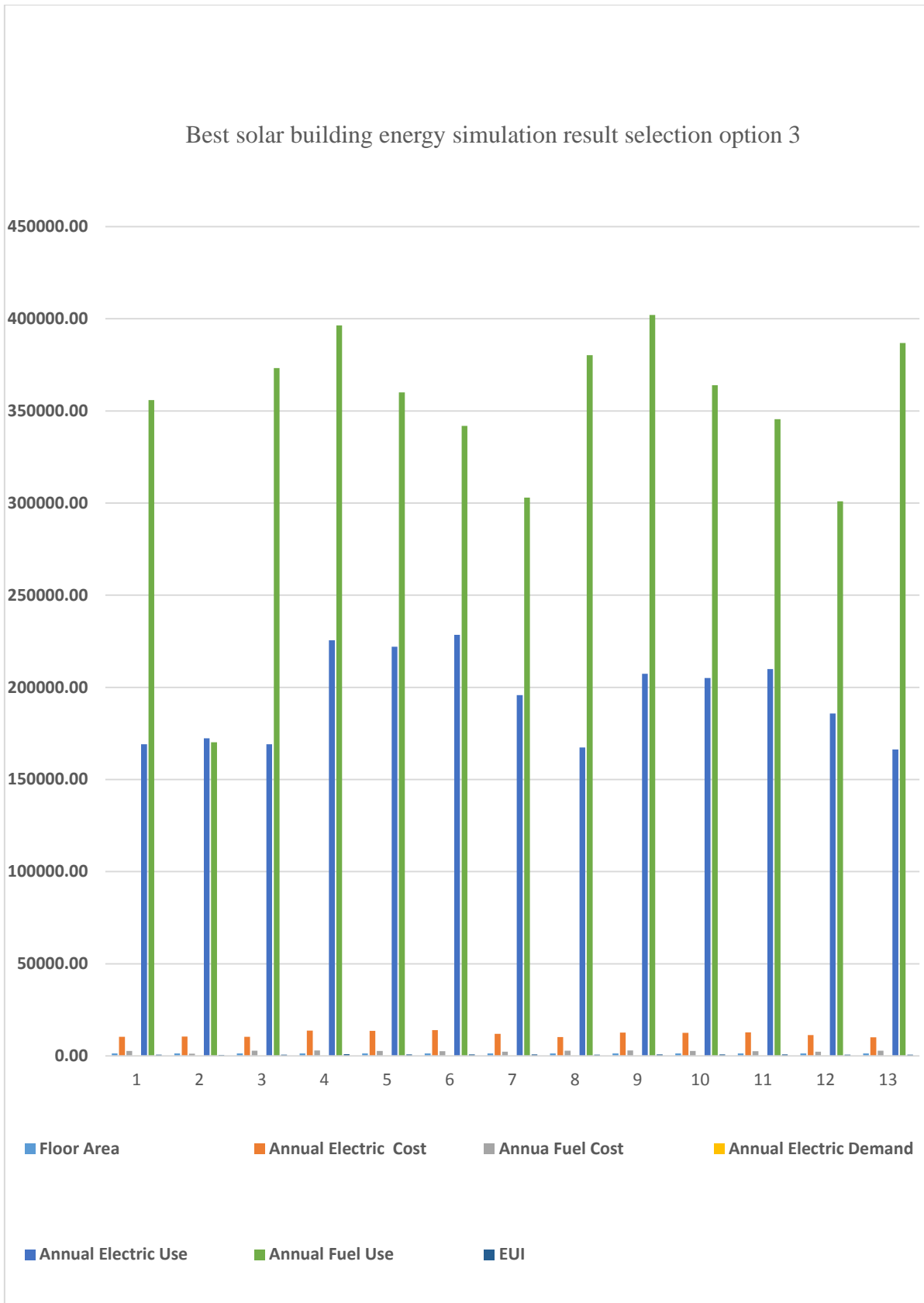


Figure 6.2: Best solar building energy simulation result chart 1

Table 6.2: Alternative design, energy simulation package result list number 2

<input type="checkbox"/>	WWR - Northern Walls_95% -- Window Shades - North_2/3 Win Height -- Window Glass Types - North_Sgl C	1/8/2018 12:30 AM	Berhanegw	1,358	806.5	\$0.06	\$0.007	\$11,830	\$2,950	\$14,779	193,927	397,096	101.0	
<input type="checkbox"/>	WWR - Northern Walls_95% -- Window Shades - North_2/3 Win Height -- Window Glass Types - North_Dbl C	1/8/2018 12:30 AM	Berhanegw	1,358	772.3	\$0.06	\$0.007	\$11,726	\$2,650	\$14,376	192,231	356,764	98.3	
<input type="checkbox"/>	WWR - Northern Walls_95% -- Window Shades - North_2/3 Win Height -- Window Glass Types - North_Dbl L	1/8/2018 12:30 AM	Berhanegw	1,358	767.7	\$0.06	\$0.007	\$11,947	\$2,507	\$14,453	195,845	337,496	98.9	
<input type="checkbox"/>	WWR - Northern Walls_95% -- Window Shades - North_2/3 Win Height -- Window Glass Types - North_Tp L	1/8/2018 12:30 AM	Berhanegw	1,358	691.5	\$0.06	\$0.007	\$10,887	\$2,202	\$13,089	178,480	296,444	89.1	
<input type="checkbox"/>	WWR - Northern Walls_65% -- Window Shades - North_No change -- Window Glass Types - North_No change	1/8/2018 12:30 AM	Berhanegw	1,358	704.2	\$0.06	\$0.007	\$10,206	\$2,629	\$12,835	167,306	353,929	87.0	
<input type="checkbox"/>	WWR - Northern Walls_65% -- Window Shades - North_No change -- Window Glass Types - North_Sgl Clr	1/8/2018 12:30 AM	Berhanegw	1,358	805.8	\$0.06	\$0.007	\$12,477	\$2,658	\$15,135	204,536	357,849	103.9	
<input type="checkbox"/>	WWR - Northern Walls_65% -- Window Shades - North_No change -- Window Glass Types - North_Dbl Clr	1/8/2018 12:30 AM	Berhanegw	1,358	776.7	\$0.06	\$0.007	\$12,262	\$2,459	\$14,721	201,020	331,043	100.9	
<input type="checkbox"/>	WWR - Northern Walls_65% -- Window Shades - North_No change -- Window Glass Types - North_Dbl LoE	1/8/2018 12:30 AM	Berhanegw	1,358	777.1	\$0.06	\$0.007	\$12,495	\$2,361	\$14,856	204,829	317,874	102.0	
<input type="checkbox"/>	WWR - Northern Walls_65% -- Window Shades - North_No change -- Window Glass Types - North_Tp LoE	1/8/2018 12:30 AM	Berhanegw	1,358	700.8	\$0.06	\$0.007	\$11,215	\$2,153	\$13,368	183,850	289,838	91.2	
<input type="checkbox"/>	WWR - Northern Walls_65% -- Window Shades - North_1/3 Win Height -- Window Glass Types - North_No ch	1/8/2018 12:30 AM	Berhanegw	1,358	705.1	\$0.06	\$0.007	\$10,143	\$2,685	\$12,829	166,286	358,829	86.7	
<input type="checkbox"/>	WWR - Northern Walls_65% -- Window Shades - North_1/3 Win Height -- Window Glass Types - North_Sgl C	1/8/2018 12:30 AM	Berhanegw	1,358	778.1	\$0.06	\$0.007	\$11,819	\$2,668	\$14,487	193,756	359,170	99.1	
<input type="checkbox"/>	WWR - Northern Walls_65% -- Window Shades - North_1/3 Win Height -- Window Glass Types - North_Dbl C	1/8/2018 12:30 AM	Berhanegw	1,358	751.1	\$0.06	\$0.007	\$11,664	\$2,463	\$14,127	191,219	331,538	96.6	
<input type="checkbox"/>	WWR - Northern Walls_65% -- Window Shades - North_1/3 Win Height -- Window Glass Types - North_Dbl L	1/8/2018 12:30 AM	Berhanegw	1,358	748.5	\$0.06	\$0.007	\$11,849	\$2,356	\$14,205	194,249	317,131	97.2	
<input type="checkbox"/>	WWR - Northern Walls_65% -- Window Shades - North_1/3 Win Height -- Window Glass Types - North_Tp L	1/8/2018 12:30 AM	Berhanegw	1,358	685.9	\$0.06	\$0.007	\$10,864	\$2,156	\$13,020	178,100	290,248	88.6	
<input type="checkbox"/>	WWR - Northern Walls_65% -- Window Shades - North_2/3 Win Height -- Window Glass Types - North_No ch	1/8/2018 12:30 AM	Berhanegw	1,358	707.1	\$0.06	\$0.007	\$10,103	\$2,704	\$12,807	165,629	363,992	86.7	

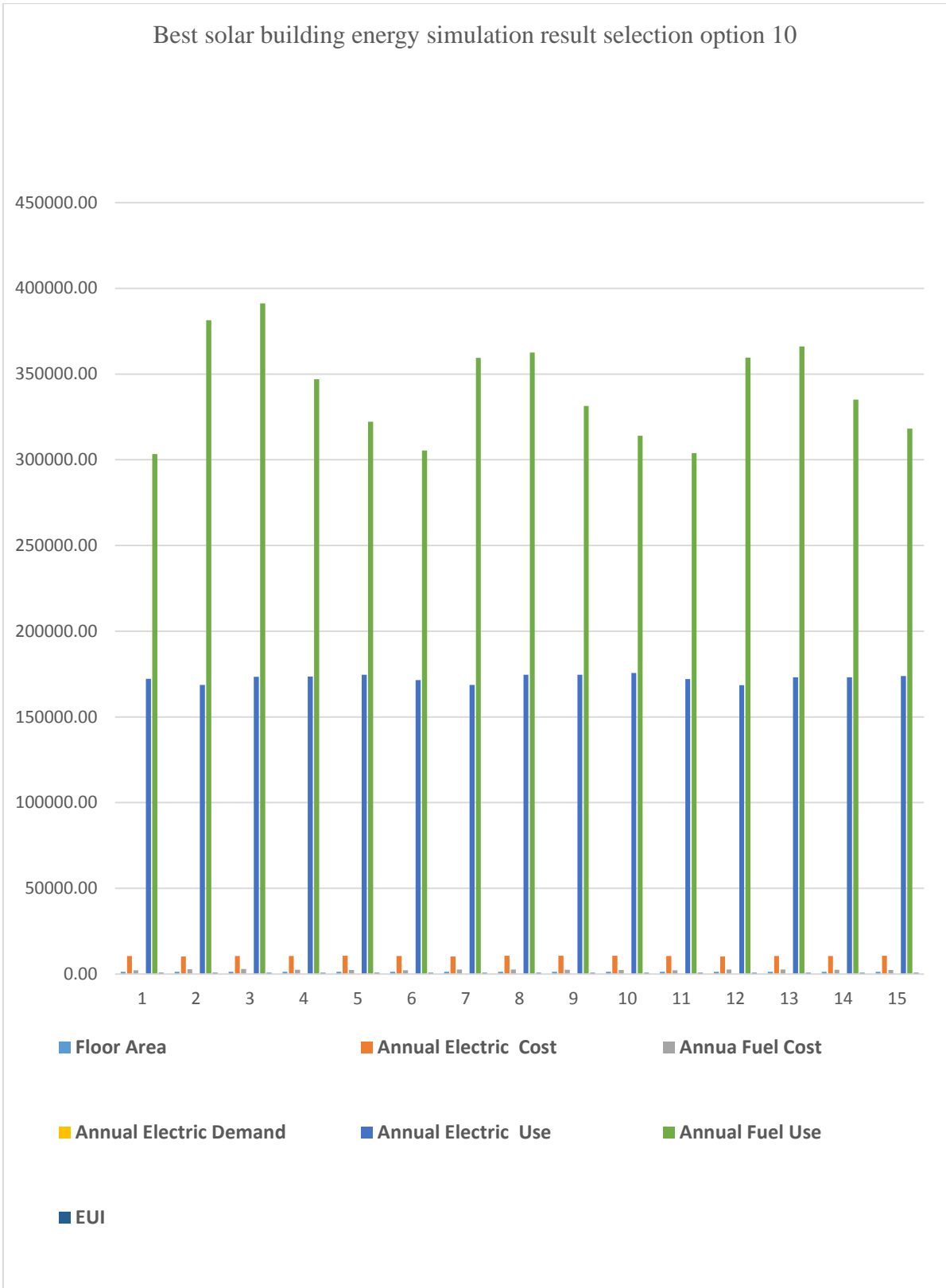


Figure 6.3: Best solar building energy simulation result chart 2

Table 6.3: Alternative design, energy simulation package result list number 3

☐	WWR - Northern Walls 30% -- Window Shades - North 2/3 Win Height -- Window Glass Types - North_Dbl L	1/8/2018 12:30 AM	Berhanegw	1,358	676.8	\$0.06	\$0.007	\$10,559	\$2,198	\$12,757	173,106	295,800	86.7	
☐	WWR - Northern Walls 30% -- Window Shades - North 2/3 Win Height -- Window Glass Types - North_Trp L	1/8/2018 12:30 AM	Berhanegw	1,358	666.3	\$0.06	\$0.007	\$10,258	\$2,224	\$12,481	168,157	299,390	84.6	
☐	WWR - Northern Walls 0% -- Window Shades - North_No change -- Window Glass Types - North_No change	1/8/2018 12:30 AM	Berhanegw	1,358	673.1	\$0.06	\$0.007	\$10,078	\$2,371	\$12,449	165,213	319,245	84.3	
☐	WWR - Southern Walls 95% -- Window Shades - South_No change -- Window Glass Types - South_No change	1/8/2018 12:30 AM	Berhanegw	1,358	729.0	\$0.06	\$0.007	\$10,313	\$2,832	\$13,146	169,070	381,315	89.1	
☐	WWR - Southern Walls 95% -- Window Shades - South_No change -- Window Glass Types - South_Sgl Clr	1/8/2018 12:30 AM	Berhanegw	1,358	752.0	\$0.06	\$0.007	\$10,845	\$2,832	\$13,676	177,781	381,202	93.0	
☐	WWR - Southern Walls 95% -- Window Shades - South_No change -- Window Glass Types - South_Dbl Clr	1/8/2018 12:30 AM	Berhanegw	1,358	719.1	\$0.06	\$0.007	\$10,839	\$2,502	\$13,341	177,686	336,857	90.8	
☐	WWR - Southern Walls 95% -- Window Shades - South_No change -- Window Glass Types - South_Dbl LoE	1/8/2018 12:30 AM	Berhanegw	1,358	705.2	\$0.06	\$0.007	\$10,945	\$2,316	\$13,260	179,420	311,776	90.3	
☐	WWR - Southern Walls 95% -- Window Shades - South_No change -- Window Glass Types - South_Trp LoE	1/8/2018 12:30 AM	Berhanegw	1,358	681.7	\$0.06	\$0.007	\$10,610	\$2,225	\$12,835	173,932	299,609	87.2	
☐	WWR - Southern Walls 95% -- Window Shades - South 1/3 Win Height -- Window Glass Types - South_No ch	1/8/2018 12:30 AM	Berhanegw	1,358	728.2	\$0.06	\$0.007	\$10,294	\$2,832	\$13,126	168,753	381,314	89.0	
☐	WWR - Southern Walls 95% -- Window Shades - South 1/3 Win Height -- Window Glass Types - South_Sgl C	1/8/2018 12:30 AM	Berhanegw	1,358	748.5	\$0.06	\$0.007	\$10,661	\$2,877	\$13,538	174,772	387,301	92.0	
☐	WWR - Southern Walls 95% -- Window Shades - South 1/3 Win Height -- Window Glass Types - South_Dbl C	1/8/2018 12:30 AM	Berhanegw	1,358	716.6	\$0.06	\$0.007	\$10,667	\$2,552	\$13,219	174,870	343,559	89.8	
☐	WWR - Southern Walls 95% -- Window Shades - South 1/3 Win Height -- Window Glass Types - South_Dbl L	1/8/2018 12:30 AM	Berhanegw	1,358	701.4	\$0.06	\$0.007	\$10,744	\$2,365	\$13,108	176,127	318,357	89.1	

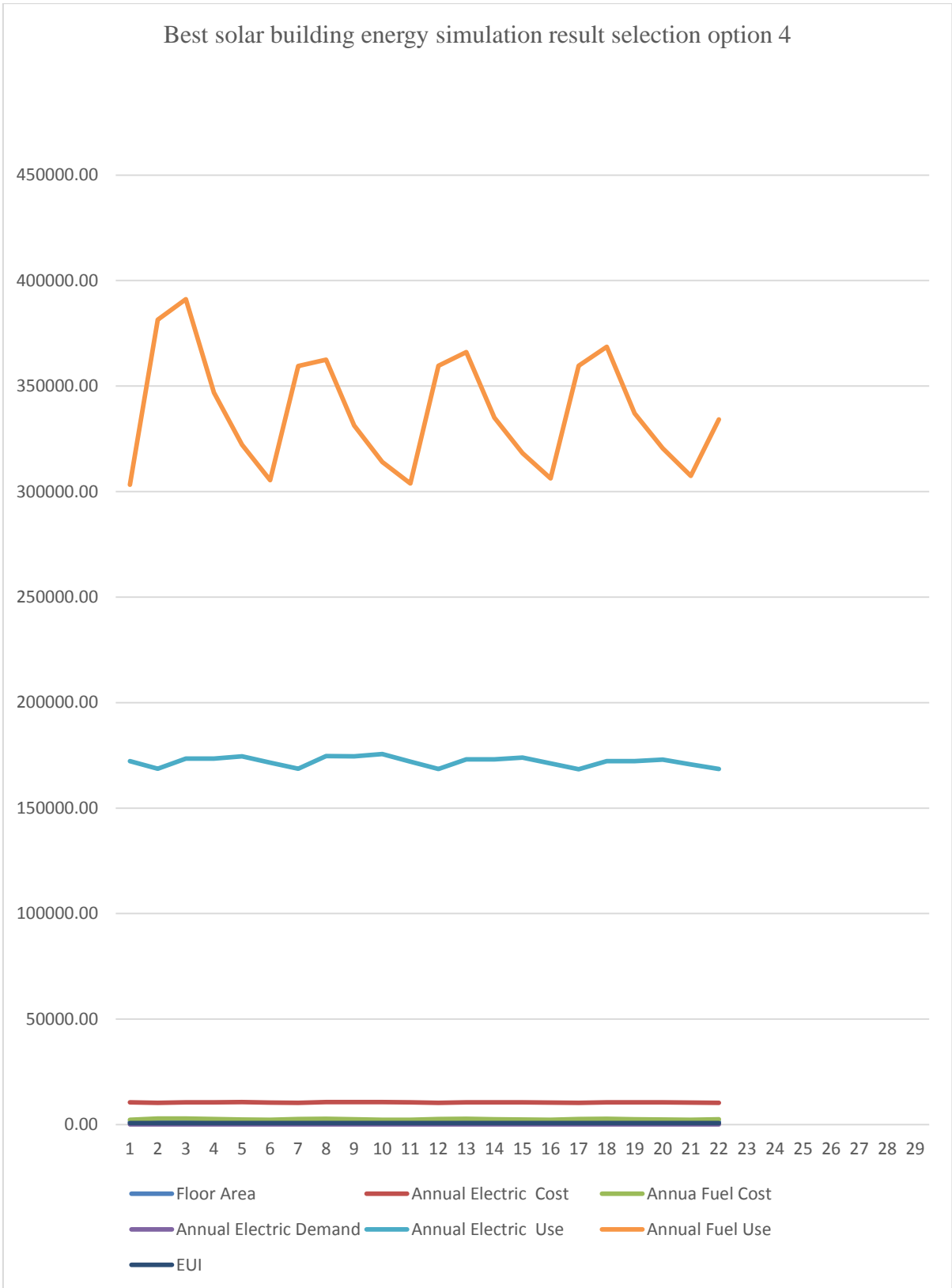


Figure 6.4: Best solar building energy simulation result chart 3

Table 6.4: Alternative design, energy simulation package result list number 4

<input type="checkbox"/>	Shades - South 1/3 Win Height -- Window Glass Types - South_Dbl L	1/8/2018 12:30 AM	Berhanegw	1,358	701.4	\$0.06	\$0.007	\$10,744	\$2,365	\$13,108	176,127	318,357	89.1	
<input type="checkbox"/>	WWR - Southern Walls 95% -- Window Shades - South 1/3 Win Height -- Window Glass Types - South_Trp L	1/8/2018 12:30 AM	Berhanegw	1,358	680.0	\$0.06	\$0.007	\$10,508	\$2,253	\$12,760	172,257	303,253	86.6	
<input type="checkbox"/>	WWR - Southern Walls 95% -- Window Shades - South 2/3 Win Height -- Window Glass Types - South_No ch	1/8/2018 12:30 AM	Berhanegw	1,358	727.9	\$0.06	\$0.007	\$10,285	\$2,834	\$13,119	168,608	381,477	88.9	
<input type="checkbox"/>	WWR - Southern Walls 95% -- Window Shades - South 2/3 Win Height -- Window Glass Types - South_Sgl C	1/8/2018 12:30 AM	Berhanegw	1,358	747.8	\$0.06	\$0.007	\$10,578	\$2,906	\$13,484	173,414	391,224	91.6	
<input type="checkbox"/>	WWR - Southern Walls 95% -- Window Shades - South 2/3 Win Height -- Window Glass Types - South_Dbl C	1/8/2018 12:30 AM	Berhanegw	1,358	715.4	\$0.06	\$0.007	\$10,582	\$2,577	\$13,159	173,483	346,887	89.4	
<input type="checkbox"/>	WWR - Southern Walls 95% -- Window Shades - South 2/3 Win Height -- Window Glass Types - South_Dbl L	1/8/2018 12:30 AM	Berhanegw	1,358	700.0	\$0.06	\$0.007	\$10,647	\$2,393	\$13,040	174,537	322,180	88.6	
<input type="checkbox"/>	WWR - Southern Walls 95% -- Window Shades - South 2/3 Win Height -- Window Glass Types - South_Trp L	1/8/2018 12:30 AM	Berhanegw	1,358	679.5	\$0.06	\$0.007	\$10,461	\$2,268	\$12,729	171,489	305,400	86.4	
<input type="checkbox"/>	WWR - Southern Walls 65% -- Window Shades - South No change -- Window Glass Types - South_No change	1/8/2018 12:30 AM	Berhanegw	1,358	712.0	\$0.06	\$0.007	\$10,291	\$2,670	\$12,961	168,712	359,450	87.9	
<input type="checkbox"/>	WWR - Southern Walls 65% -- Window Shades - South No change -- Window Glass Types - South_Sgl Cir	1/8/2018 12:30 AM	Berhanegw	1,358	729.9	\$0.06	\$0.007	\$10,652	\$2,693	\$13,345	174,625	362,519	90.7	
<input type="checkbox"/>	WWR - Southern Walls 65% -- Window Shades - South No change -- Window Glass Types - South_Dbl Cir	1/8/2018 12:30 AM	Berhanegw	1,358	706.7	\$0.06	\$0.007	\$10,647	\$2,461	\$13,107	174,533	331,300	89.1	
<input type="checkbox"/>	WWR - Southern Walls 65% -- Window Shades - South No change -- Window Glass Types - South_Dbl LoE	1/8/2018 12:30 AM	Berhanegw	1,358	696.8	\$0.06	\$0.007	\$10,712	\$2,332	\$13,045	175,613	313,986	88.7	
	Created from base run: intelligent Commercial Green Building Analysis													
<input type="checkbox"/>	WWR - Southern Walls 65% -- Window Shades - South No change -- Window Glass Types - South_Trp LoE	1/8/2018 12:30 AM	Berhanegw	1,358	679.9	\$0.06	\$0.007	\$10,496	\$2,257	\$12,752	172,059	303,839	86.6	
<input type="checkbox"/>	WWR - Southern Walls 65% -- Window Shades - South 1/3 Win Height -- Window Glass Types - South_No ch	1/8/2018 12:30 AM	Berhanegw	1,358	711.5	\$0.06	\$0.007	\$10,278	\$2,671	\$12,949	168,496	359,600	87.8	
<input type="checkbox"/>	WWR - Southern Walls 65% -- Window Shades - South 1/3 Win Height -- Window Glass Types - South_Sgl C	1/8/2018 12:30 AM	Berhanegw	1,358	728.4	\$0.06	\$0.007	\$10,557	\$2,719	\$13,276	173,065	366,108	90.1	
<input type="checkbox"/>	WWR - Southern Walls 65% -- Window Shades - South 1/3 Win Height -- Window Glass Types - South_Dbl C	1/8/2018 12:30 AM	Berhanegw	1,358	705.5	\$0.06	\$0.007	\$10,556	\$2,489	\$13,045	173,056	335,065	88.6	
<input type="checkbox"/>	WWR - Southern Walls 65% -- Window Shades - South 1/3 Win Height -- Window Glass Types - South_Dbl L	1/8/2018 12:30 AM	Berhanegw	1,358	695.3	\$0.06	\$0.007	\$10,608	\$2,364	\$12,971	173,894	318,194	88.1	

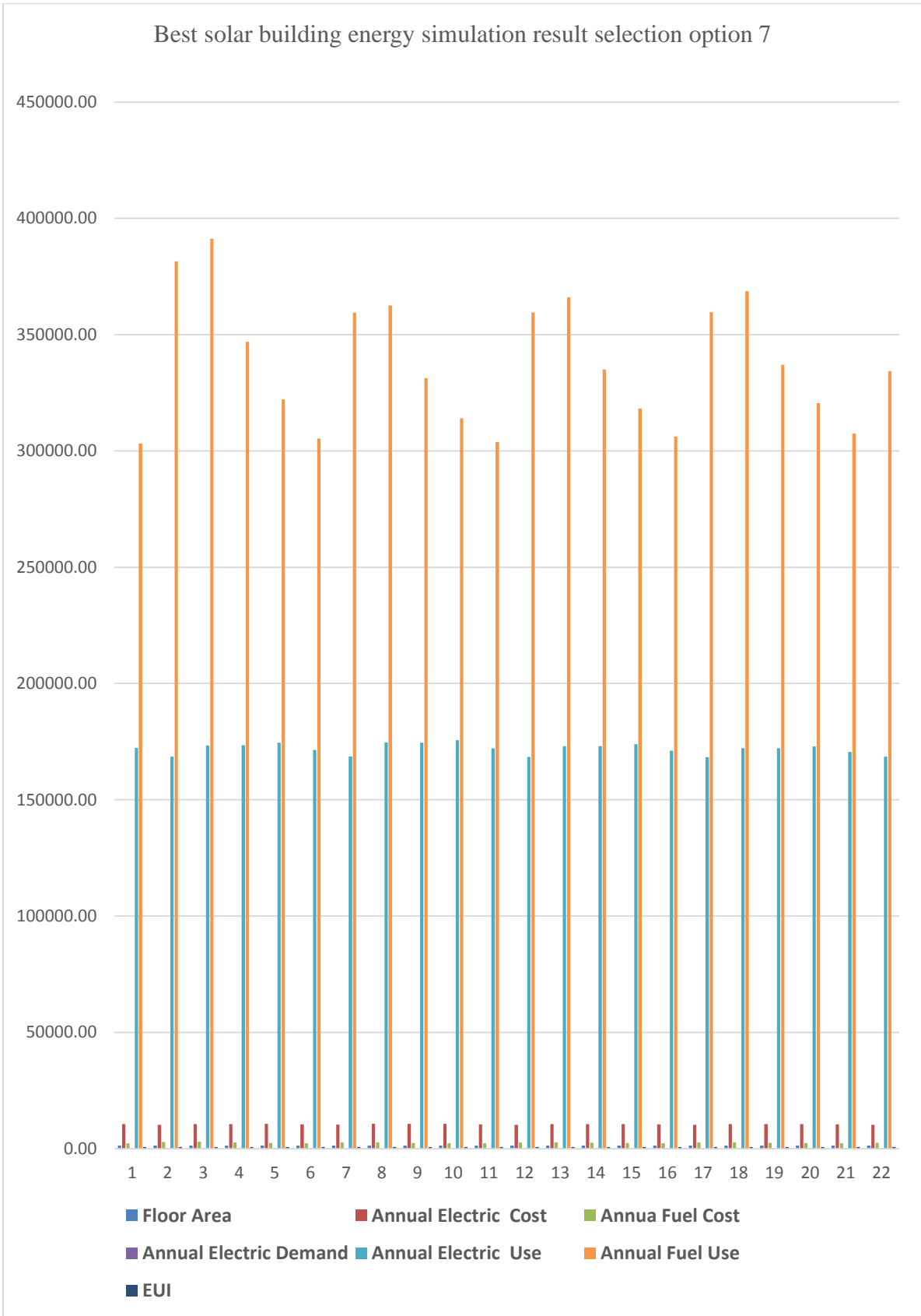


Figure 6.5: Best solar building energy simulation result chart 4

Table 6.5: Alternative design, energy simulation package result list number 5

☐	WWR - Southern Walls 65% -- Window Shades - South 1/3 Win Height -- Window Glass Types - South_Trp L	1/8/2018 12:30 AM	Berhanegw	1,358	679.3	\$0.06	\$0.007	\$10,441	\$2,274	\$12,716	171,167	306,196	86.3	
☐	WWR - Southern Walls 65% -- Window Shades - South 2/3 Win Height -- Window Glass Types - South_No ch	1/8/2018 12:30 AM	Berhanegw	1,358	711.2	\$0.06	\$0.007	\$10,270	\$2,671	\$12,942	168,368	359,651	87.7	
☐	WWR - Southern Walls 65% -- Window Shades - South 2/3 Win Height -- Window Glass Types - South_Sgl C	1/8/2018 12:30 AM	Berhanegw	1,358	728.0	\$0.06	\$0.007	\$10,506	\$2,738	\$13,244	172,222	368,620	89.9	
☐	WWR - Southern Walls 65% -- Window Shades - South 2/3 Win Height -- Window Glass Types - South_Dbl C	1/8/2018 12:30 AM	Berhanegw	1,358	704.7	\$0.06	\$0.007	\$10,504	\$2,504	\$13,008	172,198	337,065	88.3	
☐	WWR - Southern Walls 65% -- Window Shades - South 2/3 Win Height -- Window Glass Types - South_Dbl L	1/8/2018 12:30 AM	Berhanegw	1,358	694.6	\$0.06	\$0.007	\$10,551	\$2,381	\$12,932	172,965	320,577	87.8	
☐	WWR - Southern Walls 65% -- Window Shades - South 2/3 Win Height -- Window Glass Types - South_Trp L	1/8/2018 12:30 AM	Berhanegw	1,358	678.8	\$0.06	\$0.007	\$10,409	\$2,284	\$12,693	170,645	307,498	86.1	
☐	WWR - Southern Walls 30% -- Window Shades - South No change -- Window Glass Types - South_No change	1/8/2018 12:30 AM	Berhanegw	1,358	693.0	\$0.06	\$0.007	\$10,283	\$2,483	\$12,766	168,577	334,247	86.5	
☐	WWR - Southern Walls 30% -- Window Shades - South No change -- Window Glass Types - South_Sgl Clr	1/8/2018 12:30 AM	Berhanegw	1,358	701.3	\$0.06	\$0.007	\$10,447	\$2,494	\$12,940	171,254	335,758	87.8	
☐	WWR - Southern Walls 30% -- Window Shades - South No change -- Window Glass Types - South_Dbl Clr	1/8/2018 12:30 AM	Berhanegw	1,358	689.3	\$0.06	\$0.007	\$10,439	\$2,377	\$12,816	171,128	320,044	87.0	
☐	WWR - Southern Walls 30% -- Window Shades - South No change -- Window Glass Types - South_Dbl LoE	1/8/2018 12:30 AM	Berhanegw	1,358	684.5	\$0.06	\$0.007	\$10,466	\$2,316	\$12,782	171,570	311,827	86.8	
☐	WWR - Southern Walls 30% -- Window Shades - South No change -- Window Glass Types - South_Trp LoE	1/8/2018 12:30 AM	Berhanegw	1,358	677.8	\$0.06	\$0.007	\$10,373	\$2,290	\$12,663	170,044	308,281	85.9	
☐	WWR - Southern Walls 30% -- Window Shades - South 1/3 Win Height -- Window Glass Types - South_No ch	1/8/2018 12:30 AM	Berhanegw	1,358	692.9	\$0.06	\$0.007	\$10,278	\$2,484	\$12,762	168,500	334,378	86.5	
☐	WWR - Southern Walls 30% -- Window Shades - South 1/3 Win Height -- Window Glass Types - South_Sgl C	1/8/2018 12:30 AM	Berhanegw	1,358	701.0	\$0.06	\$0.007	\$10,415	\$2,505	\$12,921	170,745	337,280	87.7	
☐	WWR - Southern Walls 30% -- Window Shades - South 1/3 Win Height -- Window	1/8/2018 12:30 AM	Berhanegw	1,358	689.2	\$0.06	\$0.007	\$10,411	\$2,388	\$12,799	170,674	321,499	86.8	

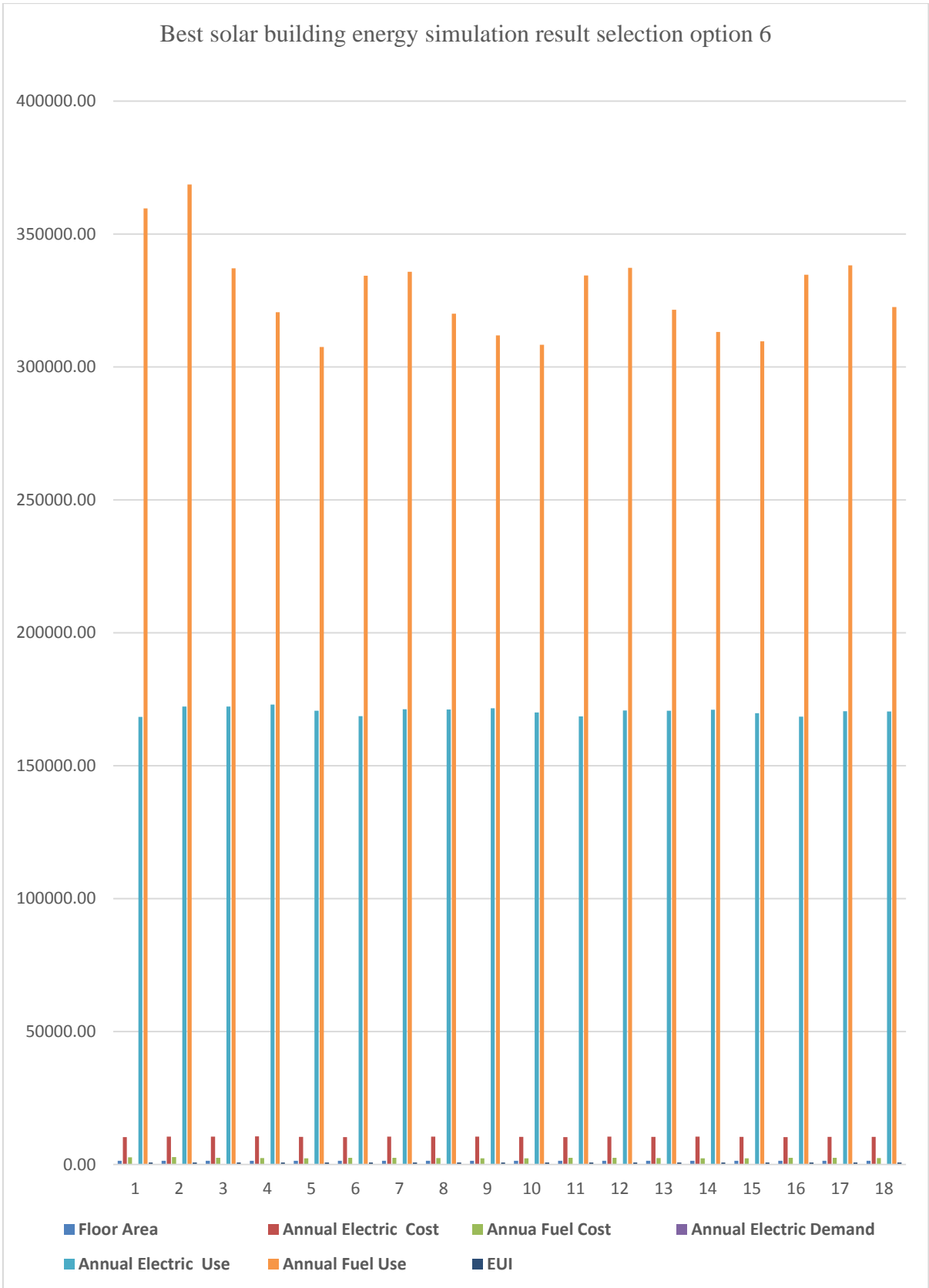


Figure 6.6: Best solar building energy simulation result chart 5

Table 6.6: Alternative design, energy simulation package result list number 6

<input type="checkbox"/>	WWR - Southern Walls_30% -- Window Shades - South_1/3 Win Height -- Window Glass Types - South_Dbl C	1/8/2018 12:30 AM	Berhanegw	1,358	689.2	\$0.06	\$0.007	\$10,411	\$2,388	\$12,799	170,674	321,499	86.8	
<input type="checkbox"/>	WWR - Southern Walls_30% -- Window Shades - South_1/3 Win Height -- Window Glass Types - South_Dbl L	1/8/2018 12:30 AM	Berhanegw	1,358	684.0	\$0.06	\$0.007	\$10,433	\$2,326	\$12,759	171,037	313,167	86.6	
<input type="checkbox"/>	WWR - Southern Walls_30% -- Window Shades - South_1/3 Win Height -- Window Glass Types - South_Trp L	1/8/2018 12:30 AM	Berhanegw	1,358	678.1	\$0.06	\$0.007	\$10,356	\$2,300	\$12,657	169,777	309,662	85.9	
<input type="checkbox"/>	WWR - Southern Walls_30% -- Window Shades - South_2/3 Win Height -- Window Glass Types - South_No ch	1/8/2018 12:30 AM	Berhanegw	1,358	693.0	\$0.06	\$0.007	\$10,275	\$2,486	\$12,760	168,436	334,644	86.5	
<input type="checkbox"/>	WWR - Southern Walls_30% -- Window Shades - South_2/3 Win Height -- Window Glass Types - South_Sgl C	1/8/2018 12:30 AM	Berhanegw	1,358	701.0	\$0.06	\$0.007	\$10,398	\$2,512	\$12,910	170,453	338,234	87.6	
<input type="checkbox"/>	WWR - Southern Walls_30% -- Window Shades - South_2/3 Win Height -- Window Glass Types - South_Dbl C	1/8/2018 12:30 AM	Berhanegw	1,358	689.2	\$0.06	\$0.007	\$10,394	\$2,395	\$12,789	170,394	322,491	86.8	
<input type="checkbox"/>	WWR - Southern Walls_30% -- Window Shades - South_2/3 Win Height -- Window Glass Types - South_Dbl L	1/8/2018 12:30 AM	Berhanegw	1,358	684.0	\$0.06	\$0.007	\$10,415	\$2,334	\$12,749	170,737	314,181	86.5	
<input type="checkbox"/>	WWR - Southern Walls_30% -- Window Shades - South_2/3 Win Height -- Window Glass Types - South_Trp L	1/8/2018 12:30 AM	Berhanegw	1,358	678.3	\$0.06	\$0.007	\$10,345	\$2,306	\$12,652	169,595	310,501	85.8	
<input type="checkbox"/>	WWR - Southern Walls_0% -- Window Shades - South_No change -- Window Glass Types - South_No change	1/8/2018 12:30 AM	Berhanegw	1,358	676.5	\$0.06	\$0.007	\$10,284	\$2,315	\$12,600	168,598	311,722	85.4	
<input type="checkbox"/>	WWR - Western Walls_95% -- Window Shades - West_No change -- Window Glass Types - West_No change	1/8/2018 12:30 AM	Berhanegw	1,358	721.7	\$0.06	\$0.007	\$10,344	\$2,745	\$13,089	169,577	369,570	88.8	
<input type="checkbox"/>	WWR - Western Walls_95% -- Window Shades - West_No change -- Window Glass Types - West_Sgl Clr	1/8/2018 12:30 AM	Berhanegw	1,358	814.6	\$0.06	\$0.007	\$11,956	\$2,975	\$14,931	196,001	400,524	102.2	
<input type="checkbox"/>	WWR - Western Walls_95% -- Window Shades - West_No change -- Window Glass Types - West_Dbl Clr	1/8/2018 12:30 AM	Berhanegw	1,358	795.6	\$0.06	\$0.007	\$11,895	\$2,810	\$14,706	195,008	378,319	100.6	
<input type="checkbox"/>	WWR - Western Walls_95% -- Window Shades - West_No change -- Window Glass Types - West_Dbl LoE	1/8/2018 12:30 AM	Berhanegw	1,358	797.4	\$0.06	\$0.007	\$12,093	\$2,742	\$14,835	198,241	369,166	101.6	
<input type="checkbox"/>	WWR - Western Walls_95% -- Window Shades - West_No change -- Window Glass Types - West_Trp LoE	1/8/2018 12:30 AM	Berhanegw	1,358	735.8	\$0.06	\$0.007	\$11,177	\$2,522	\$13,699	183,235	339,526	93.4	
<input type="checkbox"/>	WWR - Western Walls_95% -- Window Shades - West_1/3 Win Height -- Window Glass Types - West_No chang	1/8/2018 12:30 AM	Berhanegw	1,358	720.2	\$0.06	\$0.007	\$10,294	\$2,752	\$13,046	168,754	370,537	88.4	

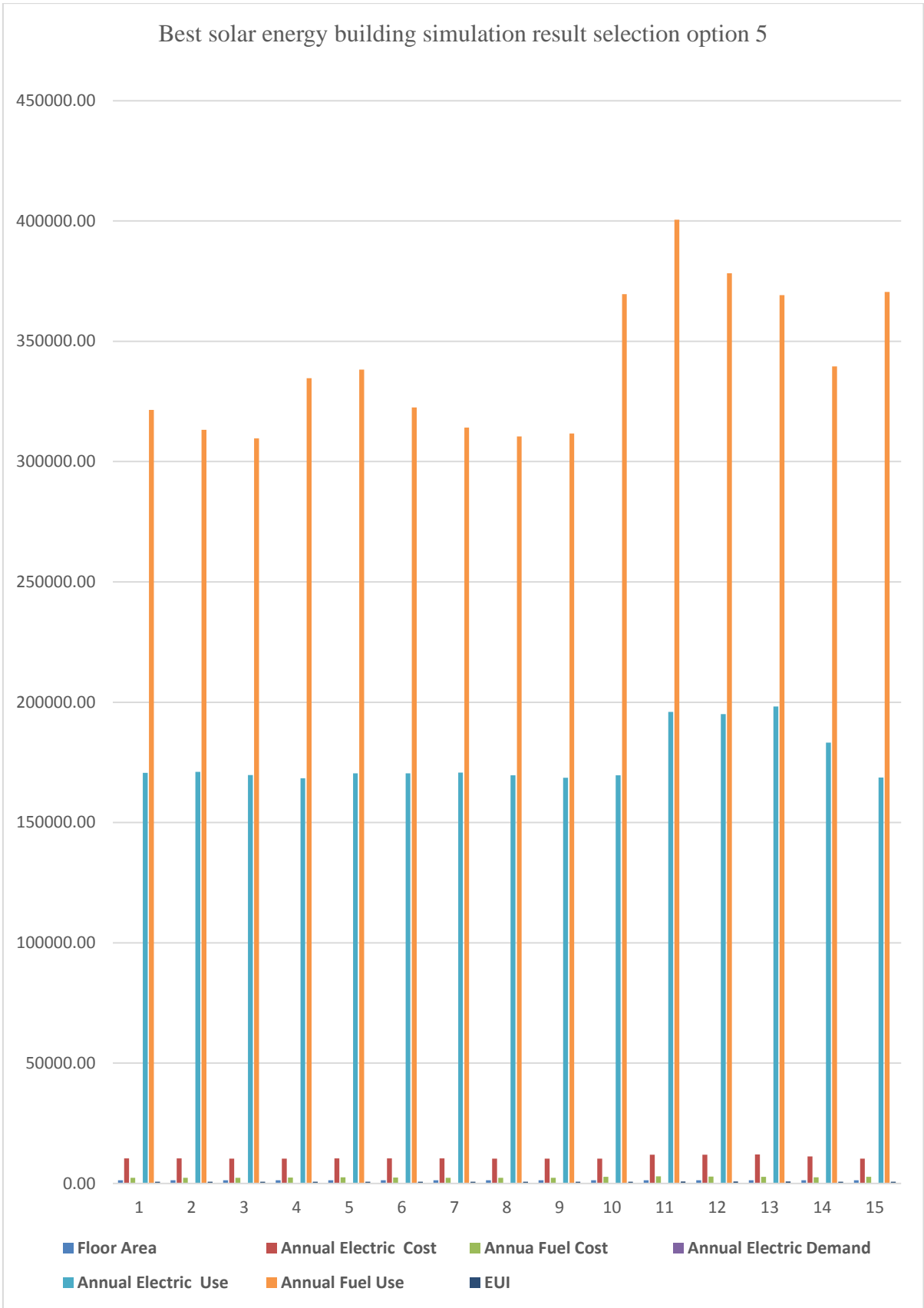


Figure 6.7: Best solar building energy simulation result chart 6

Table 6.7: Alternative design, energy simulation package result list number 7

☐	WWR - Western Walls 95% -- Window Shades - West 1/3 Win Height -- Window Glass Types - West_Sgl Clr	1/8/2018 12:30 AM	Berhanegw	1,358	794.7	\$0.06	\$0.007	\$11,552	\$2,952	\$14,504	189,379	397,436	99.0	
☐	WWR - Western Walls 95% -- Window Shades - West 1/3 Win Height -- Window Glass Types - West_Dbl Clr	1/8/2018 12:30 AM	Berhanegw	1,358	777.3	\$0.06	\$0.007	\$11,518	\$2,792	\$14,310	188,813	375,877	97.7	
☐	WWR - Western Walls 95% -- Window Shades - West 1/3 Win Height -- Window Glass Types - West_Dbl LoE	1/8/2018 12:30 AM	Berhanegw	1,358	777.3	\$0.06	\$0.007	\$11,676	\$2,721	\$14,398	191,418	366,372	98.4	
☐	WWR - Western Walls 95% -- Window Shades - West 1/3 Win Height -- Window Glass Types - West_Trp LoE	1/8/2018 12:30 AM	Berhanegw	1,358	725.6	\$0.06	\$0.007	\$10,953	\$2,518	\$13,471	179,558	338,949	91.7	
☐	WWR - Western Walls 95% -- Window Shades - West 2/3 Win Height -- Window Glass Types - West_No chang	1/8/2018 12:30 AM	Berhanegw	1,358	719.4	\$0.06	\$0.007	\$10,262	\$2,758	\$13,020	168,231	371,248	88.2	
☐	WWR - Western Walls 95% -- Window Shades - West 2/3 Win Height -- Window Glass Types - West_Sgl Clr	1/8/2018 12:30 AM	Berhanegw	1,358	781.5	\$0.06	\$0.007	\$11,283	\$2,937	\$14,219	184,962	395,344	96.9	
☐	WWR - Western Walls 95% -- Window Shades - West 2/3 Win Height -- Window Glass Types - West_Dbl Clr	1/8/2018 12:30 AM	Berhanegw	1,358	764.7	\$0.06	\$0.007	\$11,258	\$2,778	\$14,036	184,551	374,040	95.7	
☐	WWR - Western Walls 95% -- Window Shades - West 2/3 Win Height -- Window Glass Types - West_Dbl LoE	1/8/2018 12:30 AM	Berhanegw	1,358	763.8	\$0.06	\$0.007	\$11,399	\$2,707	\$14,107	186,871	364,492	96.3	
☐	WWR - Western Walls 95% -- Window Shades - West 2/3 Win Height -- Window Glass Types - West_Trp LoE	1/8/2018 12:30 AM	Berhanegw	1,358	718.5	\$0.06	\$0.007	\$10,797	\$2,514	\$13,311	176,996	338,459	90.5	
☐	WWR - Western Walls 65% -- Window Shades - West No change -- Window Glass Types - West_No change	1/8/2018 12:30 AM	Berhanegw	1,358	710.2	\$0.06	\$0.007	\$10,277	\$2,659	\$12,936	168,474	357,984	87.7	
☐	WWR - Western Walls 65% -- Window Shades - West No change -- Window Glass Types - West_Sgl Clr	1/8/2018 12:30 AM	Berhanegw	1,358	770.0	\$0.06	\$0.007	\$11,381	\$2,778	\$14,159	186,574	374,010	96.6	
☐	WWR - Western Walls 65% -- Window Shades - West No change -- Window Glass Types - West_Dbl Clr	1/8/2018 12:30 AM	Berhanegw	1,358	754.5	\$0.06	\$0.007	\$11,306	\$2,655	\$13,961	185,341	357,420	95.2	
☐	WWR - Western Walls 65% -- Window Shades - West No change -- Window Glass Types - West_Dbl LoE	1/8/2018 12:30 AM	Berhanegw	1,358	754.7	\$0.06	\$0.007	\$11,431	\$2,602	\$14,033	187,391	350,304	95.8	
☐	WWR - Western Walls 65% -- Window Shades - West No change -- Window Glass Types - West_Trp LoE	1/8/2018 12:30 AM	Berhanegw	1,358	716.2	\$0.06	\$0.007	\$10,821	\$2,481	\$13,302	177,397	333,989	90.5	

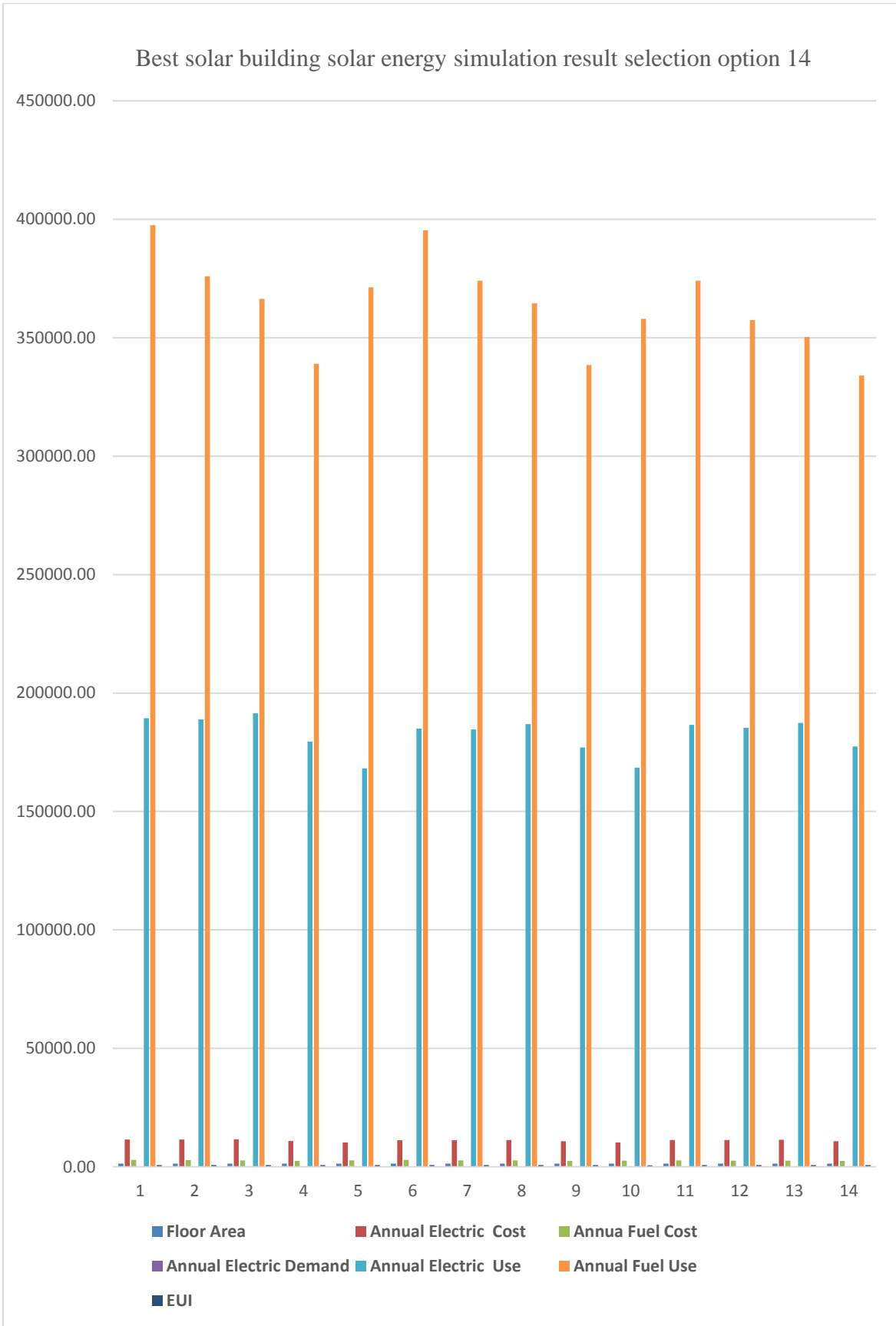


Figure 6.8: Best solar building energy simulation result chart 7

Table 6.8: Alternative design, energy simulation package result list number 8

<input type="checkbox"/>	WWR - Western Walls 65% -- Window Shades - West 1/3 Win Height -- Window Glass Types - West_No chang	1/8/2018 12:30 AM	Berhanegw	1,358	709.6	\$0.06	\$0.007	\$10,249	\$2,665	\$12,914	168,019	358,726	87.5	
<input type="checkbox"/>	WWR - Western Walls 65% -- Window Shades - West 1/3 Win Height -- Window Glass Types - West_Sgl Clr	1/8/2018 12:30 AM	Berhanegw	1,358	758.7	\$0.06	\$0.007	\$11,143	\$2,768	\$13,911	182,671	372,621	94.8	
<input type="checkbox"/>	WWR - Western Walls 65% -- Window Shades - West 1/3 Win Height -- Window Glass Types - West_Dbl Clr	1/8/2018 12:30 AM	Berhanegw	1,358	744.4	\$0.06	\$0.007	\$11,089	\$2,648	\$13,736	181,781	356,472	93.6	
<input type="checkbox"/>	WWR - Western Walls 65% -- Window Shades - West 1/3 Win Height -- Window Glass Types - West_Dbl LoE	1/8/2018 12:30 AM	Berhanegw	1,358	743.6	\$0.06	\$0.007	\$11,195	\$2,594	\$13,788	183,518	349,182	94.0	
<input type="checkbox"/>	WWR - Western Walls 65% -- Window Shades - West 1/3 Win Height -- Window Glass Types - West_Trp LoE	1/8/2018 12:30 AM	Berhanegw	1,358	710.6	\$0.06	\$0.007	\$10,688	\$2,483	\$13,171	175,210	334,253	89.5	
<input type="checkbox"/>	WWR - Western Walls 65% -- Window Shades - West 2/3 Win Height -- Window Glass Types - West_No chang	1/8/2018 12:30 AM	Berhanegw	1,358	709.7	\$0.06	\$0.007	\$10,231	\$2,673	\$12,904	167,723	359,897	87.4	
<input type="checkbox"/>	WWR - Western Walls 65% -- Window Shades - West 2/3 Win Height -- Window Glass Types - West_Sgl Clr	1/8/2018 12:30 AM	Berhanegw	1,358	750.5	\$0.06	\$0.007	\$10,971	\$2,761	\$13,732	179,857	371,673	93.5	
<input type="checkbox"/>	WWR - Western Walls 65% -- Window Shades - West 2/3 Win Height -- Window Glass Types - West_Dbl Clr	1/8/2018 12:30 AM	Berhanegw	1,358	736.8	\$0.06	\$0.007	\$10,928	\$2,642	\$13,569	179,143	355,645	92.3	
<input type="checkbox"/>	WWR - Western Walls 65% -- Window Shades - West 2/3 Win Height -- Window Glass Types - West_Dbl LoE	1/8/2018 12:30 AM	Berhanegw	1,358	735.4	\$0.06	\$0.007	\$11,018	\$2,587	\$13,606	180,627	348,341	92.6	
<input type="checkbox"/>	WWR - Western Walls 65% -- Window Shades - West 2/3 Win Height -- Window Glass Types - West_Trp LoE	1/8/2018 12:30 AM	Berhanegw	1,358	706.6	\$0.06	\$0.007	\$10,590	\$2,485	\$13,075	173,608	334,503	88.8	
<input type="checkbox"/>	WWR - Western Walls 30% -- Window Shades - West_No change -- Window Glass Types - West_No change	1/8/2018 12:30 AM	Berhanegw	1,358	698.1	\$0.06	\$0.007	\$10,215	\$2,564	\$12,779	167,461	345,118	86.6	
<input type="checkbox"/>	WWR - Western Walls 30% -- Window Shades - West_No change -- Window Glass Types - West_Sgl Clr	1/8/2018 12:30 AM	Berhanegw	1,358	719.5	\$0.06	\$0.007	\$10,702	\$2,566	\$13,268	175,441	345,427	90.2	
<input type="checkbox"/>	WWR - Western Walls 30% -- Window Shades - West_No change -- Window Glass Types - West_Dbl Clr	1/8/2018 12:30 AM	Berhanegw	1,358	712.0	\$0.06	\$0.007	\$10,649	\$2,513	\$13,162	174,574	338,333	89.4	
<input type="checkbox"/>	WWR - Western Walls 30% -- Window Shades - West_No change -- Window Glass Types - West_Dbl LoE	1/8/2018 12:30 AM	Berhanegw	1,358	711.1	\$0.06	\$0.007	\$10,697	\$2,484	\$13,181	175,358	334,386	89.6	

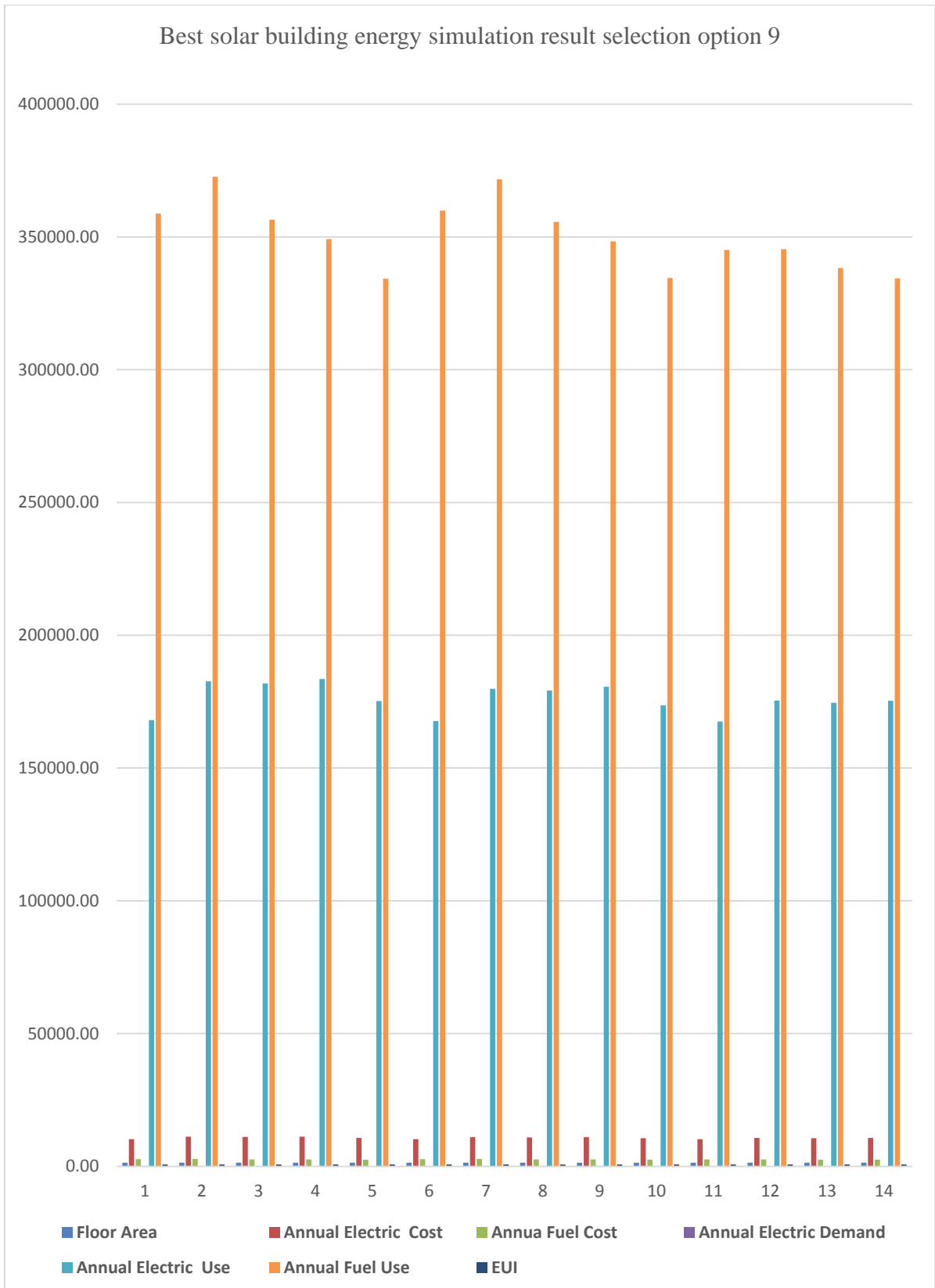


Figure 6.9: Best solar building energy simulation result chart 8

Table 6.9: Alternative design, energy simulation package result list number 9

<input type="checkbox"/>	WWR - Western Walls 30% -- Window Shades - West No change -- Window Glass Types - West_Trp LoE	1/8/2018 12:30 AM	Berhanegw	1,358	697.3	\$0.06	\$0.007	\$10,427	\$2,462	\$12,890	170,941	331,476	87.5	
<input type="checkbox"/>	WWR - Western Walls 30% -- Window Shades - West 1/3 Win Height -- Window Glass Types - West_No chang	1/8/2018 12:30 AM	Berhanegw	1,358	698.3	\$0.06	\$0.007	\$10,206	\$2,569	\$12,775	167,316	345,878	86.6	
<input type="checkbox"/>	WWR - Western Walls 30% -- Window Shades - West 1/3 Win Height -- Window Glass Types - West_Sgl Clr	1/8/2018 12:30 AM	Berhanegw	1,358	715.2	\$0.06	\$0.007	\$10,598	\$2,568	\$13,166	173,732	345,731	89.4	
<input type="checkbox"/>	WWR - Western Walls 30% -- Window Shades - West 1/3 Win Height -- Window Glass Types - West_Dbl Clr	1/8/2018 12:30 AM	Berhanegw	1,358	708.1	\$0.06	\$0.007	\$10,557	\$2,515	\$13,072	173,067	338,585	88.8	
<input type="checkbox"/>	WWR - Western Walls 30% -- Window Shades - West 1/3 Win Height -- Window Glass Types - West_Dbl LoE	1/8/2018 12:30 AM	Berhanegw	1,358	707.1	\$0.06	\$0.007	\$10,599	\$2,486	\$13,085	173,756	334,719	88.9	
<input type="checkbox"/>	WWR - Western Walls 30% -- Window Shades - West 1/3 Win Height -- Window Glass Types - West_Trp LoE	1/8/2018 12:30 AM	Berhanegw	1,358	695.0	\$0.06	\$0.007	\$10,370	\$2,464	\$12,835	170,008	331,763	87.1	
<input type="checkbox"/>	WWR - Western Walls 30% -- Window Shades - West 2/3 Win Height -- Window Glass Types - West_No chang	1/8/2018 12:30 AM	Berhanegw	1,358	698.4	\$0.06	\$0.007	\$10,199	\$2,573	\$12,773	167,201	346,464	86.5	
<input type="checkbox"/>	WWR - Western Walls 30% -- Window Shades - West 2/3 Win Height -- Window Glass Types - West_Sgl Clr	1/8/2018 12:30 AM	Berhanegw	1,358	712.7	\$0.06	\$0.007	\$10,531	\$2,572	\$13,103	172,640	346,281	89.0	
<input type="checkbox"/>	WWR - Western Walls 30% -- Window Shades - West 2/3 Win Height -- Window Glass Types - West_Dbl Clr	1/8/2018 12:30 AM	Berhanegw	1,358	705.9	\$0.06	\$0.007	\$10,497	\$2,518	\$13,016	172,090	338,996	88.4	
<input type="checkbox"/>	WWR - Western Walls 30% -- Window Shades - West 2/3 Win Height -- Window Glass Types - West_Dbl LoE	1/8/2018 12:30 AM	Berhanegw	1,358	704.6	\$0.06	\$0.007	\$10,534	\$2,489	\$13,023	172,686	335,088	88.4	
<input type="checkbox"/>	WWR - Western Walls 30% -- Window Shades - West 2/3 Win Height -- Window Glass Types - West_Trp LoE	1/8/2018 12:30 AM	Berhanegw	1,358	694.0	\$0.06	\$0.007	\$10,336	\$2,469	\$12,805	169,445	332,391	86.8	
<input type="checkbox"/>	WWR - Western Walls 0% -- Window Shades - West No change -- Window Glass Types - West_No change	1/8/2018 12:30 AM	Berhanegw	1,358	689.2	\$0.06	\$0.007	\$10,179	\$2,490	\$12,669	166,877	335,182	85.8	
<input type="checkbox"/>	WWR - Eastern Walls 95% -- Window Shades - East No change -- Window Glass Types - East_No change	1/8/2018 12:30 AM	Berhanegw	1,358	721.5	\$0.06	\$0.007	\$10,333	\$2,748	\$13,081	169,395	369,924	88.7	
<input type="checkbox"/>	WWR - Eastern Walls 95% -- Window Shades - East No change -- Window Glass Types - East_Sgl Clr	1/8/2018 12:30 AM	Berhanegw	1,358	758.9	\$0.06	\$0.007	\$11,085	\$2,795	\$13,881	181,728	376,333	94.5	
<input type="checkbox"/>	WWR - Eastern Walls 95% -- Window Shades - East No change -- Window Glass Types - East_Dbl Clr	1/8/2018 12:30 AM	Berhanegw	1,358	747.7	\$0.06	\$0.007	\$11,096	\$2,678	\$13,774	181,900	360,488	93.8	

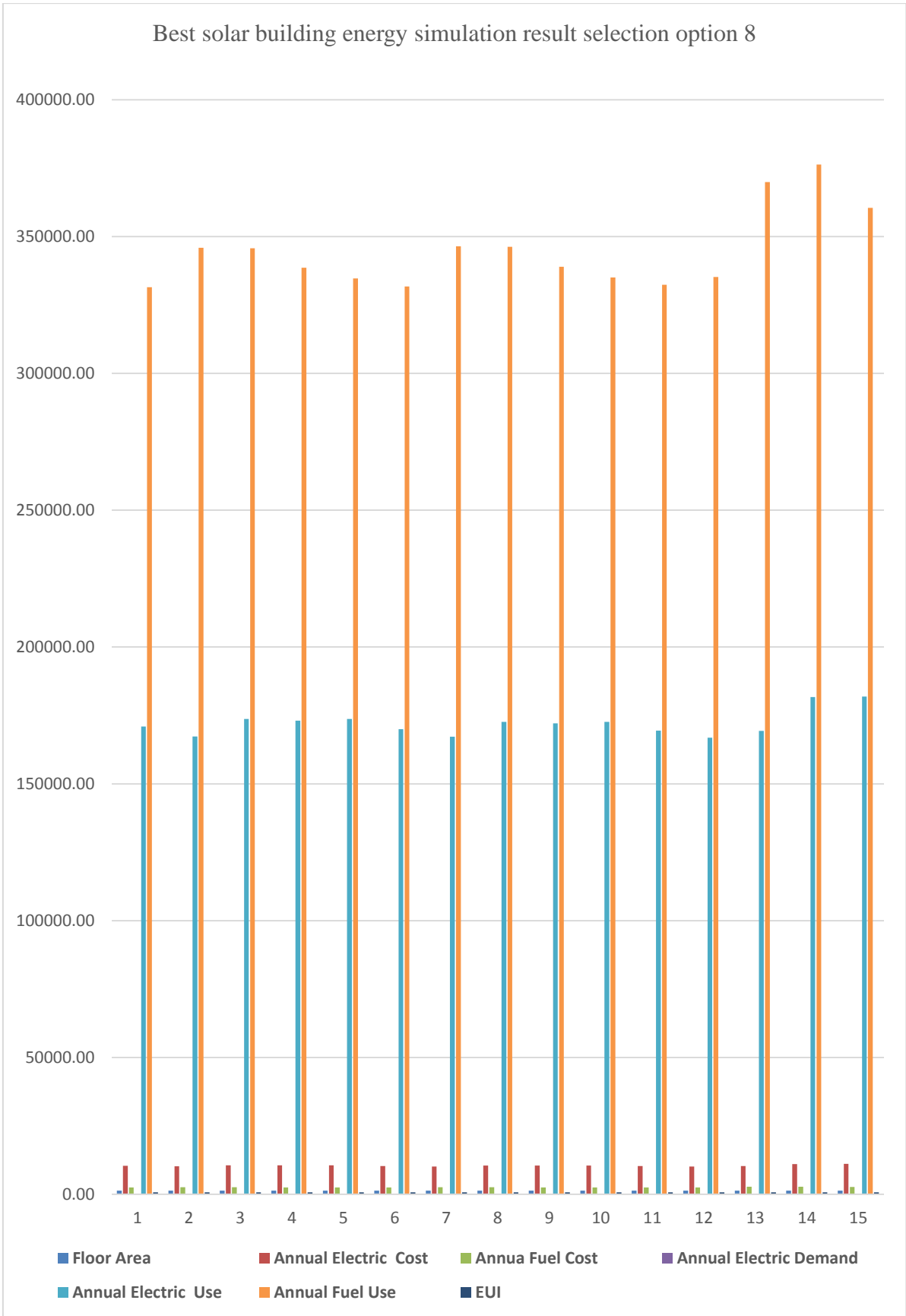


Figure 6.10: Best solar building energy simulation result chart 9

Table 6.10: Alternative design, energy simulation package result list number 10

☐	WWR - Eastern Walls_95% -- Window Shades - East_No change -- Window Glass Types - East_Dbl LoE	1/8/2018 12:30 AM	Berhanegw	1,358	748.1	\$0.06	\$0.007	\$11,230	\$2,623	\$13,853	184,106	353,084	94.4	
☐	WWR - Eastern Walls_95% -- Window Shades - East_No change -- Window Glass Types - East_Trp LoE	1/8/2018 12:30 AM	Berhanegw	1,358	712.2	\$0.06	\$0.007	\$10,726	\$2,482	\$13,208	175,835	334,148	89.8	
☐	WWR - Eastern Walls_95% -- Window Shades - East_1/3 Win Height -- Window Glass Types - East_No chang	1/8/2018 12:30 AM	Berhanegw	1,358	722.1	\$0.06	\$0.007	\$10,313	\$2,763	\$13,076	169,062	371,987	88.6	
☐	WWR - Eastern Walls_95% -- Window Shades - East_1/3 Win Height -- Window Glass Types - East_Sgl Clr	1/8/2018 12:30 AM	Berhanegw	1,358	745.1	\$0.06	\$0.007	\$10,799	\$2,782	\$13,581	177,033	374,498	92.3	
☐	WWR - Eastern Walls_95% -- Window Shades - East_1/3 Win Height -- Window Glass Types - East_Dbl Clr	1/8/2018 12:30 AM	Berhanegw	1,358	734.5	\$0.06	\$0.007	\$10,824	\$2,664	\$13,488	177,437	358,671	91.7	
☐	WWR - Eastern Walls_95% -- Window Shades - East_1/3 Win Height -- Window Glass Types - East_Dbl LoE	1/8/2018 12:30 AM	Berhanegw	1,358	733.5	\$0.06	\$0.007	\$10,929	\$2,608	\$13,537	179,158	351,145	92.1	
☐	WWR - Eastern Walls_95% -- Window Shades - East_1/3 Win Height -- Window Glass Types - East_Trp LoE	1/8/2018 12:30 AM	Berhanegw	1,358	705.7	\$0.06	\$0.007	\$10,568	\$2,486	\$13,054	173,250	334,675	88.7	
☐	WWR - Eastern Walls_95% -- Window Shades - East_2/3 Win Height -- Window Glass Types - East_No chang	1/8/2018 12:30 AM	Berhanegw	1,358	722.7	\$0.06	\$0.007	\$10,301	\$2,774	\$13,075	168,863	373,516	88.6	
☐	WWR - Eastern Walls_95% -- Window Shades - East_2/3 Win Height -- Window Glass Types - East_Sgl Clr	1/8/2018 12:30 AM	Berhanegw	1,358	739.1	\$0.06	\$0.007	\$10,648	\$2,787	\$13,435	174,559	375,239	91.3	
☐	WWR - Eastern Walls_95% -- Window Shades - East_2/3 Win Height -- Window Glass Types - East_Dbl Clr	1/8/2018 12:30 AM	Berhanegw	1,358	726.7	\$0.06	\$0.007	\$10,658	\$2,658	\$13,316	174,726	357,866	90.5	
☐	WWR - Eastern Walls_95% -- Window Shades - East_2/3 Win Height -- Window Glass Types - East_Dbl LoE	1/8/2018 12:30 AM	Berhanegw	1,358	724.2	\$0.06	\$0.007	\$10,739	\$2,597	\$13,336	176,046	349,676	90.7	
☐	WWR - Eastern Walls_95% -- Window Shades - East_2/3 Win Height -- Window Glass Types - East_Trp LoE	1/8/2018 12:30 AM	Berhanegw	1,358	702.6	\$0.06	\$0.007	\$10,480	\$2,493	\$12,972	171,799	335,591	88.1	
☐	WWR - Eastern Walls_65% -- Window Shades - East_No change -- Window Glass Types - East_No change	1/8/2018 12:30 AM	Berhanegw	1,358	714.5	\$0.06	\$0.007	\$10,313	\$2,686	\$12,999	169,067	361,602	88.1	
☐	WWR - Eastern Walls_65% -- Window Shades - East_No change -- Window Glass Types - East_Sgl Clr	1/8/2018 12:30 AM	Berhanegw	1,358	735.0	\$0.06	\$0.007	\$10,795	\$2,681	\$13,476	176,967	360,970	91.6	

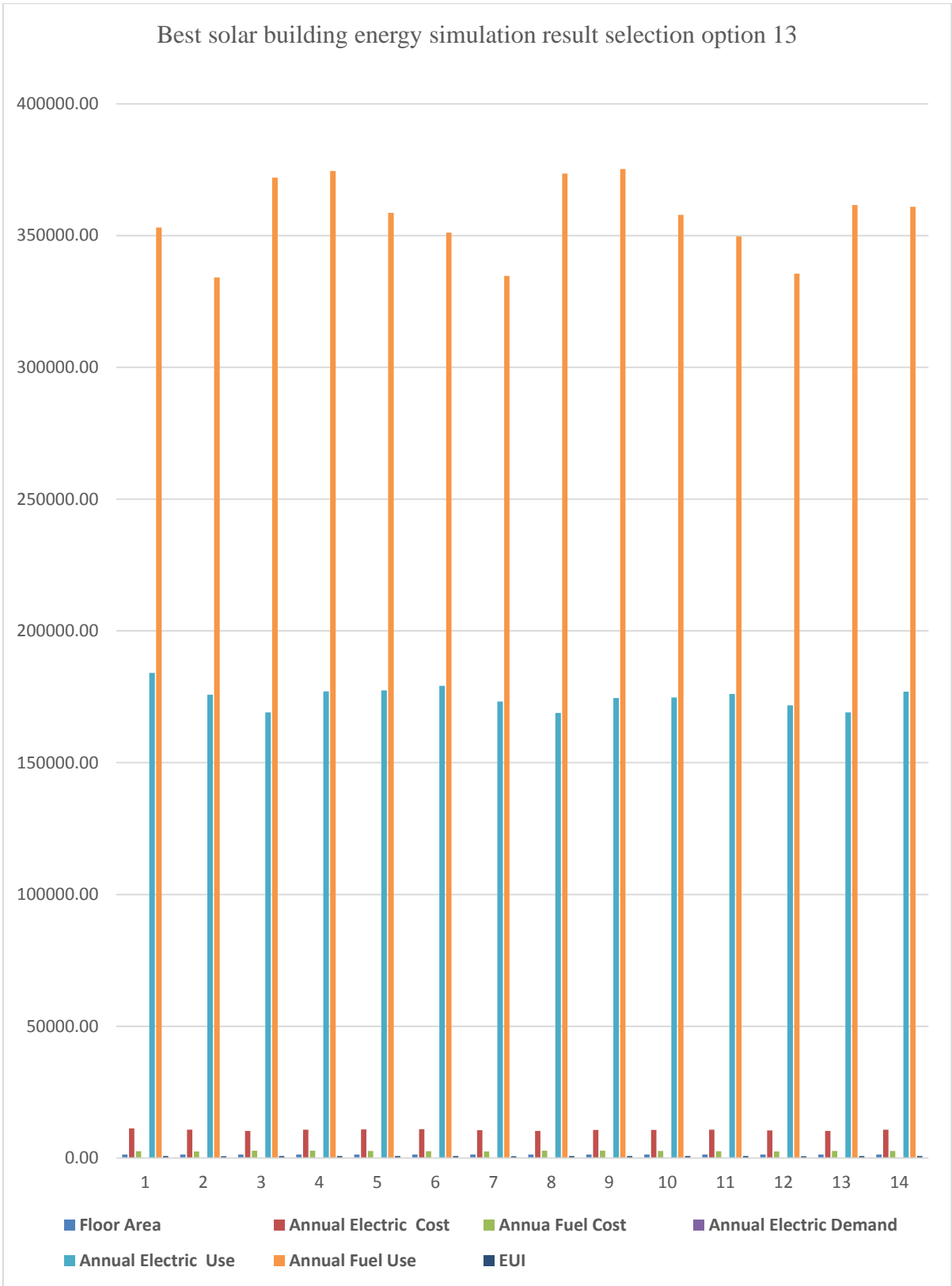


Figure 6.11: Best solar building energy simulation result chart 10

Table 6.11: Alternative design, energy simulation package result list number 11

☐	WWR - Eastern Walls_65% -- Window Shades - East_No change -- Window Glass Types - East_Dbl Clr	1/8/2018 12:30 AM	Berhanegw	1,358	725.4	\$0.06	\$0.007	\$10,782	\$2,591	\$13,373	176,752	348,813	90.9	
☐	WWR - Eastern Walls_65% -- Window Shades - East_No change -- Window Glass Types - East_Dbl LoE	1/8/2018 12:30 AM	Berhanegw	1,358	725.0	\$0.06	\$0.007	\$10,867	\$2,550	\$13,416	178,140	343,258	91.3	
☐	WWR - Eastern Walls_65% -- Window Shades - East_No change -- Window Glass Types - East_Tip LoE	1/8/2018 12:30 AM	Berhanegw	1,358	704.4	\$0.06	\$0.007	\$10,550	\$2,480	\$13,030	172,956	333,843	88.5	
☐	WWR - Eastern Walls_65% -- Window Shades - East_1/3 Win Height -- Window Glass Types - East_No chang	1/8/2018 12:30 AM	Berhanegw	1,358	715.2	\$0.06	\$0.007	\$10,300	\$2,699	\$12,998	168,851	363,308	88.1	
☐	WWR - Eastern Walls_65% -- Window Shades - East_1/3 Win Height -- Window Glass Types - East_Sgl Clr	1/8/2018 12:30 AM	Berhanegw	1,358	720.2	\$0.06	\$0.007	\$10,635	\$2,684	\$13,319	174,346	361,286	90.5	
☐	WWR - Eastern Walls_65% -- Window Shades - East_1/3 Win Height -- Window Glass Types - East_Dbl Clr	1/8/2018 12:30 AM	Berhanegw	1,358	718.5	\$0.06	\$0.007	\$10,627	\$2,589	\$13,216	174,207	348,541	89.8	
☐	WWR - Eastern Walls_65% -- Window Shades - East_1/3 Win Height -- Window Glass Types - East_Dbl LoE	1/8/2018 12:30 AM	Berhanegw	1,358	717.2	\$0.06	\$0.007	\$10,695	\$2,545	\$13,241	175,332	342,665	90.0	
☐	WWR - Eastern Walls_65% -- Window Shades - East_1/3 Win Height -- Window Glass Types - East_Tip LoE	1/8/2018 12:30 AM	Berhanegw	1,358	701.8	\$0.06	\$0.007	\$10,467	\$2,490	\$12,958	171,594	335,266	87.9	
☐	WWR - Eastern Walls_65% -- Window Shades - East_2/3 Win Height -- Window Glass Types - East_No chang	1/8/2018 12:30 AM	Berhanegw	1,358	715.5	\$0.06	\$0.007	\$10,291	\$2,705	\$12,997	168,712	364,209	88.1	
☐	WWR - Eastern Walls_65% -- Window Shades - East_2/3 Win Height -- Window Glass Types - East_Sgl Clr	1/8/2018 12:30 AM	Berhanegw	1,358	724.2	\$0.06	\$0.007	\$10,532	\$2,688	\$13,220	172,649	361,896	89.7	
☐	WWR - Eastern Walls_65% -- Window Shades - East_2/3 Win Height -- Window Glass Types - East_Dbl Clr	1/8/2018 12:30 AM	Berhanegw	1,358	714.7	\$0.06	\$0.007	\$10,530	\$2,593	\$13,123	172,616	349,094	89.1	
☐	WWR - Eastern Walls_65% -- Window Shades - East_2/3 Win Height -- Window Glass Types - East_Dbl LoE	1/8/2018 12:30 AM	Berhanegw	1,358	712.7	\$0.06	\$0.007	\$10,588	\$2,548	\$13,136	173,571	342,990	89.2	
☐	WWR - Eastern Walls_65% -- Window Shades - East_2/3 Win Height -- Window Glass Types - East_Tip LoE	1/8/2018 12:30 AM	Berhanegw	1,358	700.6	\$0.06	\$0.007	\$10,413	\$2,502	\$12,915	170,709	336,772	87.6	
☐	WWR - Eastern Walls_30% -- Window Shades - East_No change -- Window Glass Types - East_No change	1/8/2018 12:30 AM	Berhanegw	1,358	706.6	\$0.06	\$0.007	\$10,297	\$2,614	\$12,911	168,810	351,875	87.5	
☐	WWR - Eastern Walls_30% -- Window Shades - East_No change -- Window Glass Types - East_Sgl Clr	1/8/2018 12:30 AM	Berhanegw	1,358	711.8	\$0.06	\$0.007	\$10,494	\$2,580	\$13,074	172,035	347,300	88.7	

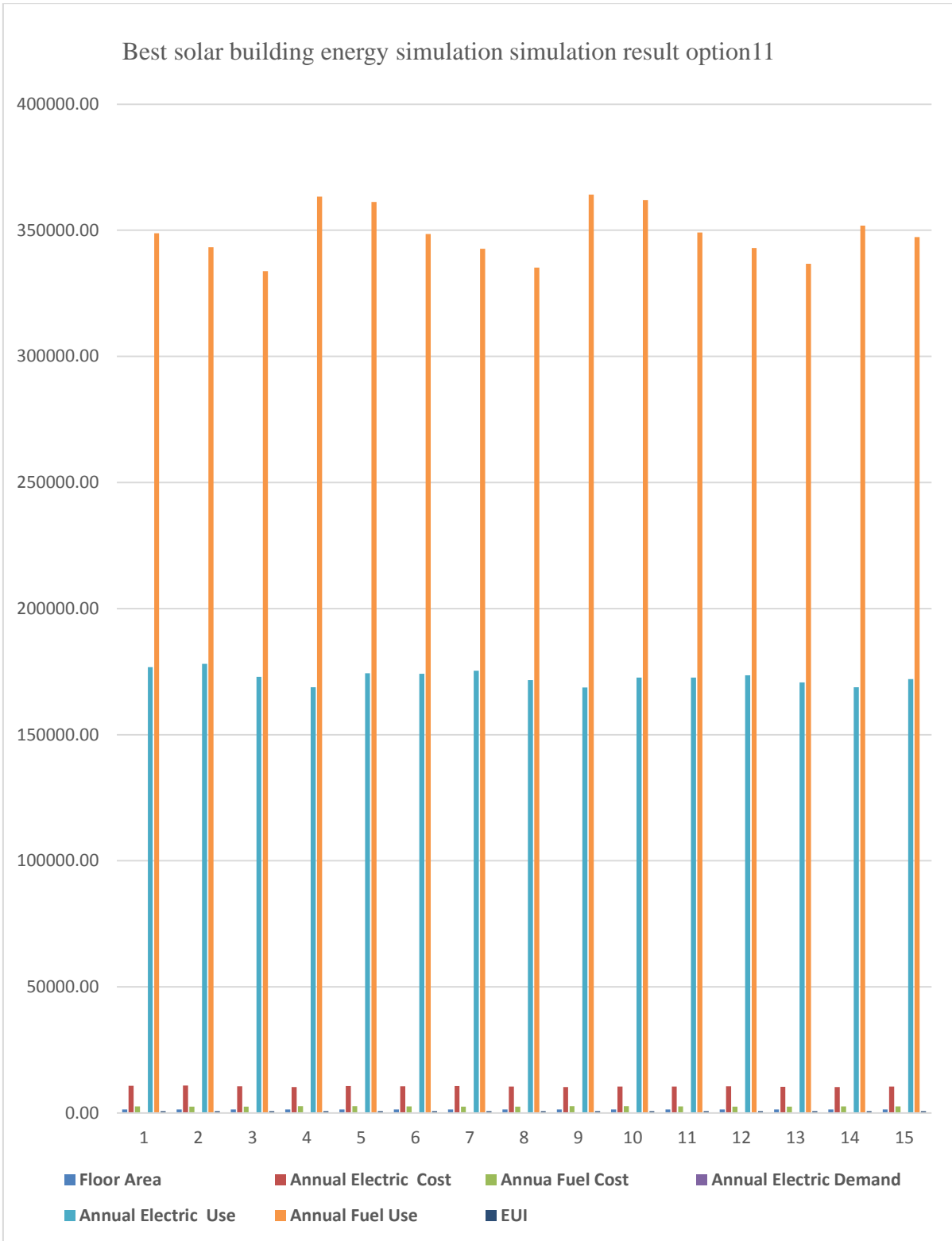


Figure 6.12: Best solar building energy simulation result chart 11

Table 6.12: Alternative design, energy simulation package result list number 12

<input type="checkbox"/>	WWR - Eastern Walls_30% -- Window Shades - East_No change -- Window Glass Types - East_Dbl Clr	1/8/2018 12:30 AM	Berhanegw	1,358	706.2	\$0.06	\$0.007	\$10,472	\$2,533	\$13,005	171,670	340,965	88.3	
<input type="checkbox"/>	WWR - Eastern Walls_30% -- Window Shades - East_No change -- Window Glass Types - East_Dbl LoE	1/8/2018 12:30 AM	Berhanegw	1,358	704.8	\$0.06	\$0.007	\$10,499	\$2,506	\$13,005	172,115	337,430	88.3	
<input type="checkbox"/>	WWR - Eastern Walls_30% -- Window Shades - East_No change -- Window Glass Types - East_Trp LoE	1/8/2018 12:30 AM	Berhanegw	1,358	699.6	\$0.06	\$0.007	\$10,380	\$2,506	\$12,886	170,167	337,369	87.4	
<input type="checkbox"/>	WWR - Eastern Walls_30% -- Window Shades - East_1/3 Win Height -- Window Glass Types - East_No chang	1/8/2018 12:30 AM	Berhanegw	1,358	707.2	\$0.06	\$0.007	\$10,292	\$2,621	\$12,913	168,722	352,894	87.5	
<input type="checkbox"/>	WWR - Eastern Walls_30% -- Window Shades - East_1/3 Win Height -- Window Glass Types - East_Sgl Clr	1/8/2018 12:30 AM	Berhanegw	1,358	710.4	\$0.06	\$0.007	\$10,437	\$2,590	\$13,028	171,106	348,751	88.4	
<input type="checkbox"/>	WWR - Eastern Walls_30% -- Window Shades - East_1/3 Win Height -- Window Glass Types - East_Dbl Clr	1/8/2018 12:30 AM	Berhanegw	1,358	705.1	\$0.06	\$0.007	\$10,423	\$2,544	\$12,966	170,864	342,431	88.0	
<input type="checkbox"/>	WWR - Eastern Walls_30% -- Window Shades - East_1/3 Win Height -- Window Glass Types - East_Dbl LoE	1/8/2018 12:30 AM	Berhanegw	1,358	703.4	\$0.06	\$0.007	\$10,445	\$2,516	\$12,961	171,226	338,713	88.0	
<input type="checkbox"/>	WWR - Eastern Walls_30% -- Window Shades - East_1/3 Win Height -- Window Glass Types - East_Trp LoE	1/8/2018 12:30 AM	Berhanegw	1,358	699.4	\$0.06	\$0.007	\$10,353	\$2,516	\$12,869	169,723	338,727	87.3	
<input type="checkbox"/>	WWR - Eastern Walls_30% -- Window Shades - East_2/3 Win Height -- Window Glass Types - East_No chang	1/8/2018 12:30 AM	Berhanegw	1,358	707.4	\$0.06	\$0.007	\$10,287	\$2,625	\$12,913	168,646	353,434	87.5	
<input type="checkbox"/>	WWR - Eastern Walls_30% -- Window Shades - East_2/3 Win Height -- Window Glass Types - East_Sgl Clr	1/8/2018 12:30 AM	Berhanegw	1,358	710.0	\$0.06	\$0.007	\$10,407	\$2,600	\$13,007	170,605	350,033	88.2	
<input type="checkbox"/>	WWR - Eastern Walls_30% -- Window Shades - East_2/3 Win Height -- Window Glass Types - East_Dbl Clr	1/8/2018 12:30 AM	Berhanegw	1,358	704.8	\$0.06	\$0.007	\$10,393	\$2,553	\$12,946	170,374	343,705	87.8	
<input type="checkbox"/>	WWR - Eastern Walls_30% -- Window Shades - East_2/3 Win Height -- Window Glass Types - East_Dbl LoE	1/8/2018 12:30 AM	Berhanegw	1,358	702.7	\$0.06	\$0.007	\$10,409	\$2,525	\$12,934	170,646	339,943	87.8	
<input type="checkbox"/>	WWR - Eastern Walls_30% -- Window Shades - East_2/3 Win Height -- Window Glass Types - East_Trp LoE	1/8/2018 12:30 AM	Berhanegw	1,358	699.4	\$0.06	\$0.007	\$10,337	\$2,524	\$12,860	169,453	339,744	87.2	
<input type="checkbox"/>	WWR - Eastern Walls_0% -- Window Shades - East_No change -- Window Glass Types - East_No change	1/8/2018 12:30 AM	Berhanegw	1,358	700.5	\$0.06	\$0.007	\$10,290	\$2,555	\$12,845	168,685	344,023	87.1	
<input type="checkbox"/>	Building Orientation (Degrees)_0	1/8/2018 12:30 AM	Berhanegw	1,358	711.2	\$0.06	\$0.007	\$10,324	\$2,648	\$12,971	169,243	356,453	87.9	
<input type="checkbox"/>	Building Orientation (Degrees)_45	1/8/2018 12:30 AM	Berhanegw	1,358	709.8	\$0.06	\$0.007	\$10,293	\$2,648	\$12,940	168,731	356,454	87.7	
<input type="checkbox"/>	Building Orientation (Degrees)_90	1/8/2018 12:30 AM	Berhanegw	1,358	709.6	\$0.06	\$0.007	\$10,285	\$2,649	\$12,934	168,607	356,564	87.7	

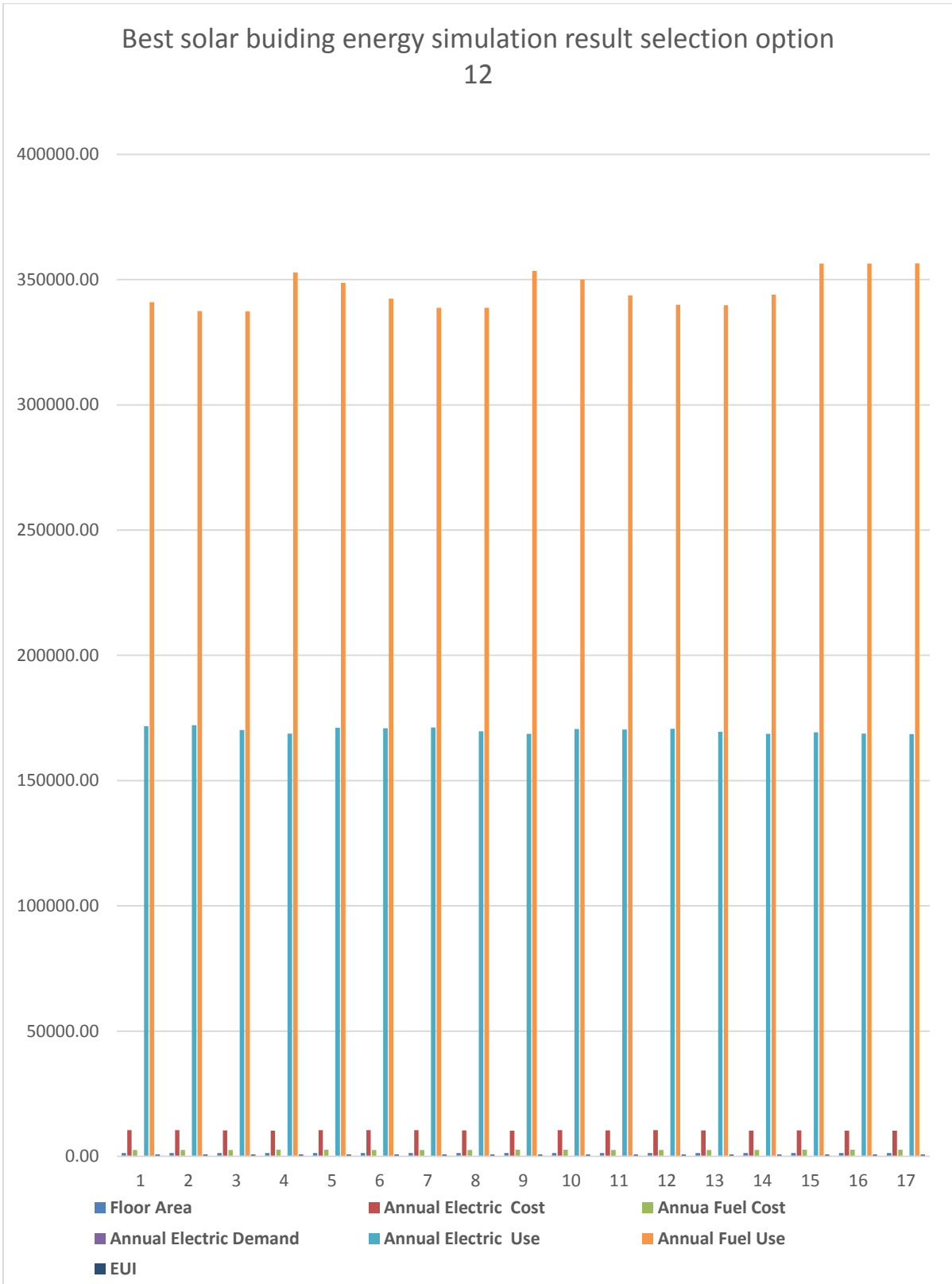


Figure 6.13: Best solar building energy simulation result chart 12

Table 6.13: Alternative design, energy simulation package result list number 13

Building Orientation (Degrees)_135	1/8/2018 12:30 AM	Berhanegw	1,358	707.1	\$0.06	\$0.007	\$10,257	\$2,636	\$12,893	168,151	354,847	87.4
Building Orientation (Degrees)_180	1/8/2018 12:30 AM	Berhanegw	1,358	707.5	\$0.06	\$0.007	\$10,260	\$2,639	\$12,899	168,204	355,240	87.4
Building Orientation (Degrees)_225	1/8/2018 12:30 AM	Berhanegw	1,358	709.8	\$0.06	\$0.007	\$10,251	\$2,666	\$12,917	168,050	358,905	87.5
Building Orientation (Degrees)_270	1/8/2018 12:30 AM	Berhanegw	1,358	711.4	\$0.06	\$0.007	\$10,303	\$2,659	\$12,962	168,901	357,965	87.9
Building Orientation (Degrees)_315	1/8/2018 12:30 AM	Berhanegw	1,358	709.7	\$0.06	\$0.007	\$10,306	\$2,641	\$12,947	168,955	355,559	87.8
Wall Construction_Uninsulated	1/8/2018 12:30 AM	Berhanegw	1,358	724.5	\$0.06	\$0.007	\$10,345	\$2,773	\$13,118	169,594	373,284	88.9
Wall Construction_R13 Metal	1/8/2018 12:30 AM	Berhanegw	1,358	703.2	\$0.06	\$0.007	\$10,372	\$2,546	\$12,918	170,029	342,823	87.6
Wall Construction_R13 Wood	1/8/2018 12:30 AM	Berhanegw	1,358	694.2	\$0.06	\$0.007	\$10,453	\$2,420	\$12,873	171,353	325,862	87.4
Wall Construction_R13+R10 Metal	1/8/2018 12:30 AM	Berhanegw	1,358	688.7	\$0.06	\$0.007	\$10,448	\$2,367	\$12,815	171,272	318,710	87.0
Wall Construction_14-inch ICF	1/8/2018 12:30 AM	Berhanegw	1,358	687.7	\$0.06	\$0.007	\$10,479	\$2,343	\$12,822	171,787	315,377	87.0
Wall Construction_R38 Wood	1/8/2018 12:30 AM	Berhanegw	1,358	687.7	\$0.06	\$0.007	\$10,508	\$2,330	\$12,839	172,266	313,746	87.2
Wall Construction_R2 CMU	1/8/2018 12:30 AM	Berhanegw	1,358	711.3	\$0.06	\$0.007	\$10,335	\$2,644	\$12,979	169,428	355,968	88.0
Wall Construction_12.25-inch SIP	1/8/2018 12:30 AM	Berhanegw	1,358	688.5	\$0.06	\$0.007	\$10,503	\$2,340	\$12,844	172,185	315,070	87.2
Roof Construction_Uninsulated	1/8/2018 12:30 AM	Berhanegw	1,358	696.8	\$0.06	\$0.007	\$10,254	\$2,533	\$12,787	168,096	341,013	86.7
Roof Construction_R10	1/8/2018 12:30 AM	Berhanegw	1,358	677.6	\$0.06	\$0.007	\$10,092	\$2,411	\$12,502	165,438	324,547	84.6
Roof Construction_R19	1/8/2018 12:30 AM	Berhanegw	1,358	676.0	\$0.06	\$0.007	\$10,080	\$2,399	\$12,480	165,250	323,028	84.5
Roof Construction_R38	1/8/2018 12:30 AM	Berhanegw	1,358	674.3	\$0.06	\$0.007	\$10,063	\$2,391	\$12,453	164,963	321,831	84.3
Roof Construction_R60	1/8/2018 12:30 AM	Berhanegw	1,358	674.0	\$0.06	\$0.007	\$10,058	\$2,389	\$12,447	164,891	321,636	84.3
Roof Construction_10.25-inch SIP	1/8/2018 12:30 AM	Berhanegw	1,358	674.4	\$0.06	\$0.007	\$10,064	\$2,391	\$12,455	164,982	321,938	84.3
Roof Construction_R15	1/8/2018 12:30 AM	Berhanegw	1,358	676.6	\$0.06	\$0.007	\$10,082	\$2,405	\$12,487	165,272	323,781	84.5
Infiltration (ACH)_0.17 ACH	1/8/2018 12:30 AM	Berhanegw	1,358	707.3	\$0.06	\$0.007	\$10,327	\$2,607	\$12,934	169,290	350,986	87.7
Infiltration (ACH)_0.4 ACH	1/8/2018 12:30 AM	Berhanegw	1,358	711.2	\$0.06	\$0.007	\$10,324	\$2,648	\$12,971	169,242	356,453	87.9
Infiltration (ACH)_0.8 ACH	1/8/2018 12:30 AM	Berhanegw	1,358	718.0	\$0.06	\$0.007	\$10,327	\$2,716	\$13,042	169,293	365,582	88.4
Infiltration (ACH)_1.2 ACH	1/8/2018 12:30 AM	Berhanegw	1,358	725.6	\$0.06	\$0.007	\$10,337	\$2,788	\$13,125	169,466	375,303	89.0
Infiltration (ACH)_1.6 ACH	1/8/2018 12:30 AM	Berhanegw	1,358	733.7	\$0.06	\$0.007	\$10,353	\$2,863	\$13,216	169,724	385,388	89.6
Infiltration (ACH)_2.0 ACH	1/8/2018 12:30 AM	Berhanegw	1,358	743.1	\$0.06	\$0.007	\$10,384	\$2,943	\$13,328	170,236	396,259	90.4
Lighting Efficiency_0.3 W/sf	1/8/2018 12:30 AM	Berhanegw	1,358	660.7	\$0.06	\$0.007	\$8,043	\$3,139	\$11,182	131,856	422,579	74.5
Lighting Efficiency_0.7 W/sf	1/8/2018 12:30 AM	Berhanegw	1,358	691.4	\$0.06	\$0.007	\$9,449	\$2,832	\$12,281	154,904	381,211	82.7
Lighting Efficiency_1.1 W/sf	1/8/2018 12:30 AM	Berhanegw	1,358	727.2	\$0.06	\$0.007	\$10,895	\$2,559	\$13,454	178,605	344,503	91.6
Lighting Efficiency_1.5 W/sf	1/8/2018 12:30 AM	Berhanegw	1,358	772.6	\$0.06	\$0.007	\$12,396	\$2,359	\$14,754	203,209	317,544	101.2
Lighting Efficiency_1.9 W/sf	1/8/2018 12:30 AM	Berhanegw	1,358	823.8	\$0.06	\$0.007	\$13,945	\$2,197	\$16,142	228,603	295,752	111.6

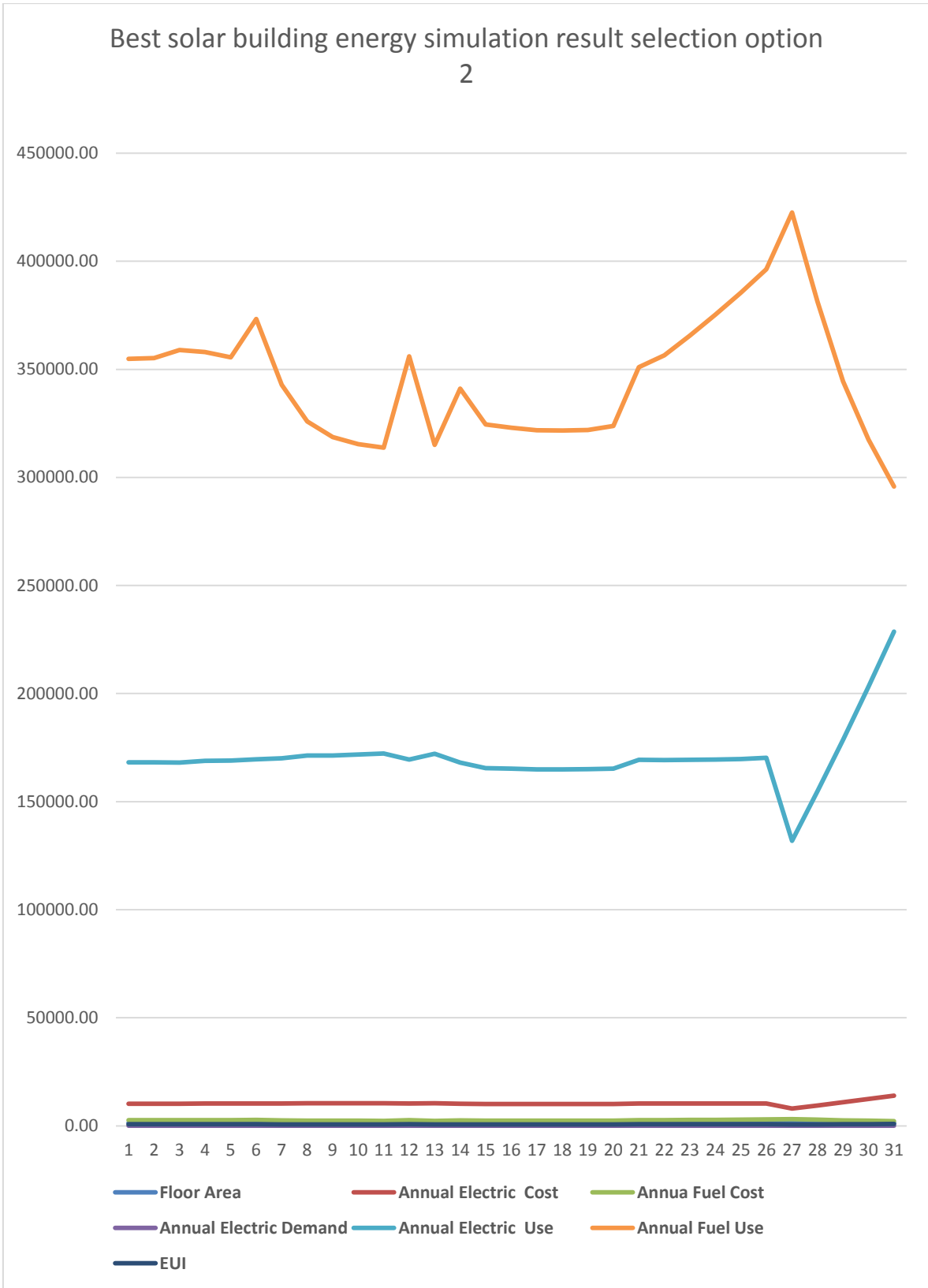


Figure 6.14: Best solar building energy simulation result chart 13

Table 6.14: Alternative design, energy simulation package result list number 14

☐	Daylighting & Occupancy Contro_None	1/8/2018 12:30 AM	Berhanegw	1,358	711.2	\$0.06	\$0.007	\$10,324	\$2,648	\$12,971	169,242	356,453	87.9	
☐	Daylighting & Occupancy Contro_Daylighting Controls	1/8/2018 12:30 AM	Berhanegw	1,358	706.3	\$0.06	\$0.007	\$10,175	\$2,664	\$12,839	166,807	358,590	87.0	
☐	Daylighting & Occupancy Contro_Occupancy Controls	1/8/2018 12:30 AM	Berhanegw	1,358	698.7	\$0.06	\$0.007	\$9,815	\$2,745	\$12,560	160,896	369,611	84.9	
☐	Daylighting & Occupancy Contro_Daylighting & Occupancy Contro	1/8/2018 12:30 AM	Berhanegw	1,358	694.6	\$0.06	\$0.007	\$9,689	\$2,759	\$12,448	158,840	371,445	84.0	
☐	Plug Load Efficiency_0.6 W/sf	1/8/2018 12:30 AM	Berhanegw	1,358	668.2	\$0.06	\$0.007	\$8,187	\$3,151	\$11,339	134,221	424,239	75.6	
☐	Plug Load Efficiency_1.0 W/sf	1/8/2018 12:30 AM	Berhanegw	1,358	691.3	\$0.06	\$0.007	\$9,367	\$2,866	\$12,233	153,559	385,884	82.4	
☐	Plug Load Efficiency_1.3 W/sf	1/8/2018 12:30 AM	Berhanegw	1,358	709.6	\$0.06	\$0.007	\$10,268	\$2,657	\$12,924	168,325	357,640	87.6	
☐	Plug Load Efficiency_1.6 W/sf	1/8/2018 12:30 AM	Berhanegw	1,358	735.1	\$0.06	\$0.007	\$11,202	\$2,504	\$13,706	183,640	337,094	93.4	
☐	Plug Load Efficiency_2.0 W/sf	1/8/2018 12:30 AM	Berhanegw	1,358	774.2	\$0.06	\$0.007	\$12,495	\$2,332	\$14,827	204,836	313,902	101.8	
☐	Plug Load Efficiency_2.6 W/sf	1/8/2018 12:30 AM	Berhanegw	1,358	843.5	\$0.06	\$0.007	\$14,488	\$2,157	\$16,645	237,511	290,398	115.3	
☐	HVAC Types_ASHRAE Package System	1/8/2018 12:30 AM	Berhanegw	1,358	582.7	\$0.06	\$0.007	\$10,525	\$1,264	\$11,788	172,533	170,136	80.1	
☐	HVAC Types_High Eff. Heat Pump	1/8/2018 12:30 AM	Berhanegw	1,358	479.9	\$0.06	\$0.007	\$10,634	\$179	\$10,813	174,323	24,088	73.7	
☐	HVAC Types_ASHRAE Heat Pump	1/8/2018 12:30 AM	Berhanegw	1,358	515.4	\$0.06	\$0.007	\$11,401	\$201	\$11,602	186,902	27,100	79.4	
☐	HVAC Types_High Eff. Package System	1/8/2018 12:30 AM	Berhanegw	1,358	561.6	\$0.06	\$0.007	\$10,317	\$1,142	\$11,460	169,134	153,806	77.8	
☐	HVAC Types_ASHRAE VAV	1/8/2018 12:30 AM	Berhanegw	1,358	722.6	\$0.06	\$0.007	\$10,580	\$2,651	\$13,231	173,448	356,881	89.9	
☐	HVAC Types_High Eff. VAV	1/8/2018 12:30 AM	Berhanegw	1,358	667.3	\$0.06	\$0.007	\$8,960	\$2,803	\$11,763	146,883	377,331	79.0	
☐	HVAC Types_ASHRAE Package Terminal Heat P	1/8/2018 12:30 AM	Berhanegw	1,358	417.8	\$0.06	\$0.007	\$9,154	\$201	\$9,356	150,074	27,100	62.9	
☐	HVAC Types_High Eff. Package Terminal AC	1/8/2018 12:30 AM	Berhanegw	1,358	577.8	\$0.06	\$0.007	\$9,157	\$1,814	\$10,971	150,114	244,241	73.8	
☐	Operating Schedule_24/7	1/8/2018 12:30 AM	Berhanegw	1,358	1,109.9	\$0.06	\$0.007	\$15,825	\$4,258	\$20,083	259,432	573,201	139.2	
☐	Operating Schedule_12/7	1/8/2018 12:30 AM	Berhanegw	1,358	788.6	\$0.06	\$0.007	\$13,019	\$2,247	\$15,266	213,432	302,483	105.1	
☐	Operating Schedule_12/6	1/8/2018 12:30 AM	Berhanegw	1,358	703.4	\$0.06	\$0.007	\$11,964	\$1,851	\$13,815	196,135	249,153	94.7	
☐	Operating Schedule_12/5	1/8/2018 12:30 AM	Berhanegw	1,358	585.9	\$0.06	\$0.007	\$9,809	\$1,610	\$11,418	160,801	216,693	77.2	
☐	Min / Max Internal Loads_Max Internal Loads	1/8/2018 12:30 AM	Berhanegw	1,358	996.9	\$0.06	\$0.007	\$18,113	\$2,115	\$20,228	296,939	284,727	141.7	
☐	Min / Max Internal Loads_Min Internal Loads	1/8/2018 12:30 AM	Berhanegw	1,358	611.6	\$0.06	\$0.007	\$5,779	\$3,636	\$9,415	94,735	489,510	61.1	
☐	Min / Max Envelope_Max Envelope	1/8/2018 12:30 AM	Berhanegw	1,358	708.2	\$0.06	\$0.007	\$10,266	\$2,643	\$12,909	168,296	355,803	87.5	
☐	Min / Max Envelope_Min Envelope	1/8/2018 12:30 AM	Berhanegw	1,358	648.6	\$0.06	\$0.007	\$10,261	\$2,045	\$12,305	168,207	275,258	83.4	
☐	Min / Max Form_Max Form	1/8/2018 12:30 AM	Berhanegw	1,358	1,040.5	\$0.06	\$0.007	\$15,932	\$3,512	\$19,444	261,180	472,767	135.0	
☐	Min / Max Form_Min Form	1/8/2018 12:30 AM	Berhanegw	1,358	606.2	\$0.06	\$0.007	\$9,918	\$1,767	\$11,685	162,595	237,852	79.0	

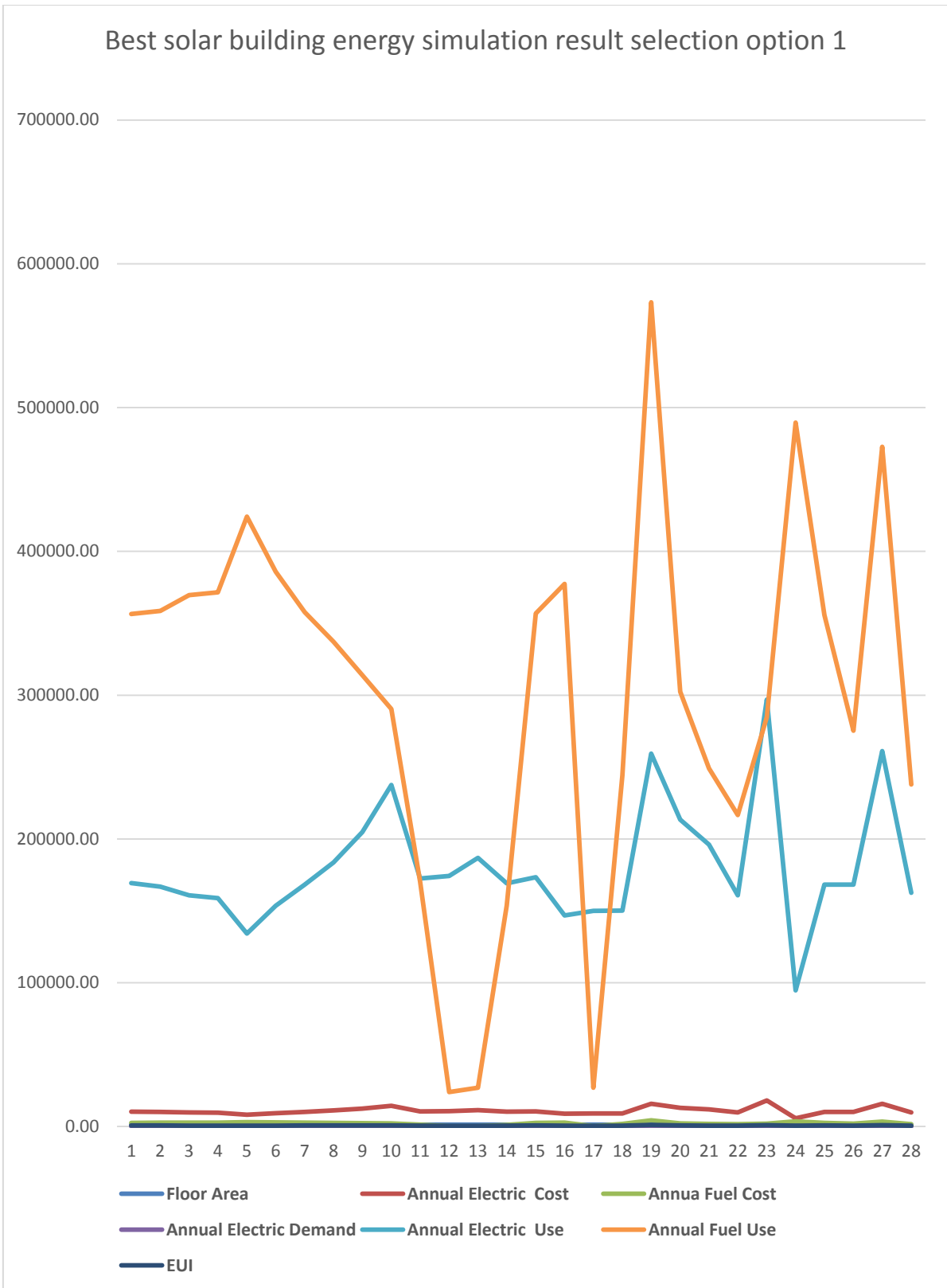


Figure 6.15: Best solar building energy simulation result chart 14

6.3 Alternative Design Best Energy Simulation

Energy simulation results shown in Table 6.15 are the best alternative design energy reduction obtained by comparison to similar alternative designs. This comparison method is used to identify the packages with most energy reduction. Hence, significant energy reduction is found in one of the ASHRAE energy packages, and most of the reduction occurred through the HVAC design system. Further, Table 6.15 is a form of summary report that contains three important columns. The first column contains the base run simulation results, the second contains the alternative design run simulation results and the third column contains the carbon footprint data. Thus, this Table demonstrates significant reductions, that is, the total annual energy cost and the life-cycle cost are reduced to \$9,365 and \$127,426 respectively. Conversely, the alternative design annual electricity energies show only slight decrease, 19,073 kWh, and this is a minor amount of change when compared with the fuel energy change of 13,386,202 MJ. However, as this research project focused on overall energy saving and because significant reductions were obtained for annual fuel energy, negligible weight was assigned to electricity energy usage decrease/reduction. In addition, the carbon footprint data also show a reasonable approach towards negative carbon neutral potential. As observed from the third column of Table 6.15, the annual electric and fuel CO₂ emissions reduced from 70.1 to 61.6 Mg and 17.7 to 1.4 Mg respectively. In parallel CO₂ emission reductions, the carbon footprint (carbon neutral potential) also shows significant reduction from 87.9 Mg to 62.9 Mg. These are other significant reductions in relation to greenhouse gas emissions that demonstrate GB makes the lowest contribution to global CO₂ emissions.

Details of energy simulations conducted in this research project are presented in three chapters. The first simulation is discussed in Chapter 4 (space heating/cooling). The second simulation is detailed in Chapter 5 (base run), which is the basic energy simulation conducted. The third is discussed in this chapter (alternative designs) and was run using automatic selections (generated by the system). Thus, the computer software energy simulation process chooses building materials that are energy efficient or changes the orientation of the building to obtain better energy reduction results and less contribution to carbon emissions and footprint. This chapter also uses manual selection of building materials by which energy efficient materials are selected

manually by the designer's specifications. Tables 6.2 to 6.14 above demonstrate, in the first column, the name/or the type of energy simulation followed by the other columns, which present data such as the dates, users, floor areas, energy use intensities, electric costs, fuel costs, annual electric costs, annual fuel costs, total annual electric energy, total annual fuel energy and annual carbon footprints. As mentioned previously, when these energy simulation results are compared (the alternative designs' simulation results with the Base Run simulation result), it was found that the 'HVAC TYPES_ASHRAE package Terminal Heat Pump,' has significantly less fuel usage and cost reduction, while the electricity energy usage and cost are similar to that of the base run simulation result. Further, average estimated annual energy was sorted according to monthly usage. The total space heating, space cooling and area lights in each month are indicated using different colour codes. For example, space heating is indicated using red, space cooling using blue and area lighting, yellow. The usage of these different energy types comprises the overall energy usage for each month and their percentage share in the overall energy usage is represented as shown in the charts in Figures 6.16 to 6.18. The highest monthly space heating energy usage is in June followed by July and August, and 70% of the total energy is consumed by space heating while only 3% is consumed by space cooling during the same season. During the opposite season, which is the hot season, space cooling and spacing heating do not significantly differ. For example, as shown in Figure 6.18, in January the space cooling usage is more than that of space heating by only a few kWh. The electrical energy usage including lighting accounts for only 31%. As can be observed from these figures, lighting consumption is very limited while space heating and space cooling are substantial. This shows that the GB lighting control system BACS did not waste unused energy. Comparison was conducted previously to determine the final best (HVAC TYPES_ASHRAE package Terminal Heat Pump) energy simulation results with base run and the rest of alternative design energy simulation results. Similarly, the final best result energy end use chart is compared with the base run energy simulation result energy end use chart as shown in Figs 6.16 and 6.17. This is to identify how the end use loads are connected and also to know where energy is saved. Thus, the end use energy loads are composed of two main types of energy, the annual electricity energy end use and the annual fuel energy end use. The electricity energy end use is supplied to the HVAC loads (34.4% and 40.7%), to the lighting loads (29.9% and 27.0%) and to the other electrical loads (35.7% and 32.3%) respectively. Conversely, the fuel energy end use is supplied to the HVAC loads

(92.4% and 00.0%) and to the other minor fuel loads (7.6% and 32.3%) respectively. On analysing these charts, the base run chart simply equivalently balances loads while the final best alternative design charts save significant fuel energy on the HVAC and lighting loads.

Table 6.15: Alternative design, best energy simulation package result

Run Name: HVAC Types_ASHRAE Package Terminal Heat P								
Energy and Carbon Results		US EPA Energy Star	Water Usage	Photovoltaic Analysis	LEED Daylight	3D VRML View	Export and Download Data Files	Design Alternatives
Project Template Applied: Intelligent Commercial Green		Building Type: Office		Electric Cost: \$0.06 / kWh		Utility Data Used: Project Default Utility Rates		
Building (4)_default		Floor Area: 1,358 m ²		Fuel Cost: \$0.01 / MJ				
Location: Wynyard, NSW								
1 Base Run		2 Design Alternative		Carbon Footprint				
Energy, Carbon and Cost Summary		Estimated Energy & Cost Summary		Alternate Run Carbon Neutral Potential				
Annual Energy Cost \$12,961		Annual Energy Cost \$9,356		Annual CO ₂ Emissions		Mg		
Lifecycle Cost \$176,526		Lifecycle Cost \$127,426		1 Base Run		87.9		
Annual CO₂ Emissions		Annual CO₂ Emissions		2 Alternate Run		62.9		
Electric 70.1 Mg		Electric 61.6 Mg		Onsite Renewable Potential		-1.0		
Onsite Fuel 17.7 Mg		Onsite Fuel 1.4 Mg		Natural Ventilation Potential		-6.7		
Large SUV Equivalent 8.8 SUVs / Year		Large SUV Equivalent 6.3 SUVs / Year		Onsite Biofuel Use		-1.4		
Annual Energy		Annual Energy		Net CO ₂ Emissions		53.9		
Energy Use Intensity (EUI) 418 MJ / m ² / year		Energy Use Intensity (EUI) 418 MJ / m ² / year		Net Large SUV Equivalent: 5.4 SUVs / Year				
Electric 169,127 kWh		Electric 150,074 kWh		Assumptions				
Fuel 365,886 MJ		Fuel 27,100 MJ		Electric Power Plant Sources in Your Region				
Annual Peak Demand 54.5 kW		Annual Peak Demand 45.2 kW		Fossil		92 %		
Lifecycle Energy		Lifecycle Energy		Nuclear		N/A		
Electric 5,073,816 kWh		Electric 4,502,208 kWh		Hydroelectric		5 %		
Fuel 10,676,574 MJ		Fuel 812,989 MJ		Renewable		3 %		
				Other		N/A		

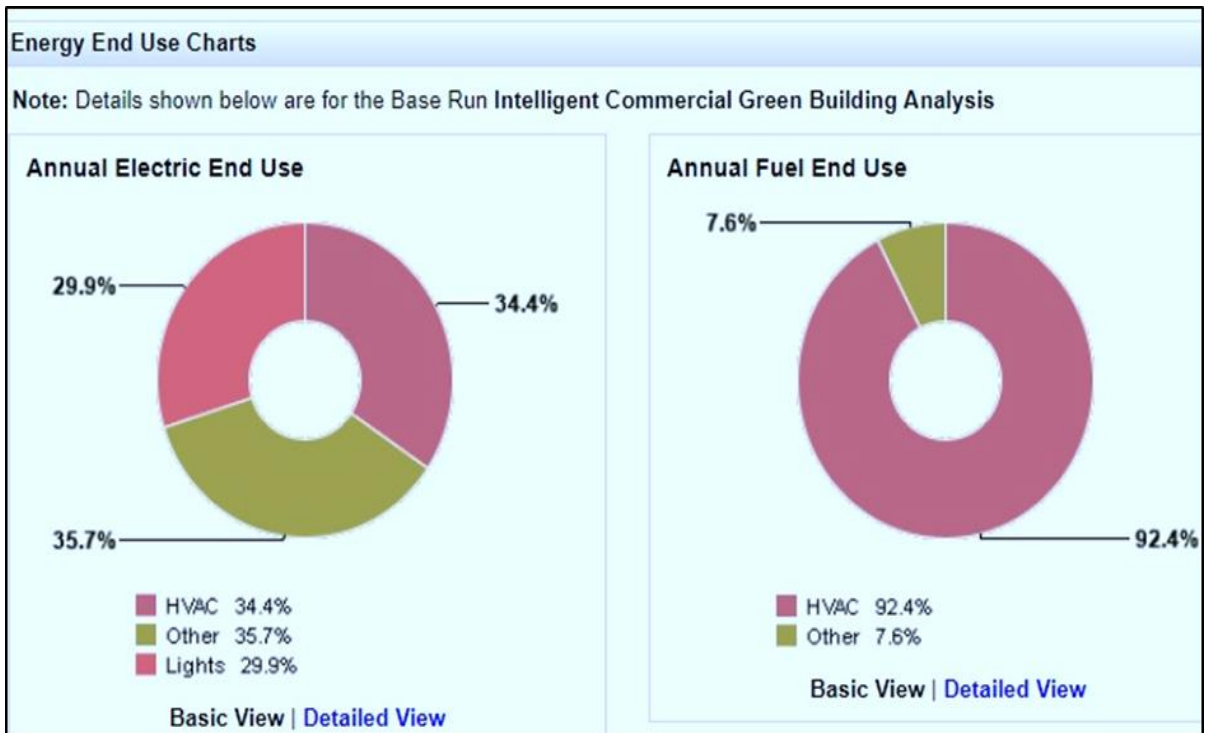


Figure 6.16: Base run energy simulation, energy end use result

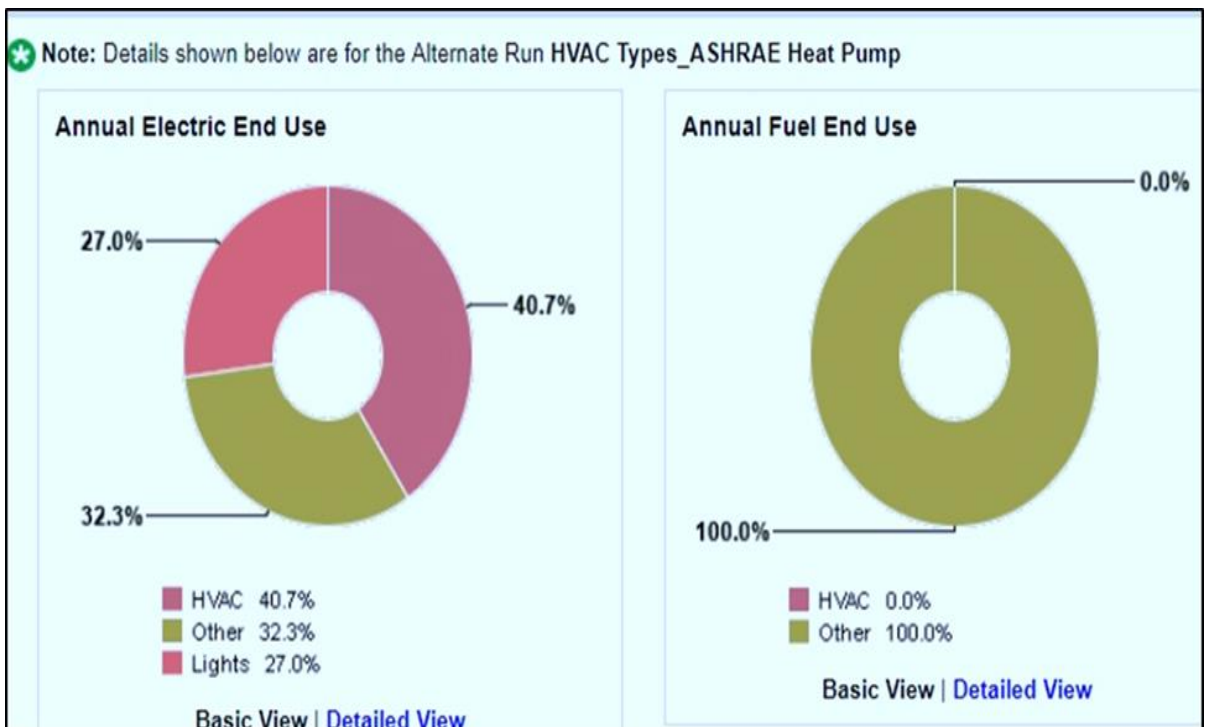


Figure 6.17: Best simulation package, energy end use result

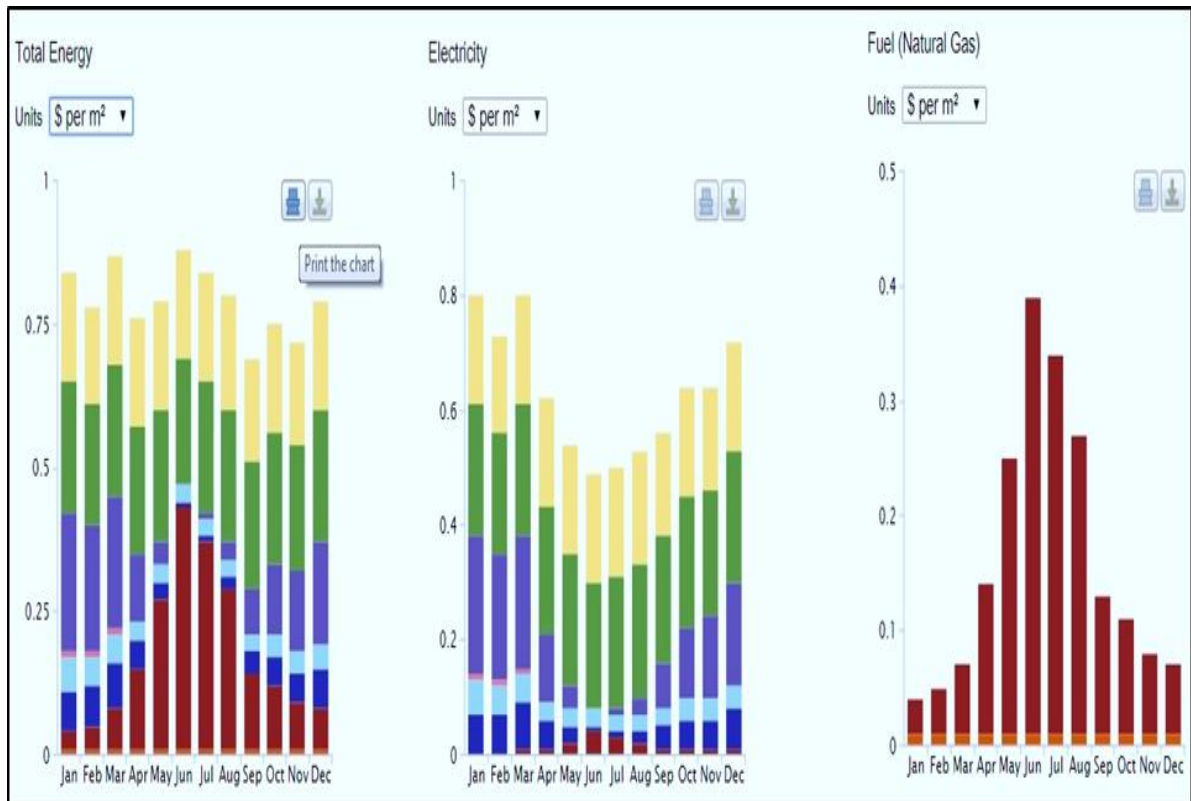


Figure 6.18 Building energy simulation, annual energy intensity result chart

6.4 Alternative Design Water Efficiency

In this chapter, the building energy simulation is shown to achieve significant savings in GB annual water usage, which increases water efficiency and reduces energy costs. Reducing the amount of water for cooling and heating minimises the amount of energy needed to perform these tasks, which in turn reduces costs. Numerous studies show that up to 15% [76] of a commercial building’s energy consumption is owing to water heating. Efficient hot water usage and generation through alternative methods, such as ‘geothermal heating’, can lead to significant energy savings and also reduce the amount of pollution related to energy production.

Alternative design building’s water efficiency is a continuation of base run water efficiency. In the base run simulation, all the water sources are configured as standard usage, owing to which no significant measures were taken to reduce water use, while in the alternative design, significant measures were taken to reduce water usage; as shown in Table 6.16, the annual water usage significantly reduced to 1,118,633 L/year. When this result is compared with the base run result (2,326,326 – 1,118,633 =

1,207,693 L/year) significant saving is achieved and as a result, NetZero saving is approached as shown in Table 6.17.

Table 6.16: Alternative design, water usage improved efficiency

LEED® Water Efficiency
Help

Water Usage and Costs

Total:	1,118,833 L / yr	\$691 / yr
Indoor:	688,879 L / yr	\$580 / yr
Outdoor:	429,754 L / yr	\$112 / yr
Net Utility:	440,782 L / yr	\$314 / yr

Source: AWWA Research Foundation 2000 Residential / Commercial and Institutional End Uses of Water.

Water Usage Estimator

Change inputs and click "Estimate" to update Water Usage and Costs

Indoor Water Factors

Number of People: 54
(Typical people for this building type/size: 52)

Percent of Time Occupied (%): 26

General Information

Project Title: Intelligent Commercial Green Building (4)

Run Title: HVAC Types_ASHRAE Heat Pump

Building Type: Office

Floor Area: 1,358 m²

Unit Water Prices

Water: \$ / m³ Sewer: \$ / m³

Outdoor Water Factors

Irrigated Area* (m²): *Irrigated area is a placeholder. Site data from Building Information Model is not incorporated.

Timed Sprinklers: ▼

Pool: ▼

Other Equipment Fixtures: ▼ Usage: L / day

Efficiency Savings

	Total	Male	Female	Employee Only	Efficiency	Percent of Indoor Usage (%)	Gallons per Year	Annual Cost Savings (\$)	
Toilets:	<input type="text" value="5"/>	<input type="text" value="1"/>	<input type="text" value="2"/>	<input type="text" value="2"/>	Low-Flow ▼	11.8	94,468	152	
Urinals:	<input type="text" value="2"/>	<input type="text" value="1"/>		<input type="text" value="1"/>	Standard ▼	0	0	0	
Sinks:	<input type="text" value="4"/>	<input type="text" value="1"/>	<input type="text" value="1"/>	<input type="text" value="2"/>	Low-Flow ▼	1.2	9,989	16	
Showers:	<input type="text" value="5"/>	<input type="text" value="2"/>	<input type="text" value="3"/>		Low-Flow ▼	0.8	6,215	10	
Clothes Washers:	<input type="text" value="5"/>				Horizontal-Av ▼	0	0	0	
Dishwashers:	<input type="text" value="5"/>				Efficient ▼	0	176	0	
Cooling Towers:	<input type="text" value="0"/>				Ozone ▼	0	0	0	
<input checked="" type="checkbox"/> Include cooling tower blowdown in sewer costs						Total Efficiency Savings:	13.9%	110,848	\$178

Source: 2000 Uniform Plumbing Code of the IAPMO, Tables 4-1 and 4-3.

Net-Zero Measures

	Annual Rainfall (mm)*	Catchment Area (m ²)	Surface Type	Liters per Year	Annual Cost Savings (\$)	
Rainwater Harvesting:	<input type="button" value="Yes"/> ▼	<input type="text" value="1215"/>	<input type="text" value="358"/>	Concrete/Asphalt ▼	391,473	270
Native Vegetation Landscaping:	<input type="button" value="Yes"/> ▼				642,756	444
Greywater Reclamation:	<input type="button" value="Yes"/> ▼				268,128	432

Table 6.17: Alternative design, water usage, approaching NetZero savings

Net-Zero Measures	Net-Zero Savings					
		Annual Rainfall (mm)*	Catchment Area (m ²)	Surface Type	Liters per Year	Annual Cost Savings (\$)
Rainwater Harvesting:	Yes ▾	1215	358	Concrete/Asphalt ▾	391,473	270
Native Vegetation Landscaping:	Yes ▾				642,756	444
Greywater Reclamation:	Yes ▾				268,128	432
Site Potable Water Sources:	Yes ▾	Yield:	50	L / day	18,250	13
Total Net-Zero Savings:					1,320,607	\$1,168

*Source: National Climatic Data Center: #CLIN81.

6.5 Green Building Energy Efficient Achievements

The ultimate building energy simulation is conducted to meet the objectives and the scope of GB to minimise the annual energy usage, cost and global CO₂ emissions and to increase occupant comfort. Hence, the overall aim is to achieve a sustainable, energy sufficient commercial building. In addition, the buildings have to be structurally stable to avoid or resist internal and external forces. When the building complies with the requirement of energy saving and stability, then it is energy efficient and stable for living.

Tables 6.18 and 6.19 display the GB base run and final alternative design best simulation package results respectively. Energy simulation results from the alternative design packages achieved significant reductions as shown in Table 6.19. In particular, over 90% reduction in fuel energy is obtained. Hence, the sums of the total annual energy reduction are calculated according to the simulation results from both building, solar energy simulation runs, base run and alternative design, in addition to the renewable energies potentials, and in particular from the PV cell simulation efficiency improvements. The total addition is as follows: (electricity usages + PV cell with 25% efficiency increase + wind turbine + fuel usages) respectively,

$$\left[\frac{\{169127 - (150074 - (34302.5 - 2208))\}}{169127} = \frac{169127 - 113563.5}{169127} = \frac{55563.5}{169127} = 0.3385 \times 100 \right] =$$

33.5%.

$$\left[\frac{98857.22 - 7527.78}{98857.78} = \frac{91329.44}{98857.78} = 0.9238 \cong 0.93 = 0.93 \times 100 \right] = 93\%. \quad \text{The average}$$

reduction from these two energies is $\frac{33.5\% + 93\%}{2} = \frac{126.5\%}{2} = 63.5\%$. This result indicates substantial energy usage reduction, indicating that buildings could be energy self-

sufficient in the near future. Indeed, this result is just from the building solar irradiation energy simulation and renewable energy, which does not include the energy reduction that could be obtained from the BACS, which ranges from 15 to 30% as shown in the literature review.

Table 6.18: Base run simulation annual total energy result

Base Run Annual Usage Simulation Results of Electricity Energy	169,127 kWh
Annual Electricity Cost	\$10,317
Base Run Annual Usage Simulation Results of Fuel Energy	98,857.22 kWh
Annual Fuel Energy Cost	\$2,643
Annual Footprint	22,168.86 Mg
PV Cell Potential Annual Energy at 15% Efficiency	27,442 kWh
Annual Potential Renewable Wind Energy	2,208 kWh

Table 6.19: HVACTYPE_ASHRAE_Package Terminal Heat Pump

Annual Electricity Energy	150,074 kWh
Annual Total Electricity Cost	\$9,154
Annual Fuel Energy	7,527.78 kWh
Annual Cost of Fuel	\$201
PV Cell Increased to 40% Efficiency: Ref: Section: 5.8.5	34,302.5 kWh

6.6 Conclusion

This chapter focuses mainly on building solar energy irradiation simulation to determine the extent of energy reduction possible when the ultimate energy simulation is conducted. Achieving a fully energy efficient commercial GB is stills complex process with many significant unsolved issues. Although the simulations generated energy reductions up to 50 to 63.5%. However, these significant results are not yet proven practically, especially for commercial buildings. This research project demonstrates a method to achieve ultimate energy reduction by designing, modelling and running simulations of a five-storey hexagonal-curve shape commercial office building. The research method has three main steps: (1) the build was initially constructed using randomly selected materials. (2) Base run energy simulation was conducted. (3) Multiple automatic alternative designs using automatic construction material selection

were tested in GBS. This last and final simulation was conducted to determine the best among the alternative designs. Hence, the 'HVACTYPES_ASHRAE_Package Terminal Heat Pump', was selected since it shows the highest energy reduction among all of the multiple alternative designs.

Chapter 7: Sustainable Building Achievement

7.1 Introduction

This chapter covers three main topics: building structural stability simulation, building occupants' comfort and BACS. Hence their introductory descriptions are outlined:

(1) Building structural simulation

Building structural stability simulation is conducted using Autodesk Revit and Autodesk structural analysis software applications to confirm that the building is not only energy efficient but also firmly stable to resist any external or internal load/force. Building structures are designed to withstand numerous frequently occurring actions, expected extreme forces and events. During construction time and over the building lifetime, structures are also exposed to many unexpected events, although structures are generally not specifically designed to withstand these events. However, it is generally expected that the building structure can withstand these accidental actions without being damaged disproportionately [88]. This is generally known as structural robustness or prevention of progressive and/or disproportionate collapse. The importance of structural robustness in structural design is universally acknowledged. Thus, all structural regulations and codes of practice include structural robustness as a fundamental requirement. The public has a general expectation that building are safe structurally and able to resist high frequency events, wind, snow and earthquakes. However, structures can also be subjected to accidental actions, such as explosion, which are difficult to define. Structural robustness is the means to protect structures against these unforeseen actions and regardless of how the buildings is designed; the damage should be proportional to the magnitude of the accidental loading. Most structures have some degree of built-in structural robustness since horizontal resistance is provided for wind and earthquake actions. The building code summaries the expected characteristics of structural robustness [89]. In this section, simulations are presented of building structure stability to correct any building structural defected elements prior to commencement of practical work; significant results are achieved in this regard.

(2) Building occupants' comfort

This section of the chapter demonstrates buildings occupants' comfort, because currently, building occupant comfort has become a significant factor in GB objectives and scope. This is because the GB is equipped with the latest modern technology and these technologies enable the building to react to the occupants' requirements/interests, instead of the occupants acting to obtain a response. Thus, modern technology, especially after the introduction of BIOT, the control system, facilitates the control of almost every action indoors/outdoors, such as air quality and monitoring occupants' health issues. In addition to the GB being smart, it is also physically firmly stable to resist any internal and external forces or loads. In this research thesis, comfort and stability are not the main subjects since the focus is on reducing GB energy consumption and CO₂ emissions. However, occupants should find the GB comfortable and stable in terms of structural firmness.

(3) Building automation control system

The GB automation control system demonstrated in this chapter focuses on three main objectives of the current GB control system. These are energy savings, energy consumption costs and occupants' comfort. Using this method, the higher annual energy usages and cost of GB are minimised while occupant comfort is maximised. However, this method is proved only theoretically using simulations and further practical research is necessary to validate the research results.

7.2 Green Building Sustainability

Building stability is a general guide for all buildings, whether a conventional building or smart/intelligent/GB; the term stability is applicable to buildings of all sizes. GB construction must comply with the National Building Code (NBC). For example, in Australia, the Building Code Australia (BCA) regulates the building regularly and all the codes emphasise structural stability. In addition, the term building stability is also defined in relation to the forces acting on the building from different directions and these directions are classified as lateral, spine and vertical [90]. The response is how the building resists these forces. Stability is not a concern unique to GB but it has to be stable in terms of both energy and structure.

The most important applications of this concept are vibrations of structures that interact with external or internal fluid flows: buildings, antennas and fluid pipes among others. The steady speed of the flow can be taken as parameter. At a certain flow of speed, increasing oscillations may be triggered this is called flutter [91], or a non-oscillatory unbounded motion occurs-this is caused by divergence. Hence, this chapter is just an introduction to the concept of building stability to demonstrate that in the design and modelling of GB it is also necessary to include basic building stability information data. Thus, the stability simulation result only shows how to correct defects prior to commencing practical work: When defects are corrected, the building is firmly stable.

7.3 Green Building Stability Simulation

A commercial office building is designed architecturally and structurally and categorised according NCC building classification code as class 7, regardless of the building height. However, typically, a medium-commercial office building is designed to be a few meters high from the ground. Conversely, highly structural reinforced commercial office buildings vary from medium height to very high and are constructed using concrete columns, beams and concrete slabs or structural steels. In both scenarios, stability is very crucial, such that the building has to be stably erected and must be able to withstand or resist all external forces. Thus, stability simulation is conducted, prior to practical design, to analyse and correct defects.

Figure 7.1 shows the structural design of a five-storey hexagonal-curve shape commercial office building designed by the architectural software application for energy and stability purpose. Five types of forces, dead load, live load, wind load, roof live load and seismic load, are applied and act on the edge of floor slabs as shown in Figure 7.1. The different colour on the edge of the floor slabs indicates the different types of forces.

External or internal forces push or pull. Forces act on all type of building structures, regardless of whether the structure is small, medium or a large-size high-rise and the building must be designed and built to withstand these forces. In case the building structure is not strong enough, it may experience structural failure. Conversely, if it is too strong, time and resources might be wasted. Since all building structures experience forces at all times, in some cases, the effects of those forces may not apparent until later.

Thus, it is important to design a building structure carefully and monitor it diligently throughout its useful life [92].



Figure 7.1: Building structure internal & external force stability simulation

7.4 Building Structural View

The building structural stability structural view is part of the simulation process, which commences with the structural erection view of the building. The building has been designed structurally clearly visible as shown in Figures 7.2 and 7.3, which show all the building supporters clearly erect with no defects of bending/shear. This is to help the structural engineer to have a clear view of the elements or the part of the building skeleton that require a defect analysis.

The building structural analysis simulation process is the basis of a modular software system application particularly programmed to function interoperability with BIM. The program is used to define structures, materials and loads for planar and spatial structural

systems consisting of plates, walls, shells and members. The program also allows to create combined structures as well as model solid and contact elements.

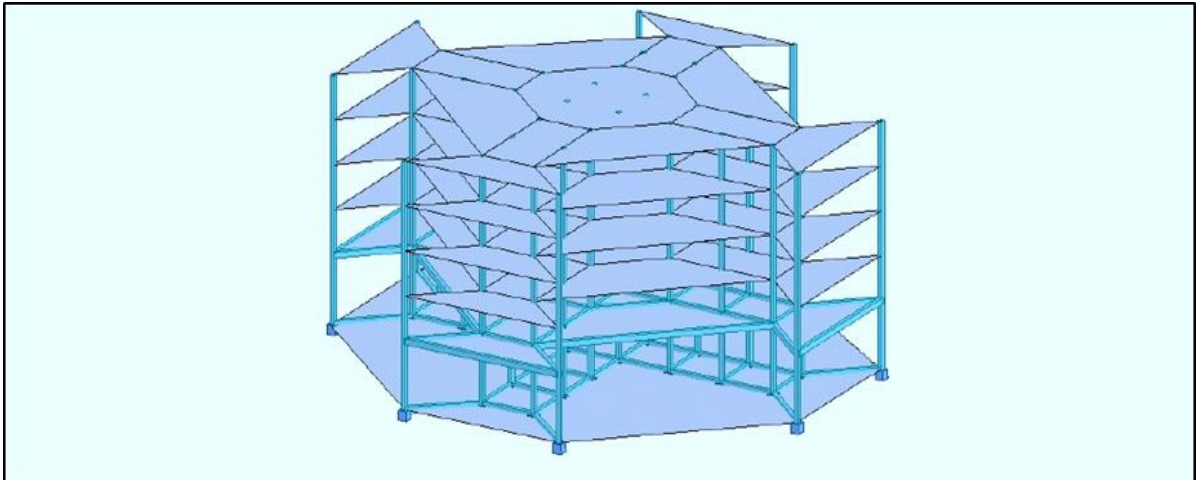


Figure 7.2: Building structure view

7.5 Building Structural Modelling

The building structural stability simulation process report included, in particular, the model of the structural analysis that has been conducted for structural stability cases. The purpose of this building structural model report is to demonstrate the type of model that has been simulated for any stability defects. Figure 7.3 shows the internal and external structure of the building; thus, the structural model provides information on deformations, internal forces, stresses, support forces and soil contact stresses. The corresponding add-on modules facilitate data input by automatic generation of structures and connections or can be used to perform further analyses and designs according to various standards. When analysing structural components of reinforced concrete structures, it is often necessary to design deep in to the model structures. These are mainly the connections between split-level slabs, and frame systems [93].

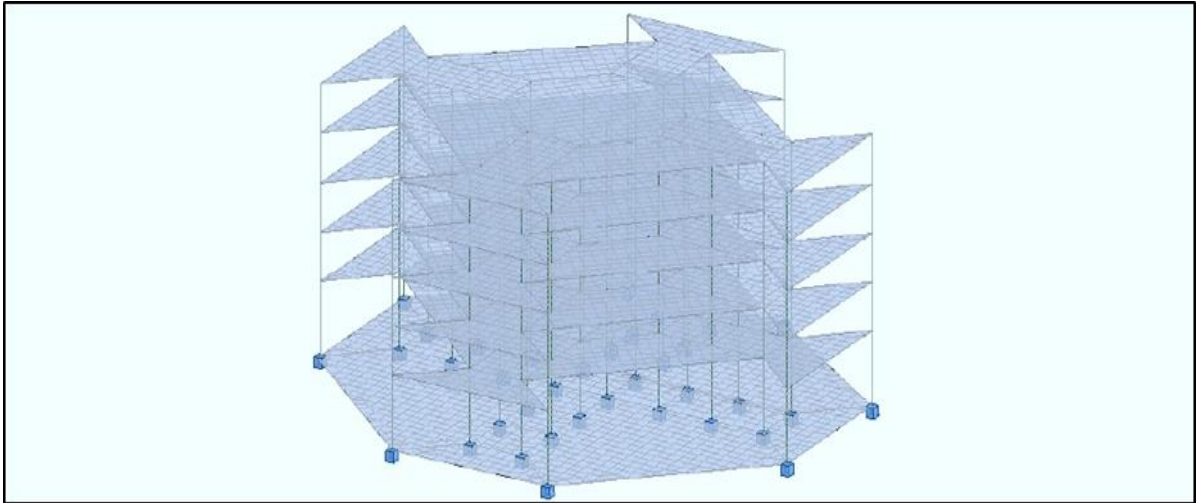


Figure 7.3: Model of building structural view

7.6 Building Structure Load Cases

During the structural analysis, loads or forces are applied to the structure and the resulting deflections are measured. Tables 7.1 and 7.2 show types of loads that defines the external forces, the centrifugal forces and the angular acceleration forces, which are their forces can be analysed to design structures for the building. Hence, these structures are associated with the ground footing, such as columns, beams and slabs; the analysis also includes the basement soils.

Autodesk Revit structural analysis defines masses/weights added to nodes and bars as well as conversion of loads to masses. Added masses are primarily used in dynamic analyses (dynamic, harmonic, spectral, seismic and time history). However, the added masses need to be considered in static calculations when generating forces for body loads.

Earthquake loads are defined as lateral live loads. Lateral loads are very complex, uncertain and potentially more damaging than wind loads. Earthquakes create ground movements that can be categorised as a shake, rattle or roll. Building structures in an earthquake zone must be able to withstand all three of these loadings of different intensities.

Seismic force is another force that is part of an earthquake but acts differently from the lateral force [94]. The aforementioned seismic measures are used to calculate forces that earthquakes impose on buildings, such as the ground shaking, pushing back and forth,

sideways and up and down, which generate internal forces within buildings called the inertial forces, which in turn cause most seismic damage. $F = \text{Mass (M)} \times \text{Acceleration (A)}$. The greater the mass/weight of the building, the greater the internal inertial forces generated [95]. If building structures constructed with lightweight construction materials, which means with less mass, it is typically an advantage in seismic design because greater mass generates greater lateral forces.

Earthquakes generate waves that may be slow and long or short and abrupt. The length of a full cycle in seconds is the period of the wave and also the inverse of the frequency [96]. Hence, all objects, including buildings, have a natural or fundamental period at which the objects vibrate if jolted by a shock. The natural period is a primary consideration for seismic design. However, other aspects of the building design can also contribute to a lesser degree to mitigation measures [97]. If the period of the shock wave and the natural period of the building coincide, then the building will resonate and its vibration will increase or amplify several times [98]. Highly amplified vibrations can cause major damages.

Table 7.1: Building structure acting load

Loads				
Load Cases				
Case	Label	Case name	Nature	Analysis type
1	DL1	DL1	dead	Static - Linear
2	LL1	LL1	live	Static - Linear
3	WIND1	WIND1	wind	Static - Linear
4	LR1	LR1	live	Static - Linear
5	SEIS1	SEIS1	seismic	Static - Linear

Table 7.2: Building structure acting load combinations

Load Combinations					
Table of Load Combinations					
Combinations	Name	Analysis type	Combination type	Case nature	Definition
6 (C)	Current work	Linear Combination	SLS	live	(1+1)*1.00
7 (C)	Ultimate	Linear Combination	ULS	live	1*1.40+1*1.60

7.7 Building Structure Load Reaction

Load reaction is considered mainly since heat affects building components in various ways. Some components burn and add fuel to the fire; others absorb heat for a time and conduct it through the structural component to another location. Understanding the compression, tension and shear stresses of the structural components assist in determining the reactions that can occur when these components are exposed to heat from a fire. Heat elongates metal objects; thus, the reaction to heating is manifested by exactly the same force the tensioned object is resisting. This is thermal expansion; when heated, the atoms that make up the material increase movement. For the most part, tensioned members are smaller than compressive members; thus, the mass is not present to absorb the heat transfer. The structural component will elongate or deform. Simply playing a hose stream on the structural components and cooling them below the reaction temperature will return steel components to near their original strength. However, the defected part of the component will not return to its original shape. The defected structural element may not now be shaped to support the structure, but it will not be strong [99]. Thus, Figure 7.4 and Tables 7.3 and 7.4 show the load reactions in load supporter elements specified in each of the five caseloads applied to the building.

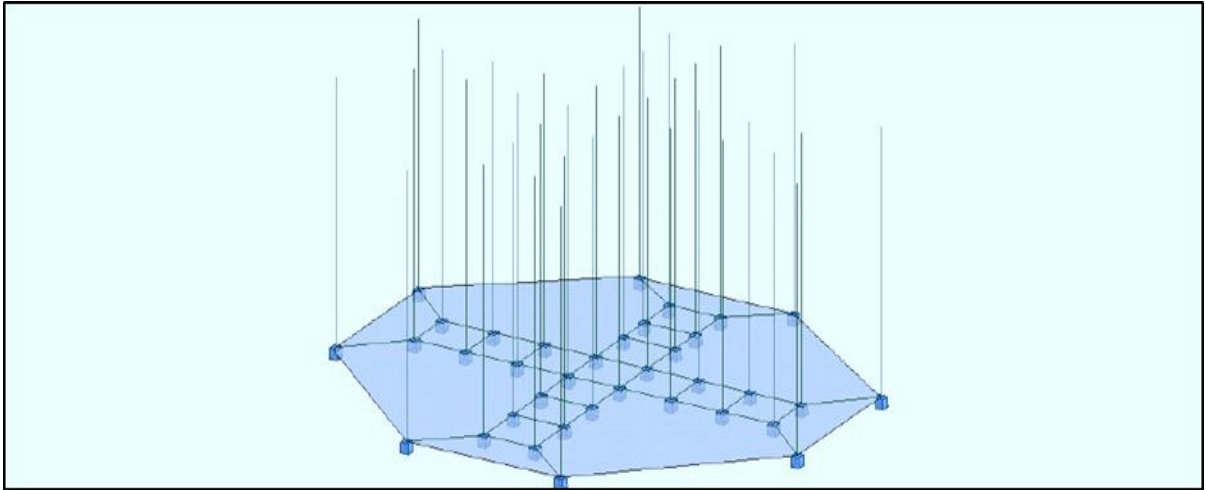


Figure 7.4: Building structure elements load supporter reaction view

Table 7.3: Building structure load reaction

Reactions in the coordinate system: global - Cases: 1 to 5 . Sum of Reactions.						
Node/Case	FX (kN)	FY (kN)	FZ (kN)	MX (kNm)	MY (kNm)	MZ (kNm)
Case 1	DL1					
Sum of value.	0.0	0.0	0.0	0.0	0.0	0.0
Sum of reaction.	-6.02e-09	-6.66e-08	2.68e+04	1.33e+05	-4.87e+05	1.61e-02
Sum of force.	0.0	0.0	-2.68e+04	-1.33e+05	4.87e+05	0.0
Check value.	-6.02e-09	-6.66e-08	-5.19e-06	-3.90e-05	4.17e-05	1.61e-02
Precision	8.85688e-08	1.02168e-15				
Case 2	LL1					
Sum of value.	0.0	0.0	0.0	0.0	0.0	0.0
Sum of reaction.	2.79e-09	-1.69e-08	8.00e+03	3.86e+04	-1.45e+05	3.02e-03
Sum of force.	0.0	0.0	-8.00e+03	-3.86e+04	1.45e+05	0.0
Check value.	2.79e-09	-1.69e-08	-1.36e-06	-1.02e-05	1.09e-05	3.02e-03
Precision	1.35281e-07	4.07079e-16				
Case 3	WIND1					
Sum of value.	0.0	0.0	0.0	0.0	0.0	0.0
Sum of reaction.	0.0	0.0	0.0	0.0	0.0	0.0
Sum of force.	0.0	0.0	0.0	0.0	0.0	0.0
Check value.	0.0	0.0	0.0	0.0	0.0	0.0
Precision	0.0	0.0				
Case 4	LR1					
Sum of value.	0.0	0.0	0.0	0.0	0.0	0.0
Sum of reaction.	0.0	0.0	0.0	0.0	0.0	0.0
Sum of forc.	0.0	0.0	0.0	0.0	0.0	0.0
Check value.	0.0	0.0	0.0	0.0	0.0	0.0
Precision	0.0	0.0				

Table 7.4: Building structure load reaction cases

Reactions in the coordinate system: global - Cases: 7 - Global extremes.						
	FX (kN)	FY (kN)	FZ (kN)	MX (kNm)	MY (kNm)	MZ (kNm)
MAX	2.80e+01	2.57e+01	3.46e+03	7.19e+02	5.05e+02	9.60e-02
Node	178811	174327	182448	170960	178756	174065
Case	7 (C)	7 (C)	7 (C)	7 (C)	7 (C)	7 (C)
MIN	-3.26e+01	-3.02e+01	7.87e+02	-6.55e+02	-5.10e+02	-1.69e-01
Node	178756	182448	178496	180397	177264	176089
Case	7 (C)	7 (C)	7 (C)	7 (C)	7 (C)	7 (C)

7.8 Nodal Supporter Load Reactions

For the force exerted on the building, it is also possible to display values of linear reactions for FX supports defined as linear on edges. These are displayed at nodes

belonging to the linear support on the edge. Nodal reaction forces, which are defined as linear reactions forces, are calculated as a value of the nodal reaction divided by half the length of sides of the elements adjoining the node. A linear reaction unit is force or moment per length unit, as shown in Figure 7.5, which indicates nodal supporter elements experiencing extreme reactions [100].

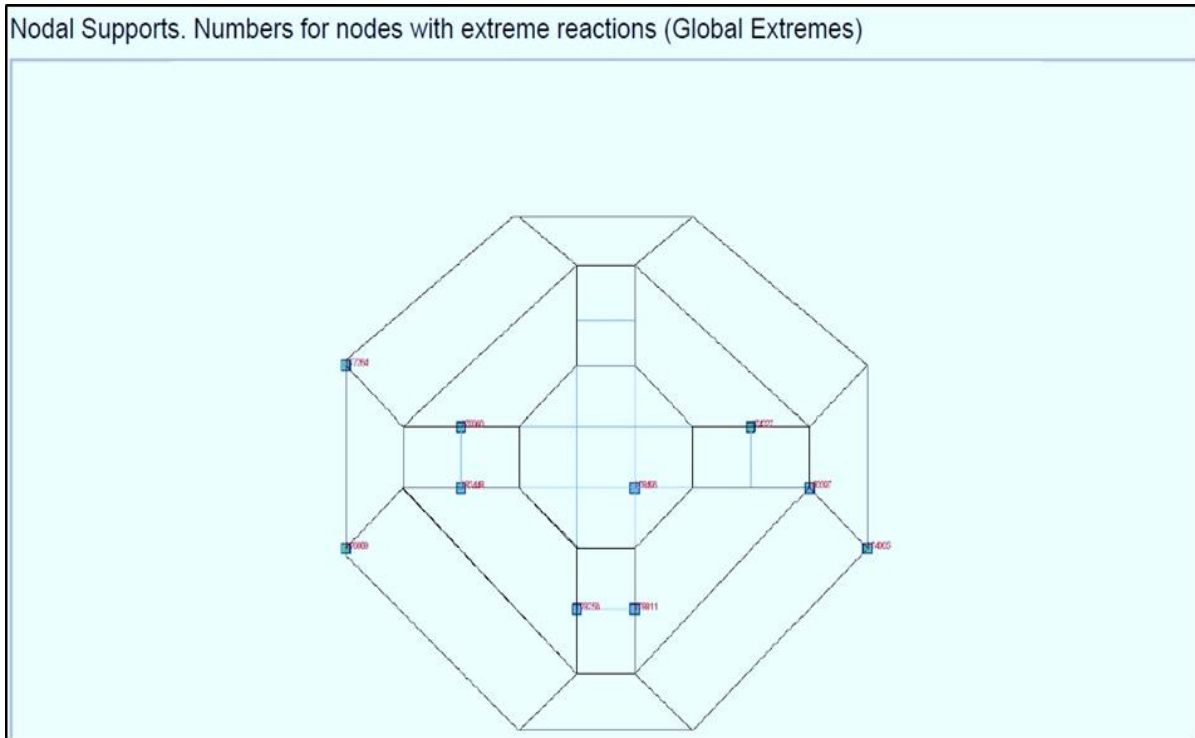


Figure 7.5: Building structure load nodal supports

7.9 Structural Building Load Displacement

Load displacement in regard to the performance of the building is evaluated based on lateral displacement. Examples of load displacements are storey shear, storey drifts, base shear and demand capacity or performance point. It is highly recommended to make use of the best type of steel bracing system, because it can significantly develop the firmness of the structure and hence minimise the maximum interstorey drift, lateral displacement and demand capacity or performance point of a reinforced cement concrete building than the shear wall system [101]. Table 7.5 and Figure 7.6 examine the load displacement of case 6, which specified the maximum and the minimum load displacement of the building in its life span.

Table 7.5: Building structure load displacement

Displacements						
Displacements - Cases: 6 : Global extremes:						
	UX (cm)	UY (cm)	UZ (cm)	RX (Rad)	RY (Rad)	RZ (Rad)
MAX	6.23e-02	0.0	1.56e+00	6e-02	6e-02	4e-04
Node	189537	5219	6427	6348	6654	189537
Case	6 (C)	6 (C)	6 (C)	6 (C)	6 (C)	6 (C)
MIN	-1.91e-02	-4.73e-01	-3.88e+01	-5e-02	-6e-02	-4e-04
Node	7560	189531	6384	6371	6363	189547
Case	6 (C)	6 (C)	6 (C)	6 (C)	6 (C)	6 (C)

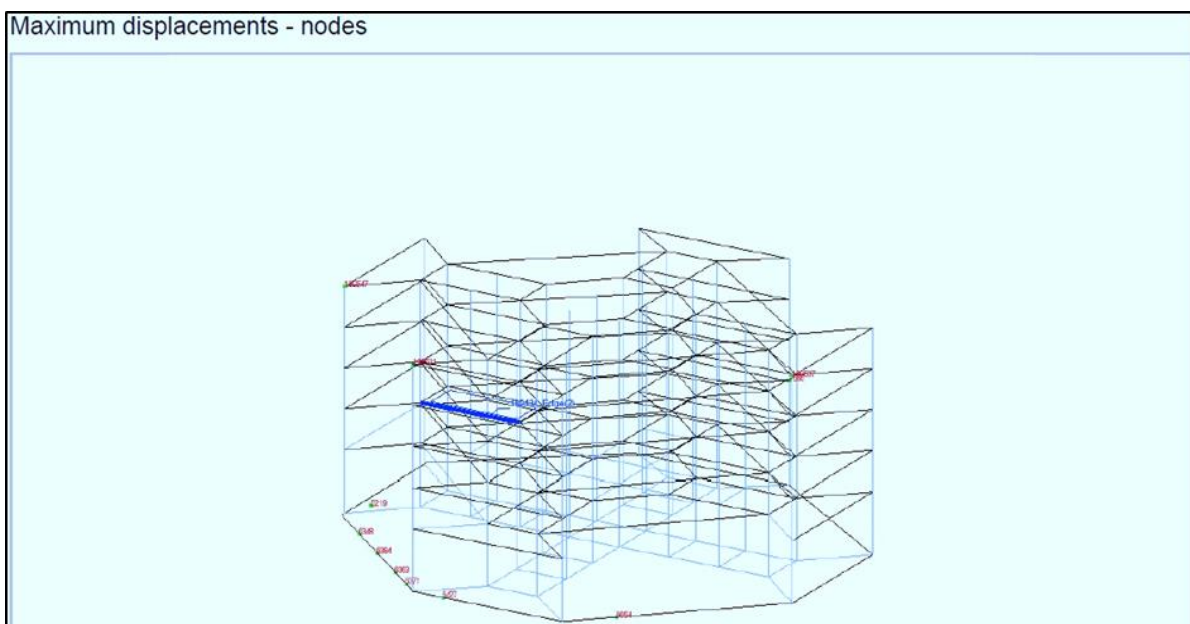


Figure 7.6: Building structure maximum load displacement

7.10 Force on Building Structure Elements

A column is a structural member that under compression transfers its load along a straight path in the direction of the column. Columns are normally thought to be vertical but can be horizontal or diagonal. A beam/girder transmits forces in a direction perpendicular to such forces to points of reaction. A girder is a beam that supports other beams. The loading delivered to a girder is the same as the load delivered to a beam. As the beam receives the load, the force is transmitted perpendicularly or at a right angle to the supporting members of the beam. Thus, loading of a beam will cause the beam to bend downward. The bending action causes the top of the beam to be in compression and the bottom under tension.

Beam load also places an attached supporting member in tension. In the arrangement of suspended beams, the top portion of the beam will be under compression and the bottom portion will be under tension; this phenomenon applies to all beam types. Thus, a beam supported on each end with a load placed in the middle of the span will deflect. This deflection results in the top portion of the beam being placed in compression and the bottom portion of the beam being placed in tension. There will be a small portion of material in the centre of the beam that has no stress applied; this is known as the neutral plane. This neutral plane serves only to keep the compressed and tensioned portions of the beam separated at an equal distance along the length of the beam. Less material is needed in this neutral plane. In addition, beam loading refers to the distribution of the load on the beam. The more the load is distributed, the better; concentrated loads may lead to collapse [102].

Tables 7.6 and 7.7 and Figures 7.7 and 7.8 show the case 7 building structural stability simulation results specified as maximum and minimum load force in building material element members, which are known as short word force in members. The load forces have distributions and directions among the members. Hence, these distributed load forces and direction are not always uniform or equal in magnitude and directions. In some cases, the load force can be extreme on any one member and then be transmitted to the other members, such faulty designs make the building structure vulnerable in the case of extreme disaster and the building can collapse. Thus, the purpose of building structural simulation prior to commencing construction is highly recommended to detect the defects at an early stage, as shown in Figure 7.7 and 7.8, in which the blue member parts are shown loaded with extreme forces and hence must be modified.

Table 7.6: Building structure force on column members

Forces in Members						
Forces in Columns						
Forces - Cases: 7 : ULS Combinations. Global extremes:						
	FX (kN)	FY (kN)	FZ (kN)	MX (kNm)	MY (kNm)	MZ (kNm)
MAX	2.79e+03	1.09e+02	9.72e+01	2.30e+00	1.62e+02	1.94e+02
Bar	178502	178762	170776	176038	170776	178699
Node	178567	189563	189523	189547	189523	189561
Case	7 (C)	7 (C)	7 (C)	7 (C)	7 (C)	7 (C)
MIN	7.17e+01	-1.17e+02	-1.09e+02	-2.29e+00	-1.81e+02	-1.82e+02
Bar	179532	178699	180403	173996	180403	178762
Node	189567	189561	189581	189537	189581	189563
Case	7 (C)	7 (C)	7 (C)	7 (C)	7 (C)	7 (C)

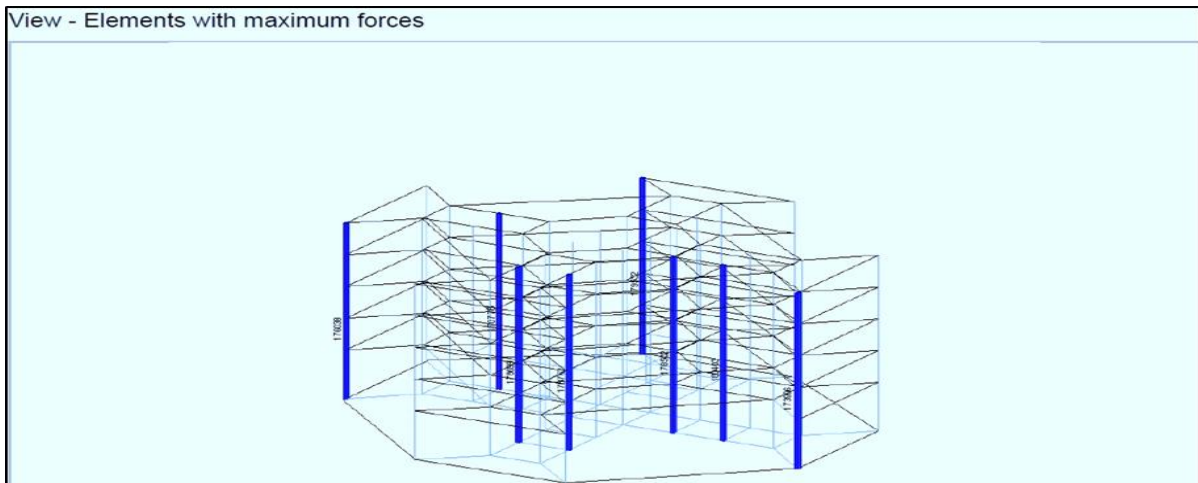


Figure 7.7: Maximum force in column members

Table 7.7: Force in beam members

Forces in Beams						
Forces - Cases: 7 : ULS Combinations. Global extremes:						
	FX (kN)	FY (kN)	FZ (kN)	MX (kNm)	MY (kNm)	MZ (kNm)
MAX	3.27e+01	1.11e+01	2.33e+02	3.06e+02	1.59e-12	1.36e-13
Bar	183583	182016	189037	190771	181994	182016
Node	170962	170962	180399	177264	170962	170962
Case	7 (C)					
MIN	-3.14e+01	-9.73e+00	-4.35e+02	-4.05e+02	-7.69e-13	-8.53e-16
Bar	183410	181994	182016	191947	189037	189037
Node	176091	170962	170962	175464	180399	180399
Case	7 (C)					

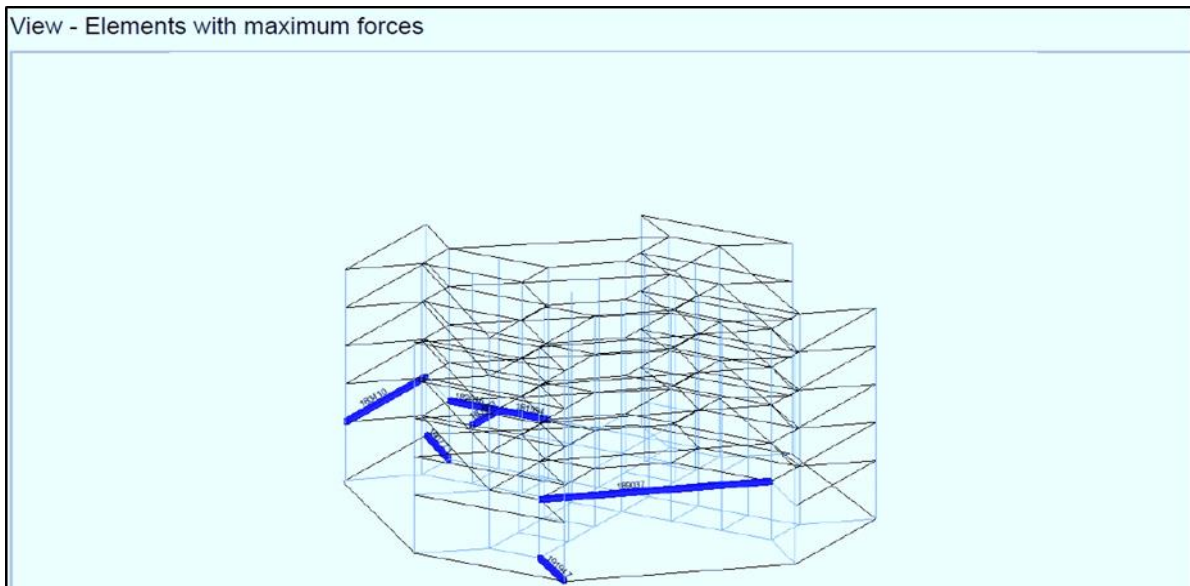


Figure 7.8: Maximum force in beam members

7.11 Load Forces in Slab Members

Slab floor boards transmit loads to joists with the beams. The amount of the load transmitted depends on the distance from the load point and direction from the joist. Floors slabs are designed to support heavy loads in the commercial building. The load is transferred from slab to beams by distributing the load over the beam. The slab loads (dead and live) are expressed in units of weight per area and are converted into weight per length of the beam [103]. The slab should rest on the beam that carries its weight. Similarly, the area weight is distributed along the beam by three methods depending on the reinforcement direction and the geometrical dimension of the slab, as shown in Figures 7.9 and 7.10. When the slab is rectangular in shape, and the ratio of its long side

to short side < 2 , it is reinforced in two directions. Each direction of reinforcement is supposed to carry and transfer a portion of the slab load to the adjacent beam. Conversely, when the slab is rectangular and the ratio of its longer side to shorter side > 2 , then it is reinforced in one way, which is the short direction, or as one-way ribbed concrete slab. Thus, the slab load is divided equally between adjacent beams. For an interior beam, the slab areas of both sides are divided by the corresponding width to obtain the lineal load of the beam [104]. The lineal load is a continuous consisting load of force with the beams. Hence, Figures 7.9 to 7.18 show the results of the structural building slab load forces with their directions. Forces are classified as horizontal (MXX) and vertical (MYY).

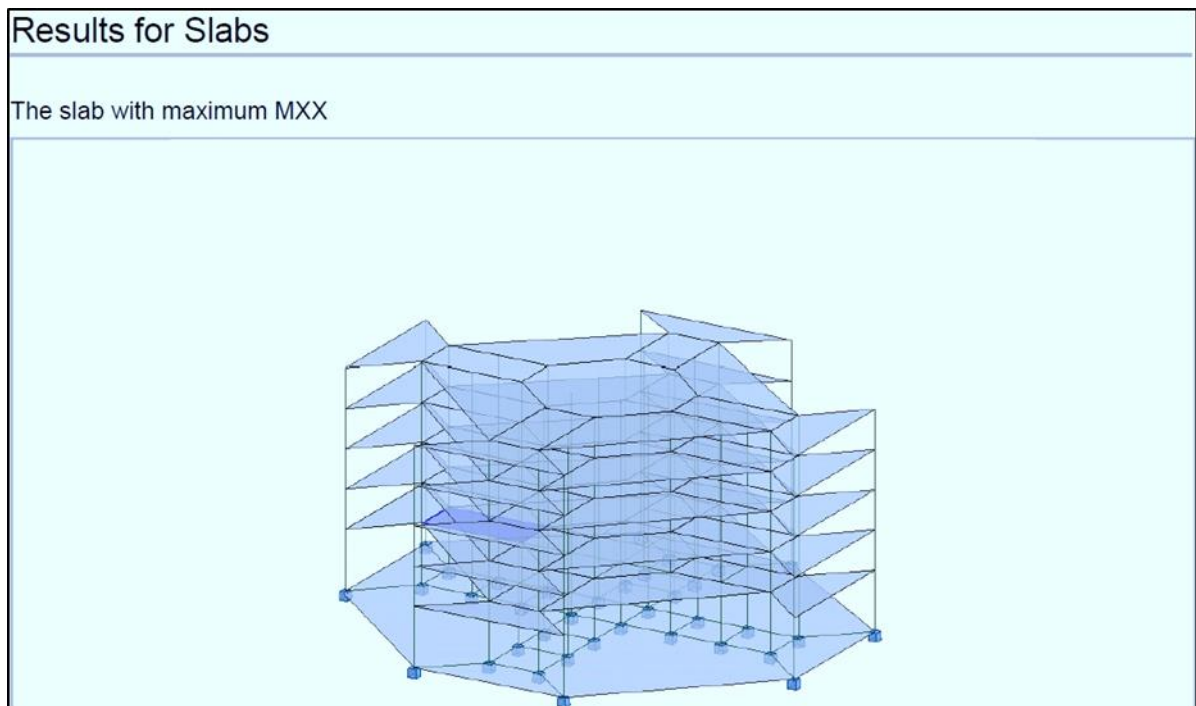


Figure 7.9: View of Building structure slab load

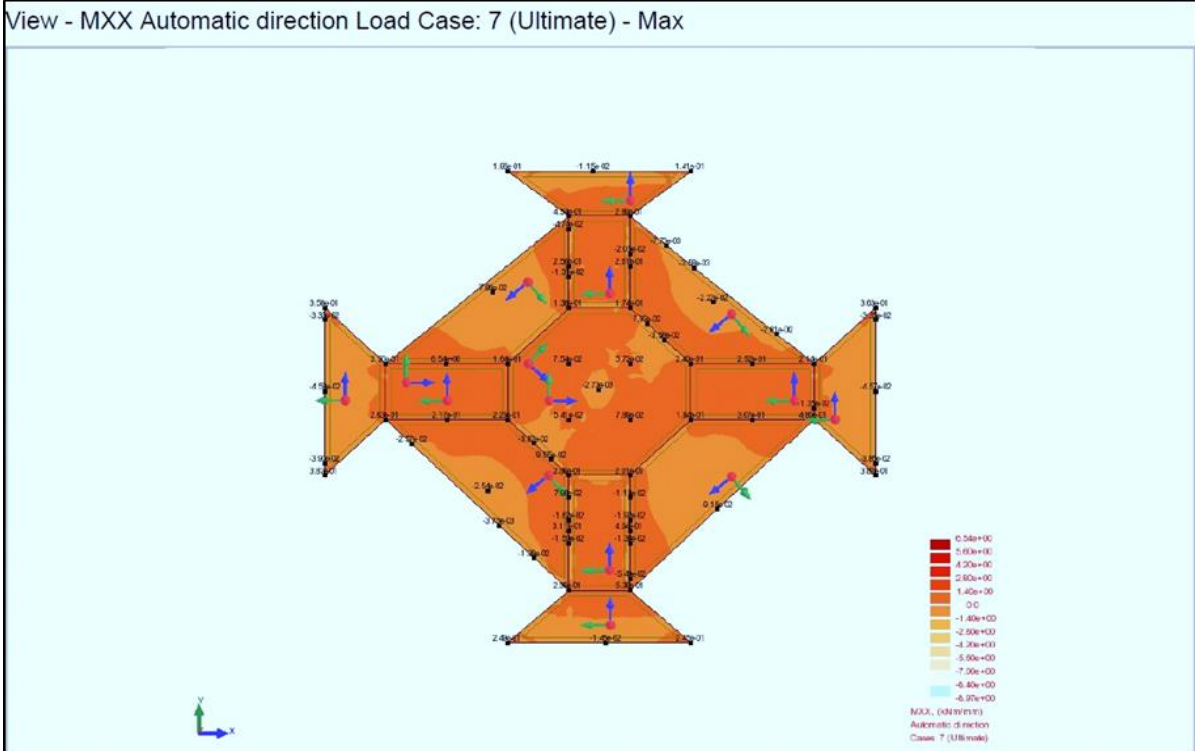


Figure 7.10: Building structure slab with maximum load and directions

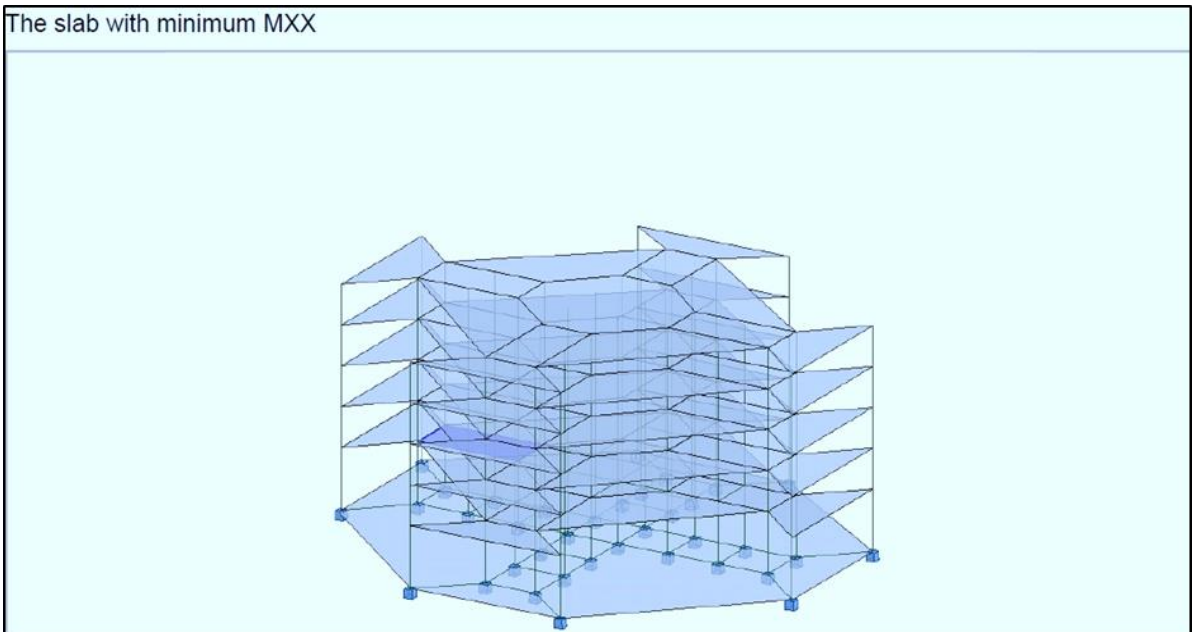


Figure 7.11: Building structure minimum force in slabs

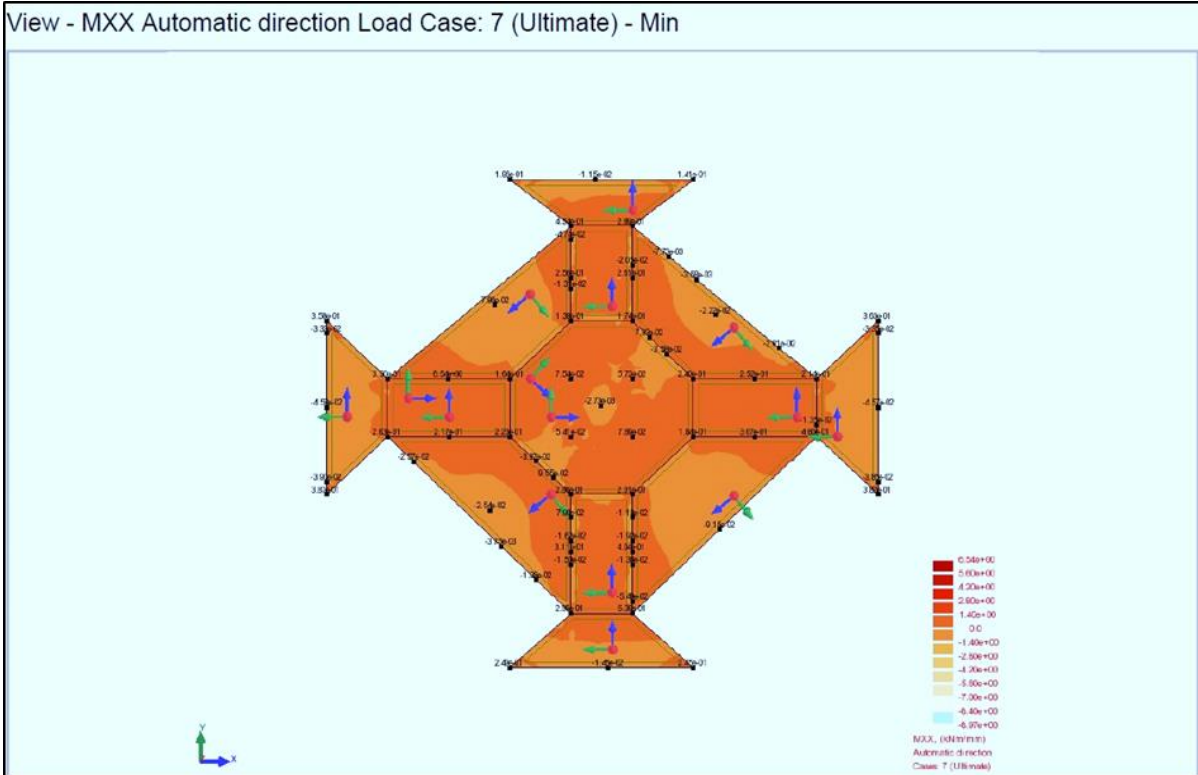


Figure 7.12: Building structure minimum slab’s loads and directions

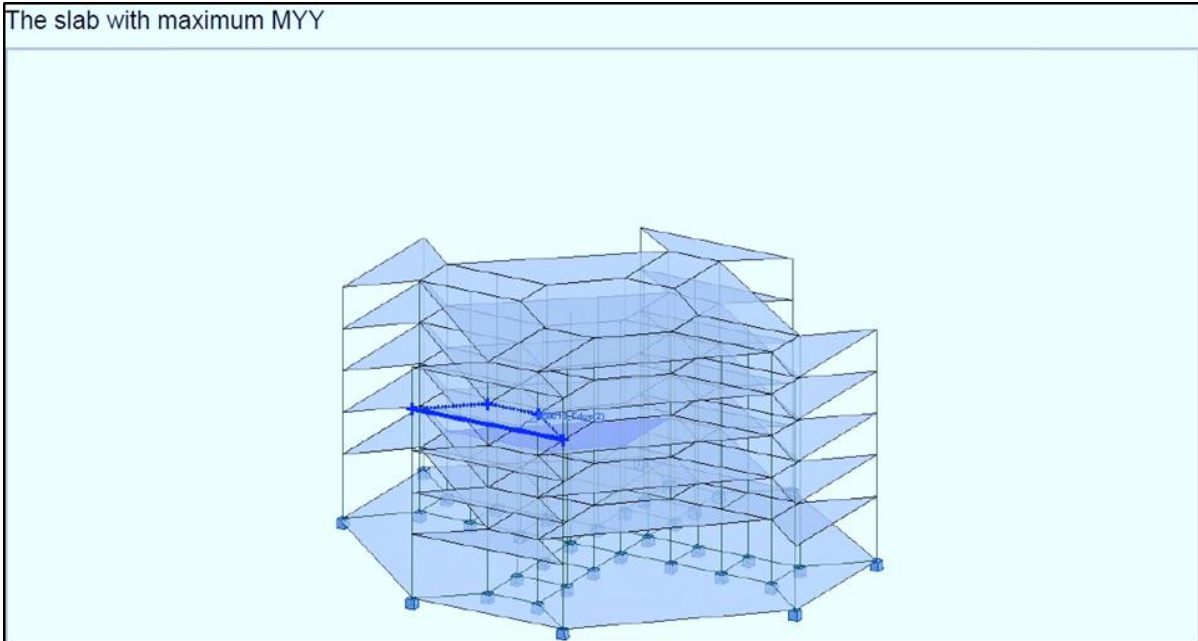


Figure 7.13: Building structure with maximum of MYY slab loads

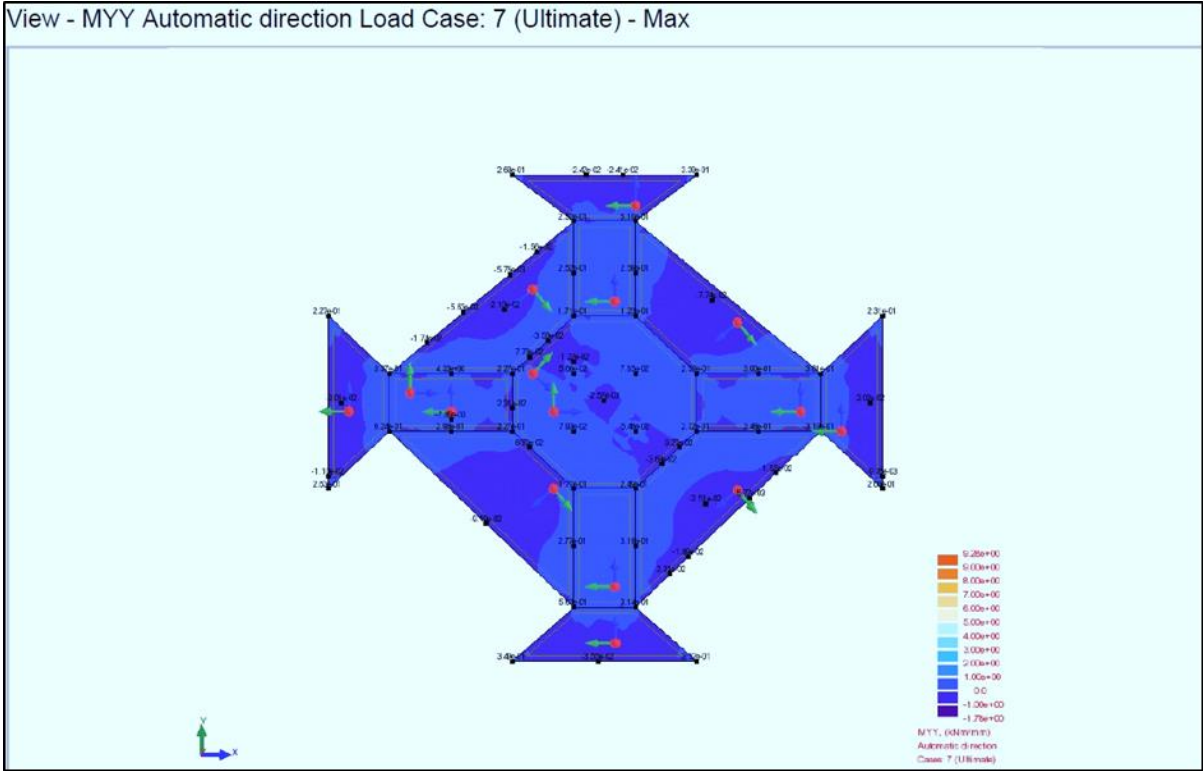


Figure 7.14: Building structure load case slab loads automatic direction

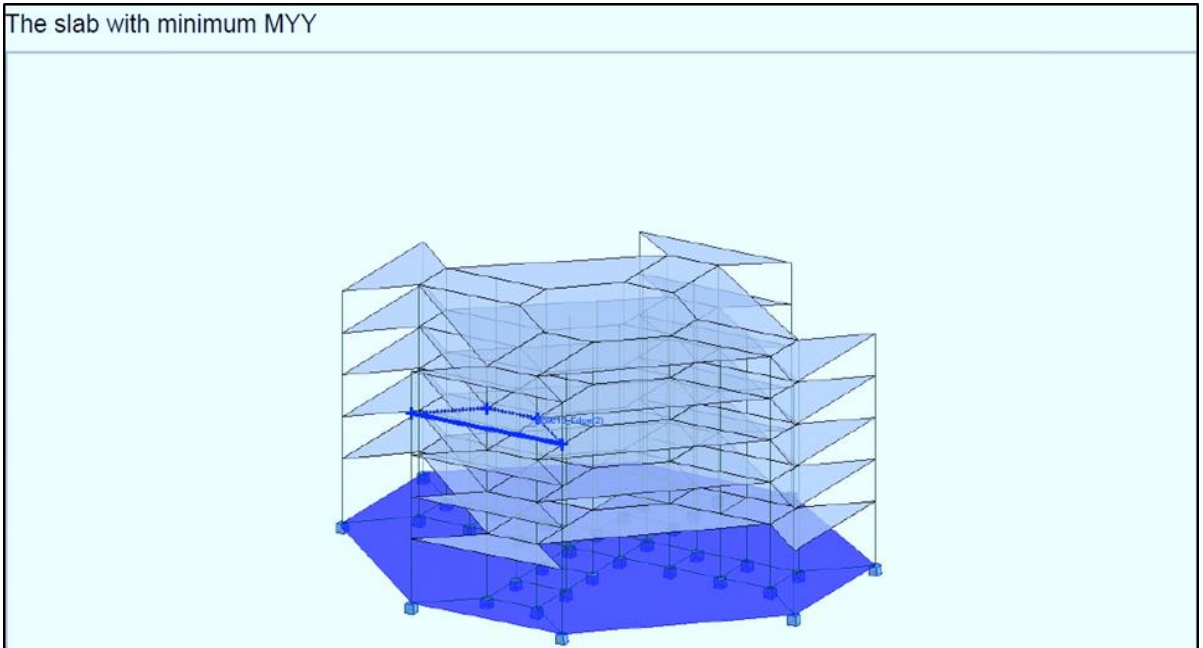


Figure 7.15: Building structure with minimum force in slabs

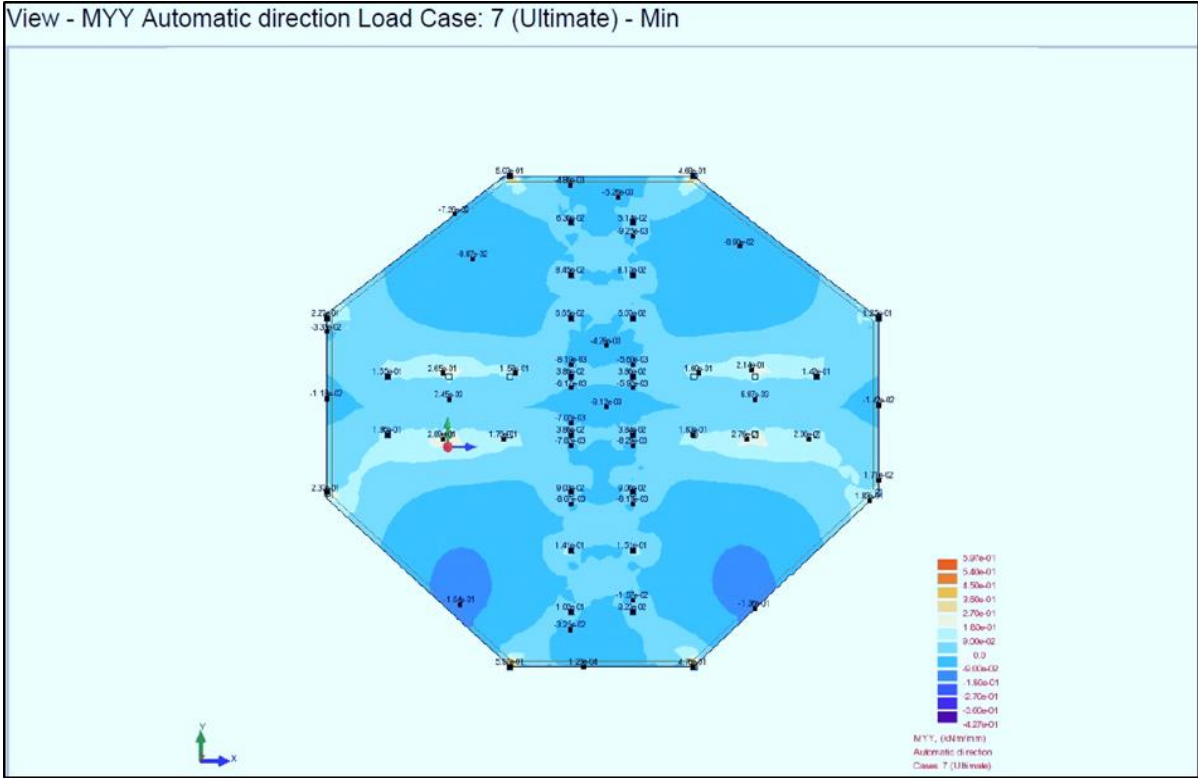


Figure 7.16: Building structure minimum slab loads with automatic direction

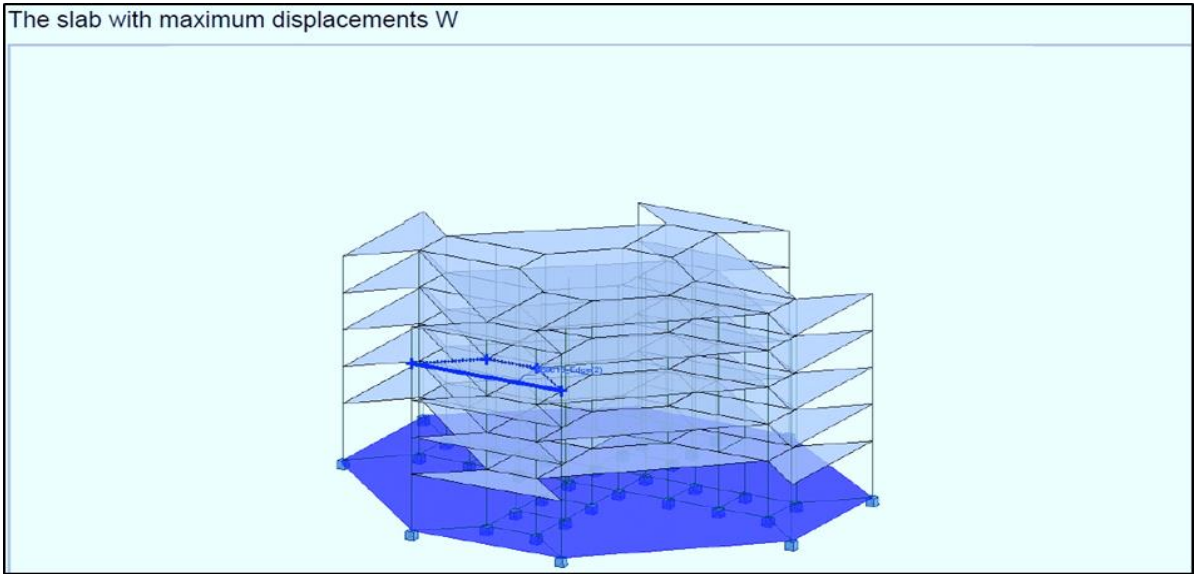


Figure 7.17: Building structure slab loads with maximum displacement

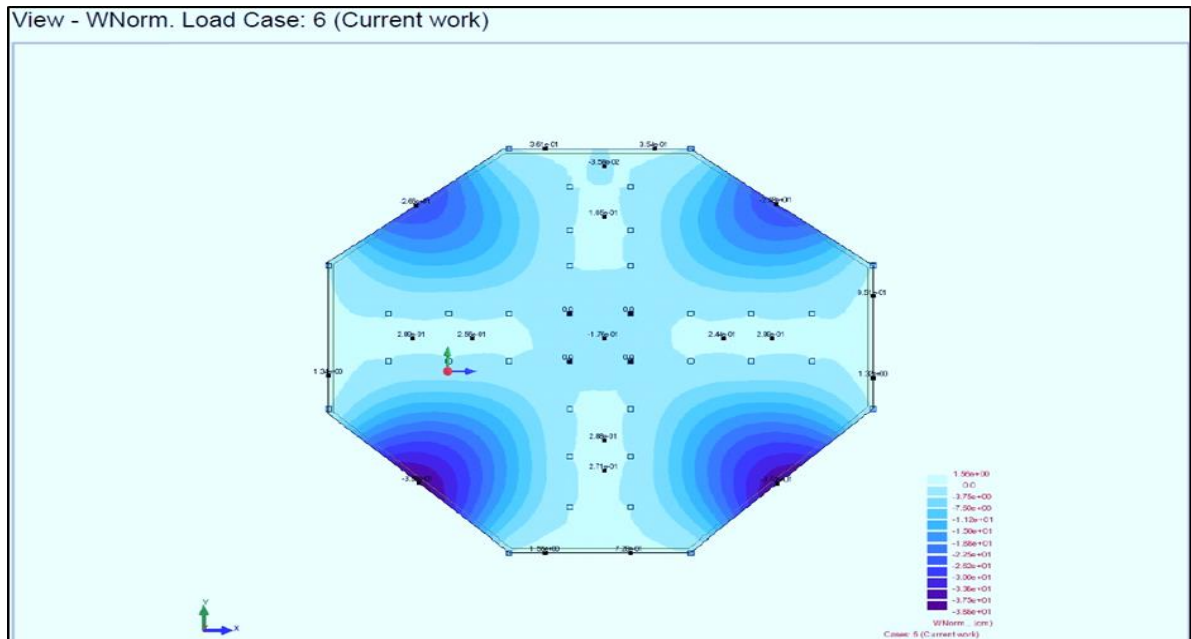


Figure 7.18: Slab load case with directions

7.12 Building Occupant Comfort

Buildings are designed for people, and those people accomplish their tasks inside the building. The building needs to keep people comfortable, efficient, healthy and safe, while they perform their tasks. Green design seeks to create buildings that keep people comfortable while minimising negative environmental effects. The current smart building is very comfortable for the occupant in the way the building provides services [105]. However, a smart building designed/equipped with most modern extended technologies, such as wireless technologies, reduces occupant comfort or make them feel their comfort is not optimised because of the side effects produced by excessive wireless power density. This is owing to wireless technologies that use high radio frequencies that cause health issues [106]. When a smart building is designed, the comfort it provides should be free of worries. This is because if there are worries, there is no comfort. Thus, in this research thesis, the use of a single-cable two-wire control system is preferred to eliminate the wireless control system devices currently used in GB.

7.12.1 Occupants' comfort satisfaction

To ensure people are comfortable, the building needs to provide the right mixture of temperature, humidity, radiant temperature and air speed. However, the right level of

these variables depends on the activities of occupants, namely, how active the occupants are, as well as the type of clothing they use. This is owing to the fact that each individual has slightly different criteria as regards comfort. Hence, comfort is often measured by the percentage of occupants who report they are satisfied with the provided service conditions [107, 108].

7.12.2 Indoor air quality

Indoor air quality (IAQ) in buildings refers to the quality of the air inside the building as represented by the concentration of pollutants, thermal temperature and relative humidity conditions that affect the health, the comfort and performance of the occupants. In addition to the growing proliferation of chemical pollutants in consumer and commercial products, modern building construction tends towards tighter building envelopes and reduced ventilation to save energy. Further, the pressures to defer maintenance and other building services to reduce costs have fostered IAQ problems in many buildings [109]. Hence, those measures significantly reduce air circulation in the building. Air circulation and ventilation rates are the quantity of outdoor air introduced into the building and the method of ventilation controls are the same as applied in the IAQ. Thus, consistent air quantities and an effective control system must be provided as demanded. Demand-controlled ventilation is applied based on the uses of air quantity and CO₂ sensors. This model uses one of the best approachable methods, especially when the CO₂ concentration set point is selected in accordance with the credit quality of indoor air. Hence, the coefficient of performance, such as a factor of 0.8, can be introduced to compensate for the actual variability in occupancy between zones and imperfect control system of dampers that do not maintain proportionality across the control range [110].

7.12.3 Energy consumption and greenhouse gas emissions calculation

According to the GBCA Guide 6, in multi-zone systems the calculation must be based on dynamic application of AS1668.2.2012 or ASHRAE 2010 multiple enclosure rules. The rate of bio-effluent CO₂ emissions to the space shall be based on the equation

$$q\text{CO}_2 = \frac{0.00276\text{ADMQR}}{0.23\text{QR} + 0.77}$$

where q_{CO_2} is the rate of CO₂ emission (L/s/person), AD is the body surface area (m²) (approx. 1.8 m² for a typical adult), M is the occupant metabolic activity rate (met) and QR is the respiratory quotient (the relative volumetric rates of CO₂ produced to oxygen consumed; approximately 0.83 for sedentary-light activity, and increasing to 1.0 for heavy physical activity (5 met)). The occupant activity level used for each space type must be consistent with the inputs used for the thermal comfort credit; assume $AD = 1.8 \text{ m}^2$ and linear variation of QR from 0.83 at 1.2 met, when met is decreasing, and 1.0 at 5 met, when met is increasing.

7.12.4 Outdoor air quality

Outdoor air enters and leaves a building by infiltration, natural ventilation and mechanical ventilation. In a process known as infiltration, outdoor air flows into the building through openings, joints and cracks in walls, floors and ceilings and around windows and doors. In natural ventilation, air moves through open windows and doors. Air movement associated with infiltration and natural ventilation is caused by air temperature differences between indoors and outdoors as well as by wind. The rate at which outdoor air replaces indoor air is described as the air exchange rate. When there is little infiltration and natural ventilation, or mechanical ventilation, the air exchange rate is low and pollutant levels can increase [111].

7.12.5 Environmental comfort stability

The goal of environmental sustainability is to conserve natural resources and to develop alternate sources of power while reducing pollution and harm to the environment. For environmental sustainability, the state of the future is measured in 50-, 100- and 1,000-year intervals. This is defined as the guiding principle of the state environmental stability [112]. Thus, many of the projects that are rooted in environmental sustainability will involve replanting forests, preserving wetlands and protecting natural areas from resource harvesting. The biggest criticism of environmental sustainability initiatives is that their priorities can be at odds with the needs of a growing industrialised society. Sustainable development is the practice of developing land and construction projects in a manner that reduces their impact on the environment by allowing them to create energy efficient models of self-sufficiency. This can take the form of installing solar panels or wind generators on factory sites, using geothermal

heating techniques or even participating in cap and trade agreements. The biggest criticism of sustainable development is that it does not do enough to conserve the environment in the present and is based on the belief that the harm done in one area of the world can be counter-balanced by environmental protection in others [113].

7.13 Building Management Control System

A building insulation system to reduce energy usage system was first used in the late 1980s [114], when energy demand increased and created a gap between energy supply and demand, leading to an energy crisis especially in the United States. Further, the building energy control system was enhanced following the increasing awareness of global warming from 1990. The two issues are the main reasons that led to the global emergence of measures to rapidly save energy in all sectors. Building is among the sectors that consume a large amount of energy. Hence, building energy saving started with simply installing an automatic ON/OFF system for lighting and rapidly increased to the extent of smart/intelligent building and, at present, with the help of BIOT is moving towards building smart cities. However, smart buildings/cities also have side effects: (1) Construction costs increase by 10 to 20%. (2) Smart buildings equipped with an extended wireless control RF system reduce occupant comfort. Thus, the importance of this thesis is that to eliminate these two factors, it progress a method that enable smart buildings can be cost-effective and offer maximum comfort, namely, the use of 'AS-Interface network protocol'.

7.13.1 AS-Interface network protocol method

The AS-Interface network protocol is an industrial network solution specifically designed for simplicity, flexibility and reliability. This decentralised installation method replaces the clutter, disorder and frustration arising from traditional cabling methods. It is all about simplifying the design of a control system, reducing wiring complexity, cutting installation costs, improving diagnostics and ultimately making automation more productive. Moreover, this research project is aimed to replace the BAS, BEMS and BACS, which are currently used in the building sector, by the modern and advanced technology of the AS-Interface protocol used in the industrial automation sector for saving power and installation wiring as aforementioned. Hence, to satisfy the objectives of GB, it is necessary to use minimum resources of building materials and EEB

materials and implement an IB control system, as shown in Figure 7.19. The advantage of the AS-Interface protocol over the current building control system is that the current GB construction costs are higher than those of the conventional building [69]. This is because any GB constructed with the current building control system consumes a huge quantum of wiring cables and requires several large cabinets. Thus, when the GB is constructed with the AS-Interface protocol, the number of electrical or electronic devices used in the building will be reduced, as shown in Figure 7.19. Consequently, the installation and the tradesmen costs will also be significantly reduced. The AS-Interface protocol requires three main wiring systems, namely, for the main grid supply, the AC power supply and the 30VDC power supply. The AS-Interface power supply uses the same wire for transmitting/receiving signal messages and to power the slave nodes and it also has a capability of handling up to maximum of 8 Amps per network with minimum 3 V voltage drop. There is no change with the grid main supply wiring. The changes are only in AC power supply wiring system and in the control wiring system. Hence, the AS-Interface protocol wiring method is distinguished from the other wiring method; because the former uses one continuous AC power supply cable, running to every device from the main C/B without entering ON/OFF switches or needing control of switches. Then, a separate AS-Interface bus cable runs to each device (slave nodes), as shown in Figures 7.19 and 7.20. This type of wiring method eliminates the need for using several C/B, switches, cables, relays and contactors and uses a minimum-size control cabinet.

Further, the AS-Interface protocol is a communication network protocol used mostly in industrial areas for data access, input/output (I/O) exchange for programmable logic control (PLC), decentralised control system (DCS), gateway devices and PC-based automation system [115]. Currently, it is an open protocol technology supported by many automation manufacturers and vendors. Moreover, it is an industrial automation system initially formed by PROFIBUS International (PI). Hence, the AS-Interface network protocol is considered the most economical and ideal for communication between actuators and sensors.

7.13.2 Reasons to migrate to AS-Interface protocol for building automation

The AS-Interface is the most essential and ideal for economical communication protocol between the higher controller level devices and the I/O devices. The benefit of

using it ranges from hardware savings to the commissioning. It has huge advantages over the current BASs.

(1) Simplicity

The AS-Interface network protocol is very simple and needs only one cable to connect the input and output modules from any manufacturer. Its users do not need deep knowledge of automation systems or communication protocols. Unlike other digital networks, it does not need terminators or equipment description files. Simplicity is its main strong point.

(2) Performance

The AS-Interface network protocol system is efficient and moderately fast, enabling its use to replace large and high-cost projects. Its master is specially designed to communicate with legacy control systems and provide smooth integration with the existing technologies. Notably, this is accomplished in a simple and reliable way.

(3) Flexibility

Expansibility is a flexibility option of the AS-Interface protocol. To add a module, just connect the module to cable and enable it. Moreover, the AS-Interface network protocol supports any cabling technology: star, bus, tree, ring or other configurations up to 100 meters of cable. Moreover, by adding repeaters it is possible to expand the system up to 300 meters. The protocol is easy to install since it needs no terminators at the ends.

(4) Cost

This protocol typically reduces cabling and installation costs by 50% in comparison to other conventional networks. The use of a single cable for connection to discrete devices reduces the need for cabinets, conduits and trays. The savings obtained in the network are really significant, since using few cables decreases installation, commissioning costs and engineering time.

(5) Moderately faster data transmitting/receiving system

Data transfer is moderately fast on less than 10 ms on a fully loaded system. For example, at one cycle up to 248 inputs and 248 outputs can be transferred without any

issues. It can also operate directly in conjunction with an existing PLC, PC and variable speed drive or can be linked to a higher-level bus system. For example, with the PROFINET Ethernet, PROBUS and HMI, which are commonly applied as the networking protocol for higher automation and plant control system.

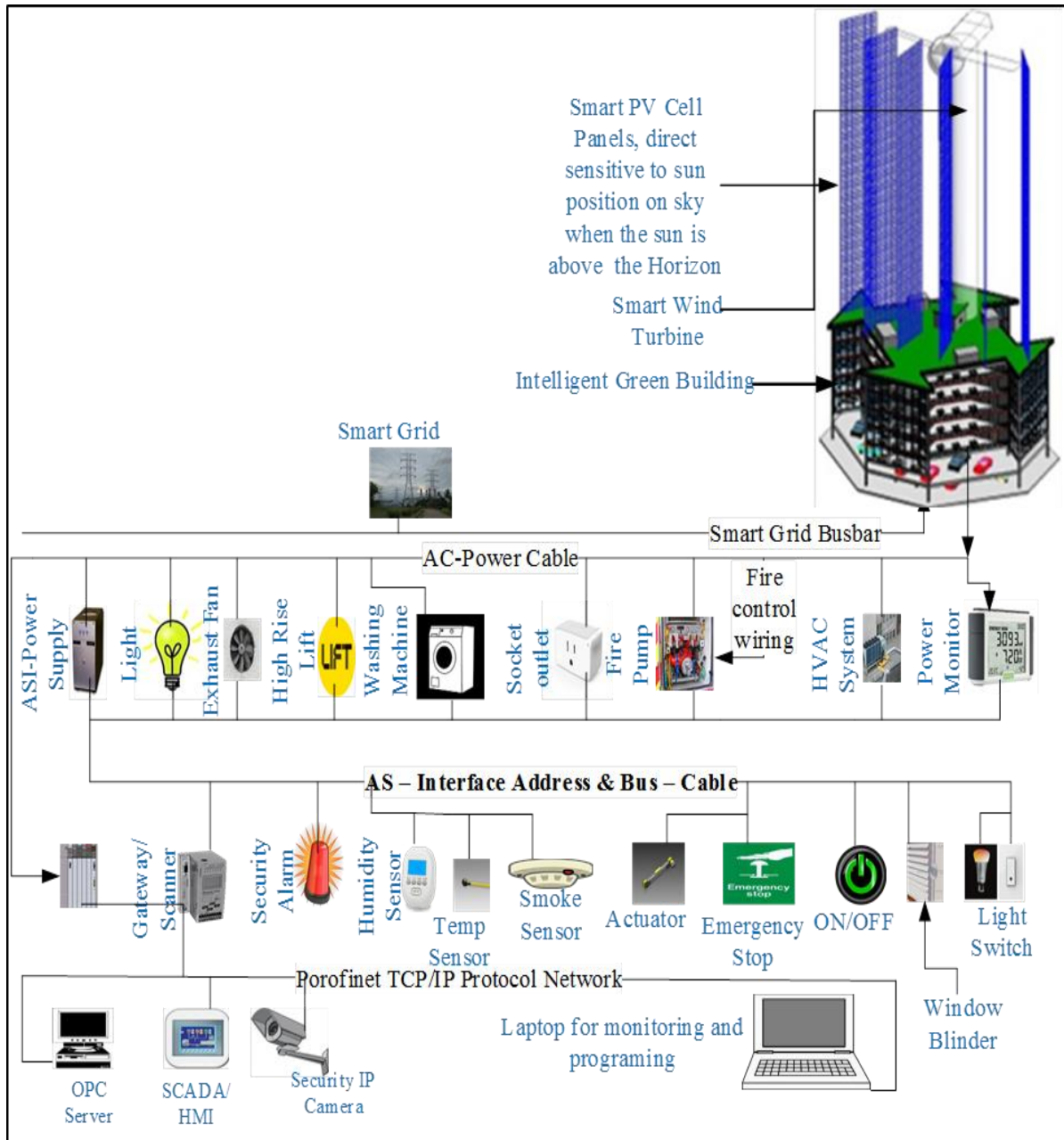


Figure 7.19: AS-Interface network protocol wiring method

7.13.3 AS-Interface network protocol hierarchy

The AS-Interface can be connected to the main controllers, such as OPC, Shell Processing Support, Computer Literacy Project, Inter-process Communication and PC.

In the AS-Interface network protocol; there are two types of wiring methods: the first is a direct connection from the higher controller (PLC) to the AS-Interface protocol slave nodes; in this case, the master has built-in AS-Interface protocol. The second type is through a gateway/scanner. Figure 7.20 shows both methods; for the purpose of this thesis research method, the second method is chosen, connecting the master PLC and the gateway/scanner via the PROFINET protocol. PROFINET offers a highly sophisticated, modern, standard Ethernet method of communication protocol devised by PI. Currently, PROFINET is also an open vendor-based protocol [116]. OPC and the other higher-level controllers are server-based computer system communication, mainly used in industrial manufacturing sectors for fast and reliable real-time communication. OPC significantly reduces the time, cost and effort required to write custom interfaces for each different device [117]. At present, OPC is widely used in most advanced industrial manufacturing sectors.

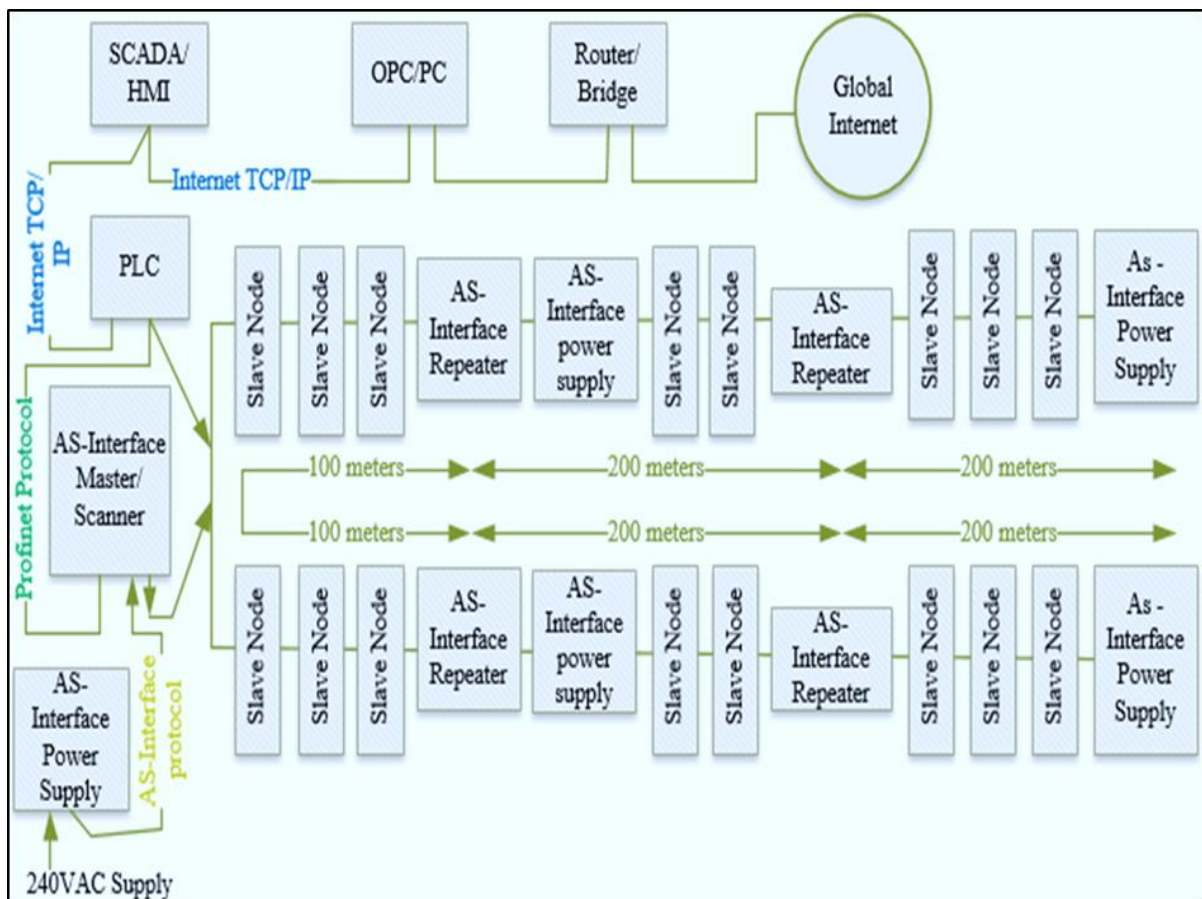


Figure 7.20: AS-Interface network protocol configuration method

7.13.4 AS-Interface network protocol

The AS-Interface protocol power supply unit supplies voltages ranging from 25.5 to 30.5 VDC and also supplies a total current of 8 Amps. The power unit supplies to the slave nodes as well as to the master or gateway/scanner through the two bus wires; the same bus wires transmit and receive AS-Interface signal data, connected at any point on the network. In case of long bus lines, the voltage drops must be taken into account and should not exceed 3 VDC on the whole 100-meter distance bus cable. This type of AS-Interface protocol power supply has an internal overload protection circuit to limit any overcurrent drawn. It has also power-balancing and data-coupling capabilities. It balances the entire AS-Interface network protocol. The data-coupling circuit sends signal messages superimposed on the AS-Interface network protocol through the power supply voltage. This network consists of two inductors and two resistors, connected in parallel. The inductors perform a differentiation function on the voltage pulses to convert the current pulses generated by the transmitters connected to the network. At the same time, the resistors prevent short circuits on the cable. The coupling between the inductors should be as close as possible to 1, meaning that the mutual inductance must tend to be 200 μ H. Slave nodes receive a permanent address from the master using software or a hand-held programming tool and up to 62 standard and A/B slaves nodes are possible, per network. The I/O data comprise four inputs and four or three outputs for each device.

7.13.5 Building internet of things

The current IB, now referred to as GB or intelligent GB has been developing since the early 1990s, and many competing definitions and names were proposed. The definitions of IB focused on the role of technology for building automation and control of building functions [118]. In the late 1990s and early 2000s, with the introduction of BREEAM codes and the LEED program, the IB spotlight tilted towards energy efficiency and sustainability.

The IOT is advancing a new type of smart buildings that are better aligned with the priorities of building owners or managers. IOT enables operational systems that deliver more accurate and useful information for improving operations and providing the best experience for building occupants. Hence, IOT accelerates the transformation of

building blocks that simplify how building systems talk to the cloud and exhaustively analyse building data to develop new business for investment, and offers insights capable of driving real value for greater performance. The BIOT takes the concept of IOT and applies it to function in commercial buildings [119]. Currently, the concept of BIOT is growing fast, because of the rapid expansion of the internet and it is being implemented in many types of building.

BIOT is changing the building industry; now, buildings have a level of intelligence built in, memory storage for HVAC, lighting, security equipment, digital signage for fire safety and current and past information to make fast and accurate decisions. Thus, BIOT makes all these things more efficient and cost-effective [120]. Hence, it reduces usage of energy.

In this research thesis, BIOT is implemented as the head of the control system, which connects the building devices with the AS-Interface protocol master gateway/scanner and with OPC as shown in Figure 7.20, using the transmission control protocol/IP PROFINET communication protocol.

7.13.6 Benefit of AS-Interface protocol

Designing and modelling GB is considered advanced step processing task, in reality, it is a complex process in which it requires an involvement of collection of engineering expertise, green energy researchers, construction contractors and an echo chart organisation contribute. In addition, the design and the modelling of GB, appropriate modern technology must be carefully selected, to satisfy the objectives of GB without adding extra construction costs over that for conventional buildings. For example, when erecting two buildings of the same size, one conventional and the other with GB, apart from the quality of the material and locations, these two buildings should not have significant difference in their construction costs since the minimum and maximum amount of construction materials used to build is specified by the building code regulations. The main significant difference occurs in the implementing of insulation, installation of renewable energy and installation of electrical and electronic devices, which make the building smart. Figure 7.21 shows a brief summary of the potential influence factors of the AS-Interface network protocol control system, in the top section

in regard to its limitation, and in the bottom section in regard to the possible response. In addition, Figure 7.22 shows the wiring reduction when the proposed method is used.

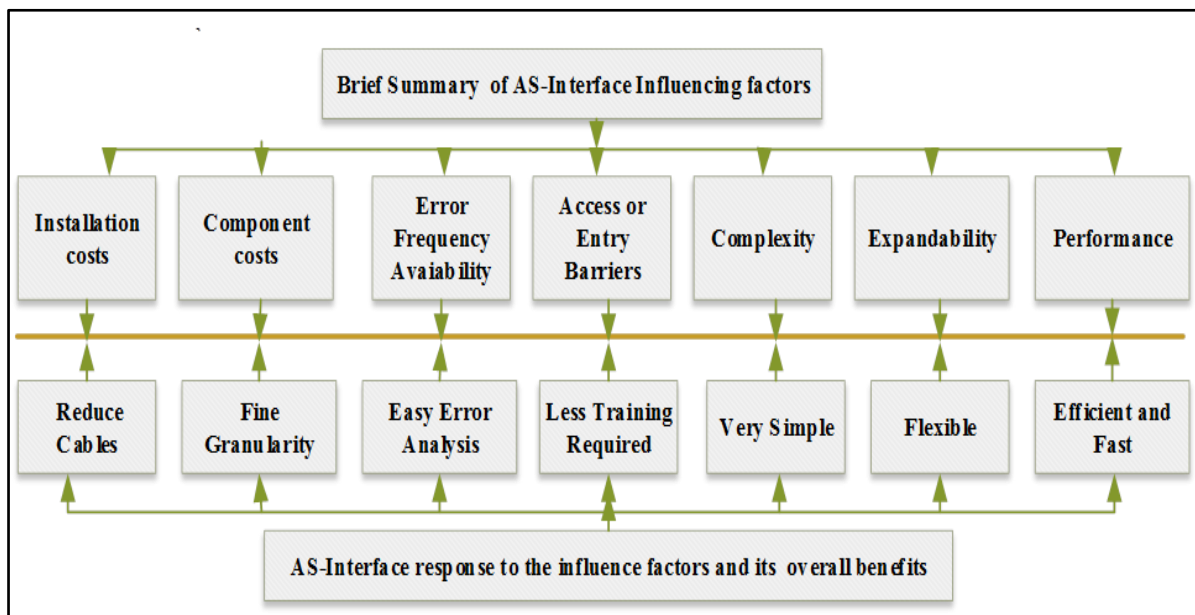
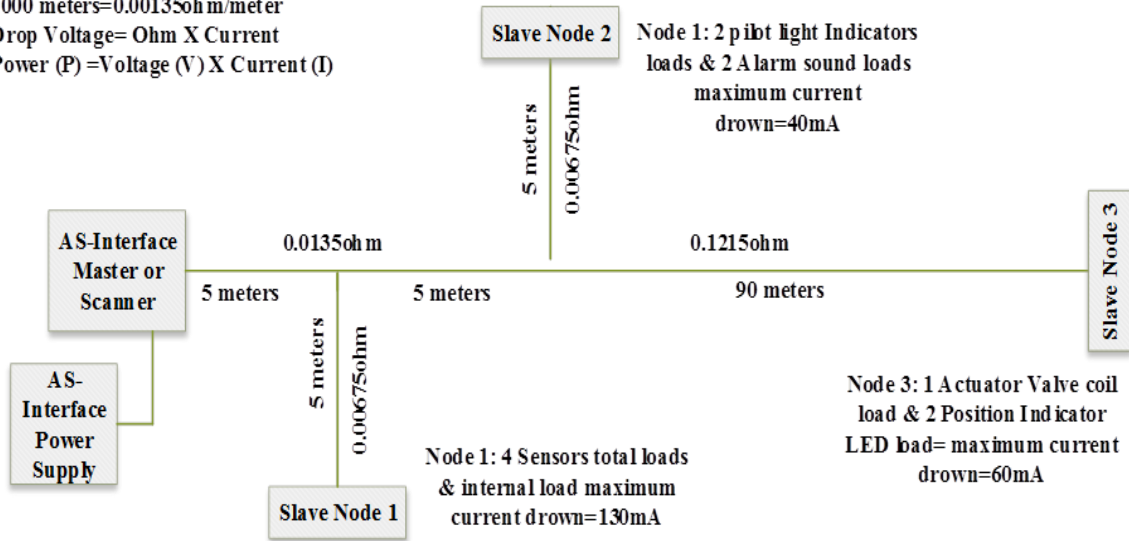


Figure 7.21: AS-Interface network protocol influence factors & response

AS-Interface Power Calculation

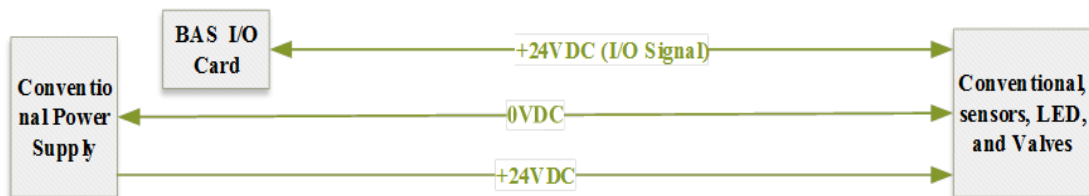
Bus-Cable Resistance=1.135ohms per 1000 meters=0.001135ohm/meter
 Drop Voltage= Ohm X Current
 Power (P) =Voltage (V) X Current (I)



The Total Impedance (Z) = $[(0.1215/0.00675+0.00675)/0.00675]+0.00675=0.01289\text{ohms}$

Load one (L1) drop voltage = 2.43mV, Load two (L2) drop voltage = 2.498mV, Load three (L3) = 9.52mV

If we wire up with Conventional wiring, there will be 11 individual signal wires (I/O) from, BAS I/O Card to BAS convention wiring Sensors, LED and Valves.



$Z1=4(0.00675+0.00675) = 0.054\text{ Oms}$, $Z2=4(0.0135 + 0.00675) = 0.081\text{ohm}$, $Z3= 3(0.033750 +0.1215) = 0.466\text{ohm}$,

Load one (L1) drop voltage = $0.054 \times 130 = 7.02\text{mV}$, Load two (L2) drop Voltage = $0.081 \times 40 = 3.24\text{mV}$, Load three (L3) drop voltage $0.44 \times 60 = 27.96\text{mV}$

Figure 7.22: Benefit of AS-Interface protocol wiring configuration

7.14 Conclusion

The first part of this chapter discusses the building structural stability simulation, which was not the main part of this study. However, as the aim of this thesis is to achieve ultimate energy saving (almost to approach NetZero energy reductions in commercial building), the concept of building physical stability is introduced as a subchapter section. Hence, when the commercial building theoretically becomes stable in regard to

energy consumption, it is also physically and structurally stable. This allows occupants of the building to not only feel safe and secure in terms of energy consumption and security purposes, but also in terms of the building's physical firmness and safety. Thus, building occupants are satisfied with the comfort offered. Owing to these reasons, the building structural stability simulation was carried out prior to energy simulation. The generated report indicates the defects of the building elements and where these defected elements should be subject to adjustment prior to commencing practical work.

The second part of this chapter demonstrates buildings occupants' comfort; currently, their comfort is a significant factor in achieving GB objectives and in its scope. Thus, to satisfy these objectives and scope, occupant comfort is one of main significant selection criteria. This is because the GB is equipped with the latest modern technology and these technologies makes the building react to the occupants' requirements/interests, instead of the occupants acting to obtain a response. In addition, modern technology, especially with introduction of BIOT, the control system, facilitates the control of almost every action indoors/outdoors, such as IAQ/outdoor air quality, fresh air ventilation and monitoring occupant health issues.

The third part of this chapter introduces a new method for the BACS that intentionally focuses on the main issues of the current building control system objectives and scope: (1) ultimate building energy reductions (2) higher energy consumption costs and (3) occupant comfort. Using this method, the higher energy consumption cost is reduced and total ultimate energy reduction is approached while occupant comfort is maximised. However, this method is only proved theoretically using computer simulation software applications and further practical research is necessary to validate the research outcomes.

Chapter 8: Conclusion and Further Research

8.1 Building Energy Simulation

The objectives of comprehensive energy efficiency in commercial GB is still complex with many significant unsolved issues. However, research to solve these issues has also increased recently, resulting in the development of many different methods. This research project also demonstrates the method of achieving ultimate energy reduction using design, modelling and simulation of a five-storey hexagonal-curve shape commercial office building. The research method consists of three main steps. (1) The building was initially constructed using randomly selected materials. (2) The primary (known as base run) energy simulation was conducted. (3) Multiple automatic alternative designs using automatic construction material selection were considered in GBS. In conclusion, these steps were conducted to choose the best method which the simulation results demonstrate maximum energy reduction. Thus, from the automatic alternative designs, the ‘HVACTYPES_ASHRAE_Package Terminal Heat Pump,’ shows a significant energy reduction over all of the multiple alternative designs.

In this research, an overall building energy simulation of GB, using a computer software application system, achieved significant reduced results from 50 to 63.5%. This result does not include the energy reduction obtained from BACS, which ranges from 15 to 30, as the literature review shows. This result is just obtained when effective control counter-measures are adopted in all the energy sectors of the commercial building.

8.2 Choosing Best Energy Simulation Results Package

The ASHRAE ‘HVACTYPES_ASHRAE_Package Terminal Heat Pump’ is selected, which is the best energy reduction package in this research project. The method and type of the building automation and HVAC that should be used with this package are yet to be identified. To this end, further practical research focusing on ASHRAE’s energy packages is necessary, which is beyond the scope of this research project. Thus, for this case, as mentioned in the previous paragraph, the energy reduction that could be obtained from BACS is excluded when the total annual energy reduction is calculated. In addition, all the other significant energy simulation results demonstrated in this research project are not yet proven practically for commercial buildings.

8.3 Building Integrating with Renewable Energy

Currently, renewable energy is considered the main solution to tackle the rising energy costs, shortage of sustainable supply and the global climate pollution produced by fossil oils. Increasing the productivity of renewable energy with optimised usage pushes the building towards energy self-sustainability and hence eliminates the usage of grid supply electricity produced by fossil oil in long term. Thus, this research focusses on comprehensive resource usage in predesigning energy efficient GB. Chapter 5 (Base run energy simulation) proposed three types of PV cells with their basic efficiency ranging from 5 to 15% and one 15-inch wind turbine for this building. In this chapter, the basic 15% efficiency of PV cell is increased to 41% and the performance of wind turbine is theoretically maintained at its optimised rated power. Hence, this renewable energy potential is maximised using different techniques to achieve energy efficient commercial GB.

8.4 Building Structure Stability

Building predesign focuses on the basic term of building structural stability simulations. The term of building stability refers to physical firmness in regard to occupant safety to live or work inside the building. Owing to these reasons, building structural stability simulation was carried out prior to building energy simulation. Hence, the generated report indicates minor defects of building element members. These defected building members should be subject to adjustment prior to commencing practical work. Thus, building occupant comfort satisfaction is achieved (EEB + structurally stable building = ultimate occupant satisfaction).

8.5 Building Occupant Comfort

In this research, comfort and stability are not main subjects; this is owing to the focus on reducing GB annual energy consumption and CO₂ emission. However, occupant comfort is highly enhanced in the entire research. This is to minimise the perception that GB is designed and modelled for thermal comfort alone. In reality, GB extends beyond such perceptions. Moreover, it provides maximised energy usage reductions and thermal comfort, and is also becoming the ultimate multi-automatic service provider to

occupants living or working in it. Modern airports, healthcare buildings, hotels and large-commercial enterprise buildings are few examples of smart buildings.

8.6 Building Management Control System

The main criterion of GB is to minimise resource usage and thus to reduce the installation, maintenance, labour and annual energy cost. In this research thesis project, a simple cost-effective control method is introduced, ‘AS-Interface protocol’, which has not attracted as much attention as the other highly sophisticated network technologies, such as the Ethernet and PROFIBUS decentralised process, but completes the job fast at low cost. The AS-Interface protocol is also available in the market as an alternative for any automation control system sectors and its users are satisfied with the cost reduction obtained from this control system. This research project demonstrates the method to design and model the GB with the AS-Interface protocol for commercial buildings to minimise the initial construction, maintenance and energy consumption costs.

8.7 Further Research Recommendations

This research project attempts comprehensive energy simulation using computer simulation software applications and achieves significant reduction in annual energy consumption. The achieved result indicates that the commercial building shall be self-sufficient or, in other words, approach NetZero energy. This will be true if more research focusing on cost-effective, resource-minimised and occupant-centred perception on the GB revolution is conducted globally. Further, the GB revolution should emphasises concepts such as green energy, green economy, green leader, green living world and green perception to make buildings self-energy sufficient. Hence, in conclusion, it is recommended that further practical research be conducted to prove the significant results obtained using computer-aided simulation software application, which is beyond the capability of this research thesis project. Such further research should focus mainly on four parts of this project:

- (1) on ASHRAE’s energy packages, especially the ‘HVACTYPES_ASHRAE Package Terminal Heat Pump’, ‘HVACTYPES_High Efficiency Heat Pump’ and ‘HVACTYPES_ASHRAE Heat Pump’

- (2) practical research work, on solar energy simulation for the whole commercial building
- (3) practical research work using the AS-Interface network protocol as BACS in commercial buildings
- (4) practical research work on the PV cell Sun intensity tracking system using the method demonstrated in Chapter 7.

References

- [1] D. P. Mehta and M. Wiesehan, "Sustainable Energy in Building Systems," *Procedia Computer Science*, vol. 19, pp. 628-635, 1/1/2013 2013.
- [2] D. Milovanovic, "Energy efficiency in buildings, industry and transportation," *AIP Conference Proceedings*, vol. 1499, pp. 71-82, 2012.
- [3] C. Tih-Ju, C. An-Pi, H. Chao-Lung, and L. Jyh-Dong, "Intelligent Green Buildings Project Scope Definition Using Project Definition Rating Index (PDRI)," *Procedia Economics and Finance*, vol. 18, pp. 17-24, 1/1/2014 2014.
- [4] L. Zhu, R. Hurt, D. Correia, and R. Boehm, "Detailed energy saving performance analyses on thermal mass walls demonstrated in a zero energy house," *Energy & Buildings*, vol. 41, pp. 303-310, 1/1/2009 2009.
- [5] H. J. Kwon, S. H. Yeon, K. H. Lee, and K. H. Lee, "Evaluation of Building Energy Saving Through the Development of Venetian Blinds' Optimal Control Algorithm According to the Orientation and Window-to-Wall Ratio," *International Journal of Thermophysics*, vol. 39, pp. 0-0, 2018.
- [6] A. Sherif, H. Sabry, and T. Rakha, "External perforated Solar Screens for daylighting in residential desert buildings: Identification of minimum perforation percentages," *Solar Energy*, vol. 86, pp. 1929-1940, 2012.
- [7] C.-F. J. Kuo, C.-H. Lin, and M.-W. Hsu, "Analysis of intelligent green building policy and developing status in Taiwan," *Energy Policy*, vol. 95, pp. 291-303, 2016.
- [8] S. Wang, Z. Xu, H. Li, J. Hong, and W.-z. Shi, "Investigation on intelligent building standard communication protocols and application of IT technologies," *Automation in Construction*, vol. 13, pp. 607-619, 1/1/2004 2004.
- [9] M. Āček, "Knowledge Formalization of Intelligent Building," *AIP Conference Proceedings*, vol. 1738, pp. 120005-1-120005-4, 2016.
- [10] K. Chan, "Integrating Traditional Commercial Buildings With Intelligent Building Concepts," *Cost Engineering*, vol. 49, pp. 25-36, 2007.
- [11] T. Gadakari, S. Mushatat, and R. Newman, "Intelligent Buildings: Key to Achieving Total Sustainability in the Built Environment," *Journal of Engineering, Project & Production Management*, vol. 4, pp. 2-16, 2014.
- [12] G. Lilis, G. Conus, N. Asadi, and M. Kayal, "Towards the next generation of intelligent building: An assessment study of current automation and future IoT based systems with a proposal for transitional design," *Sustainable Cities and Society*, 8/12 2016.
- [13] J. Wong and H. Li, "Development of a conceptual model for the selection of intelligent building systems," *Building and Environment*, vol. 41, pp. 1106-1123, 1/1/2006 2006.
- [14] H. Alwaer and D. J. Clements-Croome, "Key performance indicators (KPIs) and priority setting in using the multi-attribute approach for assessing sustainable intelligent buildings," *Building and Environment*, vol. 45, pp. 799-807, 1/1/2010 2010.
- [15] B. Lin and I. Ahmad, "Analysis of energy related carbon dioxide emission and reduction potential in Pakistan," *Journal of Cleaner Production*, 12/20 2016.
- [16] G. Günel, "What Is Carbon Dioxide? When Is Carbon Dioxide?," *PoLAR: Political & Legal Anthropology Review*, vol. 39, pp. 33-45, 2016.
- [17] E. S. F. Berman, M. Fladeland, J. Liem, R. Kolyer, and M. Gupta, "Greenhouse gas analyzer for measurements of carbon dioxide, methane, and water vapor aboard an unmanned aerial vehicle," *Sensors & Actuators: B. Chemical*, vol. 169, pp. 128-135, 7/5/5 July 2012 2012.
- [18] B.-J. Huang, Y.-C. Huang, G.-Y. Chen, P.-C. Hsu, and K. Li, "Improving Solar PV System Efficiency Using One-Axis 3-Position Sun Tracking," *Energy Procedia*, vol. 33, pp. 280-287, 1/1/2013 2013.

- [19] D. Guirguis, D. A. Romero, and C. H. Amon, "Toward efficient optimization of wind farm layouts: Utilizing exact gradient information," *Applied Energy*, vol. 179, pp. 110-123, 2016.
- [20] D. K. Jha and R. Shrestha, "Measuring Efficiency of Hydropower Plants in Nepal Using Data Envelopment Analysis," *IEEE Transactions on Power Systems*, vol. 21, pp. 1502-1511, 2006.
- [21] A. Zhang, Y. Chen, and J. Yan, "Optimal Design and Simulation of High-Performance Organic-Metal Halide Perovskite Solar Cells," *IEEE Journal of Quantum Electronics*, vol. 52, pp. 1-6, 2016.
- [22] X. Qiu, B. Cao, S. Yuan, X. Chen, Z. Qiu, Y. Jiang, *et al.*, "From unstable CsSnI₃ to air-stable Cs₂SnI₆: A lead-free perovskite solar cell light absorber with bandgap of 1.48 eV and high absorption coefficient," *Solar Energy Materials & Solar Cells*, vol. 159, pp. 227-234, 2017.
- [23] M. C. Hanna and A. J. Nozik, "Solar conversion efficiency of photovoltaic and photoelectrolysis cells with carrier multiplication absorbers," *Journal of Applied Physics*, vol. 100, p. 074510, 2006.
- [24] W. Li, R. Yang, and D. Wang, "CdTe solar cell performance under high-intensity light irradiance," *Solar Energy Materials and Solar Cells*, vol. 123, pp. 249-254, 4/1/April 2014 2014.
- [25] A. Haque, "Maximum Power Point Tracking (MPPT) Scheme for Solar Photovoltaic System," *Energy Technology & Policy: An Open Access Journal*, vol. 1, p. 115, 01// 2014.
- [26] I. Maqsood and M. Emziane, "Intelligent Sun Tracking for a CPV Power Plant," *AIP Conference Proceedings*, vol. 1277, pp. 157-160, 2010.
- [27] C.-H. Lin, C.-H. Huang, Y.-C. Du, and J.-L. Chen, "Maximum photovoltaic power tracking for the PV array using the fractional-order incremental conductance method," *Applied Energy*, vol. 88, pp. 4840-4847, 1/1/2011 2011.
- [28] Y.-T. Chen, Y.-C. Jhang, T.-H. Kuo, R.-H. Liang, and C.-W. Hung, "Jumping maximum power point tracking method for PV array under partially shaded conditions," *Solar Energy*, vol. 132, pp. 617-627, 2016.
- [29] L. Changshi, "Prediction of current and the maximum power of solar cell via voltage generated by light and irradiance using analytically invertible function," *Solar Energy*, vol. 113, pp. 340-346, 3/1/March 2015 2015.
- [30] A. A. Costa, P. M. Lopes, A. Antunes, I. Cabral, A. Grilo, and F. M. Rodrigues, "3I Buildings: Intelligent, Interactive and Immersive Buildings," *Procedia Engineering*, vol. 123, pp. 7-14, 1/1/2015 2015.
- [31] P. Haves, "Energy Simulation Tools for Buildings: An Overview," *AIP Conference Proceedings*, vol. 1401, pp. 313-327, 2011.
- [32] A. Zhivov, R. J. Liesen, S. Richter, R. Jank, D. M. Underwood, D. Neth, *et al.*, "Net Zero Building Cluster Energy Systems Analysis for U.S. Army Installations," *ASHRAE Transactions*, vol. 118, pp. 751-766, 2012.
- [33] B. Rismanchi, R. Saidur, H. H. Masjuki, and T. M. I. Mahlia, "Modeling and simulation to determine the potential energy savings by implementing cold thermal energy storage system in office buildings," *Energy Conversion and Management*, vol. 75, pp. 152-161, 11/1/November 2013 2013.
- [34] S. Korkmaz, J. I. Messner, D. R. Riley, and C. Magent, "High-Performance Green Building Design Process Modeling and Integrated Use of Visualization Tools," *Journal of Architectural Engineering*, vol. 16, pp. 37-45, 2010.
- [35] A. E. D. El-Alfy, "Design of sustainable buildings through Value Engineering," *Journal of Building Appraisal*, vol. 6, pp. 69-79, Summer2010 2010.

- [36] H. Kim and K. Anderson, "Energy Modeling System Using Building Information Modeling Open Standards," *Journal of Computing in Civil Engineering*, vol. 27, pp. 203-211, 2013.
- [37] M. A. Habib, M. Hasanuzzaman, M. Hosenuzzaman, A. Salman, and M. R. Mehadi, "Energy consumption, energy saving and emission reduction of a garment industrial building in Bangladesh," *Energy*, vol. 112, pp. 91-100, 2016.
- [38] G. P. Moynihan and D. Triantafillu, "Energy Savings for a Manufacturing Facility Using Building Simulation Modeling: A Case Study," *Engineering Management Journal*, vol. 24, pp. 73-84, 2012.
- [39] E. Enache-Pommer, R. Mayer, and G. Parsons, "Energy Efficiency of Building Walls: Thermal Modeling, Experimental Testing, Long Term Evaluation and Correlation of Building Wall Systems," *ASHRAE Transactions*, vol. 119, pp. 1-8, 2013.
- [40] H. Said, A. Kandil, S. B. S. Nookala, H. Cai, M. El-Gafy, A. Senouci, *et al.*, "Modeling of the sustainability goal and objective setting process in the predesign phase of green institutional building projects," *Journal of Architectural Engineering*, vol. 20, 06/01/2014.
- [41] "Using Building Information Modeling for Green Interior Simulations and Analyses," vol. 37, ed: Wiley-Blackwell, 2012, p. 35.
- [42] H. Kim, A. Stumpf, and W. Kim, "Analysis of an energy efficient building design through data mining approach," *Automation in Construction*, vol. 20, pp. 37-43, 1/1/2011 2011.
- [43] J. Zuo and Z.-Y. Zhao, "Green building research—current status and future agenda: A review," *Renewable and Sustainable Energy Reviews*, vol. 30, pp. 271-281, 2// 2014.
- [44] C. M. Stoppel and F. Leite, "Evaluating building energy model performance of LEED buildings: Identifying potential sources of error through aggregate analysis," *Energy and Buildings*, vol. 65, pp. 185-196, 10// 2013.
- [45] H. Kim, A. Stump, and W. Kim, *Analysis of an energy efficient building design through data mining approach*.
- [46] M. Assad, O. Hosny, A. Elhakeem, and S. El Hagggar, "Green building design in Egypt from cost and energy perspectives," *Architectural Engineering & Design Management*, vol. 11, pp. 21-40, 2015.
- [47] L. Xiwang, W. Jin, and W. Teresa, "Net-zero Energy Impact Building Clusters Emulator for Operation Strategy Development," *ASHRAE Transactions*, vol. 120, pp. 1-8, 2014.
- [48] C. Vander Veen, "Technology Efficiency," *Government Technology*, vol. 23, pp. 6-6, 2010.
- [49] S. A. S. Eldin, M. S. Abd-Elhady, and H. A. Kandil, *Feasibility of solar tracking systems for PV panels in hot and cold regions*.
- [50] C. Sungur, "Multi-axes sun-tracking system with PLC control for photovoltaic panels in Turkey," *Renewable Energy: An International Journal*, vol. 34, pp. 1119-1125, 2009.
- [51] R. C. Tesiero, III, "Intelligent approaches for modeling and optimizing HVAC systems," ed, 2015.
- [52] S. V. Prakash, "Renewable Energy and Sustainable Development: an Overview," *CURIE Journal*, vol. 3, pp. 59-69, 2010.
- [53] D. Oates and K. T. Sullivan, "Postoccupancy Energy Consumption Survey of Arizona's LEED New Construction Population," *Journal of Construction Engineering & Management*, vol. 138, pp. 742-750, 2012.
- [54] "Pioneer in the North Sea [History]," *IEEE Power and Energy Magazine, Power and Energy Magazine, IEEE, IEEE Power and Energy Mag.*, 2009.
- [55] H. Jiang, Y. Li, and Z. Cheng, "Performances of ideal wind turbine," *Renewable Energy: An International Journal*, vol. 83, pp. 658-662, 2015.
- [56] J. R. P. Vaz and D. H. Wood, "Performance analysis of wind turbines at low tip-speed ratio using the Betz-Goldstein model," *Energy Conversion and Management*, vol. 126, pp. 662-672, 10/15/15 October 2016 2016.

- [57] Y. Minghui, L. Weijie, C. Chi Yung, Z. Lianjun, C. Zaiyu, and Z. Yun, "Optimal torque control based on effective tracking range for maximum power point tracking of wind turbines under varying wind conditions," *IET Renewable Power Generation*, vol. 11, pp. 501-510, 2017.
- [58] K. L. Ku, J. S. Liaw, M. Y. Tsai, and T. S. Liu, *Automatic Control System for Thermal Comfort Based on Predicted Mean Vote and Energy Saving*.
- [59] S. E. Wolfe and H. Elizabeth, "Building towards water efficiency: the influence of capacity and capability on innovation adoption in the Canadian home-building and resale industries," *Journal of Housing and the Built Environment*, p. 47, 2011.
- [60] P. A. Valberg, T. E. Van Deventer, and M. H. Repacholi, "Workgroup Report: Base Stations and Wireless Networks--Radiofrequency (RF) Exposures and Health Consequences," *Environmental Health Perspectives*, vol. 115, pp. 416-424, 2007.
- [61] M. Khalid, T. Mee, A. Peyman, D. Addison, C. Calderon, M. Maslanyj, *et al.*, "Exposure to radio frequency electromagnetic fields from wireless computer networks: Duty factors of Wi-Fi devices operating in schools," *Progress in Biophysics & Molecular Biology*, vol. 107, pp. 412-420, 2011.
- [62] "Measurement of equivalent power density and RF energy deposition in the immediate vicinity of a 24-GHz traffic radar antenna," *IEEE Transactions on Electromagnetic Compatibility, Electromagnetic Compatibility, IEEE Transactions on, IEEE Trans. Electromagn. Compat.*, p. 183, 1995.
- [63] A. I. AbdelAzim, A. M. Ibrahim, and E. M. Aboul-Zahab, "Development of an energy efficiency rating system for existing buildings using Analytic Hierarchy Process – The case of Egypt," *Renewable & Sustainable Energy Reviews*, vol. 71, pp. 414-425, 2017.
- [64] J. K. W. Wong and J. Zhou, "Review: Enhancing environmental sustainability over building life cycles through green BIM: A review," *Automation in Construction*, vol. 57, pp. 156-165, 9/1/September 2015 2015.
- [65] X. Wang, N. Wang, X. Liu, and R. Shi, "Energy-saving analysis for the Modern Wing of the Art Institute of Chicago and green city strategies," *Renewable & Sustainable Energy Reviews*, vol. 73, pp. 714-729, 2017.
- [66] E. Setyowati, A. R. Harani, and Y. N. Falah, "Green Building Design Concepts of Healthcare Facilities on the Orthopedic Hospital in the Tropics," *Procedia - Social and Behavioral Sciences*, vol. 101, pp. 189-199, 11/8/8 November 2013 2013.
- [67] W. Eisenstein, G. Fuertes, S. Kaam, K. Seigel, E. Arens, and L. Mozingo, "Climate co-benefits of green building standards: water, waste and transportation," *Building Research & Information*, vol. 45, pp. 828-844, 2017.
- [68] P. MacNaughton, J. Spengler, J. Vallarino, S. Santanam, U. Satish, and J. Allen, "Environmental perceptions and health before and after relocation to a green building," *Building and Environment*, vol. 104, pp. 138-144, 8/1/1 August 2016 2016.
- [69] M. Rehm and R. Ade, "Construction costs comparison between 'green' and conventional office buildings," *Building Research & Information*, vol. 41, pp. 198-208, 2013.
- [70] S. E. Diaz-Mendez, A. A. Torres-Rodríguez, M. Abatal, M. A. E. Soberanis, A. Bassam, and G. K. Pedraza-Basulto, "Economic, environmental and health co-benefits of the use of advanced control strategies for lighting in buildings of Mexico," *Energy Policy*, vol. 113, pp. 401-409, 2/1/February 2018 2018.
- [71] I. Bartolozzi, F. Rizzi, and M. Frey, "Are district heating systems and renewable energy sources always an environmental win-win solution? A life cycle assessment case study in Tuscany, Italy," *Renewable & Sustainable Energy Reviews*, vol. 80, pp. 408-420, 2017.
- [72] N. DeForest, A. Shehabi, J. O'Donnell, G. Garcia, J. Greenblatt, E. S. Lee, *et al.*, "United States energy and CO2 savings potential from deployment of near-infrared electrochromic window glazings," *Building & Environment*, vol. 89, pp. 107-117, 2015.

- [73] A. Michopoulos, V. Voulgari, K. Papakostas, and N. Kyriakis, "Evaluation of different weather files on energy analysis of buildings," *International Journal of Energy & Environment*, vol. 3, p. 195, 03// 2012.
- [74] A. Pyrgou, V. L. Castaldo, A. L. Pisello, F. Cotana, and M. Santamouris, "Differentiating responses of weather files and local climate change to explain variations in building thermal-energy performance simulations," *Solar Energy*, vol. 153, pp. 224-237, 2017.
- [75] A. Das, D. Rossetti di Valdalbero, and M. R. Virdis, "ACROPOLIS: An example of international collaboration in the field of energy modelling to support greenhouse gases mitigation policies," *Energy Policy*, vol. 35, pp. 763-771, 1/1/2007 2007.
- [76] I. Meireles, V. Sousa, K. Adeyeye, and A. Silva-Afonso, "User preferences and water use savings owing to washbasin taps retrofit: a case study of the DECivil building of the University of Aveiro," *Environmental Science And Pollution Research International*, 2017.
- [77] C. Cheng-Li, P. Jr-Jie, H. Ming-Chin, L. Wan-Ju, and C. Szu-Jen, "Evaluation of Water Efficiency in Green Building in Taiwan," *Water, Vol 8, Iss 6, p 236 (2016)*, p. 236, 2016.
- [78] M. Chown, "Why is the Sun hot?," *New Humanist*, vol. 131, pp. 8-8, 09// 2016.
- [79] T. Alexandru Dan, "INSTRUMENTATION FOR MEASURING AND TRANSMISSION THE SOLAR RADIATION THROUGH EARTH'S ATMOSPHERE," *Current Trends in Natural Sciences, Vol 2, Iss 3, Pp 83-91 (2013)*, p. 83, 2013.
- [80] J. J. Díaz-Torres, L. Hernández-Mena, M. A. Murillo-Tovar, E. León-Becerril, A. López-López, C. Suárez-Plascencia, *et al.*, "Assessment of the modulation effect of rainfall on solar radiation availability at the Earth's surface," *Meteorological Applications*, vol. 24, pp. 180-190, 2017.
- [81] A. Hamel, "Higher values of spectral response, absorption coefficient and external quantum efficiency of solar cell in the form of pyramids," *Physics of Particles and Nuclei Letters*, vol. 14, pp. 453-458, 05/01/2017.
- [82] M. Caduff, M. A. J. Huijbregts, H.-J. Althaus, A. Koehler, and S. Hellweg, "Wind Power Electricity: The Bigger the Turbine, The Greener the Electricity?," *Environmental Science & Technology*, vol. 46, pp. 4725-4733, 2012.
- [83] B. Loganathan, I. Mustary, H. Chowdhury, and F. Alam, "Effect of sizing of a Savonius type vertical axis micro wind turbine," *Energy Procedia*, vol. 110, pp. 555-560, 3/1/March 2017 2017.
- [84] M. Ragheb and A. M. Ragheb, "Wind Turbines Theory - The Betz Equation and Optimal Rotor Tip Speed Ratio," in *Fundamental and Advanced Topics in Wind Power*, R. Cariveau, Ed., ed Rijeka: InTech, 2011, p. Ch. 02.
- [85] H. Zhao, Q. Wu, C. N. Rasmussen, and M. Blanke, "\cal L_1 Adaptive Speed Control of a Small Wind Energy Conversion System for Maximum Power Point Tracking," *IEEE Transactions on Energy Conversion*, vol. 29, pp. 576-584, 2014.
- [86] M. A. Abdullah, A. H. M. Yatim, and T. Chee Wei, "A study of maximum power point tracking algorithms for wind energy system," in *2011 IEEE Conference on Clean Energy and Technology (CET)*, 2011, pp. 321-326.
- [87] K. Kee Han, O. John Kie-Whan, and J. WoonSeong, "Study on Solar Radiation Models in South Korea for Improving Office Building Energy Performance Analysis," *Sustainability*, 2016.
- [88] L. Xu, Y. Yu, and Y. Cui, "Active vibration control for seismic excited building structures under actuator saturation, measurement stochastic noise and quantisation," *Engineering Structures*, vol. 156, pp. 1-11, 02/01/2018.
- [89] Y. Bao, J. A. Main, and S. Y. Noh, "Evaluation of structural robustness against column loss: Methodology and application to RC frame buildings," *Journal of Structural Engineering (United States)*, vol. 143, 08/01/2017.

- [90] L. Elhifnawy, H. Abou-Elfath, and E. El-Hout, "Original Article: Inelastic performance of RC buildings subjected to near-source multi-component earthquakes," *Alexandria Engineering Journal*, 3/4 2017.
- [91] B. A. Baskaran and S. K. Ping Ko, "Optimizing the Wind Uplift Resistance of Mechanically Attached Roof Systems," *Journal of Architectural Engineering*, vol. 14, pp. 65-75, 2008.
- [92] A. Valašík, V. Benko, A. Strauss, and B. Täubling, "Reliability assessment of slender concrete columns at the stability failure," *AIP Conference Proceedings*, vol. 1922, pp. 1-7, 2017.
- [93] "An InSAR-Based Temporal Probability Integral Method and its Application for Predicting Mining-Induced Dynamic Deformations and Assessing Progressive Damage to Surface Buildings," *IEEE Journal of Selected Topics in Applied Earth Observations and Remote Sensing, Selected Topics in Applied Earth Observations and Remote Sensing, IEEE Journal of, IEEE J. Sel. Top. Appl. Earth Observations Remote Sensing*, p. 472, 2018.
- [94] D. M. Sahoo and S. Chakraverty, "Functional Link Neural Network Learning for Response Prediction of Tall Shear Buildings With Respect to Earthquake Data," *IEEE Transactions on Systems, Man & Cybernetics. Systems*, vol. 48, pp. 1-10, 2018.
- [95] D. Feng Hui, L. Can Hong, L. Yuan, and S. Bao Jiang, "Numerical analysis on dynamic responses of single-storey buildings under seismic effects," *Journal of Vibroengineering*, vol. 19, p. 3581, 08// 2017.
- [96] Z. Cheng, W. Lin, and Z. Shi, "Wave dispersion analysis of multi-story frame building structures using the periodic structure theory," *Soil Dynamics & Earthquake Engineering (0267-7261)*, vol. 106, pp. 215-230, 2018.
- [97] M. I. Todorovska and M. D. Trifunac, "Earthquake damage detection in the Imperial County Services Building III: Analysis of wave travel times via impulse response functions," *Soil Dynamics and Earthquake Engineering*, vol. 28, pp. 387-404, 1/1/2008 2008.
- [98] "High-resolution Spectral-analysis for Fundamental Frequency Estimation of High-rise Buildings subjected to Earthquakes," *IEEE Latin America Transactions, Latin America Transactions, IEEE (Revista IEEE America Latina), IEEE Latin Am. Trans.*, p. 3735, 2015.
- [99] P. Khalili-Tehrani, E. R. Ahlberg, C. Rha, A. Lemnitzer, J. P. Stewart, E. Taciroglu, *et al.*, "Nonlinear Load-Deflection Behavior of Reinforced Concrete Drilled Piles in Stiff Clay," *Journal of Geotechnical & Geoenvironmental Engineering*, vol. 140, pp. 1-14, 2014.
- [100] M. Ohsaki, T. Nakajima, J. Fujiwara, and F. Takeda, "Configuration optimization of clamping members of frame-supported membrane structures," *Engineering Structures*, vol. 33, pp. 3620-3627, 2011.
- [101] J. Vaculik and M. C. Griffith, "Out-of-plane load–displacement model for two-way spanning masonry walls," *Engineering Structures*, vol. 141, pp. 328-343, 2017.
- [102] O. Mohammad Esmail Nia and M. Somayeh, "Estimation of RC columns' response under the effect of lateral blast loading by SDOF method and comparison with FEM," *Journal of Structural and Construction Engineering, Vol 4, Iss 3, Pp 81-90 (2017)*, p. 81, 2017.
- [103] Z. Yousif and R. Hindi, "AASHTO-LRFD Live Load Distribution for Beam-and-Slab Bridges: Limitations and Applicability," *Journal of Bridge Engineering*, vol. 12, pp. 765-773, 2007.
- [104] P. Olmati, J. Sagaseta, D. Cormie, and A. E. K. Jones, "Simplified reliability analysis of punching in reinforced concrete flat slab buildings under accidental actions," *Engineering Structures*, vol. 130, pp. 83-98, 1/1/1 January 2017 2017.
- [105] G. R. Newsham, B. J. Birt, C. Arsenault, A. J. L. Thompson, J. A. Veitch, S. Mancini, *et al.*, "Do 'green' buildings have better indoor environments? New evidence," *Building Research & Information*, vol. 41, pp. 415-434, 2013.

- [106] "Human Exposure to RF, Microwave, and Millimeter-Wave Electromagnetic Radiation [Health Effects]," *IEEE Microwave Magazine, Microwave Magazine, IEEE, IEEE Microwave*, p. 32, 2016.
- [107] Z. Brown and R. J. Cole, "Influence of occupants' knowledge on comfort expectations and behaviour," *Building Research & Information*, vol. 37, pp. 227-245, 2009.
- [108] R. Hitchings, "Studying thermal comfort in context," *Building Research & Information*, vol. 37, pp. 89-94, 2009.
- [109] D. Lukcso, T. L. Guidotti, D. E. Franklin, and A. Burt, "Indoor environmental and air quality characteristics, building-related health symptoms, and worker productivity in a federal government building complex," *Archives of Environmental & Occupational Health*, vol. 71, pp. 85-101, 03// 2016.
- [110] L. Asere, T. Mols, and A. Blumberga, "Assessment of Energy Efficiency Measures on Indoor Air Quality and Microclimate in Buildings of Liepaja Municipality," *Energy Procedia*, vol. 95, pp. 37-42, 9/1/September 2016 2016.
- [111] R. W. Allen, S. D. Adar, E. Avol, M. Cohen, C. L. Curl, T. Larson, *et al.*, "Modeling the Residential Infiltration of Outdoor PM_{2.5} in the Multi-Ethnic Study of Atherosclerosis and Air Pollution (MESA Air)," *Environmental Health Perspectives*, vol. 120, pp. 824-830, 06// 2012.
- [112] R. Larsen, "Experiments and observations in the study of environmental impact on historical vegetable tanned leathers," *Thermochimica Acta*, vol. 365, pp. 85-99, 1/1/2000 2000.
- [113] K. Van Looy, M. Lejeune, and W. Verbeke, "Original research paper: Indicators and mechanisms of stability and resilience to climatic and landscape changes in a remnant calcareous grassland," *Ecological Indicators*, vol. 70, pp. 498-506, 11/1/November 2016 2016.
- [114] F. Stazi, C. Di Perna, and P. Munafò, "Durability of 20-year-old external insulation and assessment of various types of retrofitting to meet new energy regulations," *Energy & Buildings*, vol. 41, pp. 721-731, 1/1/2009 2009.
- [115] C. Iain, "<E2>INTRODUCTION TO DIGITAL SYSTEMS,</E2> by Milós Ercegovac, Tomás Lang and Jaime H. Moreno, Wiley, Chichester, UK, 1999, 498 pages, inc. CD and Index (Hb; £29.50)," *Robotica*, vol. 17, p. 697, 11/01/Number 6/November 1999 1999.
- [116] A. M. Mulaosmanović, "KOMUNIKACIJA U INDUSTRIJI PRIMJENOM PROFINET PROTOKOLA," *COMMUNICATION IN INDUSTRY BY USING THE PROFINET PROTOCOL.*, vol. 63, pp. 146-160, 2015.
- [117] B. Lee, D.-K. Kim, H. Yang, and S. Oh, "Model transformation between OPC UA and UML," *Computer Standards & Interfaces*, vol. 50, pp. 236-250, 2017.
- [118] S. Macquarie Law and P. Radan, "Is Intelligent Design Science?: Who Decides if It Is?," *Macquarie Law Symposium*, p. 67, 2006.
- [119] A. Jean Yves, Z. Igor Yurievich, and M. Oleg Nikolaevich, "Smart Building Management Systems and Internet of Things," *Bezopasnost' Informacionnyh Tehnologij, Vol 24, Iss 3, Pp 18-29 (2017)*, p. 18, 2017.
- [120] M. Thibaud, H. Chi, W. Zhou, and S. Piramuthu, "Internet of Things (IoT) in high-risk Environment, Health and Safety (EHS) industries: A comprehensive review," *Decision Support Systems*, 2/17 2018.